

The Regulation of Oat Coleoptile  
Phosphoenolpyruvate Carboxylase and Malic Enzyme  
by  $H^+$  and Metabolites:  
Kinetic Evidence For and Against a Cytosolic pH-Stat

by

Ceredwyn E. Smith, B.Sc. (Hons.)

A Thesis  
submitted to the Department of Biological Sciences  
in partial fulfilment of the requirements  
for the degree of  
Master of Science

August 1979  
Brock University  
St. Catharines, Ontario

© Ceredwyn E. Smith, 1979

### Abstract

Phosphoenolpyruvate carboxylase (PEPC) and malic enzyme activities in soluble protein extracts of Avena coleoptiles were investigated to determine whether their kinetics were consistent with a role in cytosol pH regulation. Malic enzyme activity was specific for NADP<sup>+</sup> and Mn<sup>2+</sup>. Maximal labelled product formation from [<sup>14</sup>C]-substrates required the presence of all coenzymes, cofactors and substrates. Plots of rate versus malate concentration, and linear transformations thereof, indicated typical Michaelis-Menten kinetics at non-saturating malate levels and substrate inhibition at higher malate levels. pH increases between 6.5 and 7.25 increased near-optimal activity, decreased the degree of substrate inhibition and the  $K_{mapp}(Mn^{2+})$  but did not affect the  $V_{max}$  or  $K_{mapp}(malate)$ . Transformed data of PEPC activity demonstrated non-linear plots indicative of non-Michaelian kinetics. pH increases between 7.0 and 7.6 increased the  $V_{max}$  and decreased the  $K_{mapp}(Mg^{2+})$  but did not affect the  $K_{mapp}(PEP)$ . Various carboxylic acids and phosphorylated sugars inhibited PEPC and malic enzyme activities, and these effects decreased with pH increases. Metabolite inhibited malic enzyme activity was non-competitive and resulted mainly from Mn<sup>2+</sup> chelation. In contrast, metabolite inhibited PEPC activity was unique for each compound tested, being variously dependent on the PEP concentration and the pH employed.

These results indicate that fluctuations in pH and metabolite levels affect PEPC and malic enzyme activities similarly and that

the in vitro properties of PEPC are consistent with its proposed role in a pH-stat, whereas the in vitro properties of the malic enzyme cannot be interpreted in terms of a role in pH regulation.

### Acknowledgements

I sincerely thank Dr. A. W. Bown for providing me with the opportunity to undertake this project, and whose discussions helped to buffer perhaps unwarranted criticism I had for some aspects of the related literature. Secondly, I wish to thank Dr. P. Nicholls for his enlightening interpretation of some of the kinetic observations found over the course of this work. In addition, I thank Dr. S. M. Pearce for her critical discussion and optimistic support of my research.

I also wish to thank Mr. B. C. Hill, Mr. A. C. Doo and Mr. J. Engemann for their advice, moral support and their sometimes rather heated discussions regarding enzyme kinetics and plant growth. My sincere thanks is also extended to Ms. C. P. Bray for her speedy drafting of the illustrations herein, and Miss J. Hastie for the typing of this manuscript.

## Table of Contents

	Page
Abstract	2
Acknowledgements	4
List of Tables	8
List of Figures	11
Introduction	15
Review of Literature	19
I. Characteristics of Phosphoenolpyruvate Carboxylase and the Malic Enzyme	19
A. Phosphoenolpyruvate Carboxylase	20
(1) Reaction Catalyzed	20
(2) Regulatory Properties	24
(3) Concluding Statement	28
B. The Malic Enzyme	28
(1) Reactions Catalyzed	28
(2) Regulatory Properties	32
(3) Concluding Statement	37
C. Intracellular Location and Environment	38
II. Pathways of Carboxylation and Decarboxylation	40
III. Metabolic and Physiological Roles of Phosphoenolpyruvate Carboxylase and the Malic Enzyme	43
A. Anaplerotic Fluxes and Removal of TCA Cycle Intermediates	43
B. Osmoregulation	45
C. Intracellular pH Maintenance	47
D. Concluding Statement	50
IV. Hormone Stimulated Growth and Relationships with Phosphoenolpyruvate Carboxylase and the Malic Enzyme	51
Materials and Methods	
Materials	
I. Biological Materials	54
II. General Materials.	54

	Page
III. Chemical Materials	54
A. Assay Materials	54
B. Buffer Materials	55
C. Chromatographic Materials	56
D. Radiochemicals and Autoradiographic Materials	56
IV. Reagents	57
A. Enzyme Assay Reagents	57
B. Chromatographic Reagents	58
C. Radiochemicals and Scintillation Fluids	58
D. Lowry Reagents	58
Methods	
I. Source and Extraction of Enzymes	59
A. Coleoptile Tissue	59
B. Preparation of Enzyme Extract	59
II. Enzyme Assays	62
A. Phosphoenolpyruvate Carboxylase	62
(1) Spectrophotometric Assays	62
(2) Radiochemical Assays	69
B. The Malic Enzyme	74
(1) Spectrophotometric Assays	74
(2) Radiochemical Assays	83
III. Scintillation Counting and Velocity Calculations	91
IV. Protein Determinations	96
V. Data Analysis	98
Results	
I. Effects of Various Extraction Techniques and Assay Conditions on Phosphoenolpyruvate Carboxylase and Malic Enzyme Activities	101
A. Effects of Dialysis or Gel Filtration of the Protein Preparation on PEP Carboxylase Activity	101
B. Effects of Various Buffer Systems on PEP Carboxylase and Malic Enzyme Activities	109

	Page
II. Characterization of Malic Enzyme Activity	128
A. Substrate, Coenzyme and Cofactor Dependence of the Spectrophotometric Reaction Rate	128
B. Radiochemical Assays	133
C. Kinetics of the Malic Enzyme as a Function of pH	138
III. Determination of the Apparent Kinetic Constants of Phosphoenolpyruvate Carboxylase and the Malic Enzyme from Radiochemical Assays	150
A. PEP Carboxylase	150
B. The Malic Enzyme	151
IV. Effects of pH and Various Metabolites on Phosphoenolpyruvate Carboxylase and Malic Enzyme Activities	157
A. General Survey of Potential Effectors of PEP Carboxylase and Malic Enzyme Activities	157
B. Evidence for a Direct or Indirect Effect of Potential Effectors on Enzyme Activities	166
C. Effects of pH and Effectors on the Apparent Kinetic Constants of PEP Carboxylase and the Malic Enzyme	176
Discussion	198
Literature Cited	214

## List of Tables

	Page
1. Standard assay system for the spectrophotometric measurement of PEP carboxylase activity	64
2. Standard assay system for the spectrophotometric measurement of malate dehydrogenase activity	67
3. Reproducibility of the standard spectrophotometric assay of PEP carboxylase at saturated and PEP-limited substrate levels	70
4. Standard assay systems for the radiochemical measurement of PEP carboxylase activity	71
5. Reproducibility of the standard radiochemical assays of PEP carboxylase at near-saturated and PEP-limited substrate levels	75
6. Standard assay system for the spectrophotometric measurement of malic enzyme activity (NADP <sup>+</sup> reduction)	76
7. Standard assay system for the spectrophotometric measurement of malic enzyme activity (NADPH oxidation)	80
8. Reproducibility of the standard spectrophotometric assay of the malic enzyme at near-saturated and malate-limited levels of activity (a) NADP <sup>+</sup> reduction (b) NADPH oxidation	84
9. Standard assay system for the radiochemical measurement of malic enzyme activity (NADP <sup>+</sup> reduction)	85
10. Standard assay system for the radiochemical measurement of malic enzyme activity (NADPH oxidation)	86
11. Reproducibility of the standard radiochemical assays of the malic enzyme at near-saturated and malate-limited levels of activity	90
12. Effect of Tris-BES extraction buffer concentrations, and Tris-BES assay buffer concentrations and pH on PEP carboxylase activity	123



	Page
13. Effect of Tris-BES extraction buffer concentrations and Tris-BES assay buffer concentrations and pH on malic enzyme activity	125
14. Effect of various concentrations of pyruvate and $\text{NaHCO}_3$ on the rates of pyruvate carboxylation	131
15. Radioactivity recovered in the ethylacetate, ethanolamine and aqueous fractions of a malic enzyme catalyzed reaction: Dependence on substrates, coenzymes and cofactors	134
16. Radioactivity recovered in gel sections of the ethylacetate fraction of a malic enzyme catalyzed reaction: Dependence on $\text{MnCl}_2$ and $\text{NADP}^+$	137
17. Radioactivity recovered in gel sections of the aqueous fraction of a malic enzyme catalyzed reaction: Dependence on pyruvate, $\text{MnCl}_2$ and $\text{NADPH}$	140
18. Effect of spectrophotometric or radiochemical assays on the apparent $K_m(\text{PEP})$ and $V_{\text{max}}$ for PEP carboxylase	153
19. Effect of spectrophotometric or radiochemical techniques on the apparent $K_m(\text{malate})$ and $V_{\text{max}}$ for the malic enzyme	156
20. Effects of various metabolites on the spectrophotometric activities of PEPC and the malic enzyme	158
21. Effects of various metabolites on the spectrophotometric or radiochemical assay of PEPC activity	160
22. Effects of various metabolites on the spectrophotometric or radiochemical assay of malic enzyme activity	163
23. Effect of glutamate or aspartate on the radioactive accumulation of products of a PEP catalyzed reaction	167
24. Effect of glutamate or aspartate on the radioactive accumulation of products of a malic enzyme catalyzed reaction	169
25. Effect of $\text{MgCl}_2$ on PEP carboxylase activity in the presence and absence of various metabolites	171

	Page
26. Effect of $\text{MnCl}_2$ on malic enzyme activity in the presence and absence of various metabolites	174
27. Effects of pH and various metabolites on the apparent $K_m$ (PEP) and $V_{\text{max}}$ for PEP carboxylase	193
28. Effects of pH and various metabolites on the apparent $K_m$ (malate) and $V_{\text{max}}$ for the malic enzyme	197

## List of Figures

	Page
1. PEP carboxylase catalyzed absorbance decrease at 340 nm	65
2. Malic enzyme catalyzed absorbance increase at 340 nm	77
3. Effect of $\text{MnCl}_2$ on the absorbance of protein in Tris-BES buffers	79
4. Malic enzyme catalyzed absorbance decrease at 340 nm	81
5. [ $^{14}\text{C}$ ]-hexadecane standard calibration curve for colour quenched samples	92
6. Standard calibration curve for solvent quenched (colourless) samples	93
7. Bovine serum albumin standard calibration curve for the Lowry method of protein determination	97
8. Effect of dialysis or gel filtration on the time dependent stability of PEP carboxylase activity ( $\pm 0.1$ mM malate)	102
9. Effect of dialysis or gel filtration on the velocity versus PEP concentration plot of PEP carboxylase activity ( $\pm 0.1$ mM malate)	104
10. Effect of dialysis or gel filtration on the Lineweaver-Burk plot of PEP carboxylase activity	105
11. pH profiles of PEP carboxylase activity at near-saturated and PEP-limited substrate levels	107
12. Effect of pH on PEP carboxylase activity as a function of the PEP concentration	108
13. Effect of pH on linearly transformed plots of PEP carboxylase activity as a function of the PEP concentration	110
14. Effect of pH on the Hill plot of PEP carboxylase activity	113
15. Effect of pH on the $K_{m_{app}}$ ( $\text{MgCl}_2$ ) and $V_{max}$ of PEP carboxylase	114

	Page
16. Effect of pH and various extraction and assay buffer species on PEP carboxylase activity	116
17. Effect of assay buffer species and pH on malic enzyme activity from potassium phosphate extracted protein	118
18. Effect of pH and various extraction and assay buffer species on malic enzyme activity	120
19. Effect of pH and assay ionic strength on PEP carboxylase activity assayed in various Tris-BES buffers	124
20. Effect of pH and assay ionic strength on malic enzyme activity assayed in various Tris-BES buffers	127
21. Effect of malate, $\text{MnCl}_2$ and $\text{NADP}^+$ on the rates of absorbance decrease at 340 nm	129
22. Effect of pyruvate, $\text{NaHCO}_3$ , $\text{MnCl}_2$ and NADPH on the rates of absorbance increase at 340 nm	132
23. Chromatogram of the 2,4-dinitrophenylhydrazine derivatives of OAA, pyruvate and a malate, $\text{MnCl}_2$ and $\text{NADP}^+$ utilizing reaction including the scheme for gel sectioning.	135
24. Autoradiogram of the 2,4-dinitrophenylhydrazine derivatives of a malate, $\text{MnCl}_2$ and $\text{NADP}^+$ utilizing reaction	135
25. Chromatogram of malate and the aqueous fraction of a pyruvate, $\text{NaHCO}_3$ , $\text{MnCl}_2$ and NADPH utilizing reaction including the scheme for gel sectioning	139
26. pH profiles of malic enzyme activity at saturated and malate-limited substrate levels	142
27. Effect of pH on malic enzyme activity as a function of the malate concentration	143
28. Effect of pH on linearly transformed plots of malic enzyme activity as a function of the malate concentration	144
29. Effect of pH on the Hill plot of malic enzyme activity	148

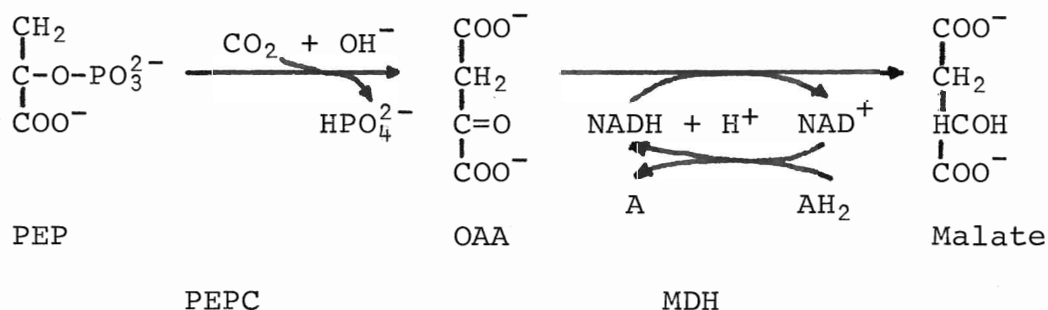
	Page
30. Effect of pH on the $K_{mapp}$ ( $MnCl_2$ ), the $K_{mapp}$ (malate) and $V_{max}$ of the malic enzyme	149
31. Effect of spectrophotometric or radiochemical measurement of activity on the kinetics of PEP carboxylase	152
32. Effect of spectrophotometric or radiochemical measurement of activity on the kinetics of the malic enzyme	154
33. Autoradiogram of the chromatography of 2,4-dinitro-phenylhydrazine derivatives of the PEP carboxylase reaction in the presence of various metabolites	162
34. Autoradiogram of the chromatography of 2,4-dinitro-phenylhydrazine derivatives of the malic enzyme catalyzed reaction in the presence of various metabolites	165
35. Effect of succinate and $MgCl_2$ on the PEP carboxylase catalysed rate of absorbance decrease at 340 nm	172
36. Effect of succinate and $MnCl_2$ on the malic enzyme catalyzed rate of absorbance change at 340 nm	175
37. Effect of fructose-1,6-diphosphate and $MnCl_2$ on the malic enzyme catalyzed rate of absorbance change at 340 nm using the standard protein preparation, or protein pre-incubated with $MnCl_2$	177
38. Effect of pH on the percent inhibition of near-saturated PEP carboxylase activity by malate, succinate, citrate, fructose-1,6-diphosphate and 3-phosphoglycerate	179
39. Effect of 0.1 mM malate on the pH profiles of PEP carboxylase activity at near-saturated and PEP limited substrate levels	180
40. Effect of pH on the percent inhibition of PEP carboxylase activity by 0.1 mM malate	181
41. Effect of pH and 0.1 mM malate on the linear transformations of PEP carboxylase activity as a function of the PEP concentration	182

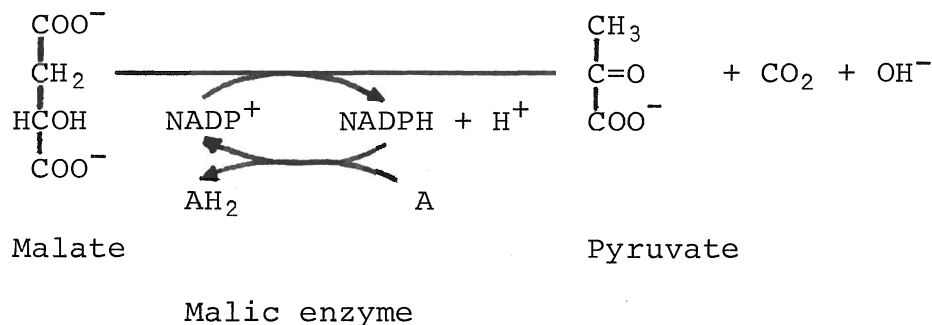
	Page
42. Effect of pH on the Dixon plot of PEP carboxylase activity in the presence of malate	186
43. Effect of pH and 1.7 mM succinate on the Lineweaver-Burk plot of PEP carboxylase activity	188
44. Effect of pH and 1.7 mM citrate on the Lineweaver-Burk plot of PEP carboxylase activity	189
45. Effect of pH and 1.7 mM fructose-1,6-diphosphate on the Lineweaver-Burk plot of PEP carboxylase activity	190
46. Effect of pH and 1.0 mM 3-phosphoglycerate on the Lineweaver-Burk plot of PEP carboxylase activity	192
47. Effect of pH on the percent inhibition of near-saturated malic enzyme activity by fructose-1,6-diphosphate, 3-phosphoglycerate, succinate and citrate	194
48. Effect of pH and 1.7 mM succinate on the Lineweaver-Burk plot of malic enzyme activity	196
49. A model for the mechanism of action of growth hormones	212

## Introduction

Cellular homeostasis depends on the maintenance of a relatively constant environment. A major factor in this balance is the regulation of inter- and intracellular pH. Acid-base balance can be achieved by buffers, which stabilize pH through an equilibrium between the protonated and the salt species of a weak acid or base. The major buffering power in animal systems results from carbon dioxide/bicarbonate and inorganic phosphate equilibria, and protein ionizations (for review see Reeves, 1977). Plant cellular homeostasis is much less understood. It has been suggested that in these organisms the cytoplasm has a finite buffering capacity which is exhausted by metabolic processes which generate acidic or basic metabolites (Davies, 1973; Smith and Raven, 1979).

Davies (1973) has postulated that the cytosolic pH of plant cells can be regulated by the number of acidic carboxyl groups present. He suggests that a metabolic pH-stat involving phosphoenolpyruvate carboxylase (PEPC) (E.C.4.1.1.31) and the malic enzyme (E.C. 1.1.1.40) could serve this function.





For involvement in a pH-stat, Davies (1973) states the following prerequisites for PEPC and malic enzyme activity:

- (1) The pH optimum of PEPC is higher than the cytosolic pH, which is higher than the pH optimum of the malic enzyme.
- (2) Increases in cytosol pH are accompanied by increases in PEPC activity and decreases in malic enzyme activity, and the converse occurs with decreases in cytosolic pH.
- (3) Metabolites that positively effect PEPC activity negatively effect malic enzyme activity, and vice versa. These effects are pH dependent with maximal effects at the pH of the cytosol.
- (4) All of the preceding characteristics are found under in vivo cellular conditions.

Thus carboxylation at high pH would lower the pH, and decarboxylation at low pH would raise the pH. Effector control of enzymic activities would serve to reinforce the regulation by pH.

Cytoplasmic pH of plant cells has been estimated to be between pH 7.0 and 7.5 (Spanswick and Miller, 1977). The pH optimum for PEPC isolated from Avena coleoptiles (Hill and Bown,



1978) and Solanum tubers (Bonugli and Davies, 1977) is approximately pH 8.0. With both maximal and sub-maximal substrate concentrations the Avena enzyme increases 80 to 110% in activity when pH is raised from 7.0 to 7.6 (Hill and Bown, 1978; Smith, Doo and Bown, 1979). Additionally, the apparent  $K_m$ (PEP) decreased 50% as pH is increased over the same range (Smith et al., 1979). Malate is a strong inhibitor of PEPC activity isolated from a variety of species (Hishikido and Takanashi, 1973). Smith et al. (1979) demonstrated that the apparent  $K_i$ (malate) increased 200% as pH was increased from 7.0 to 7.6. The Solanum enzyme was inhibited by carboxylic acids and activated by sugar phosphates, with maximal effects between pH 7.0 and 7.6 (Bonugli and Davies, 1977). The combined results indicate that the properties of in vitro PEPC are consistent with its postulated role in a metabolic pH-stat.

The pH optimum of malic enzyme activity isolated from Solanum tubers decreased from 7.6 to 6.4 as malate concentrations are decreased 10-fold (Davies and Patil, 1974). Decreases in pH are also correlated with decreases in the  $K_m$ (malate) and increases in substrate inhibition (Rutter and Lardy, 1958; Mukerji and Ting, 1968; Davies and Patil, 1974; Pupillo and Bossi, 1979). With sub-maximal concentrations of substrate enzyme activity is activated by carboxylic acids and inhibited by sugar phosphates; however, the effects of pH on inhibition and activation were not investigated (Davies and Patil, 1974).

The combined evidence from PEPC and malic enzyme activities of Solanum suggest that they could be involved in a metabolic pH-stat (Bonugli and Davies, 1977).

The pH-stat hypothesis is particularly relevant to tissue whose growth is stimulated by indoleacetic acid (IAA) mediated  $H^+$  excretion. In vivo evidence for a metabolic pH-stat in Avena coleoptiles includes IAA stimulated  $H^+$  efflux (Cleland, 1973), non-autotrophic  $CO_2$  fixation (Haschke and Lüttge, 1977), and malate accumulation (Haschke and Lüttge, 1975; Stout, Johnson and Rayle, 1978). Evidence implicating PEPC in the non-autotrophic fixation of  $CO_2$  has been reported from a number of laboratories (Bown and Lampman, 1971; Haschke and Lüttge, 1977).

Preliminary investigations in this laboratory have indicated the presence of malic enzyme activity in Avena coleoptile tissue, although a thorough characterization was not undertaken (Howe, B.Sc. Hon. Thesis, 1969; Bown and Lampman, 1971). This study was initiated to investigate the activities of Avena coleoptile PEPC and malic enzyme in relation to the hypothesized pH-stat. A primary objective of this work was the demonstration and characterization of malic enzyme activity. In addition, pH profiles of PEPC and malic enzyme activities were constructed at maximal and sub-maximal substrate concentrations, and in the presence or absence of various glycolytic and TCA cycle intermediates. The pH dependent properties of the two enzymes are discussed in light of their possible role in a metabolic pH-stat.

## Literature review

The purpose of this section is to review the properties and possible functions of phosphoenolpyruvate carboxylase (PEPC) (E.C.4.1.1.31) and the malic enzyme (E.C. 1.1.1.40) in plant tissues. These enzymes have been implicated in intracellular pH regulation, the maintenance of steady state levels of TCA cycle intermediates, and osmoregulation during periods of rapid growth. An examination of the evidence relating to these roles shall be made.

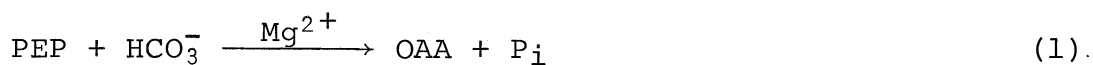
### I. Characteristics of phosphoenolpyruvate carboxylase and the malic enzyme

PEPC and the malic enzyme have been isolated from a wide variety of plant species and tissues. These can be grouped into autotrophic (photosynthetic) and non-autotrophic (non-photosynthetic) tissues. Investigations of purified enzymic activities indicate the presence of distinct isozymes with different regulatory properties for PEPC (Goatly, Coombs and Smith, 1975; Mukerji, 1977a, b and c) and the malic enzyme (Pupillo and Bossi, 1979) in autotrophic or non-autotrophic tissue. This study is concerned with PEPC and malic enzyme activities associated with non-autotrophic tissue. Consequently, the relevance of data from autotrophic tissue may be limited, and will not be discussed here. This section shall deal with isolation and characterization, in vitro regulation, and intracellular location and environment of PEPC and the malic enzyme.

## A. Phosphoenolpyruvate carboxylase

### (1) Reaction catalyzed

The catalyzed carboxylation of phosphoenolpyruvate (PEP) to oxaloacetate (OAA) and inorganic phosphate (Pi) was first indicated in 1804 (de Saussure, in Davies, Giovanelli and Aprees, 1964).



$$\Delta G^{01} = -7.9 \text{ kcal} \cdot \text{mole}^{-1}$$

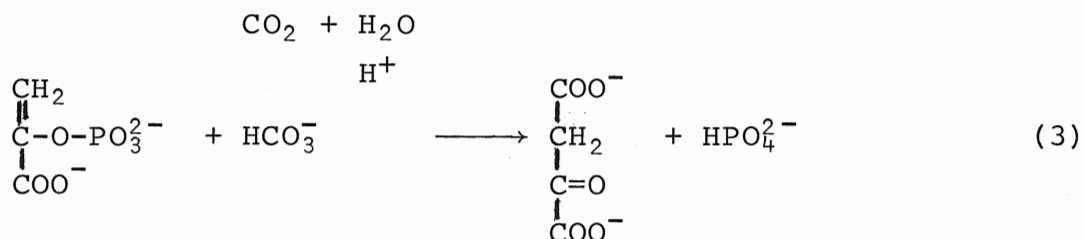
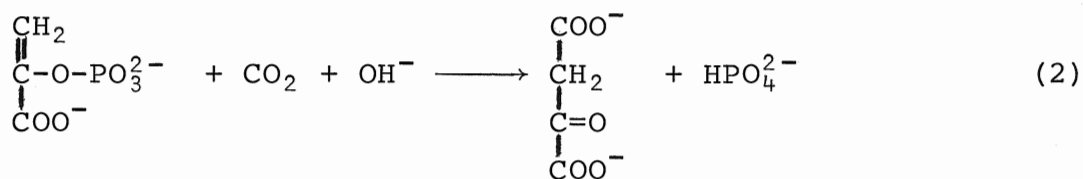
(Burton and Krebs, 1953)

Partially purified forms of phosphoenolpyruvate carboxylase (PEPC) have been obtained from a wide variety of organisms including autotrophic and heterotrophic bacteria, protozoa, algae and many higher plants.

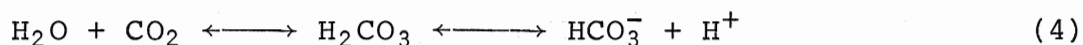
PEPC requires as substrate a CO<sub>2</sub> species and PEP. Optimal activity requires the presence of divalent metal cations. Spectrophotometric measurements of activity at 340 nm involves the addition of NADH so that OAA produced by PEPC can be reduced by malate dehydrogenase (MDH) activity. Incubation of the enzyme with [<sup>14</sup>C]-HCO<sub>3</sub><sup>-</sup> in the presence or absence of NADH and MDH indicate that the major reaction product is OAA or malate respectively (Ting, 1968; Hong, 1973).

The species of CO<sub>2</sub> utilized is still controversial. Both CO<sub>2</sub> (Waygood, Mache and Tan, 1969) and HCO<sub>3</sub><sup>-</sup> (Maruyama et al., 1966) have been proposed as substrate. Reactions (2) and (3) have been written assuming that the ionic forms indicated exist in the cytosol with a pH near 7.0. Reaction (2) involves the consumption of an OH<sup>-</sup> ion, reaction (3) the

generation of an  $H^+$  ion.



Reaction (4) takes at least one minute to equilibrate at  $10^\circ\text{C}$  when the initial reactants are  $\text{CO}_2$  and  $\text{H}_2\text{O}$  (Krebs and Roughton, 1948). The addition of the enzyme carbonic anhydrase at this temperature hastens the attainment of equilibrium (Krebs and Roughton, 1948).



pK = 6.35  
(Umbreit, Burris and Stauffer, 1964)

Reibach and Benedict (1977) investigated the activity of PEPC from Zea mays (Graminae, corn) leaves in the presence of  $\text{HCO}_3^-$ ,  $\text{CO}_2$  or  $\text{CO}_2$  plus carbonic anhydrase. Rates were determined spectrophotometrically (340 nm) at  $10^\circ\text{C}$  by coupling PEPC with MDH and following the oxidation of NADH. Results demonstrated that initial velocities were highest with the addition of  $\text{HCO}_3^-$ , lowest with the addition of  $\text{CO}_2$ , and intermediate when  $\text{CO}_2$  and carbonic anhydrase were added. Similar results indicating

that  $\text{HCO}_3^-$  is the substrate were obtained for enzyme isolated from the C4 plant Pennisetum purpureum and the C3 plant Pisum sativum (Coombs, Maw and Baldry, 1975). A radiochemical modification of the spectrophotometric technique was also utilized to attempt to determine the "CO<sub>2</sub>" species utilized. Enzyme activities isolated from Zea mays shoots and peanut cotyledons (Cooper and Wood, 1971) and Zea mays leaves (Mukerji, 1977) were measured at 10°C in the presence of  $[^{14}\text{C}]\text{-HCO}_3^- + \text{CO}_2$ ,  $\text{HCO}_3^- + [^{14}\text{C}]\text{-CO}_2$ , or  $\text{HCO}_3^- + [^{14}\text{C}]\text{-CO}_2 + \text{carbonic anhydrase}$ . Radioactivity accumulated in malate was highest when the enzyme was assayed with  $[^{14}\text{C}]\text{-HCO}_3^- + \text{CO}_2$ . However, Davies (1979) suggests that the value of this kinetic method is dependent on fulfilling two requirements. First, the buffering of the assay system must prevent any significant pH change upon the addition of the specific "CO<sub>2</sub>" species; and secondly, the concentration of the "CO<sub>2</sub>" species must be small relative to their apparent  $K_m$ . These requirements were not met in the experiments of Waygood et al. (1969); and the second requirement was not met in any of the other studies reported. Thus the value of these results is limited.

Maruyama et al. (1966) assayed enzyme isolated from peanut cotyledons with  $\text{U-}[^{18}\text{O}]\text{-HCO}_3^-$  and analyzed the reaction products. The results demonstrated a two to one ratio of the label in malate and inorganic phosphate, a result consistent with  $\text{HCO}_3^-$  being the substrate. Further evidence for this view resulted from the demonstration that  $K_m$  for CO<sub>2</sub> (1.25 mm) is much larger

than the  $K_m$  for  $\text{HCO}_3^-$  (0.11 mM) (Reibach and Benedict, 1977).

Indirect evidence for  $\text{HCO}_3^-$  being the active species is obtained from cytosolic pH estimations of between 7.0 and 7.5 (Spanswick and Miller, 1977), and the pH optimum of the enzyme being around 8.0 (Kluge and Osmond, 1972). At pH 7.4 the ratio of  $\text{HCO}_3^-:\text{CO}_2$  will be 10:1 using the pK of the dissociation of the  $\text{CO}_2 \rightleftharpoons \text{HCO}_3^- + \text{H}^+$  equilibrium (reaction (4)). The  $\text{HCO}_3^-$  would be the dominant species in the likely environmental conditions of the enzyme.

The necessity of divalent metal ions for optimal enzyme activity has been investigated in a number of laboratories. Danner and Ting (1967) observed that maximal PEPC activity from Zea mays roots was obtained when PEP,  $\text{HCO}_3^-$ ,  $\text{Mg}^{2+}$  and NADH were present in the spectrophotometric assay system. In the absence of  $\text{Mg}^{2+}$ , the initial velocity of the reaction was reduced by 90%. Hong (1973) demonstrated that  $\text{Mg}^{2+}$  was preferentially utilized over other divalent cations by enzyme isolated from Avena sativa (Graminae, oat) coleoptile tissue. The requirements for  $\text{Mg}^{2+}$  for optimal enzymic activity was further illustrated through the addition of metal ion chelating agents such as ATP, ADP and EDTA. PEPC activity is almost completely inhibited under these conditions (Ting and Osmond, 1973; Wong and Davies, 1973; Hill, 1976).

## (2) Regulatory properties

PEPC activity from non-autotrophic tissue is affected by various carboxylic and amino acids, sugar phosphates, inorganic ions and pH. Enzyme activities at saturating substrate concentrations have pH optima of approximately pH 8.0 (Kluge and Osmond, 1972). In the presence of saturating or limiting substrate levels, PEPC activity from Avena coleoptile tissue increases at least two-fold as pH is raised from 7.0 to 7.6 (Hill and Bown, 1978; Smith, Doo and Bown, 1979). Saturated activity from peanut cotyledons shows a similar increase (Maruyama et al., 1966). The authors have suggested that these pH mediated increases may be due to the increased availability of  $\text{HCO}_3^-$  resulting from the titration of  $\text{H}_2\text{CO}_3$  (Jacoby and Laties, 1971). If this were the case, then increases in enzymic activity should be proportional to increases in  $\text{HCO}_3^-$  concentration arising from the titration of  $\text{H}_2\text{CO}_3$ . Calculation of the change in  $\text{HCO}_3^-$  concentration as pH is increased indicates that between pH 7.1 and 7.5 the  $\text{HCO}_3^-$  level increases approximately 30%. It is apparent that much larger increases in enzyme activity over the same pH range involves factors other than changes in  $\text{HCO}_3^-$  concentrations.

Binding affinities of the enzyme for its substrates may be pH dependent. Maruyama et al. (1966) demonstrated that pH increases from 7.1 to 7.5 decreased the  $K_m(\text{PEP})$  and the  $K_m(\text{Mg}^{2+})$  13% and 30% respectively for enzyme isolated from peanut cotyledons. Similarly, Smith et al. (1979) observed



that the apparent  $K_m$ (PEP) decreased approximately 50% (0.17 mM to 0.08 mM) as pH was raised from 7.1 to 7.5 for enzyme extracted in soluble protein extracts of Avena coleoptiles. These results were obtained from Lineweaver-Burk and Eadie-Hofstee plots of spectrophotometric data. Wong (1975) suggests that these plots may be of limited value in determining kinetic parameters due to unequal weighting of rates obtained with low substrate concentrations. He reviews evidence indicating that the Hanes plot (substrate versus substrate $\cdot$ velocity $^{-1}$ ) is less biased in this respect and suggests that this plot should be utilized in combination with the previous two linear plots.

Evidence indicates that PEPC is a regulatory enzyme with properties typical of allosteric enzymes. Diagnostic tests for positive rate cooperativity include sigmoid plots of velocity versus substrate concentration, concave upwards Lineweaver-Burk plots, concave downwards Eadie-Hofstee plots, and Hill coefficients from Hill plots greater than one (Koshland, 1970). Positive rate cooperativity indicates positive binding cooperativity, and is the result of changes in the binding affinity of substrate for enzyme as substrate concentrations change. As each succeeding substrate molecule is bound, the affinity of the enzyme to bind more substrate increases. Hill (1976) demonstrated that PEPC activity from Avena coleoptiles exhibited sigmoid velocity versus PEP concentration plots at pH 7.6. Furthermore, he found Hill coefficients greater than two, concave upwards Lineweaver-Burk plots and concave downwards

Eadie-Hofstee plots, all of which indicate positive cooperativity. Smith (1977) demonstrated that the type of cooperativity exhibited by the Avena enzyme was pH dependent. Positive cooperativity appeared to be characteristic of activity above pH 7.2, and below this value negative cooperativity appeared to be exhibited. In contrast, enzyme from Solanum tubers exhibited hyperbolic kinetics under all assay conditions (Bonugli and Davies, 1977).

Enzyme activity isolated from a variety of tissues is inhibited by some carboxylic acids. Hishikido and Takanashi (1973) observed that L-malate inhibited PEPC from a variety of plant tissues and species, and that OAA was a still more powerful inhibitor. Enzyme isolated from P. purpureum exhibited increased activity when NADH was added to the assay system, resulting in the reduction of OAA to the less inhibitory malate (Coombs, Baldry and Bucke, 1973). PEPC from Avena coleoptiles (Hill and Bown, 1978), E. coli (Corwin and Fanning, 1968) and etiolated Z. mays seedlings (Wong and Davies, 1973) exhibited non-competitive inhibition by L-malate. Smith et al. (1979) demonstrated that the apparent  $K_i$ (malate) for the Avena enzyme increased 200% (0.03 mM to 0.09 mM) as pH was raised from 7.1 to 7.5. Succinate, fumarate and citrate were found to be mild non-competitive inhibitors of both the Solanum enzyme when assayed between pH 7.3 and 7.1 (Bonugli and Davies, 1977) and the E. coli enzyme when assayed at its pH optimum of 9.0 (Corwin and Fanning, 1968).

The amino acids aspartate and, to a lesser extent, glutamate slightly inhibited enzyme activity from E. coli (Corwin and Fanning, 1968), Z. mays roots (Ting, 1968) and etiolated leaves (Wong and Davies, 1973) and Solanum tubers (Bonugli and Davies, 1977). The latter study found the mixed-type inhibition to be most pronounced at pH 7.3. In contrast, PEPC extracted from Avena coleoptiles was not affected by aspartate when assayed at pH 7.6 (Hill, 1976).

Sugar phosphates activate PEPC activity isolated from non-autotrophic plant tissue. Enzyme from Z. mays (Wong and Davies, 1973) and Solanum tubers (Bonugli and Davies, 1977) was activated two- to three-fold in the former, and 0.2- to 0.3 fold in the latter by 5.0 mM concentrations of each of the phosphorylated 6-C glycolytic intermediates. The Z. mays enzyme was assayed at saturating substrate levels; whereas the Solanum enzyme was assayed at PEP concentrations giving half the maximal velocity. Additionally, fructose-6-phosphate activated the Solanum enzyme maximally at pH 7.1, the effect tailing off to zero at pH 6.6 and 7.9 (Bonugli and Davies, 1977).

Inorganic anions variously affected PEPC from different species. Sulphate activated both the Z. mays enzyme (Wong and Davies, 1973) and the Solanum enzyme (Bonugli and Davies, 1977). In contrast, phosphate activated only the Z. mays enzyme (Wong and Davies, 1973).

### (3) Concluding statement

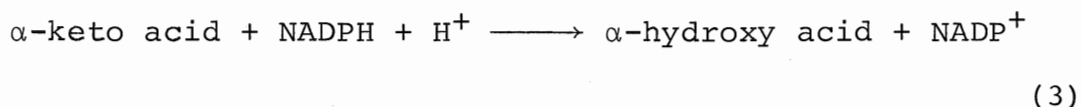
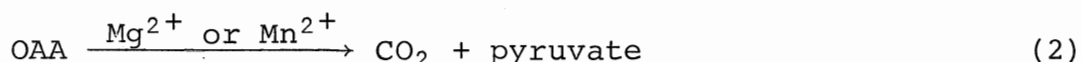
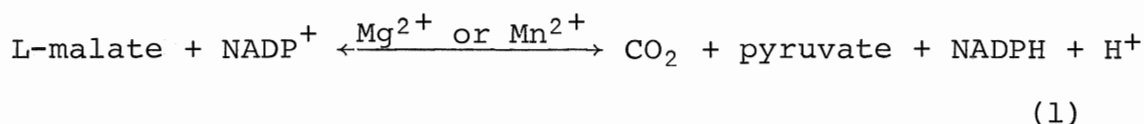
In general, the reports reviewed indicate that PEPC from a variety of species and tissues is activated by increased pH and sugar phosphates, and inhibited by carboxylic acids. Discrepancies in the literature concerning the degree of control of PEPC by various metabolites could be due to differences in the methods of enzyme isolation and assay. Loss of regulatory control is enhanced as further enzyme purification is attained (Maruyama et al., 1966; Smith, 1969; Bonugli and Davies, 1977). Coombs et al. (1973) demonstrated that enzymic activity from P. purpureum lost regulatory properties following sequential purification by ammonium sulphate precipitation and Sephadex gel filtration and chromatography. Hill and Bown (unpublished) observed that PEPC activity from Avena coleoptiles became insensitive to malate inhibition over time, even though uninhibited activity remained constant. Another reason for discrepancies may be variation in control mechanisms from species to species, and tissue to tissue.

### B. The malic enzyme

#### (1) Reactions catalyzed

Malic enzyme activity was first demonstrated in pigeon liver homogenates (Ochoa, Mehler and Kornberg, 1947) and wheat germ extracts (Kraemer, Conn and Vennesland, 1951). Studies on this enzyme by the groups led by Ochoa and Vennesland culminated in the identification of the substrates and establishment of the stoichiometry of the reactions catalyzed. Oxidative

decarboxylation of L-malate is the physiologically relevant reaction (see reaction (1)). The enzyme also catalyzes the pyridine nucleotide independent decarboxylation of oxaloacetic acid at pH values less than 5.0 (reaction (2)), and the slow reduction of a number of  $\alpha$ -keto acids (reaction (3)).



Reaction (1) has since been demonstrated in protein extracts isolated from a variety of higher vertebrates and microorganisms. Preliminary surveys of the higher plants have identified malic enzyme activity in crude extracts of autotrophic and non-autotrophic tissue from species having C-3, C-4 or crassulacean acid metabolism (Davies, Nascimento and Patil, 1974; Nishikido and Wada, 1974). This survey of the literature will report on enzyme activity from non-autotrophic plant tissue, vertebrates and microorganisms only.

Enzyme activity from all species requires L-malate as substrate, although coenzyme and cofactor requirements are less rigid. Furthermore, increasing purification procedures universally demonstrate the presence of two or more isozymes differing in their specificity for coenzyme and cofactor

requirements (Davies and Patil, 1974; Pupillo and Bossi, 1979).

NADP<sup>+</sup> is the coenzyme utilized although enzyme isolated from etiolated maize leaves and coleoptiles can reduce NAD<sup>+</sup> at two to five per cent of the rate obtained in the presence of NADP<sup>+</sup> (Pupillo and Bossi, 1979). In these studies the  $K_m$  for NAD<sup>+</sup> was at least 25-fold higher than the  $K_m$  for NADP<sup>+</sup>.

Divalent metal cations are required for maximal activity. Partially purified enzyme from E. coli exhibited a strict requirement for Mn<sup>2+</sup>, and Mg<sup>2+</sup> could not substitute (Sanwal and Smando, 1969). In contrast, the partially purified pigeon liver enzyme attained maximal activity with a MgCl<sub>2</sub> concentration that exceeded the MnCl<sub>2</sub> concentration by a factor of five times (Rutter and Lardy, 1958). The  $K_m$  (malate) for enzyme from a variety of plant species and tissues doubled when assayed with Mg<sup>2+</sup> rather than Mn<sup>2+</sup> (Davies et al., 1974; Pupillo and Bossi, 1979). The species of divalent cation utilized apparently affects the binding affinity of the enzyme for malate and the type of kinetics observed. The  $K_m$ (Mg<sup>2+</sup>) was 200-fold higher than the  $K_m$ (Mn<sup>2+</sup>) in partially purified enzyme from Solanum tuberosum tubers (Davies and Patil, 1974), rabbit heart mitochondria (Lin and Davis, 1974), and etiolated maize leaves and coleoptiles (Pupillo and Bossi, 1979).

Hyperbolic plots of velocity versus malate concentration when assayed with Mn<sup>2+</sup> or Mg<sup>2+</sup> were observed for enzyme isolated from E. coli (Sanwal and Smando, 1969), rabbit heart mitochondria (Lin and Davies, 1974) and maize coleoptiles (Pupillo and Bossi,

1979). The pigeon liver enzyme purified by Schimerlik, Grimshaw and Cleland (1977) indicated pronounced negative cooperative kinetics in the presence of varying  $\text{Mn}^{2+}$  concentrations, and Michaelis-Menten type hyperbolic kinetics when assayed with  $\text{Mg}^{2+}$ . The  $\text{Mn}^{2+}$  effect was indicated by biphasic (or concave downwards) Lineweaver-Burk plots. Conversely, a survey of malic enzyme from the higher plants prompted the suggestion that generally, hyperbolic kinetics are obtained in the presence of  $\text{Mn}^{2+}$  and alkaline conditions (Davies and Patil, 1974). Schimerlik et al. (1977) have suggested that the probable substrate for the pigeon liver enzyme in vivo is  $\text{Mg}^{2+}$ .

The oxidative decarboxylation of malate to pyruvate proceeds with a free energy change of  $-0.36 \text{ kcal} \cdot \text{mol}^{-1}$  (Burton and Krebs, 1953). The reductive carboxylation of pyruvate is thus thermodynamically unfavourable. However, by employing high concentrations of pyruvate and bicarbonate enzyme isolated from Avena coleoptiles (Howe, 1969) Solanum tubers (Davies and Patil, 1974), rabbit heart mitochondria (Lin and Davis, 1974) and pigeon liver (Schimerlik and Cleland, 1977a) can catalyze malate formation. At saturating substrate conditions, the ratio of the forward to reverse reactions was 3.5:1 (Solanum), 16.7:1 (rabbit) and 3.3:1 (pigeon). Schimerlik et al. (1977a) demonstrated that the  $K_m(\text{pyruvate})$  and the  $K_m(\text{CO}_2)$  are 36-fold and 2-fold larger than the  $K_m(\text{malate})$ .

## (2) Regulatory properties

Rates of malate decarboxylation in crude and partially purified tissue extracts are variously affected by malate levels and some metabolites and inorganic ions. Intrinsic to these possible regulatory processes is the influence of pH. The observed pH optimum at saturating malate concentrations for the E. coli enzyme was 8.2 to 8.4 (Sanwal and Smando, 1969), that from rabbit heart mitochondria was 7.0 to 8.0 (Lin and Davis, 1974), and that from etiolated maize leaves and coleoptiles was 6.8 to 7.1 (Pupillo and Bossi, 1979). These data may not represent in vivo pH optima however, as pH optima can vary as substrate levels vary (Davies, 1973). The pH optima for enzymic activity isolated from Solanum tubers (Davies and Patil, 1974) and pigeon liver (Rutter and Lardy, 1958) decrease from approximately 8.0 to 7.0 as malate levels decrease 10-fold in the former tissue and 500-fold in the latter.

Data reported for the effects of pH on the various Michaelis constants are limited. Davies et al. (1974) using a variety of plant species were unable to demonstrate a consistent effect on the  $K_m(\text{malate})$  when the pH was increased from 7.0 to 7.6. The  $K_m(\text{malate})$  of the maize enzyme increased approximately ten-fold as the pH was raised from 6.4 to 8.4 (Pupillo and Bossi, 1979). However, with  $\text{Mg}^{2+}$  as cofactor rather than  $\text{Mn}^{2+}$ , the binding affinity for malate decreased by half over the same pH range. The  $K_m(\text{NADP}^+)$  was maximal at pH 7.4 and decreased by 50% at pH 6.9 or 8.4 (Pupillo and Bossi, 1979). Schimerlik



and Cleland (1977b) observed that increases in pH resulted in increases in the  $K_m$  for  $Mn^{2+}$  or  $Mg^{2+}$  for the pigeon liver enzyme.

Inhibition of enzyme activity by high levels of malate was demonstrated in the pigeon liver enzyme (Rutter and Lardy, 1958), some species of the Graminae when assayed with  $Mn^{2+}$  but not with  $Mg^{2+}$  (Davies et al., 1974) and the maize enzyme (Pupillo and Bossi, 1979). In addition, increases in pH above neutrality released the enzyme from substrate inhibition (Rutter and Lardy, 1958; Pupillo and Bossi, 1979). All other studies did not demonstrate substrate inhibition. Furthermore, recent studies of the pigeon liver enzyme demonstrate that 500-fold increases of malate over saturation do not induce substrate inhibition at an assay pH of 7.2 (Schimerlik and Cleland, 1977a). The authors suggest that substrate inhibition is partly an artifact and that under 'properly controlled' conditions of ionic strength and concentrations this phenomenon is eliminated. Unfortunately, a systematic study of the effects of various buffer systems on enzymic activity has not been reported and the validity of the previous statement is limited.

Evidence indicates that malic enzyme isolated from some tissues, and under some conditions of assay, has properties consistent with an allosteric nature. Studies on enzymes isolated from E. coli (Sanwal and Smando, 1969), pigeon liver (Hsu, Mildwan, Chang and Fung, 1976) and etiolated maize leaves and coleotiles (Pupillo and Bossi, 1979) and subjected to

various chromatographic and electrophoretic techniques indicate a tetrameric protein with a molecular weight of 300 to 350 kDaltons. However, with only two exceptions, Michaelis-Menten type (hyperbolic) kinetics were observed for all reported enzyme activities. Previous discussions indicate that the pigeon liver enzyme is affected by  $Mn^{2+}$  in a non-linear fashion (Schimerlik et al., 1977). Binding studies of the pigeon liver enzyme indicate that  $Mn^{2+}$  binds tightly on two of the subunits and weakly on the remaining two (Hsu et al., 1976); whereas  $Mg^{2+}$  binds equally to all four monomers (Schimerlik and Cleland, 1977b).

Various carboxylic acids have been tested as potential effectors of malic enzyme activity. Succinate had no effect on the  $K_m$  (malate) for enzyme isolated from five species of the Graminae at pH 7.0 or 7.6 (Davies, et al., 1974). Enzyme from Solanum tubers was activated approximately two-fold by succinate (1.0 to 7.0 mM) assayed at pH 7.0 and an unspecified malate concentration (Davies, 1973). The author also reports activation by fumarate and oxoglutarate (1.5 to 2.0-fold) and 80% inhibition by 2.5 mM citrate without specifying malate concentrations (Davies, 1973). In a succeeding report, the Solanum enzyme assayed at pH 7.6 with a malate concentration 10% of saturation was activated maximally by 2.0 to 4.0 mM oxaloacetate, fumarate, L(+)-tartrate, 2-oxoglutarate and phosphoenolpyruvate (Davies and Patil, 1974). At concentrations greater than 2.0 mM OAA became slightly inhibitory. Davies and

Patil (1974) suggest that in general dicarboxylic acids activate the enzyme maximally at high pH and eliminate the sigmoidicity of the velocity versus malate concentration plots. The value of this generalization is limited as data is reported for only one concentration of succinate assayed at pH 7.6 alone. Schimerlik and Cleland (1977a) demonstrated that the pigeon liver enzyme assayed at pH 7.2 was competitively inhibited by succinate, fumarate, oxaloacetate and a number of malate analogues. Additionally, their results indicate that 3-C acids (mesotartrate, L-tartrate, D-tartrate and hydroxymalonate) are stronger inhibitors than the previously cited 4-C acids. Enzyme isolated from rabbit heart mitochondria was not affected by succinate or fumarate (Lin and Davis, 1974) and the E. coli enzyme was inhibited by acetyl CoA and oxaloacetate at pH 7.2 (Sanwal and Smando, 1969). The E. coli enzyme was suggested to have different binding sites for effectors, since at pH 8.5 acetyl CoA inhibition was eliminated whereas OAA was still a strong inhibitor (Sanwal and Smando, 1969).

The amino acid glycine activated the E. coli enzyme although there was wide quantitative variation from experiment to experiment (Sanwal and Smando, 1969). Assayed at pH 7.0 and an unspecified malate concentration, 6 mM aspartate inhibited the Solanum tuber enzyme 15% whereas 6 mM glutamate had no effect (Davies, 1973).

The sugar phosphates (3.0 mM), 2-phosphoglycerate, 3-phosphoglycerate and 2,3-diphosphoglycerate inhibited the

Solanum enzyme from 75 to 100% at pH 7.0 and a malate concentration giving approximately 20% of saturation (Davies and Patil, 1974). The addition of succinate to these assays decreased these effects by a maximum of 30%. Fructose-1,6-diphosphate inhibited the same assays 5 to 10% (Davies and Patil, 1974).

Various inorganic ions affect the rates of malate decarboxylation. Sanwal and Smando (1969) demonstrated that the E. coli enzyme is activated by ammonia, which increased  $V_{\max}$  and decreased the  $K_m(\text{malate})$ . They also observed a mixed-type activation by potassium ions. Rutter and Lardy (1958) demonstrated that the pigeon liver enzyme was not significantly affected by either potassium or sodium salts. Phosphate and sulphate inhibited malic enzyme activity isolated from Solanum tubers by increasing the  $K_m(\text{malate})$  1.5-fold (Davies and Patil 1974). No details of the corresponding cation were reported, again limiting the value of their results. Potassium salts of bromide, sulphate, chloride (Schimerlik and Cleland, 1977a) and copper, arsenite and iodoacetate (Rutter et al., 1959) were weak competitive inhibitors of pigeon liver enzyme. Strong competitive inhibition of the same enzyme was observed with potassium salts of nitrate, iodide, cyanide (Schimerlik et al., 1977a), mercury, p-mercuribenzoate, and o-iodosobenzoate (Rutter et al., 1958). Rutter et al. (1958) suggest that these effects may reflect the importance of chelation of metal cations in inhibition phenomena. The more recent studies by Schimerlik

and Cleland (1977a) led these authors to conclude that the strong inhibition by some inorganic anions reflects binding to a positively charged active site group. They suggest this is the group which binds the 1C carboxyl of malate and other negatively charged organics.

Evidence indicates that the effects of some regulators of malate decarboxylation can be diminished by the addition of other reagents. Davies and Patil (1974) observed that addition of phosphate at pH 7.6 had little effect on the Hill number of one obtained from activity in the absence of phosphate. With both phosphate and succinate in the assay, the Hill number was decreased from two to one. The Hill number in the presence of succinate alone was not reported; however, the data indicates that it is closer to one than two. The authors state that the inhibition produced by phosphate is partially reversed by succinate addition. Sanwal and Smando (1969) observed that glycine activation of the E. coli enzyme reduces the inhibitory effects of OAA and acetyl CoA at all pH values tested. They suggest that glycine desensitizes the enzyme to these effectors by dissociating the allosteric and catalytic subunits of the protein.

### (3) Concluding statement

The reports available indicate close similarities in substrate, coenzyme, and cofactor regulation of malic enzyme activity isolated from plants, animals and microorganisms.

However, discrepancies regarding the regulatory properties of the enzyme from species to species are documented. Different extraction and assay techniques and conditions may contribute towards such variation, as each research group employed different procedures. Conversely, these reported variations may reflect inherent properties of individual species. A potential pitfall in the literature is that in all reports data was obtained from the spectrophotometric change in absorbance of  $\text{NADP}^+$  reduction (or NADPH oxidation) at 340 nm. The dependence on one assay procedure for measuring enzyme activity could limit the value of the results.

Before conclusive evidence for pH-dependent activity in the presence and absence of effectors can be obtained, the possible influence of buffer species, and ionic strength and concentration should be investigated. In addition, product analysis should be employed to check that malic enzyme activity in the presence of various metabolites does not result from an artifact of the assay system.

### C. Intracellular location and environment

Danner and Ting (1967) investigated the distribution of enzymes involved in non-autotrophic  $\text{CO}_2$  fixation in Zea mays roots. They initiated their work with the assumption that these enzymes were PEPC, MDH and the malic enzyme (Ting and Dugger, 1966). Root tissue was fractionated into soluble and particulate

fractions, and each was investigated for PEPC, MDH and malic enzyme activities. Data indicated all three enzymes were in the soluble fraction, although an alloenzyme of MDH was also found in the particulate fraction. Furthermore, in vitro PEPC activity was sufficient to account for the CO<sub>2</sub> uptake by corn roots in vivo, although other potential carboxylating enzymes may also be present. The properties of the malic enzyme catalysed reaction indicate that it functions in decarboxylation and soluble MDH links PEPC and the malic enzyme via reduction of OAA to malate (Danner and Ting, 1967).

Higher plant cell cytosol pH measurements have been hampered due to the technical difficulties associated with vacuolate microscopic walled cells (Smith and Raven, 1979). However, cytosol pH of large algal cells measured with either glass microelectrodes or distribution patterns of the weak acid 5,5-dimethyloxazolidine-2,4-dione (DMO), and cultured Acer (maple) cells measured with the DMO technique has been estimated to be between pH 7.0 and 7.5 (Spanswick and Miller, 1977; Kurkdjian and Guern, 1978).

Determination of substrate concentrations for PEPC and the malic enzyme in plant tissues have not been reported. However, various rat tissues have been analyzed for metabolite, cofactor and divalent metal ion concentrations. Bergmeyer (1963) has reviewed much of this data. The following figures refer to rat tissues excluding the atypical liver data (e.g., heart, brain, muscle, kidney). The glycolytic intermediates, PEP and pyruvate

are present from 0.02 to 0.10  $\mu\text{mole}\cdot\text{gram fresh weight}^{-1}$ . TCA cycle intermediates excluding OAA range from 0.1 to 0.5  $\mu\text{mole}\cdot\text{gram fresh weight}^{-1}$  (OAA ranges from 0.005 to 0.01  $\mu\text{mole}\cdot\text{gram fresh weight}^{-1}$ ). Aspartate and glutamate concentrations vary from 1.0 to 4.0  $\mu\text{mole}\cdot\text{gram fresh weight}^{-1}$ .  $\text{Mg}^{2+}$  concentrations of 5 to 8 mM are present in most mammalian tissues; whereas the  $\text{Mn}^{2+}$  concentration is maintained around 10  $\mu\text{M}$  (Metzler, 1977). The ratio of cytosolic  $[\text{NAD}^+]/[\text{NADH}]$  and  $[\text{NADP}^+]/[\text{NADPH}]$  in rat liver tissue has been indicated as 700 and 0.01 respectively (Newsholme and Start, 1973). These concentrations and cytosolic pH values indicate that in vivo PEPC and malic enzyme activities are operating at sub-optimal substrate and pH levels. Consequently, small changes in these parameters could have large effects on enzymic activity. Similarly, feedback and allosteric regulation of the enzymes would be important in regulating activity.

## II. Pathways of carboxylation and decarboxylation

Feeding of  $[\text{}^{14}\text{C}]$ -bicarbonate to non-autotrophic plant tissues has been a useful technique in elucidating the pathway of dark  $\text{CO}_2$  fixation. The primary labelled products are malate, citrate, aspartate and glutamate (Splittstoesser, 1966; Howe, 1969; Bown and Lampman, 1971). Nesius and Fletcher (1975) investigated  $[\text{}^{14}\text{C}]\text{-HCO}_3^-$  incorporation in five and eleven day old cultures of Paul's Scarlet Rose. In the eleven day old cells, 80% of the label was found in the organic acid fraction,



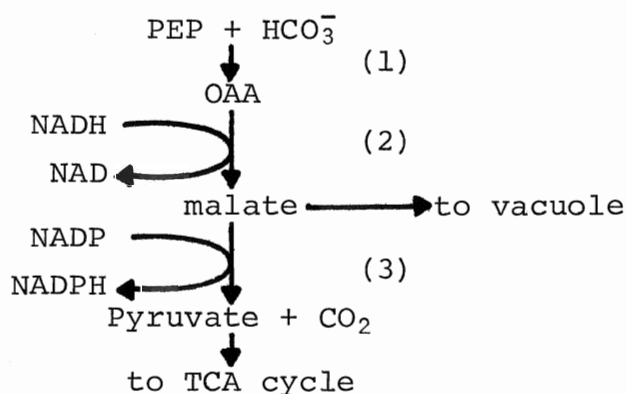
whereas 55% of the label was incorporated into the organic acids of the younger cultures. The remainder of the label was found in the protein fraction. The younger tissue is involved in cell division, whereas the older culture is primarily involved in expansion growth and vacuolar enlargement. This suggests that OAA synthesized by PEPC is mainly utilized for biosynthesis in the five day old cultures, and for vacuolar storage as malate in the older vacuolated tissue.

A number of investigators have attempted to explain the seemingly metabolically inert pool of malate formed from non-autotrophic  $\text{CO}_2$  fixation. Lips and Beevers (1966) tested the hypothesis that two or more malate pools are present in corn roots. They incubated the tissue in the presence of  $[^{14}\text{C}]\text{-HCO}_3^-$  and  $[^3\text{H}]\text{-CH}_3\text{COO}^-$  and, after short chases with unlabelled substrates found that the  $[^{14}\text{C}]\text{-malate}$  pool was subject to very little turnover, whereas the  $[^3\text{H}]\text{-malate}$  was actively metabolized and diminished rapidly. The investigators suggested the presence of at least two physically separate pools of labelled malate; mitochondrially formed from labelled acetate, and cytoplasmic and/or vacuolar from labelled bicarbonate. The former would result from reactions of the TCA cycle, while the latter results from non-autotrophic  $\text{CO}_2$  fixation. Conversely, similarly labelled organic acids such as citrate, succinate, aspartate and glutamate lost  $^3\text{H}$  and  $^{14}\text{C}$  labels at the same rate, indicating that the two labelled forms were part of the same metabolic pool. Jacoby and Laties

(1971) obtained evidence that the extramitochondrial malate pool may be vacuolar by observing that non-vacuolate barley root tips actively metabolized malate labelled from  $[^{14}\text{C}]\text{-HCO}_3^-$ , whereas older vacuolated root sections exhibited very little loss of label from malate.

In conclusion, it appears that non-vacuolate cells actively metabolize malate produced from non-autotrophic  $\text{CO}_2$  fixation, whereas more mature vacuolate cells accumulate this malate. This indicates that malate synthesis and subsequent accumulation takes place in the cytoplasm and vacuole respectively.

Radioactivity in pyruvate was not detected when 3- $[^{14}\text{C}]\text{-malate}$  was incubated with corn root tissue (Lips and Beevers, 1966). The results indicate that pyruvate produced from malate by way of the malic enzyme is actively metabolized. Osmond (1976) has suggested this process to be via the TCA cycle, and has proposed the following sequence of reactions.



Enzymes: (1) PEP carboxylase  
 (2) Malate dehydrogenase  
 (3) Malic enzyme

This scheme would necessarily require sophisticated control mechanisms for regulating the flux of malate to storage compartments or to further metabolism. Very little information is available regarding the in vivo regulation and compartmentation of the pathway(s) of carboxylation, and even less is known about decarboxylation. Data on the relative activities of tonoplast and mitochondrial membrane malate transport systems, the ratio of in vivo PEPC and malic enzyme activities, and the fate(s) of pyruvate produced by the malic enzyme are not documented, but would undoubtedly increase our understanding of the carboxylation and decarboxylation processes.

### III. Metabolic and physiological roles of PEP carboxylase and the malic enzyme

PEPC and the malic enzyme have been implicated in the maintenance of intracellular pH, osmoregulation, and the regulation of the level of TCA cycle intermediates. This section examines the literature pertinent to these roles.

#### A. Anaplerotic fluxes and removal of TCA cycle intermediates

Anaplerotic mechanisms refer to reactions which serve to build up compounds which have been depleted in specific metabolic pathways. Of relevance to the PEPC reaction is the removal of TCA cycle acids for synthesis of amino acids and other molecules. In the absence of mechanisms to replenish TCA cycle intermediates the level of OAA to accept acetyl groups would

fall, and the rate of the cycle would decrease. Malate transported into the mitochondrion would generate OAA.

Avena coleoptiles (Bown and Aung, 1974; Bown, Dymock and Aung, 1974) and maize roots (Spittstoesser, 1966) increase their rates of [ $^{14}\text{C}$ ]-leucine incorporation into protein as  $\text{CO}_2$  concentrations in the media are increased to air levels (0.03%). The data indicate that non-autotrophic  $\text{CO}_2$  fixation is involved in the biosynthesis of growing tissue, presumably via PEPC catalyzed malate formation and subsequent oxidation through the TCA cycle.

Vacuolated maize root segments can be induced to increase the rate of malate metabolism (derived from [ $^{14}\text{C}$ ]- $\text{HCO}_3^-$ , or exogenously added 3-[ $^{14}\text{C}$ ]-malate) by treating the tissue with malonate, a specific inhibitor of succinate dehydrogenase (Lips and Beevers, 1966). The authors suggest that extramitochondrial malate could replenish acetyl acceptor concentration by entering the mitochondria and undergoing oxidation to OAA.

In mammalian tissue the malic enzyme produces pyruvate and reducing equivalents which are utilized in cytoplasmic biosynthetic reactions (e.g., gluconeogenesis and fatty acid synthesis). Lee and Davis (1979) demonstrated that perfused rat skeletal muscle produced 3-carbon skeletons (pyruvate/alanine) from 4-carbon TCA cycle intermediates, presumably by decarboxylation involving the malic enzyme. Furthermore,  $^{14}\text{C}$  from [ $^{14}\text{C}$ ]- $\text{HCO}_3^-$  fluxed through malate, TCA cycle intermediates and lastly 3-carbon products. Their results indicate that  $\text{CO}_2$

is continuously fixed into carboxylates, which are continuously decarboxylated in the form of malate to pyruvate. Evidence for a similar role for plant malic enzyme is not available, however it should not be disregarded as a possibility.

#### B. Osmoregulation

Cell growth requires pressure (turgor) exerted on the cell wall. Turgor pressure results from the water potential of the cell which is lower than that of the surrounding dilute medium. Consequently water tends to enter the cell and increase the turgor. The wall yields to turgor pressure when it is made extensible by hormone action. Continued extension and water uptake will ultimately result in decreased turgor pressures unless osmotically active substances are also accumulated to maintain turgor and extension growth. When cellular water potential increases in growing tissue, various mechanisms could be activated to increase solute concentrations. Synthesis of potassium malate and its removal to an isolated extra-mitochondrial pool (e.g., vacuole) may function in this respect. Indeed, many higher plant species have as their major osmotica potassium and organic acids (Cram, 1976).

Elongation growth of cotton ovule fibres was observed to be dependent on the fibre turgor pressure (Dhindsa, Beasley and Ting, 1975). Decreases in turgor, by treatment with Carbowax 6000 inhibited growth. Increases in turgor pressure were correlated with increases in growth, and potassium and

malate accumulation. Malate accumulation was indicated through the ability of cotton ovules to fix  $[^{14}\text{C}]\text{-HCO}_3^-$ . Maximal malate and potassium accumulation occurred when the growth rate was highest. Furthermore, the authors indicate that these concentrations of malate and potassium can account for over 50% of the osmotic potential of the fibre cells. They suggest that potassium and malate act as osmoregulatory agents and that the malate accumulated is derived from non-autotrophic  $\text{CO}_2$  fixation.

In giant algal cells, where turgor dependent processes have been most actively studied, turgor appears to control membrane transport processes and the electrical properties of the membrane (for review see Zimmerman, 1978). Changes in turgor instantaneously effect changes in the membrane potential difference of Chara corallina cells (Zimmerman and Beckers, 1978). Cram (1978) suggests that cation influx and synthesis of organic anions are immediately affected by changes in the potential difference, although detectable increases in influx and synthesis show variable lag periods depending on the tissue studied. The trigger for increased malate synthesis is not understood. Osmond (1976) suggests that malate synthesis may be regulated by membrane  $\text{K}^+/\text{H}^+$  which would activate PEPC by increasing the cytosolic pH and provide  $\text{K}^+$  as a counter ion for synthesized malate, and/or the release of feedback inhibition of malate on PEPC as potassium malate is transported to the vacuole.

Evidence for a role of the malic enzyme in osmoregulatory processes is lacking. However, in Avena coleoptiles  $\text{Cl}^-$  uptake has been correlated with increased growth (Rubinstein and Light, 1973). Chloride loading of some tissues appears to decrease the influx of malate to the vacuole (Cram, 1974).

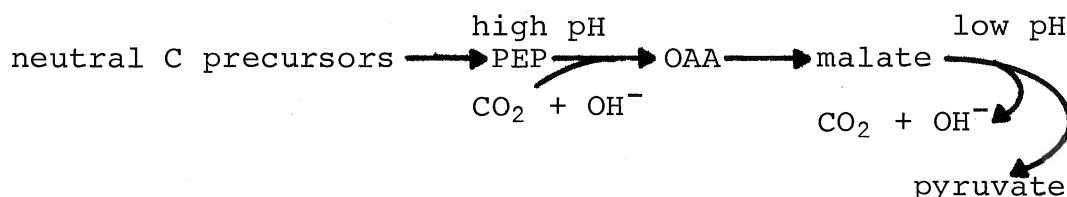
It is possible that during periods of high cytosolic water potential, KCl competes with potassium malate for transport into the vacuole, in effect increasing the substrate available for the malic enzyme. Thus an increase in non-autotrophic  $\text{CO}_2$  fixation correlated with high rates of  $\text{K}^+/\text{H}^+$  exchange and  $\text{Cl}^-$  uptake might lead to increased malic enzyme activity.

### C. Intracellular pH maintenance

There is much evidence available indicating that cytoplasmic pH in higher and lower plant cells remains relatively constant (for review see Smith and Raven, 1979). Acid-base balance can be regulated by the buffering materials present in the cytoplasm. These include weak acids or bases with  $\text{pK}_a$  values between pH 6.0 and 8.0 (bicarbonate, phosphate compounds, histidine imidazolyl group, cysteine -SH group, and the cysteine amino group). Raven and Smith (1976) calculated the theoretical cytoplasmic buffering capacity from these  $\text{pK}_a$  values and determined it to be at most  $20 \text{ mmol H}^+ \cdot \text{litre}^{-1}$  when the pH is between 6.0 and 8.0. It is suggested that buffers existing in the cytoplasm cannot effectively counter pH fluctuations, since the buffers themselves are derived from reactions which generate

or consume  $H^+$  (Smith and Raven, 1979).

Hiatt (1966) suggested that cytoplasmic pH may control rates of carboxylation by affecting carboxylase activities. Davies (1973) developed this suggestion in his pH-stat hypothesis. He suggested that the maintenance of cytoplasmic pH may be controlled by the number of 'acidic carboxyl groups' present. Carboxylation, activated by high pH would generate  $H^+$  (or consume  $OH^-$ ) resulting in a decrease of the cytoplasmic pH. Conversely, low pH would activate decarboxylation which would tend to raise the cytoplasmic pH. To function as a pH-stat, the pH optimum of the carboxylase should be higher than cytoplasmic pH, and the decarboxylase should have a pH optimum less than the cytoplasmic pH. PEPC and the malic enzyme appear suited for roles in the hypothetical pH-stat (Davies, 1973).



PEPC activity from different tissues has a pH optimum of approximately 8.0 (Kluge and Osmond, 1972); the cytoplasmic pH of plant cells has been indicated to be between 7.0 and 7.5 (Spanswick and Miller, 1977); and the pH optimum of the malic enzyme from some tissues is approximately 7.0 (Davies and Patil, 1974). A rise in cytoplasmic pH due to biochemical and/or biophysical events which remove  $H^+$  would increase PEPC activity



and increased production of carboxyl groups which would lower cytoplasmic pH. PEPC activity may also be inhibited by the increased malate concentration as well as the increased  $H^+$  concentrations.

The evidence in favour of PEPC and malic enzyme involvement in this pH-stat mechanism includes in vitro observations concerning optimal pH values, and the effects of pH on the  $K_m$ (substrate) for both enzymes and the  $K_i$ (malate) for PEPC (Pupillo and Bossi, 1979; Smith et al., 1979). In vivo evidence results from observations that malate is accumulated in tissues which are excreting  $H^+$  (Haschke and Lüttge, 1975, 1977). In vivo evidence for the involvement of the malic enzyme in the pH-stat is lacking, although malate and pyruvate accumulation during  $H^+$  excretion may provide indirect evidence against malic enzyme involvement (Caldogno et al., 1978).

Osmond (1976) and Smith and Raven (1979) suggest the malic enzyme cannot regulate fluctuations in cytoplasmic pH over the life span of a cell. They indicate that whereas carboxylation may be important in countering a high intracellular pH, decarboxylation cannot counter a low pH since the malate required for decarboxylation arises from previous synthesis of malate which is itself accompanied by  $H^+$  production. Smith and Raven (1979) further suggest that carboxylate synthesis and degradation should be considered in conjunction with the membrane transport of ions. Consequently, they proposed a model of cytoplasmic pH regulation which involves the concurrent

functioning of a biochemical and biophysical pH-stat. In contrast, short term maintenance of cytoplasmic pH may be regulated by the biochemical pH-stat alone (Smith and Raven, 1979).

#### D. Concluding Statement

The evidence available for the involvement of PEPC in various metabolic roles is well documented. Conversely, the suggested role for the malic enzyme in a pH-stat is controversial, and the metabolic role of the malic enzyme is not clear. The study conducted by Lee and Davis (1979) indicates that carboxylation reactions continuously replete TCA cycle intermediates, and that excessive buildup of 4-C intermediates is by decarboxylation reactions. The authors conclude that this would result in fine control of the steady-state level of cycle intermediates. The in vivo regulation of carboxylation and decarboxylation reactions in plant cells is poorly documented. This is compounded by the lack of information regarding malate transport mechanisms across the mitochondrial membrane and the tonoplast, relative activities of PEPC and the malic enzyme, the ratio of cytoplasmic  $\text{NADP}^+/\text{NADPH}$  and the mechanisms for maintaining this ratio, and the ultimate fate(s) of pyruvate produced from malate decarboxylation.

#### IV. Hormone stimulated growth and its relationship to PEP carboxylase and malic enzyme activities

The acid growth hypothesis states that plant cells excrete  $H^+$  into the cell wall region where they induce cell wall loosening and ultimately cell wall elongation. Thimann and Schneider (1938) observed increasingly enhanced growth rates of Avena coleoptiles as the pH of the bathing medium was decreased. Indoleacetic acid (IAA) and fusicoccin (FC) cause stem and coleoptile  $H^+$  excretion and elongation (Cleland, 1973, 1976).

IAA is a natural plant growth hormone of the auxin class. Studies by Went (1928) indicate that it is synthesized in the 3 mm apical section of the coleoptile and transported downwards. FC is a diterpene glucoside, bearing no structural similarity to auxins, which is derived from the fungus Fusicoccum amygdali. It is a higher plant toxin which initiates wilting in crop plants. However, in concentrations equivalent to those which promote growth by IAA (10  $\mu M$ ), it exhibits biological properties similar to the natural hormone (for review see Marré, 1979). Consequently, it has recently been employed as a tool in attempts to determine the mechanism(s) of IAA stimulated growth.

IAA and FC stimulated growth has been correlated with increased rates of  $H^+$  efflux,  $K^+$  influx, non-autotrophic  $CO_2$  fixation and malate accumulation, (Haschke and Lüttge, 1977, Stout et al., 1978; Beffagna, Coccuci and Marré, 1977).

Attempts to demonstrate the interrelationships of these effects have been complicated by technical differences from one laboratory to the next, however, time lags of the onset of these events after hormone application may indicate their relationship. IAA (and FC) treated coleoptile segments show increased growth rates in 15-18 minutes (within two minutes) (Rayle, 1973; Cleland, 1973; 1976) , net  $H^+$  efflux in 15-20 minutes (within one minute) (Cleland, 1973; 1976),  $K^+$  influx in 15-20 minutes (within one minute) (Stout et al., 1978) and net accumulation of  $[^{14}C]-HCO_3^-$  in malate at 45 to 60 minutes (within 30 minutes) (Stout et al., 1978). IAA or FC stimulated cation uptake is specific for  $K^+$ , whereas it has been suggested that hormone induced malate accumulation works equally well with  $K^+$  or  $Na^+$  (Stout et al., 1978). In addition, FC treated pea internode segments show an enhanced rate of pyruvate accumulation and an increase of the cytoplasmic NADPH/NADP $^+$  ratio (Caldogno et al., 1978).

Non-autotrophic  $CO_2$  fixation and malate accumulation is presumably due to PEPC activity. The time lags previously cited indicate that auxin enhanced  $CO_2$  fixation is a secondary effect of  $H^+$  excretion and elongation growth. This is consistent with the observations that in vitro PEPC activity from Avena coleoptiles is not effected by IAA (Bown, Dymock and Hill, 1976) or FC (Stout and Cleland, 1978; Smith et al., 1979). Haschke and Lüttge (1977) suggest that auxin stimulated non-autotrophic  $CO_2$  fixation is a result of auxin induced  $H^+$  efflux

causing an increase in cytoplasmic pH values and pH dependent PEPC activity. Increased pyruvate and cytosolic NADPH production may result from malic enzyme activity (Marré, 1979). Thus hormone stimulated  $H^+$  efflux and elongation growth could promote the attainment of a higher, steady state level of PEPC and malic enzyme activities.

## Materials and Methods

### Materials

#### I. Biological materials

seeds of Avena sativa

variety: Victory

Supplier

Ward's Natural Science

Establishment,

Rochester, New York

#### II. General materials

dialysis tubing, 1.0 cm diameter

column, 30 x 0.9 cm diameter

vermiculite, industrial grade no. 4

Ball-Superior Limited,

Mississauga, Ontario.

#### III. Chemical materials

Except for those listed, all chemicals were purchased from British Drug Houses Canada Ltd., Toronto, Ontario, or from Fisher Scientific Company, Fair Lawn, New Jersey, and were of analytical grade.

A. Carboxylic and amino acids, sugar phosphates and coenzymes

Supplier

D,L-aspartic acid

Eastman Organic Chemicals,

L-malic acid

Rochester, New York

phenylsuccinic acid

Aldrich Chemical Co., Inc.,

Milwaukee, Wisconsin.

The following chemicals were purchased from the Sigma Chemical Company, St. Louis, Montana.

D-fructose-1-phosphate, sodium salt	(F-1-P)
D-fructose-6-phosphate, disodium salt	(F-6-P)
D-fructose-1,6-diphosphate, trisodium salt	(F-1,6-diP)
$\alpha$ -D-glucose-1-phosphate, disodium salt	(G-1-P)
D-glucose-6-phosphate, disodium salt	(G-6-P)
L-histidine $\cdot$ HCl, monohydrate	(his)
L-leucine	(leu)
$\beta$ -nicotinamide adenine dinucleotide, reduced, disodium salt	(NADH)
$\beta$ -nicotinamide adenine dinucleotide phosphate, monosodium salt	(NADP <sup>+</sup> )
$\beta$ -nicotinamide adenine dinucleotide phosphate, reduced, tetrasodium salt	(NADPH)
cis-oxaloacetic acid	(OAA)
phospho(enol)pyruvate, tricyclohexylamine salt	(PEP)
D(-)3-phosphoglyceric acid, disodium salt	(3-PGA)
pyruvic acid, sodium salt	

#### B. Buffer materials

N,N-bis[2-hydroxyethyl]-2-aminoethane sulfonic acid (BES)

Sigma Chemical Co.

hydroxymethylaminomethane (Tris)

Calbiochem,

San Diego, California

## C. Chromatographic materials

Brom cresol green spray	Sigma Chemical Co.
phenol, liquefied (analytical reagent)	
	Mallinckrodt Chemical Works
Sephadex G-25 (coarse grade)	Pharmacia Fine Chemicals, Uppsala, Sweden
Silica Gel G	Analabs Inc., North Haven, Connecticut
Thin Layer Chromomedia CC41	W. and R. Balston Ltd., England.

## D. Radiochemical assay and autoradiographic materials

2,4-dinitrophenylhydrazine	Sigma Chemical Co.
2,5-diphenyloxazole (PPO)	Amersham/Searle Co., Arlington Heights, Is.
ethanolamine (scintillation grade)	Packard Instrument Co., Inc., Is.
[ <sup>14</sup> C]-hexadecane	Amersham/Searle Co.
Kodak Dektol Developer	Eastman Kodak Co., Rochester, New York
Kodak Medical X-ray Film	Amersham/Searle Co.
U-[ <sup>14</sup> C]-malic acid	Amersham/Searle Co.
I-[ <sup>14</sup> C]-phosphoenolpyruvate (cyclohexylammonium salt)	Amersham/Searle Co.
1,4-bis-[2-(5-phenyloxazole)]benzene (POPOP)	Amersham Searle Co.
[ <sup>14</sup> C]-sodium hydrogen carbonate	Amersham/Searle Co.
Toluene (scintillation grade)	J. T. Baker Chemical Co., Phillipsburg, New Jersey.



#### IV. Reagents

##### A. Enzyme assay reagents

###### (1) Metabolites

The following chemicals were dissolved in the assay buffer utilized to the indicated concentrations and used for PEPC or malic enzyme assays:

1.5 mM NADH, 15.0 mM NADP<sup>+</sup>, 15.0 mM PEP, 400 mM pyruvate

1.5 mM NADPH

L-Malic acid and OAA were dissolved in distilled water, neutralized with 0.1 N NaOH and made up to 15.0 mM or 50 mM respectively. OAA was used within 30 minutes of its preparation. All other acidic metabolites used in the assays were dissolved in distilled water, neutralized with 0.1 N NaOH and made up to 50 mM with distilled water.

###### (2) Buffers

BES or histidine·HCl was dissolved in distilled water and made up to 50 mM, then titrated to the required pH with 0.1 N KOH or NaOH. Tris was dissolved in distilled water and made up to 50 mM, and titrated to the desired pH with 0.1 N HCl.

20 mM potassium phosphate buffers were prepared by dissolving K<sub>2</sub>HPO<sub>4</sub> or KH<sub>2</sub>PO<sub>4</sub> in distilled water to 20 mM.

K<sub>2</sub>HPO<sub>4</sub> was titrated to the desired pH with KH<sub>2</sub>PO<sub>4</sub>.

250 mM Tris-BES buffers were prepared by dissolving Tris or BES in distilled water to 250 mM. BES was titrated with Tris to the desired pH. All buffers were prepared at 25°C.

## B. Radiochemical and scintillation fluids

$[^{14}\text{C}]\text{-NaHCO}_3$  ( $5 \times 10^3 \mu\text{Ci}$   $60 \mu\text{Ci} \cdot \mu\text{mole}^{-1}$ ) was diluted in distilled water containing dissolved  $[^{12}\text{C}]\text{-NaHCO}_3$  and made up to a specific activity of  $10 \mu\text{Ci} \cdot \mu\text{mole}^{-1}$ .

$1\text{-}[^{14}\text{C}]\text{-PEP}$  ( $50 \mu\text{Ci}$ ;  $13.1 \mu\text{Ci} \cdot \mu\text{mole}^{-1}$ ) was dissolved in 20 mM potassium phosphate buffer pH 7.4 and made up to a specific activity of  $2.0 \mu\text{Ci} \cdot \mu\text{mole}^{-1}$ .

$\text{U-}[^{14}\text{C}]\text{-malate}$  ( $50 \mu\text{Ci}$ ;  $55 \mu\text{Ci} \cdot \mu\text{mole}^{-1}$ ) was dissolved in distilled water made up to a specific activity of  $0.7 \mu\text{Ci} \cdot \mu\text{mole}^{-1}$  and neutralized with 0.1 N NaOH.

Scintillation Fluid I was prepared by dissolving 5.0 g PPO and 0.3 g POPOP in toluene and made up to one litre with toluene. Scintillation Fluid II was prepared by adding 100 ml methanol to one litre of Scintillation Fluid I.

## C. Lowry reagents

Two percent sodium carbonate was dissolved in and made up to one litre with 0.1 N NaOH (Solution A). 0.5% Cupric sulphate was dissolved in and made up to one litre with distilled water containing 1.0 g potassium tartrate (Solution B). The Alkaline Copper Reagent was prepared by mixing 50 ml Solution A and 1.0 ml Solution B immediately before using in protein determinations.

## Methods

### I. Source and extraction of enzymes

#### A. Coleoptile tissue

Seeds of Avena sativa were husked and stirred in distilled water for four hours prior to planting, embryos upwards, on a layer of Kimwipe tissue covering a vermiculite/distilled water mixture in a 1:1 ratio (v:v). The seeds were placed under a weak red light in humid conditions at 27°C for 66 to 72 hours.

#### B. Preparation of enzyme extract

Two different buffer species were used to extract PEPC or the malic enzyme. The procedure describes buffers employed to extract PEP carboxylase activity. Those buffers used in the extraction of the malic enzyme are indicated by closed brackets. Deviations from these buffer systems are noted in the Results section.

Coleoptile tissue (25-32 mm in length) was harvested by removing the primary leaf. The tissue was placed in a pre-weighed beaker containing cold (0-4°C) 1 mM potassium phosphate buffer pH 7.4 (5 mM Tris-BES buffer pH 7.4) and the weight of the tissue determined (approximately 4.0 g). All further operations were carried out in the cold (0-4°C) using glassware rinsed with 10 mM EDTA. The tissue was combined in a 1:6 ratio (w:v) with 1 mM potassium phosphate buffer pH 7.4 (5 mM Tris-BES pH 7.4) and ground with a mortar and pestle. The slurry was transferred to a Potter-Elvehjem vessel and homogenized for 45 to 60

seconds (three passes of the pestle through the slurry). The homogenate was strained through two layers of cheese cloth and centrifuged in an I.E.C. B-20 refrigerated centrifuge for five minutes at 500 g. The supernatant fluid was retained and its volume determined (12-15 ml). Ammonium sulphate was stirred in gently to bring the solution to 75% saturation (0.519 g  $(\text{NH}_4)_2\text{SO}_4$ /ml supernatant). This was allowed to sit for 15 minutes and then centrifuged for 15 minutes at 15,000 g. The pellet was retained and dissolved in 1-2 ml 20 mM potassium phosphate buffer pH 7.4 (250 mM Tris-BES buffer pH 7.4). The yellow protein solution was filtered on a column of G-25 Sephadex gel (Methods I, C), collected in the void volume and centrifuged for 15 minutes at 15,000 g. The supernatant fluid was retained, its volume determined (5-8 ml) and used for enzyme assays the same day.

In some initial experiments, the protein precipitated by ammonium sulphate was dissolved in 5-8 ml 20 mM potassium phosphate buffer pH 7.4 and dialyzed for 2 h against two changes of one litre volumes of the same buffer. After centrifugation for 15 minutes at 15,000 g, the volume of the supernatant fluid was determined (7-10 ml), and then used in PEP carboxylase assays the same day.

(C) Preparation of column for gel filtration of protein extract

Approximately 10 g of Sephadex G-25 (coarse) was swollen in 100-150 ml distilled water overnight (0-4°C) and poured into a 30 x 0.9 cm diameter glass column fitted with a small wad of fine glass wool at the base. A double layer of cheese cloth (1 cm diameter) was placed on top of the packed column. The column was equilibrated by flushing it with 250-300 ml 20 mM potassium phosphate buffer pH 7.4 (250 mM Tris-BES buffer pH 7.4). The void volume was determined by measuring the volume of buffer required to flush a 1 ml solution of blue dextran through the column (25-30 ml). The void volume passed through the column in 2-3 minutes.

## II. Enzyme assays

Spectrophotometric and radiochemical techniques were employed to assay enzyme activity. Spectrophotometric assays were carried out on an Hitachi-Coleman 124 double beam spectrophotometer equipped with a temperature controlled water circulation system and an Hitachi-Coleman 165 recorder with zero suppression control apparatus. The latter mechanism permitted adjustment of the recorder so that full scale deflection of the recorder pen corresponded to an absorbance change of 0.1 units. Assays were normally conducted at 30°C and 340 nm using a chart speed of 20 mm·min<sup>-1</sup> with full scale pen deflection equivalent to a change of absorbance of 0.2 units.

Radiochemical assays were performed in a circulating temperature controlled water bath at 30°C. Assays were normally terminated after incubating the enzyme in the presence of all assay components for five minutes.

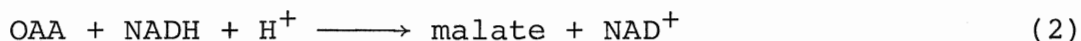
With both assay techniques, assays were conducted in duplicate for each condition tested with each enzyme extract. Each experiment was performed at least twice with two separate protein preparations.

### A. PEP carboxylase

- (1) Spectrophotometric assays
- (i) Assay system

PEP carboxylase activity was measured using the technique of Tchen and Vennesland (1955). The procedure involves the

coupling of PEPC activity (reaction (1)) with malate dehydrogenase activity (reaction(2)).



The standard 3.0 ml assay system for maximal activity at all pH values used is indicated in Table 1. Deviations from this will be noted in the results section. The reaction was begun with the addition of PEP. Figure 1 illustrates a typical recorder trace of PEPC activity. Under all conditions tested, the traces were linear for at least five minutes.

Saturation of the assay system with all substrates, coenzyme and cofactor was demonstrated by doubling the amounts of these reagents separately and observing no further increase in the rate of absorbance change. Experiments with various amounts of enzyme extract in the standard assay system demonstrated a linear relationship between the amount of enzyme and the reaction rate. The combined results of these tests indicate that the limiting factor in the oxidation of NADH is the amount of enzyme.

A Radiometer PHM64 Research pH meter equipped with a combination microelectrode was employed to determine the pH of the assay system. Studies demonstrated that the assay pH did not fluctuate during a five minute incubation. Monitoring of the assay pH was routinely accomplished by combining 3.2 ml of the buffer utilized, 2.6 ml distilled water and 0.2 ml 0.5 M sodium hydrogen carbonate. The addition of  $\text{NaHCO}_3$

Table 1: Standard assay system for the spectrophotometric measurement of PEP carboxylase activity.

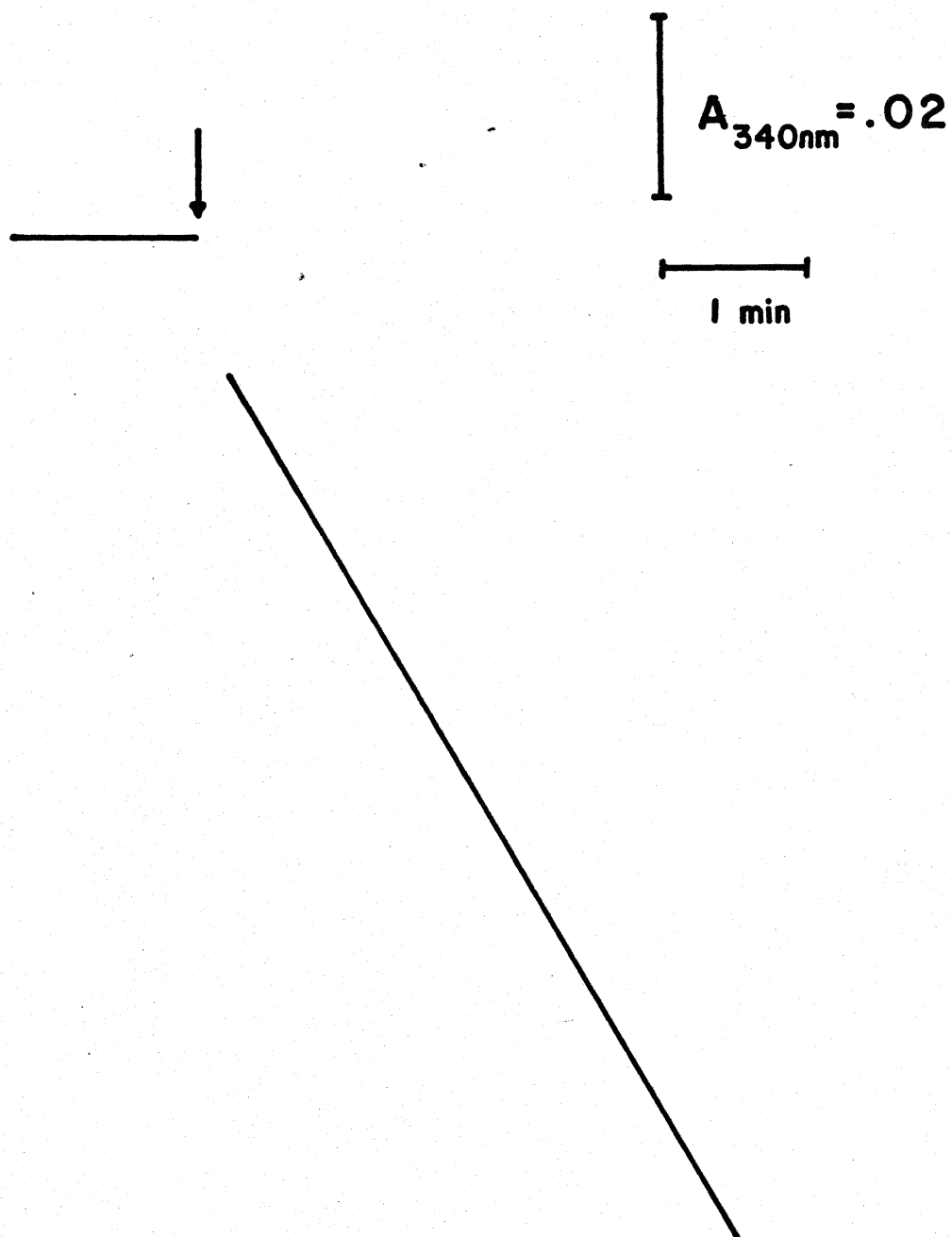
Reagent	Amount ( $\mu$ mole)	Volume (ml)
20 mM Potassium phosphate buffer, pH 6.7 to 7.4	32.0	1.6
100 mM $\text{MgCl}_2$	10.0	0.1
500 mM $\text{NaHCO}_3$	50.0	0.1
1.5 mM NADH	0.15	0.1
15 mM PEP	1.5	0.1
$\text{H}_2\text{O}$	—	0.8
Enzyme extract	—	0.2

$\text{MgCl}_2$  and  $\text{NaHCO}_3$  were prepared in distilled water. All other reagents were prepared in 20 mM K-Pi buffer pH 7.4. In the presence of potential effectors and/or different amounts of one or more of the reagents listed the volume of  $\text{H}_2\text{O}$  was adjusted so that the final volume of the assay was 3.0 ml.



Figure 1: PEP carboxylase catalyzed absorbance decrease at 340 nm.

The enzyme preparation was incubated at 30°C with 10.7 mM K-Pi buffer pH 7.4, 16.7 mM NaHCO<sub>3</sub>, 0.05 mM NADH and 3.3 mM MgCl<sub>2</sub>. Absorbance change was monitored at 340 nm with an Hitachi-Coleman 124 spectrophotometer in the split beam mode against a buffer blank. 0.5 mM PEP was added as indicated (↓).



increased the pH 0.15-0.20 units. Other components of the assay system did not detectably effect its pH.

(ii) Assay system containing potential effectors.

Various carboxylic and amino acids, and sugar phosphates (metabolites) were added to the standard assay system (Table 1). In all cases, rates in the following assays were determined prior to calculating any metabolite effect on PEPC activity.

- (1) standard assay + metabolite
- (2) standard assay - PEP + metabolite
- (3) standard assay + additional  $\text{MgCl}_2$
- (4) standard assay + additional  $\text{MgCl}_2$  + metabolite

Assay (1) was performed first, by adding PEP two minutes before the metabolite, and second by adding the metabolite two minutes before PEP and measuring the absorbance change after each addition. The same procedure was used for assays (2), (3) and (4) with the result that two, two and six measurements of absorbance change were determined respectively.

(iii) Malate dehydrogenase activity

Activity of MDH in the protein extract was determined by following the oxidation of NADH in the presence of oxaloacetic acid (OAA). The standard reaction mixture is indicated in Table 2. Under the assay conditions tabulated, MDH activity was in at least 200-fold excess of PEPC activity.

Table 2: Standard assay system for the spectrophotometric measurement of malate dehydrogenase activity.

Reagent	Amount ( $\mu$ mole)	Volume (ml)
20 mM Potassium phosphate buffer, pH 6.0 to 8.0	32.0	1.6
100 mM $MgCl_2$	10.0	0.1
1.5 mM NADH	0.15	0.1
76 mM OAA	7.6	0.1
$H_2O$	—	1.09
Enzyme extract	—	0.01

$MgCl_2$  was prepared in distilled water. NADH and OAA were prepared in 20 mM K-Pi buffer pH 7.4. OAA was used for enzyme assays within 30 minutes of its preparation.

## (iv) Calculation of velocity

Changes in absorbance per minute ( $\Delta A \cdot \text{min}^{-1}$ ) were obtained from the recorder traces. The Beer-Lambert law was employed to convert absorbance measurements to molar amounts.

$A = a_m \cdot b \cdot c$  where  $A$  = absorbance

$a_m$  = extinction coefficient ( $\text{ml} \cdot \text{mole}^{-1} \cdot \text{cm}$ )

$b$  = length of light path (1 cm)

$c$  = concentration of the absorbing species  
in  $\text{moles} \cdot \text{l}^{-1}$

A  $1 \text{ mole} \cdot \text{ml}^{-1}$  solution of NAD(P)H measured at 340 nm has an extinction coefficient of  $6.22 \times 10^6 \text{ ml} \cdot \text{mole}^{-1} \cdot \text{cm}$  when the incident light is monochromatic. A sample calculation follows.

Let  $A = 0.207$

$A = a_m \cdot b \cdot c$

$0.207 = 6.22 \times 10^6 \text{ ml} \cdot \text{mole}^{-1} \cdot \text{cm} \times 1 \text{ cm} \times c$

$$c = \frac{0.207 \text{ mole}}{6.22 \times 10^6 \text{ ml}}$$

The assay volume was 3.0 ml

$$\frac{c}{3.0 \text{ ml}} = \frac{0.207 \text{ } \mu\text{mole}}{6.22 \text{ ml}}$$

$$c = 0.1 \text{ } \mu\text{mole} \cdot \text{assay}^{-1}$$

Therefore an absorbance change of  $0.207 \cdot \text{min}^{-1}$  is equivalent to a rate of NAD(P)H oxidation (or  $\text{NADP}^+$  reduction) equal to  $0.1 \text{ } \mu\text{mole}$  per minute per assay. Since the gram fresh weight of tissue and the final volume of the enzyme extract are known, the gram fresh weight equivalent per assay can be calculated. The rate can now be expressed as  $\mu\text{moles}$  per minute per gram fresh weight ( $\mu\text{mole} \cdot \text{min}^{-1} \cdot \text{g FW}^{-1}$ ). After determining the protein

content, as outlined in Methods (IV), the assay rates can be expressed as  $\mu\text{mole} \cdot \text{min}^{-1} \cdot \text{mg protein}^{-1}$ .

(v) Reproducibility of the assay system

To determine the reproducibility of the assay system at high and low levels of activity, five assays were run with 0.5 mM PEP, and five were run with 0.01 mM PEP. Means and standard deviations were calculated (Table 3).

(2) Radiochemical assays

(i) Assay systems

The enzyme extract was incubated in the presence of either 1- $^{14}\text{C}$ -PEP or  $^{14}\text{C}$ - $\text{NaHCO}_3$  in stoppered 2.0 ml serum vials. The standard 1.0 ml assay system is indicated in Table 4. Any deviations from this will be noted in the Results section. When  $^{14}\text{C}$ - $\text{NaHCO}_3$  was employed, the reaction was begun with the addition of bicarbonate; and when 1- $^{14}\text{C}$ -PEP was employed, the reaction was begun with the addition of enzyme.

When the incubation time or the amount of enzyme was varied, results indicated that the accumulation of label was proportional to the incubation time, and the amount of enzyme present.

Whenever radiochemical assays were conducted, spectrophotometric assays were performed on the same extract to obtain a comparison of activity obtained with the two assay systems. To ensure comparability, the spectrophotometric assays were

Table 3: Reproducibility of the standard spectrophotometric assay of PEP carboxylase at near-saturated and PEP-limited substrate levels.

Assay pH	mM PEP	Activity	
		Mean	Standard Deviation
7.55	0.50	.360	.020
	0.01	.150	.011
	—	N.D. <sup>1</sup>	—
7.05	0.50	.080	.005
	0.01	.025	.002
	—	N.D.	—

<sup>1</sup>N.D., no detectable activity

Five assays were performed for each concentration of PEP in the presence of 10.7 mM K-Pi buffer pH 6.9 and 7.4, 3.3 mM MgCl<sub>2</sub>, 16.7 mM NaHCO<sub>3</sub>, 0.05 mM NADH and 0.2 ml enzyme extract. Activities are expressed as  $\mu\text{mole} \cdot \text{min}^{-1} \cdot \text{gFW}$  of coleoptile tissue.

Table 4: Standard assay systems for the radiochemical measurement of PEP carboxylase activity.

Reagent	Amount ( $\mu\text{mole}$ )	Volume (ml)
21.4 mM Potassium phosphate buffer pH 7.0	10.7	0.5
66 mM $\text{MgCl}_2$	3.3	0.1
167 mM $[^{12}\text{C}]$ - or $[^{14}\text{C}]\text{-NaHCO}_3$ (10 $\mu\text{Ci}\cdot\mu\text{mole}^{-1}$ )	16.7	0.1
5.0 mM $[^{12}\text{C}]$ - or 1- $[^{14}\text{C}]\text{-PEP}$ (2 $\mu\text{Ci}\cdot\mu\text{mole}^{-1}$ )	0.5	0.1
$\text{H}_2\text{O}$	—	0.1
Enzyme extract	—	0.1

$\text{MgCl}_2$  was prepared in distilled water.  $[^{14}\text{C}]$ -labelled reagents were prepared in distilled water and made up to the specified activities with unlabelled reagents. All other reagents were prepared in 20 mM K-Pi buffer pH 7.4. In the presence of potential effectors and/or different amounts of one or more of the reagents listed, the volume of  $\text{H}_2\text{O}$  was adjusted so that the final volume of the assay was 1.0 ml.



conducted with both the labelled and the unlabelled substrates.

(ii) Assay systems containing potential effectors

Some of the metabolites employed in Methods (II,A,1,(ii)) were tested as to their effects on the accumulation of the labelled product of PEPC activity. Assays performed with [ $^{14}\text{C}$ ]- $\text{NaHCO}_3$  were incubated with a metabolite in the presence and absence of PEP. Those performed with 1-[ $^{14}\text{C}$ ]-PEP were incubated with the metabolite in the presence of 0.5 mM PEP or 0.01 mM PEP.

(iii) Formation and detection of a 2,4-dinitrophenylhydrazine derivative of OAA

To the reaction mixtures incubated with 1-[ $^{14}\text{C}$ ]-PEP or [ $^{14}\text{C}$ ]- $\text{NaHCO}_3$  described in (i) was added 0.5 ml 4 N HCl saturated with 2,4-dinitrophenylhydrazine (2,4-DNP). The formation of the 2,4-DNP derivative of OAA was completed within three hours at 30°C or overnight (12-16 h) at 4°C. The DNP fraction was extracted from the assay mixture with three 0.5 ml washes of ethyl acetate. 95-98% of the fixed radioactivity in the reaction mixture was recovered in this fraction. The combined washes were evaporated to dryness and dissolved in 0.5 ml methanol. Volumes of 0.1 ml were added to scintillation vials containing 10 ml Scintillation Fluid I (Materials IV, B) and counted (Methods III). 5 or 10  $\mu\text{l}$  volumes were used for separation and identification of the reaction products

(Methods II, A, 2, (iv)).

(iv) Thin layer chromatography and autoradiography of the chromatograms.

The presence of 2,4-dinitrophenylhydrazine derivatives in the ethyl acetate fraction was detected according to the method of Smith (1960). To prepare the silica gel plates, Silica Gel G and water were combined in a 1:2 ratio (w:v) in a stoppered Erlenmeyer flask and vigorously shaken for sixty seconds. The silica was spread onto 20 cm square glass plates to give a thickness of 0.5 mm. Immediately prior to use, the plates were activated by heating them for one hour at 110°C.

Duplicate plates were spotted with 5 or 10  $\mu$ l volumes of the ethyl acetate fraction containing 2,4-DNP derivatives and co-chromatographed with the authentic 2,4-DNP derivative of OAA. The plates were developed using a butanol:water:ethanol solvent in a 70:20:10 (v:v:v) ratio. The solvent front was allowed to develop approximately 15 cm at which time the plates were removed from the chromatographic tanks and dried completely. The yellow areas of silica corresponding to authentic OAA-DNP were scraped from the plates, removed to scintillation vials containing 10 ml Scintillation Fluid I, and counted (Methods III). The duplicate plate was hardened by spraying with a layer of clear acrylic and exposed to medical X-ray film for three weeks before development.

(v) Reproducibility of the assay systems

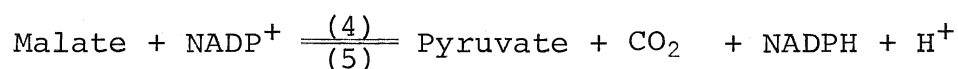
The reproducibilities of the assay systems were determined by performing four assays at high (0.5 mM) and low (0.01 mM) levels of PEP, and in the absence of PEP (when assays contained [ $^{14}\text{C}$ ]- $\text{NaHCO}_3$  and [ $^{12}\text{C}$ ]-PEP). Means and standard deviations were calculated (Table 5).

B. The malic enzyme

(1) Spectrophotometric assays

(i) Assay systems

Malic enzyme activity was followed in the forward and reverse directions.



Reaction (4) was measured by following the reduction of  $\text{NADP}^+$ . The standard 3.0 ml assay system for near-maximal activity is indicated in Table 6. Any deviations from this assay system will be noted in the results section. The reaction was begun with the addition of enzyme to the cuvette. A typical recorder trace of malic enzyme activity ( $\text{NADP}^+$  reduction) is illustrated in Figure 2. Under all conditions tested, the traces were linear for at least five minutes. Demonstrations of saturation of activity by  $\text{NADP}^+$  and malate, and dependence of the reaction rate on enzyme concentrations (as discussed in Methods (II, A, 1, (i))) indicated that when malate levels gave optimal activity, the enzyme concentration was the limiting factor in  $\text{NADP}^+$

Table 5: Reproducibility of the standard radiochemical assays of PEP carboxylase at near-saturated and PEP-limited substrate levels.

mM PEP	<sup>14</sup> C-labelled Substrate	Activity	
		Mean	Standard Deviation
0.50	1-[ <sup>14</sup> C]-PEP	81,500.0 (0.160)	7,200.0
0.01		4,075.0 (0.008)	1,035.0
0.50	[ <sup>14</sup> C]-NaHCO <sub>3</sub>	29,000.0 (0.180)	2,750.0
0.01		1,640.0 (0.010)	430.0
—		380.0 (0.002)	15.0

Five assays were performed for each concentration of PEP in the presence of 10.7 mM K-Pi buffer pH 7.0, 3.3 mM MgCl<sub>2</sub>, 16.7 mM NaHCO<sub>3</sub> and 0.1 ml enzyme extract. When labelled PEP (1.5  $\mu\text{Ci}\cdot\mu\text{mole}^{-1}$ ) was used unlabelled NaHCO<sub>3</sub> was added to the assay system, and when labelled NaHCO<sub>3</sub> (0.6  $\mu\text{Ci}\cdot\mu\text{mole}^{-1}$ ) was used the assay system contained unlabelled PEP. Activities are expressed as dpm per 1.0 ml assay and bracketed values are expressed as  $\mu\text{mole}\cdot\text{min}^{-1}\cdot\text{gFW}$  of coleoptile tissue.

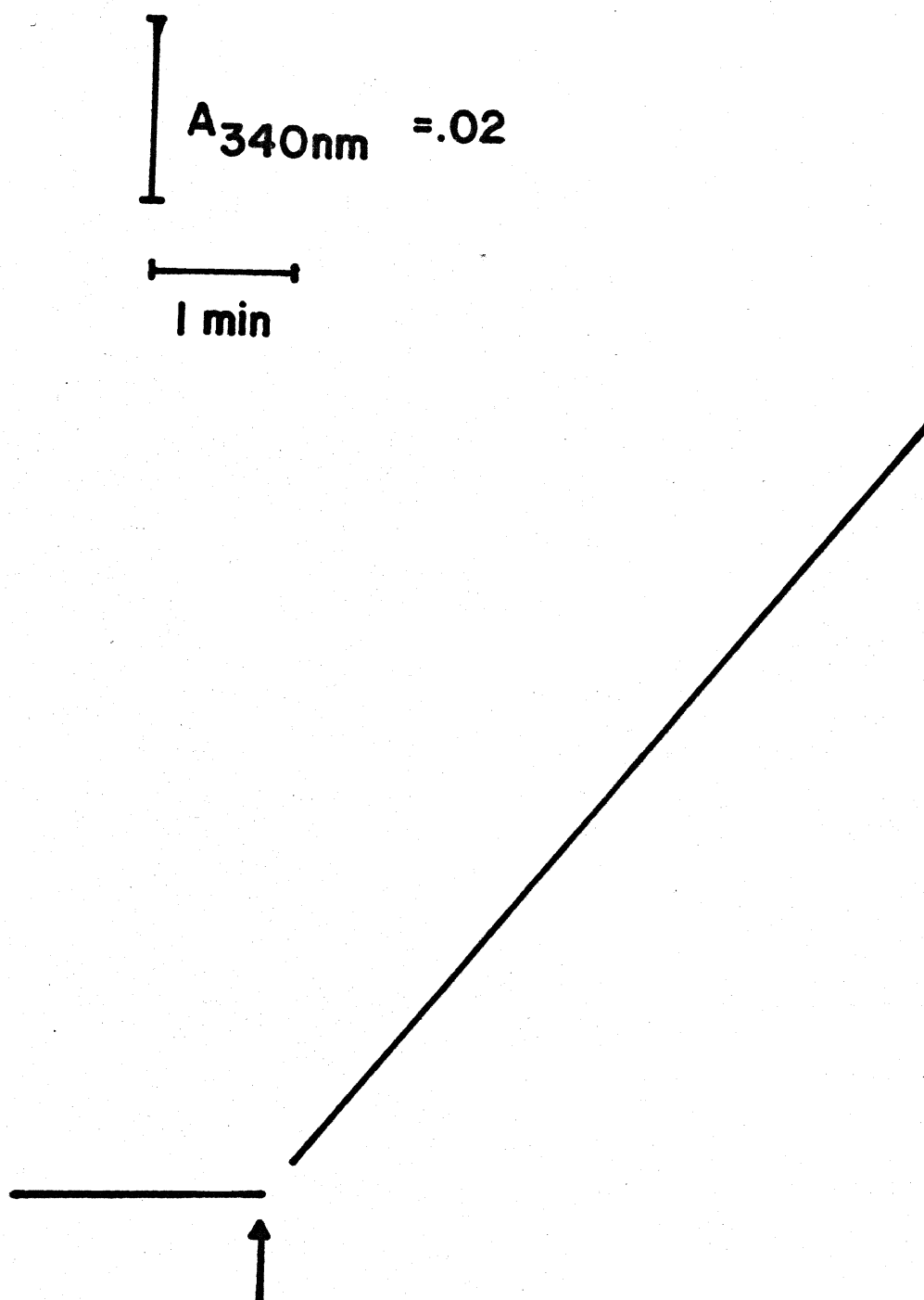
Table 6: Standard assay system for the spectrophotometric measurement of malic enzyme activity (NADP<sup>+</sup> reduction).

Reagent	Amount ( $\mu$ mole)	Volume (ml)
25 mM Tris-BES buffer, pH 6.5 to 7.25	37.5	1.5
30 mM MnCl <sub>2</sub>	3.0	0.1
15 mM NADP <sup>+</sup>	1.5	0.1
15 mM L-malate	1.5	0.1
H <sub>2</sub> O	—	1.0
Enzyme extract	—	0.2

MnCl<sub>2</sub> and L-malate were prepared in distilled water. Malate was neutralized with 0.1 N NaOH. NADP<sup>+</sup> was prepared in 25 mM Tris-BES buffer pH 7.4. In the presence of potential effectors and/or different amounts of one or more of the reagents listed, the volume of water was adjusted so that the final volume of the assay was 3.0 ml.

Figure 2: Malic enzyme catalyzed absorbance increase  
at 340 nm.

The enzyme preparation was incubated at 30°C with  
- 12.5 mM Tris-BES buffer pH 7.4, 1.0 mM  $\text{MnCl}_2$  and  
0.5 mM  $\text{NADP}^+$ . Absorbance change was monitored at  
340 nm with an Hitachi-Coleman 124 spectrophotometer  
in the split beam mode against a buffer blank.  
0.5 mM malate was added as indicated (†).



reduction. Malate concentrations greater than 0.5 mM inhibited enzyme activity.

Spectral measurements on an Aminco DW-2 UV-Vis spectrophotometer indicated that absorbance between 200 and 400 nm increased over a 15 minute period when 1.0 mM  $\text{MnCl}_2$  and enzyme extract alone were mixed (Figure 3). Consequently, demonstration of  $\text{MnCl}_2$  saturation of the system required incubation of the enzyme preparation and 2.0 mM  $\text{MnCl}_2$  for fifteen minutes prior to the addition of malate and  $\text{NADP}^+$ . The results indicated no significant difference in reaction rates with 1.0 or 2.0 mM  $\text{MnCl}_2$  present.

Routine measurements of the assay pH were followed as described earlier (Methods (II,A,1,(i))), by mixing 3.0 ml of the buffer utilized and 3.0 ml distilled water. The pH of the standard assay system did not fluctuate over a five minute incubation period.

Reaction (5) was measured by following the oxidation of NADPH. The standard 3.0 ml assay system for maximal activity is indicated in Table 7. Any deviations from this assay system will be noted in the Results section. The reaction was begun with the addition of enzyme to the cuvette. A typical recorder trace of malic enzyme activity (NADPH oxidation) is shown in Figure 4, and the traces were linear for at least five minutes. Saturation of the enzyme with all substrates and dependence of the reaction rate on the amount of enzyme present were demonstrated as previously described (Methods II, A, 1, (i)).



Figure 3: Effect of  $\text{MnCl}_2$  on the absorbance of protein in Tris-BES buffers.

12.5 mM Tris-BES buffer pH 7.4 was scanned between 210 and 410 nm in the absence (————) and presence of 0.2 ml enzyme extracted in 250 mM Tris-BES pH 7.4 (— — — —). 1.0 mM  $\text{MnCl}_2$  was added and scanned at 0 min (— · — · — · —), 15 min (-----) and 50 min (.....) after addition to the protein:buffer mixture. Absorbance change was monitored with an Aminco DW-2 spectrophotometer in the split beam mode against a buffer blank.

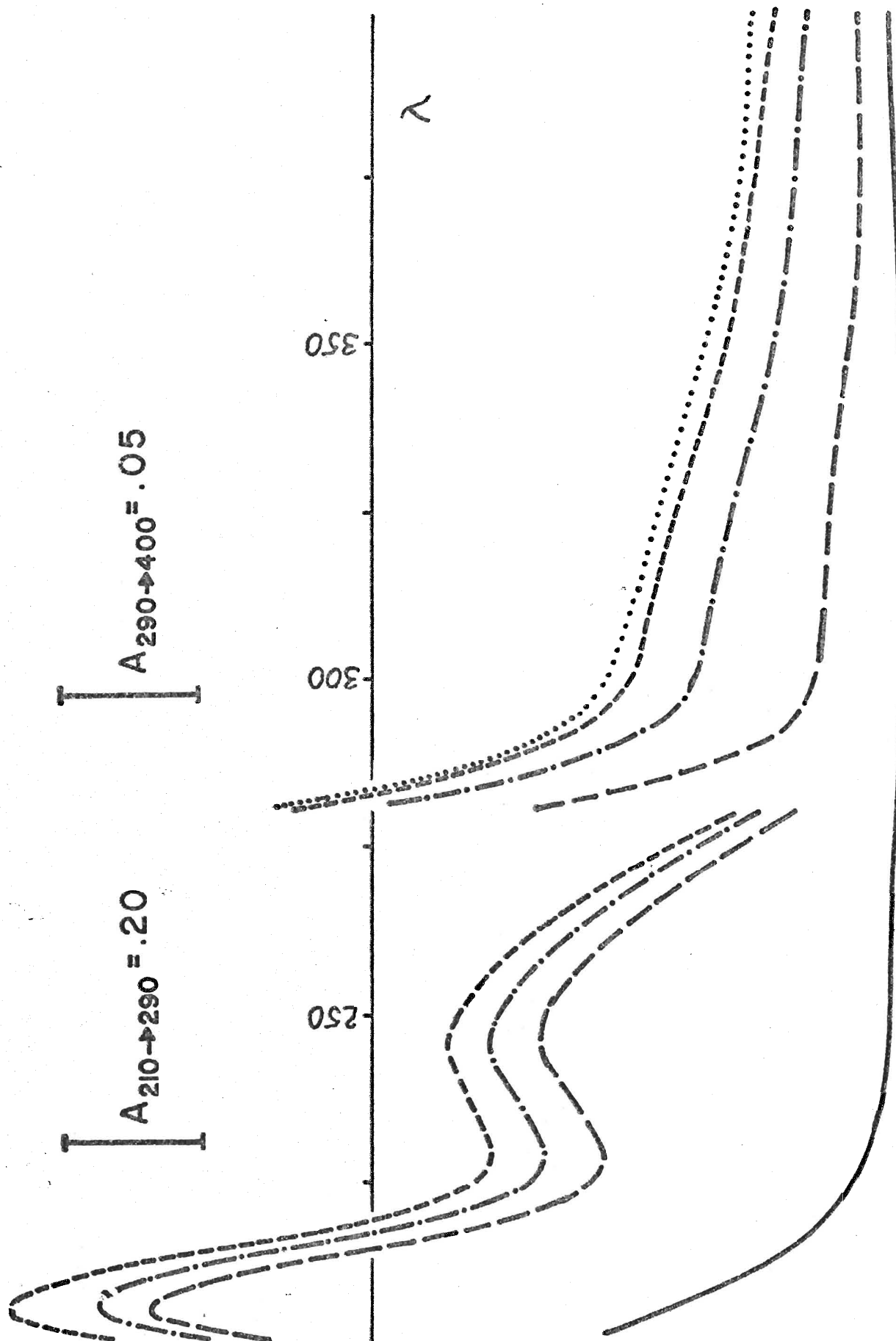


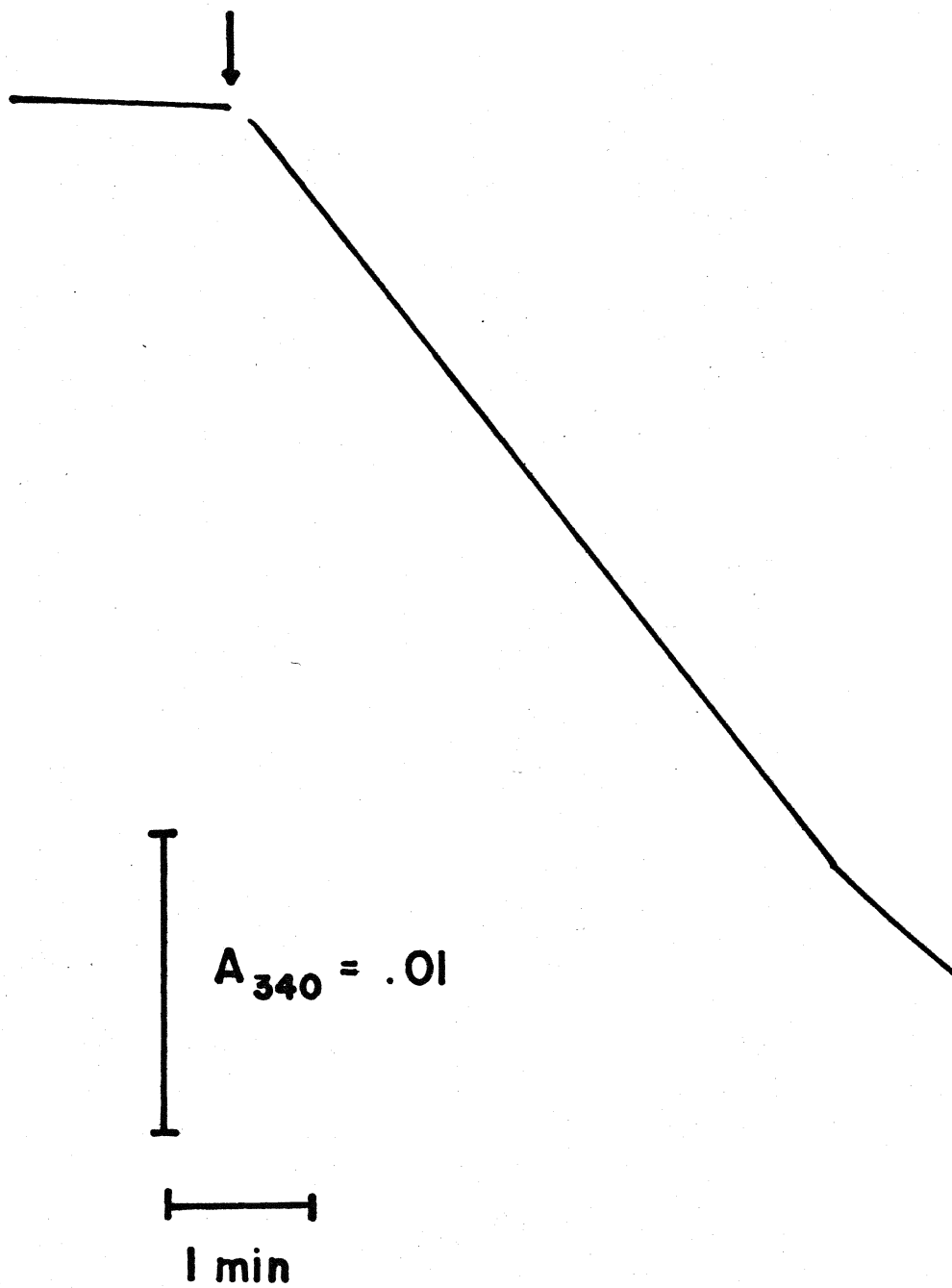
Table 7: Standard assay system for the spectrophotometric measurement of malic enzyme activity (NADPH oxidation).

Reagent	Amount ( $\mu$ mole)	Volume (ml)
25 mM Tris-BES buffer pH 7.25	37.5	1.5
30 mM $\text{MnCl}_2$	3.0	0.1
1.0 M $\text{NaHCO}_3$	100.0	0.1
1.5 mM NADPH	0.15	0.1
400 mM pyruvate	40.0	0.1
$\text{H}_2\text{O}$	—	0.9
Enzyme extract	—	0.2

$\text{MnCl}_2$  and  $\text{NaHCO}_3$  were prepared in distilled water. NADPH and pyruvate were prepared in 25 mM Tris-BES buffer pH 7.25. In the presence of different amounts of one or more of the reagents listed, the volume of water was adjusted so that the final volume of the assay was 3.0 ml.

Figure 4: Malic enzyme catalyzed absorbance decrease at 340 nm.

The enzyme preparation was incubated at 30°C with 12.5 mM Tris-BES buffer pH 7.4, 1.0 mM  $\text{MnCl}_2$ , 33.3 mM  $\text{NaHCO}_3$ , and 0.05 mM NADPH. Absorbance change was monitored at 340 nm with an Hitachi-Coleman 124 spectrophotometer in the split beam mode against a buffer blank. 13.3 mM pyruvate was added as indicated (↓).



The pH of the assay system did not fluctuate over a five minute period. Routine determinations of the assay pH were conducted with a solution containing 3.0 ml buffer, 2.8 ml distilled water and 0.2 ml 1.0 M  $\text{NaHCO}_3$ . The addition of  $\text{HCO}_3^-$  increased the pH of this solution 0.25-0.35 pH units.

(ii) Assay systems containing potential effectors

Various metabolites (Methods II, A, 1, (ii)) were tested for their effects on reaction (4) by adding them individually to the standard assay system. The following assays were performed:

- (1) standard assay + metabolite
- (2) standard assay - malate + metabolite
- (3) standard assay + additional  $\text{MnCl}_2$
- (4) standard assay + metabolite + additional  $\text{MnCl}_2$

Assay (1) was run first, by adding malate two minutes before the metabolite; and second, by adding the metabolite two minutes before malate. Rates of absorbance changes were obtained after each reagent addition.

(iii) Calculation of velocity

Velocity was determined from rates of absorbance using the procedure outlined in Methods (II, A, 1, (iv)). The extinction coefficient employed for  $\text{NADP}^+$  reduction/NADPH oxidation was  $6.22 \times 10^6 \text{ ml} \cdot \text{mole}^{-1} \cdot \text{cm}$ .

(iv) Reproducibility of the assay systems

The protocol employed in Methods (II,A,1,(v)) was followed for determining the reproducibilities of the forward and reverse reactions of the malic enzyme. Tables 8a and 8b indicate the means and standard deviations obtained for enzyme activity at maximal and sub-maximal substrate levels and in the absence of substrate.

(2) Radiochemical assays

(i) Assay systems

Malic enzyme activity was followed three ways by measuring label accumulation in a 2,4-DNP derivative of pyruvate (method (1)), carbon dioxide (method (2)), and malate (method (3)). The labelled substrate for methods (1) and (2) was U- $[^{14}\text{C}]$ -malate, and that for method (3) was  $[^{14}\text{C}]$ - $\text{NaHCO}_3$ . The standard 1.0 ml assay system for methods (1) and (2) is indicated in Table 9. Any deviations from this will be noted in the Results section. The reaction was begun with the addition of enzyme extract. In method (1), the assays were incubated in 15 ml glass conical centrifuge tubes. Stoppered Warburg manometric flasks (5.0 ml) were employed in method (2). All assay components were contained in the main vessel. A fluted filter paper saturated with 0.2 ml ethanolamine was inserted in the centre well for  $[^{14}\text{C}]$ - $\text{CO}_2$  collection and the side arm contained 0.5 ml 4 N HCl for terminating the reaction.

The standard 1.0 ml assay system for method (3) is indicated in Table 10. Any deviations from this system are

Table 8: Reproducibility of the standard spectrophotometric assays of the malic enzyme at near-saturated and substrate-limited levels of activity.

(a)  $\text{NADP}^+$  reduction

Assay pH	mM malate	Activity	
		Mean	Standard Deviation
7.25	0.50	.250	.008
	0.01	.020	.005
	—	N.D. <sup>1</sup>	—
6.50	0.50	.200	.010
	0.01	.020	.006
	—	N.D. <sup>1</sup>	—

(b) NADPH oxidation (pH 7.25)

mM pyruvate	Mean	Standard Deviation
13.3	.060	.010
1.3	.008	.001
—	.005	.001

<sup>1</sup>N.D., no detectable activity

Five assays were performed for each concentration of malate (a) or pyruvate (b) in the presence of 12.5 mM Tris-BES buffer pH as indicated, 1.0 mM  $\text{MnCl}_2$  and 0.2 ml enzyme extract plus (a) 0.5 mM  $\text{NADP}^+$  or (b) 33.3 mM  $\text{NaHCO}_3$  and 0.05 mM NADPH. Activities are expressed as  $\mu\text{mole} \cdot \text{min}^{-1} \cdot \text{gFW}$  of coleoptile tissue.



Table 9: Standard assay system for the radiochemical measurement of malic enzyme activity (NADP<sup>+</sup> reduction).

Reagent	Amount ( $\mu$ mole)	Volume (ml)
25 mM Tris-BES buffer pH 7.25	12.5	0.5
10 mM MnCl <sub>2</sub>	1.0	0.1
5 mM NADP <sup>+</sup>	1.5	0.1
5 mM U-[ <sup>14</sup> C]-malate (0.7 $\mu$ Ci· $\mu$ mole <sup>-1</sup> )	1.5	0.1
H <sub>2</sub> O	—	0.1
Enzyme extract	—	0.1

MnCl<sub>2</sub> and U-[<sup>14</sup>C]-malate were prepared in distilled water. Malate was neutralized with 0.1 N NaOH. NADP<sup>+</sup> was prepared in 25 mM Tris-BES buffer pH 7.25. In the presence of potential effectors and/or different amounts of one or more of the reagents listed, the volume of water was adjusted so that the final volume of the assay was 3.0 ml.

Table 10: Standard assay system for the radiochemical measurement of malic enzyme activity (NADPH oxidation).

Reagent	Amount ( $\mu$ mole)	Volume (ml)
25 mM Tris-BES buffer pH 7.25	12.5	0.5
20 mM $\text{MnCl}_2$	1.0	0.05
333 mM $[^{14}\text{C}]\text{-NaHCO}_3$ ( $0.1 \mu\text{Ci} \cdot \mu\text{mole}^{-1}$ )	33.3	0.1
1 mM NADPH	0.05	0.05
133 mM pyruvate	13.3	0.1
$\text{H}_2\text{O}$	—	0.1
Enzyme extract	—	0.1

$\text{MnCl}_2$  and  $[^{14}\text{C}]\text{-NaHCO}_3$  were prepared in distilled water. All other reagents were prepared in 25 mM Tris-BES buffer pH 7.25. In the absence of one or more of the reagents listed, the volume of water was adjusted so that the final volume of the assay was 1.0 ml.

noted in the Results section. The assays were run in stoppered 2.0 ml serum vials, and were begun with the addition of  $[^{14}\text{C}]\text{-NaHCO}_3$ .

In all methods, experiments were run in which the incubation time, or the amount of enzyme was varied. The results indicated a proportionality between the accumulated label, and the time of incubation and amount of enzyme present. In addition, spectrophotometric assays were performed in conjunction with the radiochemical assays to obtain a comparison of enzymic activity obtained with the two techniques.

(ii) Assay systems containing potential effectors

Some of the metabolites used in Methods (II,B,1,(ii)) were tested for their influence on the accumulation of the 2,4-DNP derivative of pyruvate. Assays were performed using the standard assay system (Table 9) in the presence of 0.5 mM malate or 0.01 mM malate.

(iii) Formation and detection of  $[^{14}\text{C}]\text{-product(s)}$

The product(s) obtained by method (1) (Methods II,B,2,(i)) were converted to 2,4-dinitrophenylhydrazine derivatives and extracted from the assay system by the procedure outlined in Methods (II, A, 2, (iii)).

The reaction described in method (2) was stopped by tipping the HCl in the side arm into the main vessel. After thirty minutes, the filter paper was removed, placed in

scintillation vials containing 10 ml Scintillation Fluid II (Materials IV, B), and counted.

The reaction mixture of method (3) was stopped by the addition of 0.5 ml 4 N HCl. To remove remaining unreacted [ $^{14}\text{C}$ ]- $\text{NaHCO}_3$ , the mixture was bubbled with 100%  $\text{CO}_2$  for fifteen minutes. Protein was removed from the system by centrifuging in an IEC clinical centrifuge at top speed for five minutes. The supernatant fluid was retained and evaporated to dryness. The residue was dissolved in 0.5 ml methanol. 0.1 ml volumes were removed and combined with 10 ml Scintillation Fluid I and counted (Methods C). 10  $\mu\text{l}$  volumes were used for separation and identification of reaction products (Methods II, B, 2, (iv)).

(iv) Thin layer chromatography and autoradiography of the chromatograms

2,4-DNP derivatives in the ethyl acetate fraction were chromatographed following the procedure outlined in Methods (II, A, 2, (iv)). Each sample was co-chromatographed with the 2,4-DNP derivatives of pyruvate and oxaloacetate. The migration path was sectioned into areas according to their correspondence with OAA-DNP, pyruvate-DNP and uncoloured regions. Silica gel from these sectioned areas was removed into scintillation vials containing 10 ml Scintillation Fluid I, and counted (Methods III). Duplicate plates were autoradiographed as described previously (Methods II, A, 2, (iv)).

The detection of malate in the aqueous fraction was accomplished by the method of Myers and Huang (1969). Cellulose plates were prepared and activated by combining cellulose CC41 and water in a 1:2 (w:v) ratio.

Duplicate plates were spotted with 10  $\mu$ l volumes of the aqueous fraction (Methods II, B, 2, (iii)), and co-chromatographed with authentic malate. Malic acid was dissolved in water and neutralized with 0.1 N NaOH. The solution was evaporated to dryness and dissolved in 2-3 ml methanol.

The plates were developed approximately 15 cm in a phenol: water:formic acid solvent in a 75:25:1 (v:v:v) ratio, and then dried completely. Malate was detected by spraying the plates with bromcresol green, and an atmosphere of ammonia was used to heighten the contrast between the yellow organic acid spots and the blue background. The areas corresponding to malate, and all other areas of the migration pathway were scraped, removed to scintillation vials containing Scintillation Fluid I, and counted (Methods III).

(v) Reproducibility of the assay systems

The reproducibility of the two assay systems (methods (1) and (3), Methods (II, B, 2, (i))) was determined following the protocol outlined in Methods II, A, 2, (v). The results are indicated in Table 11.

Table 11: Reproducibility of the standard radiochemical assay of the malic enzyme at near-saturated and malate-limited levels of activity.

mM U-[ $^{14}\text{C}$ ]-malate	Activity	
	Mean	Standard Deviation
0.50	22,500.0 (0.165)	3,250.0
0.01	2,045.5 (0.015)	550.0

Five assays were performed for each malate concentration in the presence of 12.5 mM Tris-BES buffer pH 7.25, 1.0 mM  $\text{MnCl}_2$ , 0.5mM  $\text{NADP}^+$  and 0.1 ml enzyme extract. Activities are expressed as dpm per 1.0 ml assay, and bracketed values are expressed as  $\mu\text{mole}\cdot\text{min}^{-1}\cdot\text{gFW}$  of coleoptile tissue. The specific activity of U-[ $^{14}\text{C}$ ]-malate employed was  $2.0 \mu\text{Ci}\cdot\mu\text{mole}^{-1}$ .

### III. Scintillation counting and calculation of velocity

Samples were counted for ten minutes in a Searle Delta 300 liquid scintillation counter set at 800K and using the  $^3\text{H}$  or  $^{14}\text{C}$  mode cassette. The counting efficiency of the machine is indicated by the ratio of counts generated in the two channels by an external source of radioactivity. Efficiency is always less than 100%, and efficiency was further decreased by the quenching effect of the coloured 2,4-DNP derivatives. Consequently the amount of quenching in each sample was determined by constructing a standard calibration curve of percent counting efficiency against the external standard ratio. This was done with a series of vials containing a known amount of radioactivity in [ $^{14}\text{C}$ ]-hexadecane and varying amounts of the yellow coloured pyruvate-DNP in  $\text{CH}_3\text{OH}$  in 10 ml of Scintillation Fluid I. The curve is illustrated in Figure 5. When colourless samples were counted, a calibration curve was constructed with a series of purchased internal standards (Figure 6).

Counts per minute (cpm) were obtained from the scintillation counter recorder tapes. The figures on the tape indicate the following parameters:

vial no. → xx	:	xx.xx	counting time
		xxxx.x	cpm in Channel A
		xxxx.x	cpm in Channel B
		x.xxx	sample channel ratio
		x.xxx	external standard ratio (ESR)

A calibration curve and the ESR of a sample were used to determine the counting efficiency of the sample.

Figure 5:  $[^{14}\text{C}]$ -hexadecane standard calibration curve  
for colour quenched samples

0.04 Ci  $[^{14}\text{C}]$ -hexadecane was counted in the presence of a series of concentrations of the 2,4-dinitrophenyl hydrazine derivative of pyruvate dissolved in methanol. The counting efficiency of each sample was determined as a percent of the cpm obtained for  $[^{14}\text{C}]$ -hexadecane and methanol, and plotted against the external standard ratio obtained for each sample.



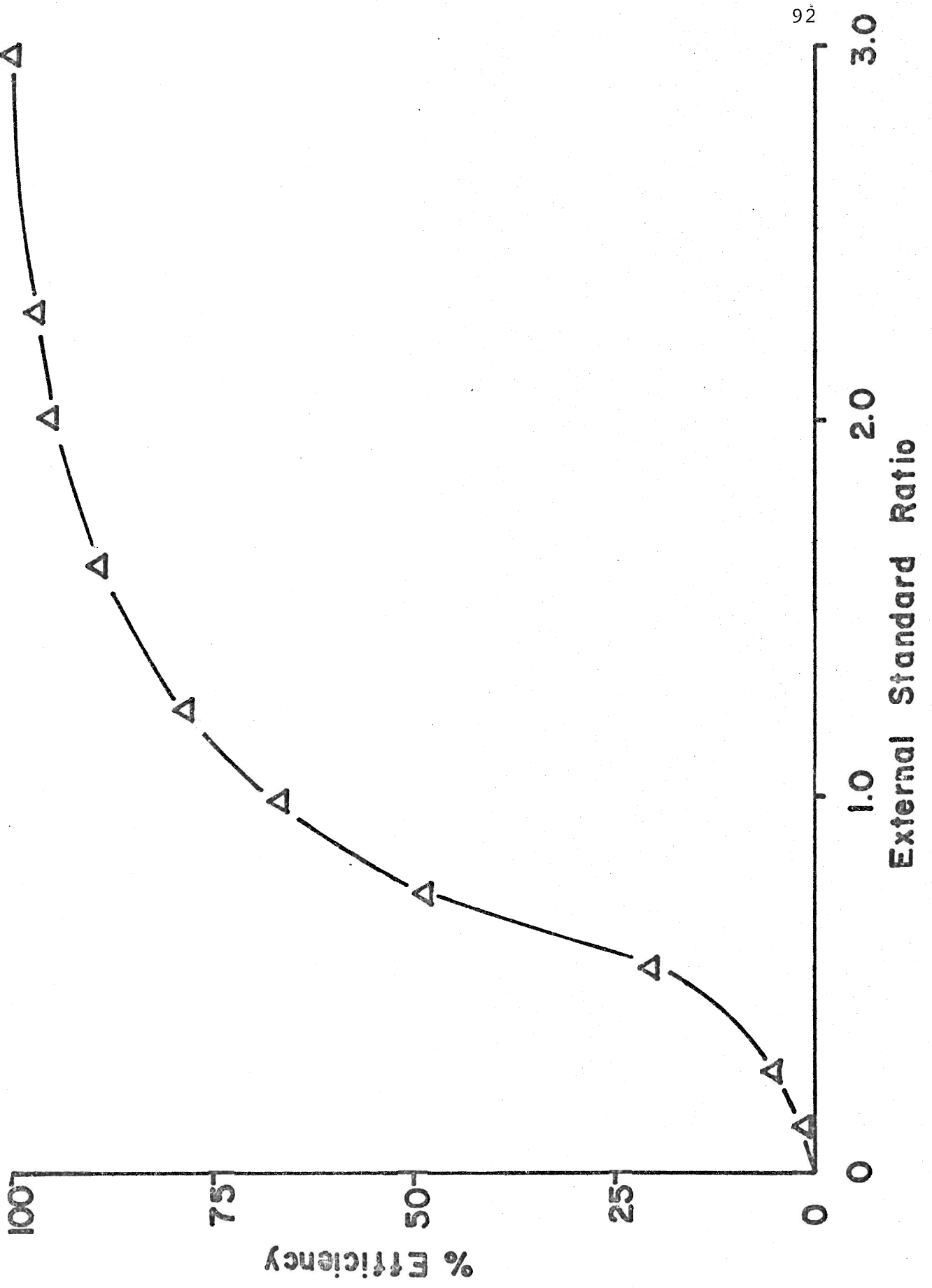
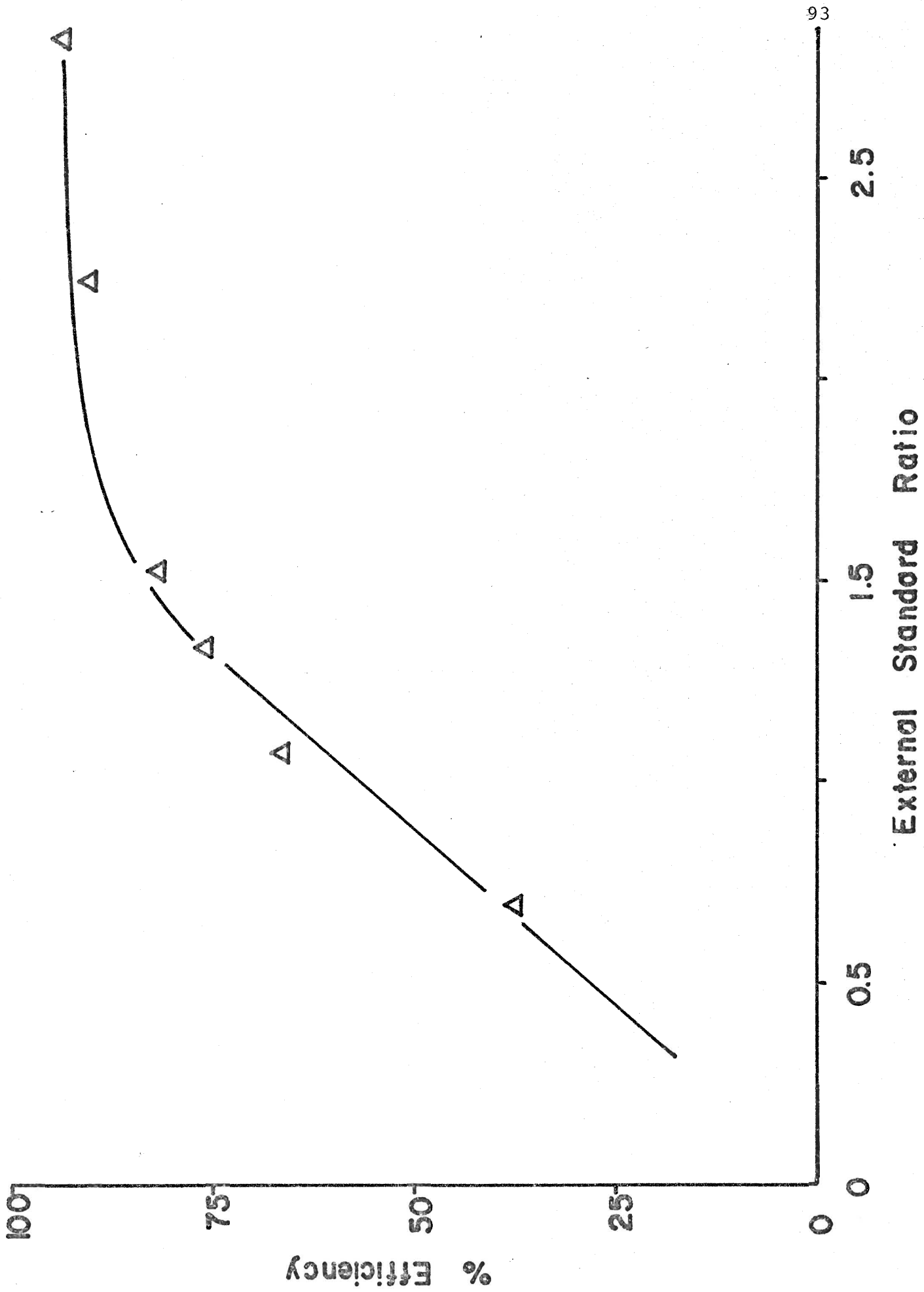


Figure 6: Standard calibration curve for solvent quenched (colourless) samples.

Purchased internal standards containing 100,000 dpm and variously quenched with solvent were counted. The counting efficiency of each sample was determined as a percent of the cpm obtained and plotted against the external standard ratio obtained for each sample.



The cpm of the samples ranged from 500 to 20,000, depending on the assay conditions employed, and the counting efficiencies were between 85 and 95%. The cpm of the sample was converted to dpm as follows:

$$\text{dpm} = \frac{\text{cpm} \times 100}{\% \text{ counting efficiency}}$$

The following sample calculation illustrates the determination of velocity ( $\mu\text{mole} \cdot \text{min}^{-1} \cdot 1.0 \text{ ml assay}$ ) from the dpm of the sample.

$$\begin{aligned} \text{velocity} = & \frac{\text{dpm}}{\text{volume counted (ml)}} \times \frac{1 \mu\text{Ci}}{2.2 \times 10^6 \text{ dpm}} \times \frac{\text{specific activity of label}}{(\mu\text{mol} \cdot \mu\text{Ci}^{-1})} \\ & \times \frac{\text{total volume of sample (ml)}}{\text{incubation time (min)}} \end{aligned} \quad (6)$$

For example,

$$\text{dpm} \cdot 0.1 \text{ ml}^{-1} = 10,000 \text{ dpm}$$

$$\text{specific activity of label added} = 1 \mu\text{mole} \cdot \mu\text{Ci}^{-1}$$

$$\text{total volume of ethylacetate fraction in CH}_3\text{OH} = 0.5 \text{ ml}$$

$$\text{incubation time} = 5.0 \text{ min}$$

$$\begin{aligned} \text{velocity} = & \frac{10,000 \text{ dpm}}{0.1 \text{ ml}} \times \frac{1 \mu\text{Ci}}{2.2 \times 10^6 \text{ dpm}} \times \frac{1 \mu\text{mole}}{\mu\text{Ci}} \\ & \times \frac{0.5 \text{ ml}}{5.0 \text{ min}} \\ = & 0.0045 \mu\text{mole} \cdot \text{min}^{-1} \cdot 1 \text{ ml assay} \end{aligned}$$

As in the spectrophotometric assays, this figure was expressed as a specific activity in  $\mu\text{mole} \cdot \text{min}^{-1} \cdot \text{g FW}$

Equation (6) was modified when determining activity from radioactivity recovered in the ethylacetate or ethanolamine fractions. In the former case, equation (6) was multiplied by  $1/0.75$  to compensate for loss of  $^{14}\text{C}$  and  $^{14}\text{CO}_2$  when U- $^{14}\text{C}$ -malate is converted to U- $^{14}\text{C}$ -pyruvate; and in the latter case the multiplication factor was  $1/0.25$  to compensate for the loss of  $^{14}\text{C}$  as U- $^{14}\text{C}$ -pyruvate in the non-ethanolamine fraction.

#### IV. Protein determinations

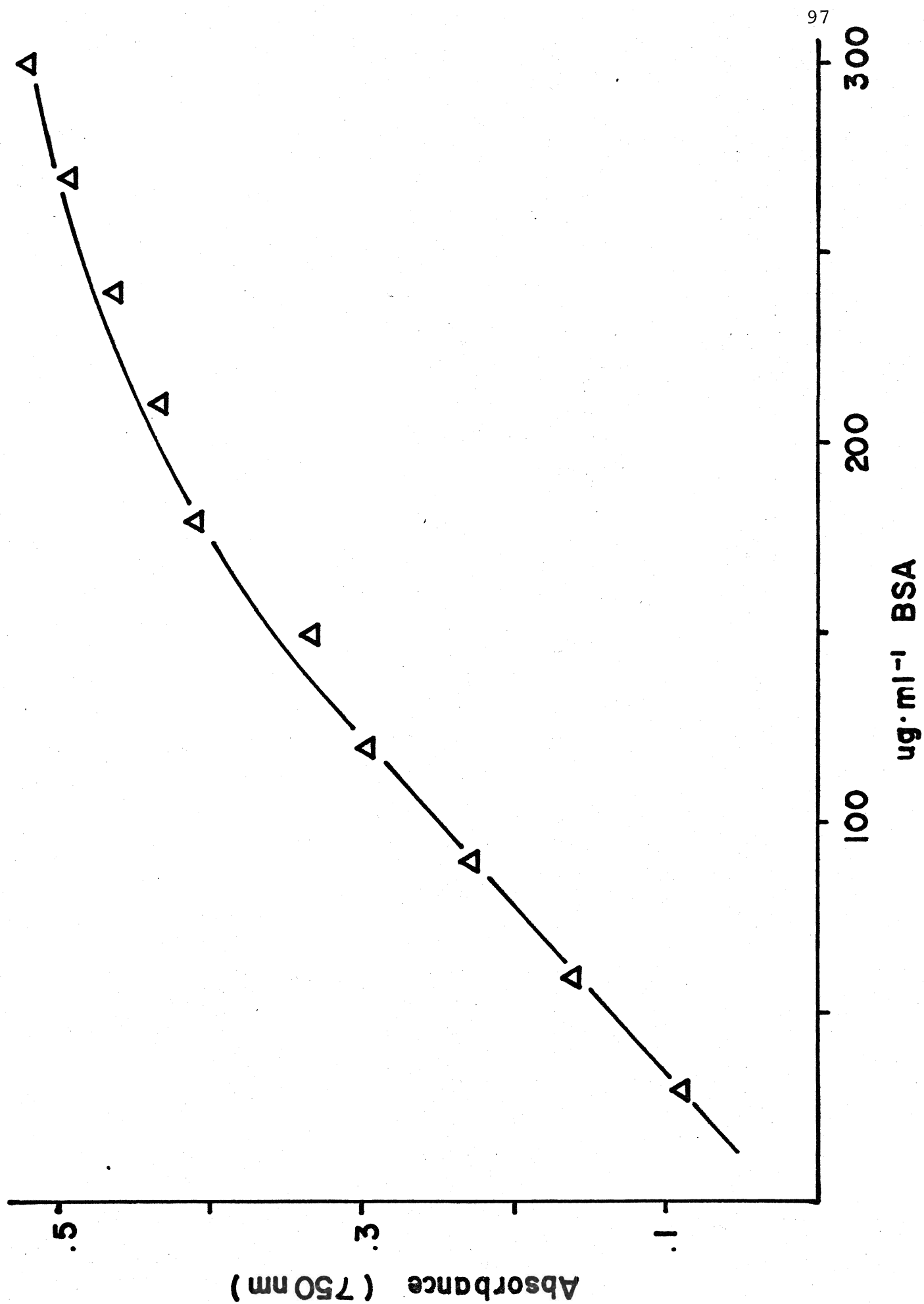
The method of Lowry et al. (1951) was employed to determine the protein content of each enzyme preparation. An aliquot (0.3 ml) of the enzyme preparation extracted in potassium phosphate was stored before determination in 0.1 N NaOH (2.7 ml). 1.0 ml of the alkaline protein solution was combined with 5.0 ml Alkaline Copper Reagent (Materials IV, C) and allowed to sit at room temperature for ten minutes. 0.5 ml Folin Reagent was added and mixed immediately, after which the solution was incubated for thirty minutes. The optical density at 750 nm was determined. The protein content was determined by comparing the absorbance with a standard calibration curve obtained with a series of known bovine serum albumin concentrations ( $30 \mu\text{g}\cdot\text{ml}^{-1}$  to  $300 \mu\text{g}\cdot\text{ml}^{-1}$ ; Figure 7). Mean maximal PEPC activity obtained throughout this investigation was  $0.1 \mu\text{mole}\cdot\text{min}^{-1}\cdot\text{mg}$  protein with a standard deviation of  $0.01 \mu\text{mole}\cdot\text{min}^{-1}\cdot\text{mg}$  protein.

Tris-BES buffers were observed to react with the Lowry reagents resulting in colour formation of approximately the same absorbance as a  $300 \mu\text{g}\cdot\text{ml}^{-1}$  BSA solution. No other satisfactory technique was discovered, and consequently the protein content of enzyme preparations extracted in Tris-BES buffers could not be determined.

Figure 7: Bovine serum albumin standard calibration curve for the Lowry method of protein determination.

A series of known concentrations of bovine serum albumin (0 to 300  $\mu\text{g}\cdot\text{ml}^{-1}$ ) were reacted with the Lowry reagents and plotted against their absorbance at 750 nm.

Absorbance was monitored with an Hitachi-Coleman 124 spectrophotometer in the split beam mode against a water blank treated with the Lowry reagents.





## V. Data analysis

Various graphical methods were employed to determine a number of kinetic constants. It was assumed that velocity data directly reflected the degree of substrate binding.

pH profiles (velocity versus assay pH) were constructed for each substrate concentration used. Percent modulation of activity by metabolites was calculated and plotted as a function of assay pH and substrate concentration.

Approximations of  $V_{\max}$  and apparent  $K_m$  were determined from velocity versus substrate concentration plots. Linear transformations of the Michaelis-Menton equation were used to construct straight line plots of the data which yield more accurate estimates of  $V_{\max}$ ,  $K_{m_{app}}$  and  $K_{i_{app}}$ . These plots included Lineweaver-Burk ( $1/v \times 1/s$ ), Eadie-Hofstee ( $v \times v/s$ ) and Hanes ( $s/v \times s$ ) transformations. Deviations from linearity may indicate co-operative substrate binding or substrate inhibition. Shifting of the plots in the presence of added metabolites may indicate an activation or inhibition of enzymic activity. The type of modulation (competitive, non-competitive, un-competitive) can be estimated from the relationship of plots in the presence of effectors to those in the absence of effectors.

The kinetic constants which were determined from the linear transformations can be described.  $V_{\max}$  refers to the maximal velocity of activity in the enzyme preparation.  $K_{m_{app}}$  is the apparent substrate concentration giving half the maximal velocity.  $K_{i_{app}}$  is the effector concentration giving half the maximal velocity obtained in the presence of the effector.

Estimations of co-operative kinetics were made from Hill coefficients obtained from the slopes of Hill plots ( $\log [s] \times \log (v/V_{\max} - v)$ ) of the data.

## Results

The results are divided into four sections. Each section indicates the influence of pH on PEPC or malic enzyme activities in addition to results concerning specific problems investigated. The first section involves a survey of extraction procedures and assay conditions to determine which of these result in optimal PEPC and malic enzyme activities as measured spectrophotometrically. The second section deals with the characterization of malic enzyme activity, and analysis of the reaction products. Section three presents the kinetic constants for PEPC and the malic enzyme obtained from radiochemical assays. The final section looks at possible metabolic effectors of PEPC and the malic enzyme activities as measured spectrophotometrically and radiochemically. In all sections the results of representative experiments are demonstrated.

I. Effect of various extraction techniques and assay conditions on PEP carboxylase and malic enzyme activities

A. Effect of dialysis or gel filtration on PEP carboxylase activity

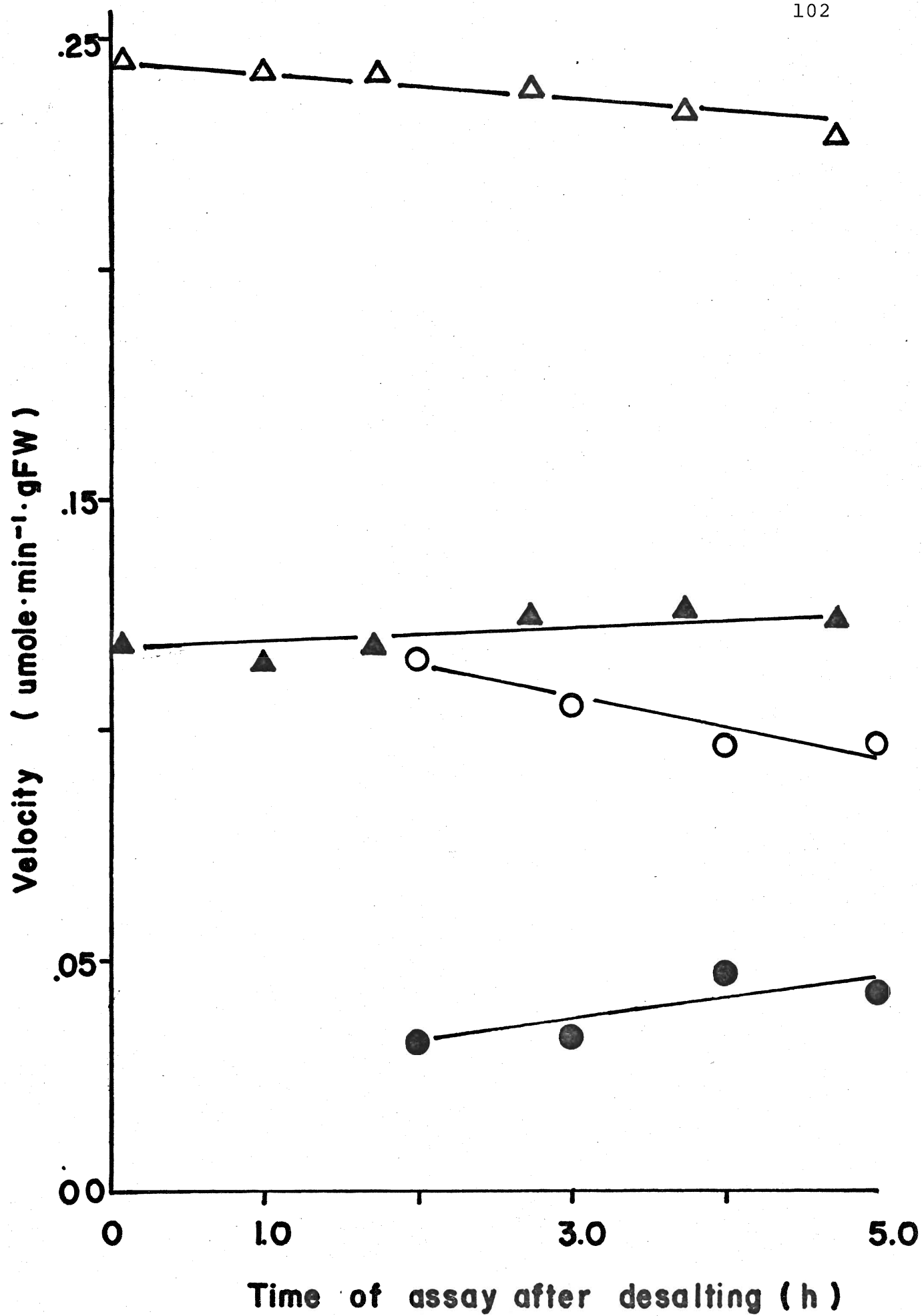
Ammonium sulphate, used in the precipitation of soluble proteins, was removed from the enzyme preparation by dialysis or gel filtration (Methods I,B). This section deals first with the effect of each technique on the time dependent stability of PEPC activity. The influence of pH and extraction technique on the kinetic constants of PEPC are also reported.

(1) Effect of dialysis or gel filtration on the stability of PEP carboxylase activity

Saturated PEPC activity from dialyzed or gel filtrated protein extracts was assayed spectrophotometrically at pH 7.27 in the presence and absence of 0.1 mM malate. Assays were conducted at hourly intervals, starting five minutes after the preparation of the gel filtrated extract to five hours after this time. Dialysis resulted in an additional two hours preparation time; therefore, assays with dialyzed protein were conducted from time two hours to time five hours. Figure 8 demonstrates that PEPC activity from gel filtrated protein extracts decreased  $1.0\% \cdot \text{hr}^{-1}$ , whereas that from dialyzed protein extracts was less stable, decreasing  $7.0\% \cdot \text{hr}^{-1}$ . Ratios of activity from filtrated and dialyzed protein extracts increased from 2:1 at the two hour assay, to 2.5:1.0 at the five hour assay.

Figure 8: Effect of dialysis or gel filtration on the time dependent stability of near-saturated PEP carboxylase activity ( $\pm 0.1$  mM malate).

Enzyme activity was assayed spectrophotometrically at 340 nm in the presence of 10.7 mM K-Pi buffer pH 7.27, 16.7 mM  $\text{NaHCO}_3$ , 3.3 mM  $\text{MgCl}_2$ , 0.5 mM PEP, 0.05 mM NADH and 0.2 ml enzyme desalted either via dialysis ( $\Delta$ ) or gel filtration ( $\bigcirc$ ). Closed symbols indicate activity in the presence of 0.1 mM malate.



Malate (0.1 mM) inhibition of PEPC activity also exhibited less stability after dialysis (Figure 8). Malate inhibited activity after filtration increased  $0.5\% \cdot \text{hr}^{-1}$ , and the per cent inhibition remained relatively constant with time at approximately 50%. In contrast, the dialyzed protein lost sensitivity to malate at a rate of approximately  $12\% \cdot \text{hr}^{-1}$ . The percent inhibition decreased from 72% at time two hours to 52% at time five hours.

(2) Effect of dialysis or gel filtration on the apparent  $K_m(\text{PEP})$  and  $V_{\text{max}}$  of PEP carboxylase

PEPC activity from dialyzed or gel filtrated extracts was assayed at pH 7.27 with PEP concentrations from 0.01 to 0.5 mM. Figure 9 indicates that  $V_{\text{max}}$  was lower for the dialyzed enzyme, and that 0.1 mM malate inhibited enzyme activity from both protein extracts by decreasing  $V_{\text{max}}$ . Apparent binding affinity constants for PEP and malate were determined from linear plots of these data (Methods V). Lineweaver-Burk, Eadie-Hofstee, and Hanes plots were non-linear for enzyme activity from both preparations. This phenomenon was more pronounced in the presence of malate. Results indicated that the binding affinity of PEPC for PEP and malate was dependent on the PEP concentration and independent of the desalting procedure employed. At low levels of PEP (less than 0.05 mM), the  $K_{\text{mapp}}(\text{PEP})$  was 0.03 mM, and PEP concentrations greater than 0.05 mM, the  $K_{\text{mapp}}(\text{PEP})$  was increased to 0.8 mM (Figure 10).

Figure 9: Effect of dialysis or gel filtration on the velocity versus PEP concentration plot of PEP carboxylase activity ( $\pm$  0.1 M malate)

Enzyme activity was assayed spectrophotometrically at 340 nm in the presence of 10.7 mM K-Pi buffer pH 7.27, 16.7 mM NaHCO<sub>3</sub>, 3.3 mM MgCl<sub>2</sub>, 0.01 to 0.5 mM PEP, 0.05 mM NADH and 0.2 ml enzyme desalted either via dialysis (○) or gel filtration (Δ). Closed symbols indicate activity in the presence of 0.1 mM malate.



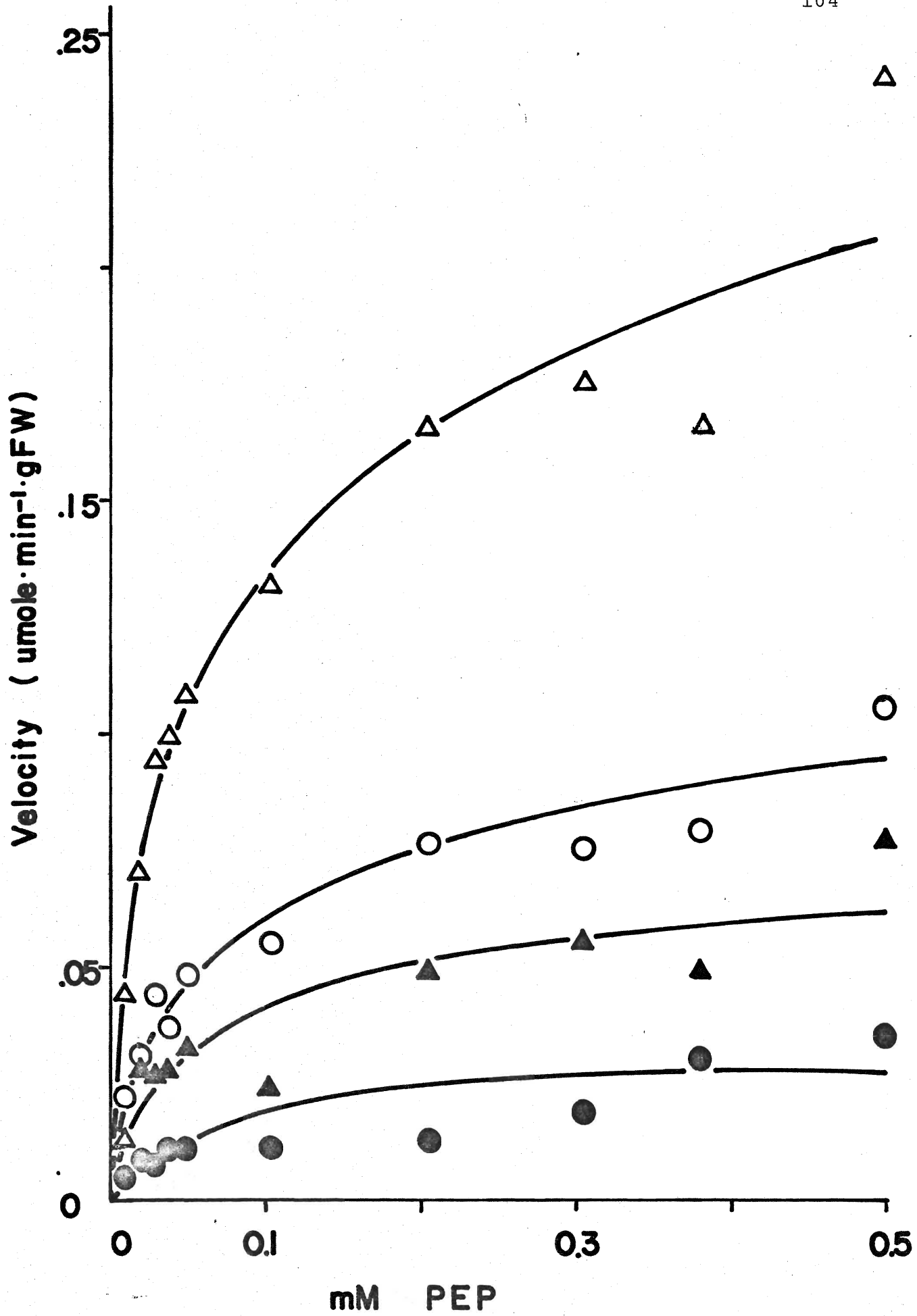
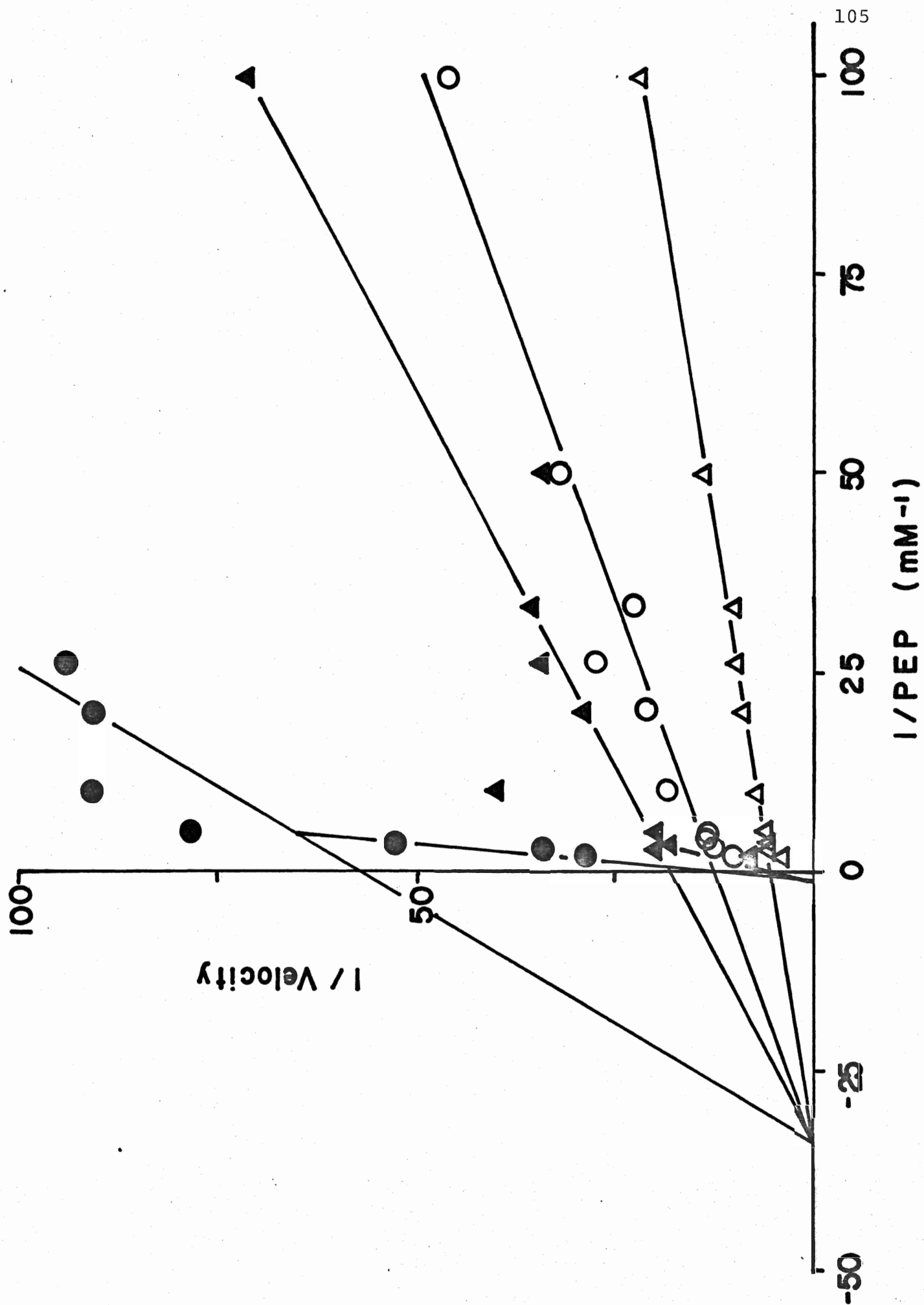


Figure 10: Effect of dialysis or gel filtration on the Lineweaver-Burk plot of PEP carboxylase activity ( $\pm 0.1$  mM malate).

Enzyme activity was assayed spectrophotometrically at 340 nm in the presence of 10.7 mM K-Pi buffer pH 7.27, 16.7 mM NaHCL, 3.3 mM MgCl, 0.05 mM NADH, 0.01 to 0.5 mM PEP and 0.2 ml enzyme desalted either via dialysis ( $\blacktriangle$ ) or gel filtration ( $\bullet$ ). Closed symbols indicate activity in the presence of 0.1 mM malate.



In the presence of malate, the low and high  $K_{m_{app}}$ (PEP) were not changed and the  $V_{max}$  were decreased, indicative of non-competitive inhibition.

Since filtration of the protein extract increased the stability of the enzyme, decreased the time required for preparation, and did not affect the kinetics compared with dialyzed enzyme, this procedure was employed in all further experiments.

### (3) Characterization of PEP carboxylase activity after gel filtration

The effect of pH on enzyme activity was investigated between pH 7.0 and 7.6 using the standard enzyme assay (Table 1) and PEP concentrations from 0.01 to 0.5 mM. Assays at low PEP levels and low pH (7.05; 7.18) resulted in minimal activity and these values were not reported.

pH profiles of PEPC activity were constructed for all PEP concentrations used (Figure 11). Increases in pH from 7.1 to 7.5 resulted in the most pronounced increase in activity which was stimulated three to four times at all levels of PEP.

Velocity versus PEP concentrations plots of the same data demonstrate hyperbolic kinetics and a decrease in  $V_{max}$  as pH decreased (Figure 12). Approximate estimates of the  $K_{m_{app}}$ (PEP) from these plots indicate pH independence.

Estimations of the  $K_{m_{app}}$ (PEP) and  $V_{max}$  were obtained from linear derivations of the same data. At all pH values tested

Figure 11: pH profiles of PEP carboxylase activity at near-saturated and PEP-limited substrate levels.

Enzyme activity was assayed spectrophotometrically at 340 nm in the presence of 10.7 mM K-Pi buffers pH 6.9 to 7.4, 16.7 mM  $\text{NaHCO}_3$ , 3.3 mM  $\text{MgCl}_2$ , 0.05 mM NADH, 0.2 ml enzyme extract and 0.5 ( $\Delta$ ), 0.3 ( $\blacktriangledown$ ), 0.1 ( $\bigcirc$ ) and 0.05 ( $\square$ ) mM PEP.

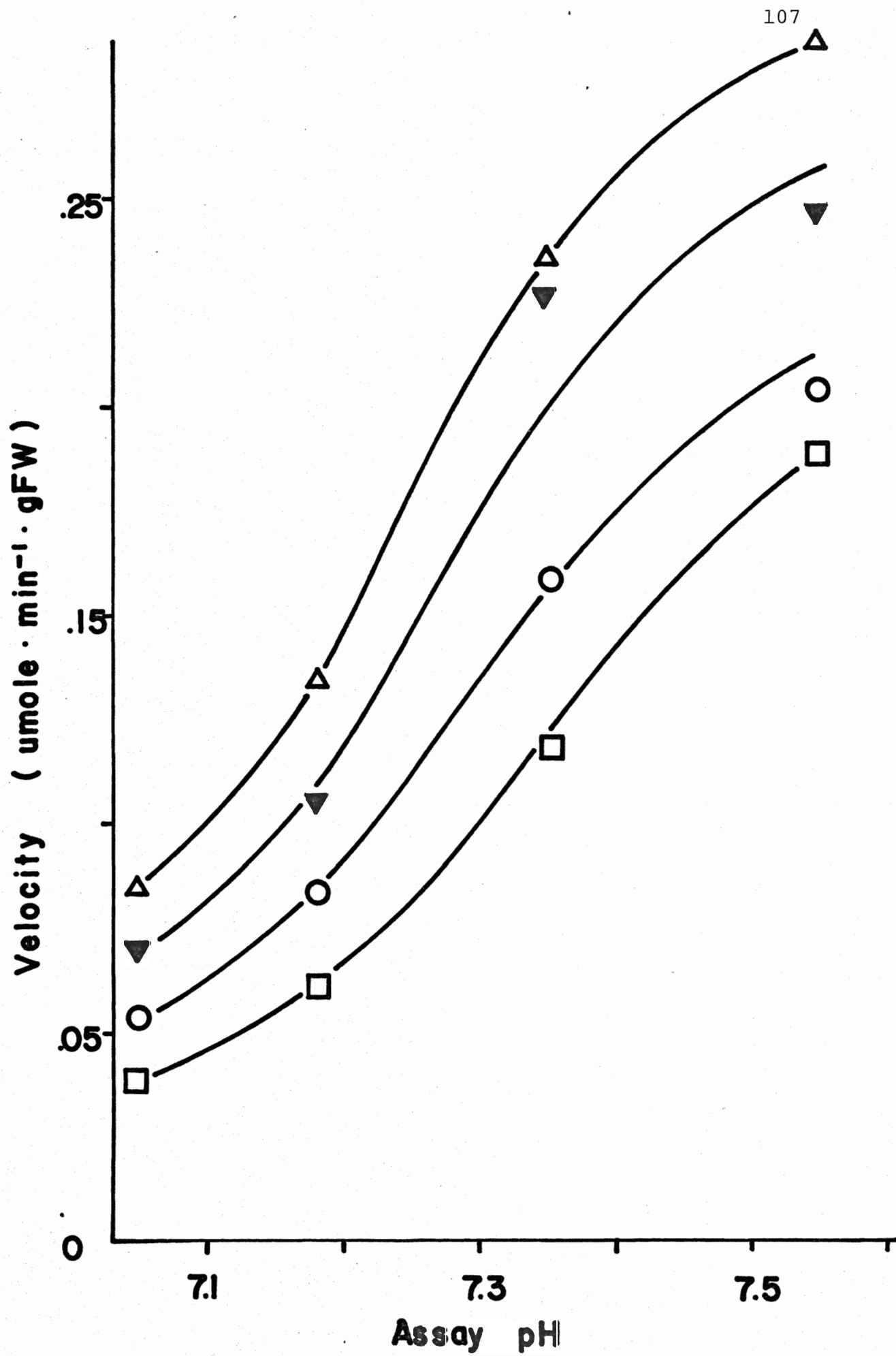
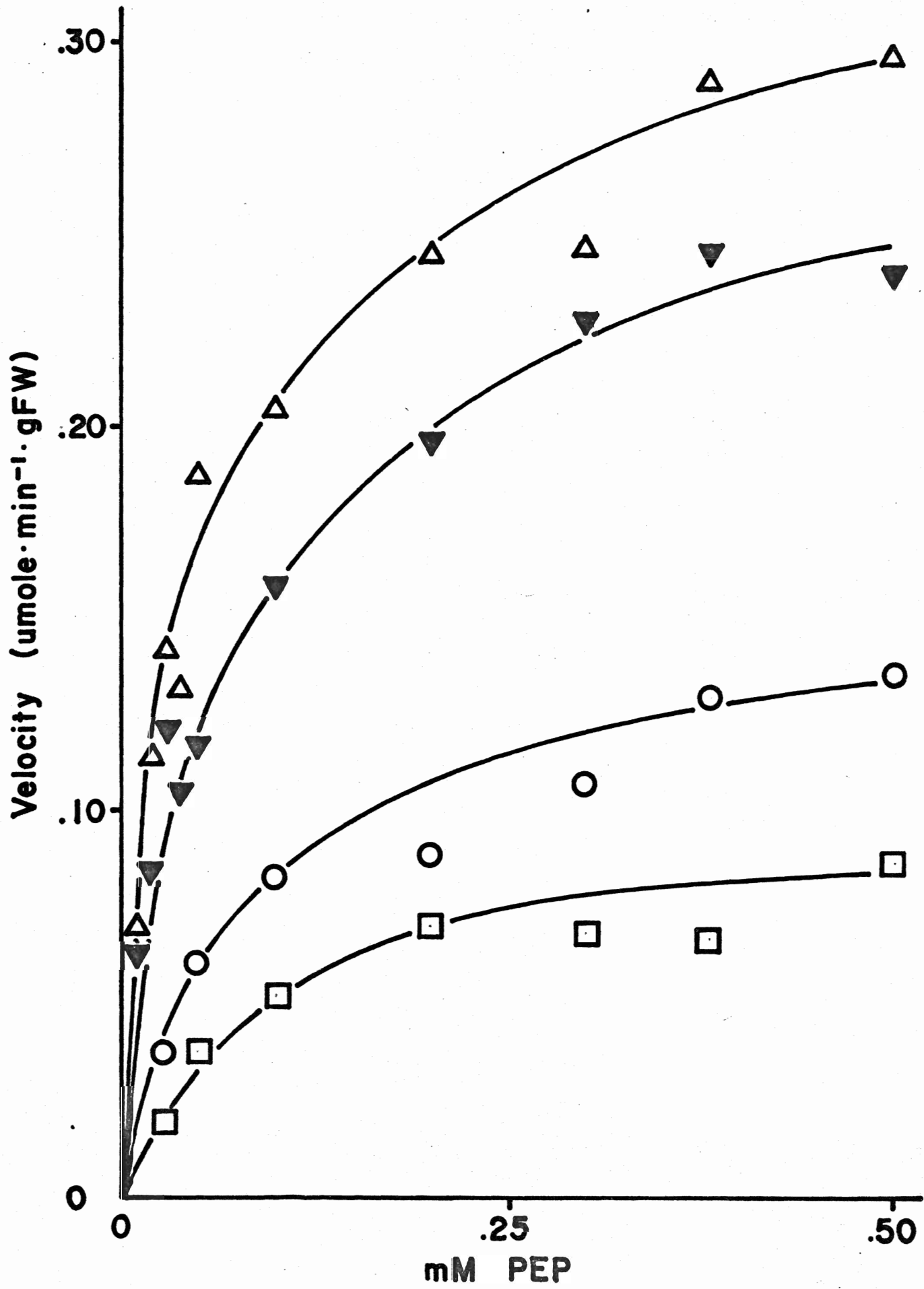


Figure 12: Effect of pH on PEP carboxylase activity as a function of the PEP concentration.

Enzyme activity was assayed spectrophotometrically at 340 nm in the presence of 16.7 mM  $\text{NaHCO}_3$ , 3.3 mM  $\text{MgCl}_2$ , 0.05 mM NADH, 0.01 to 0.5 mM PEP, 0.2 ml enzyme extract and 10.7 mM K-Pi buffers pH 6.9 ( $\square$ ), 7.05 ( $\circ$ ), 7.25 ( $\blacktriangledown$ ) and 7.4 ( $\triangle$ ).





the Lineweaver-Burk, Eadie-Hofstee, and Hanes plots were non-linear (Figure 13a, b and c) confirming the results obtained in Section (I,A,2). Both the high  $K_{mapp}(\text{PEP})$  of 0.6 to 1.0 mM and the low  $K_{mapp}(\text{PEP})$  of 0.02 to 0.04 mM were pH independent. Under conditions of high binding affinity,  $V_{max}$  decreased from  $0.35 \mu\text{mole} \cdot \text{min}^{-1} \cdot \text{g FW}$  at pH 7.55 to  $0.07 \mu\text{mole} \cdot \text{min}^{-1} \cdot \text{g FW}$  at pH 7.05. In contrast, conditions resulting in low binding affinity showed a higher turnover, as indicated by a  $V_{max}$  of  $0.67 \mu\text{mole} \cdot \text{min}^{-1} \cdot \text{g FW}$  at pH 7.55 and  $0.23 \mu\text{mole} \cdot \text{min}^{-1} \cdot \text{g FW}$  at pH 7.05.

Non-linear plots of linear transformations of Michaelis-Menton curve may indicate co-operative kinetics. However, Hill coefficients derived from Hill plots of these data are approximately equal to one and are not affected by pH (Figure 14).

The effect of pH on the  $K_{mapp}(\text{MgCl}_2)$  was determined by assaying the enzyme with 0.5 mM PEP and various  $\text{MgCl}_2$  concentrations (0.17 to 3.33 mM) from pH 7.05 to 7.70. The results demonstrate that the  $K_{mapp}(\text{MgCl}_2)$  decreased from 0.55 at pH 7.20 to 0.15 mM at pH 7.70 (Figure 15). The combined results of this section indicate that as pH is increased, so is catalytic efficiency and binding affinity for  $\text{MgCl}_2$ .

#### B. Effects of various buffer systems on PEP carboxylase and malic enzyme activities.

This section presents the results obtained for PEPC and malic enzyme activities in protein preparations extracted and

Figure 13: Effect of pH on linearly transformed plots of PEP carboxylase activity as a function of the PEP concentration.

Enzyme activity was assayed spectrophotometrically at 340 nm in the presence of 16.7 mM  $\text{NaHCO}_3$ , 3.3 mM  $\text{MgCl}_2$ , 0.5 mM NADH, 0.01 to 0.5 mM PEP, 0.2 ml enzyme extract and 10.7 mM K-Pi buffers pH 6.9 ( $\square$ ), 7.05 ( $\circ$ ), 7.25 ( $\blacktriangledown$ ) and 7.4 ( $\triangle$ ).

Figure 13(a): Lineweaver-Burk plot

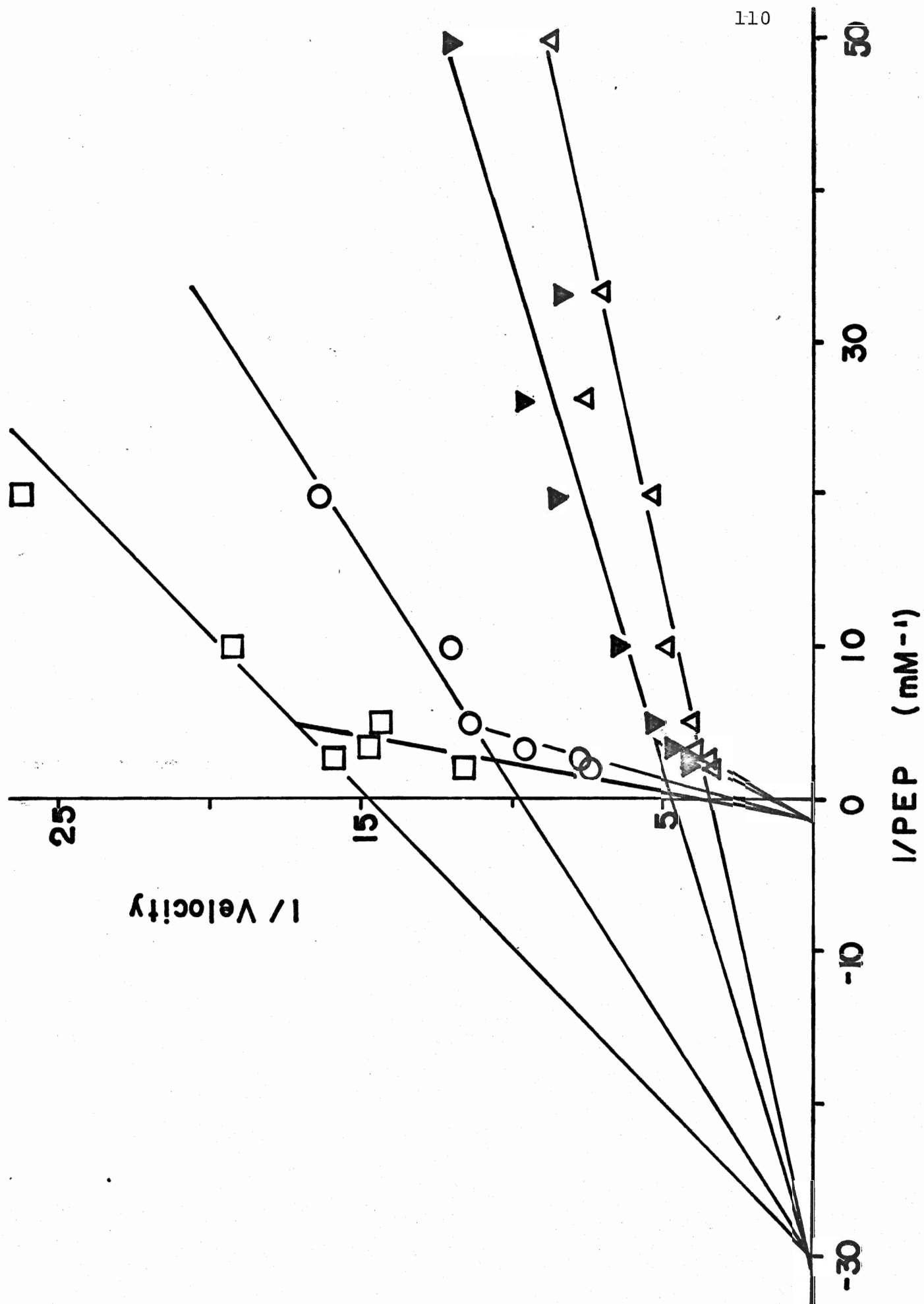


Figure 13(c): Hanes plot

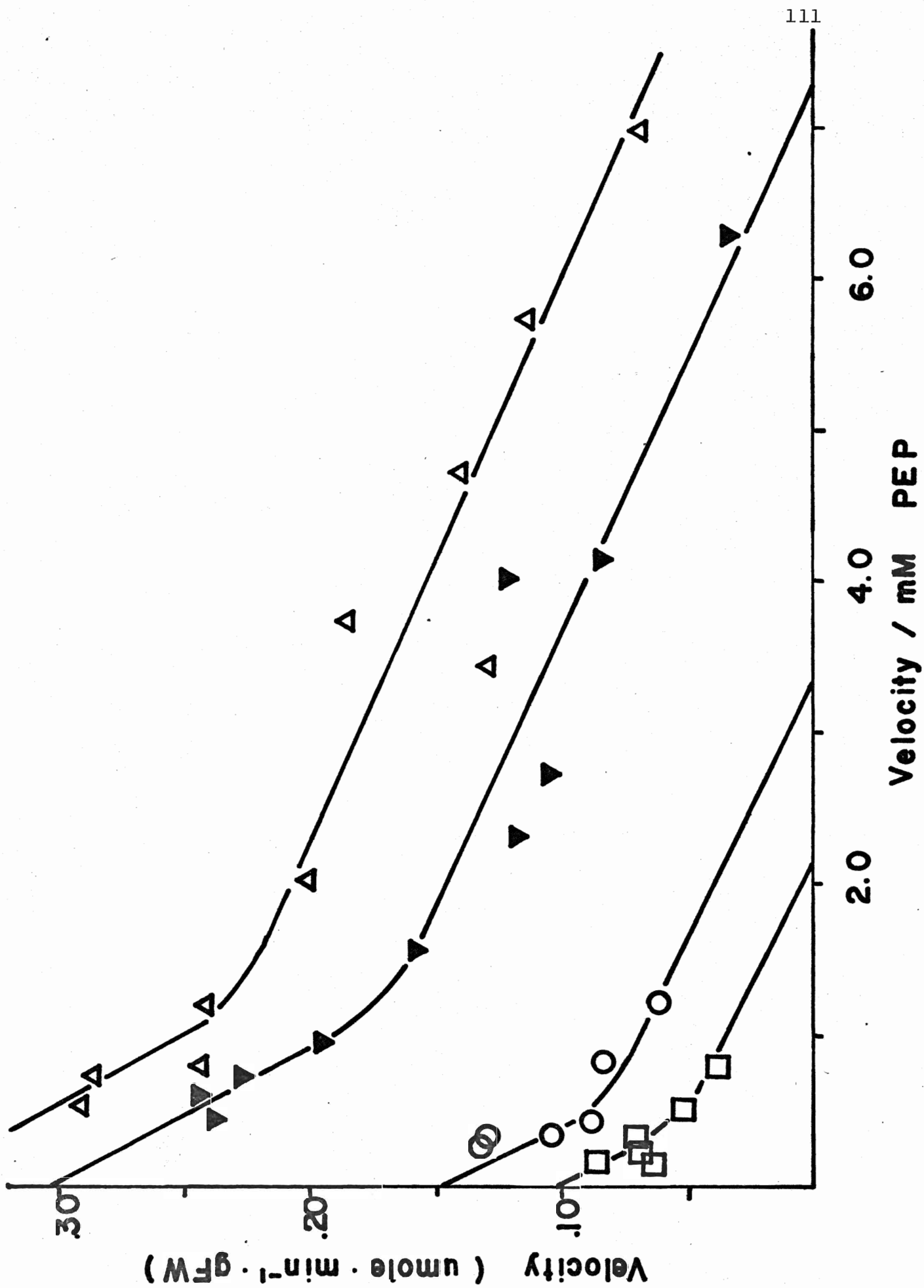


Figure 13(b): Eadie-Hofstee plot

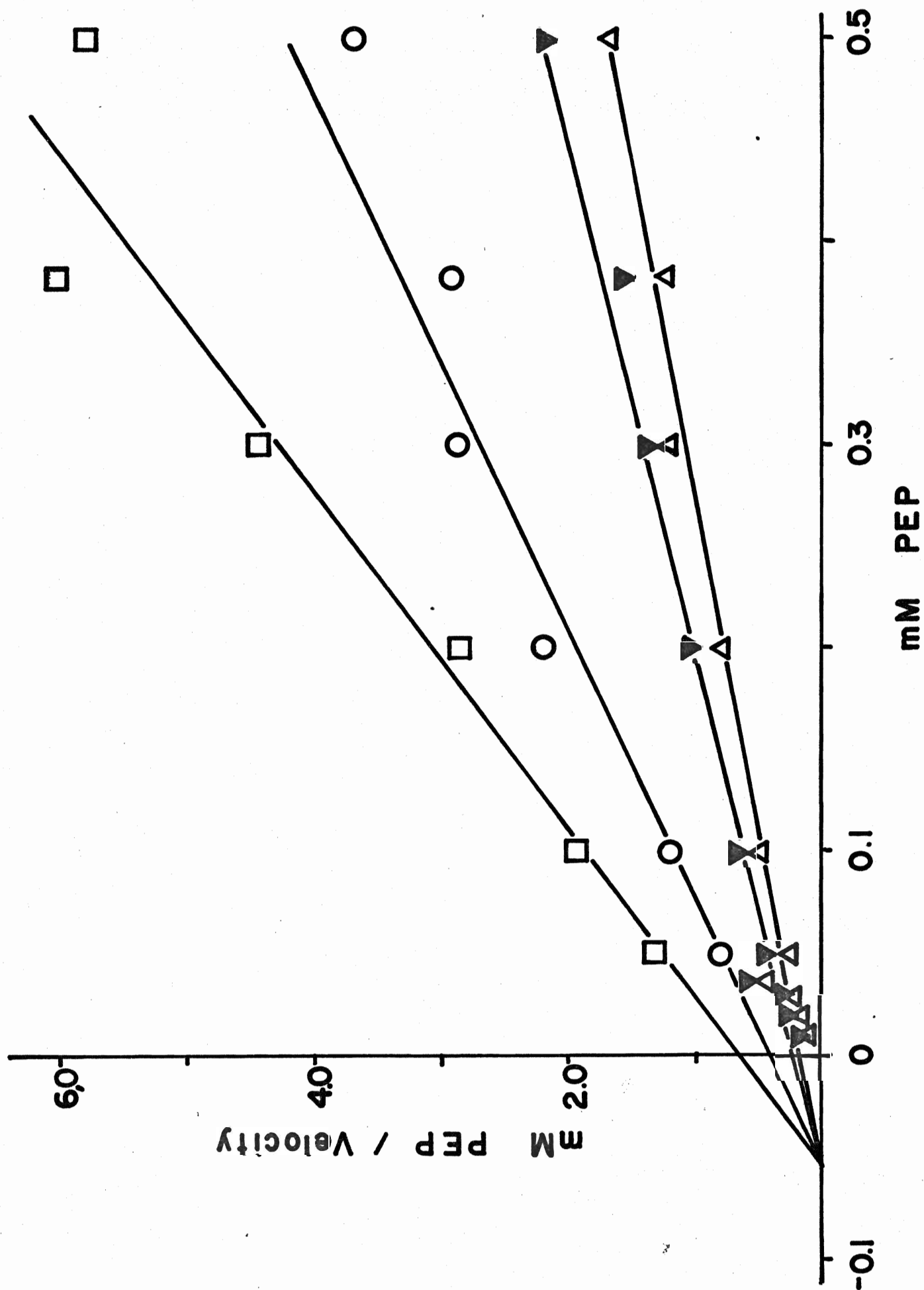


Figure 14: Effect of pH on the Hill plot of PEP carboxylase activity.

Enzyme activity was assayed spectrophotometrically at 340 nm in the presence of 16.7 mM  $\text{NaHCO}_3$ , 3.3  $\text{MgCl}_2$ , 0.05 mM NADH, 0.01 to 0.5 mM PEP, 0.2 ml enzyme extract and 10.7 mM K-Pi buffers pH 6.9 ( $\square$ ), 7.05 ( $\circ$ ), 7.25 ( $\blacktriangledown$ ) and 7.4 ( $\triangle$ ).



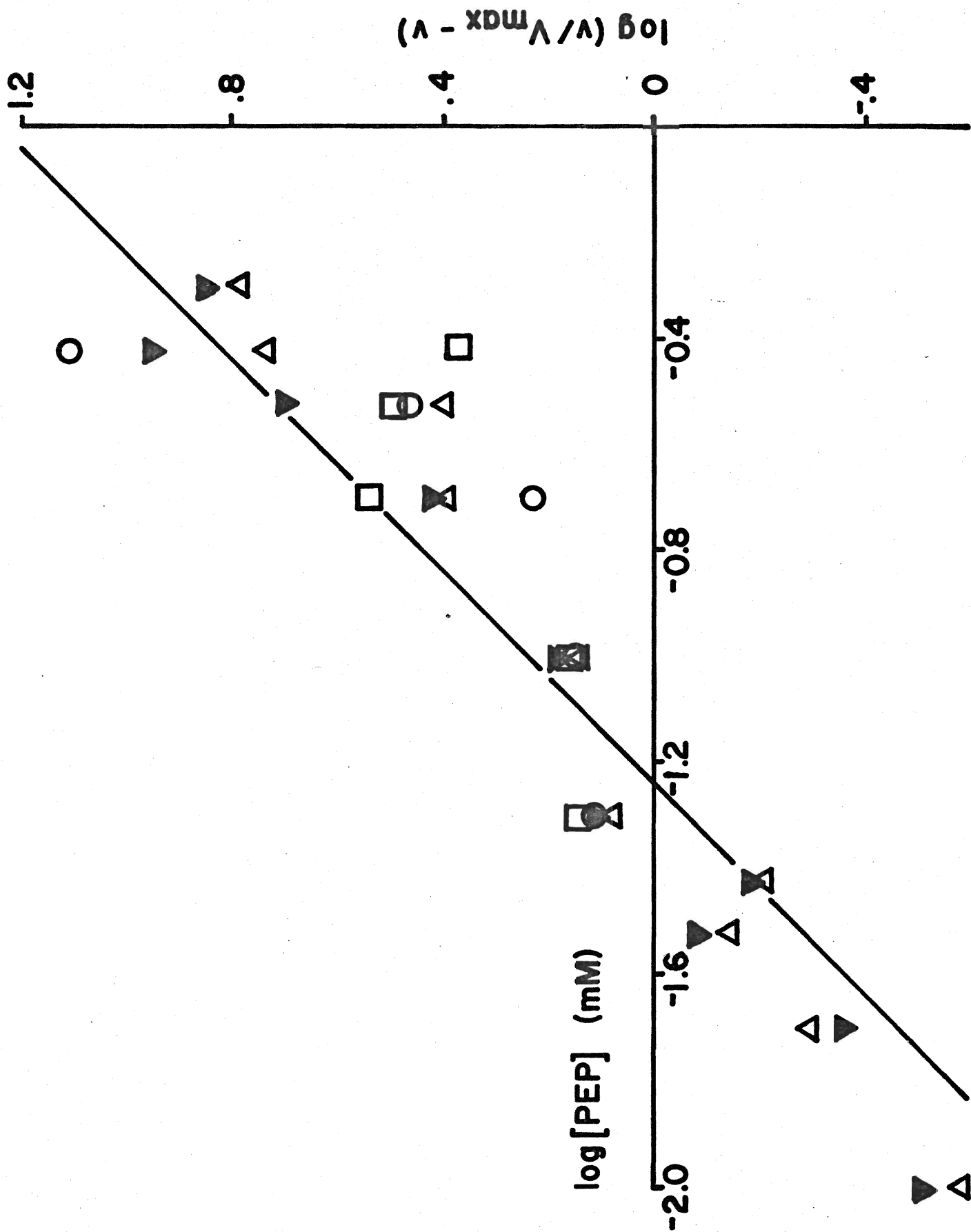
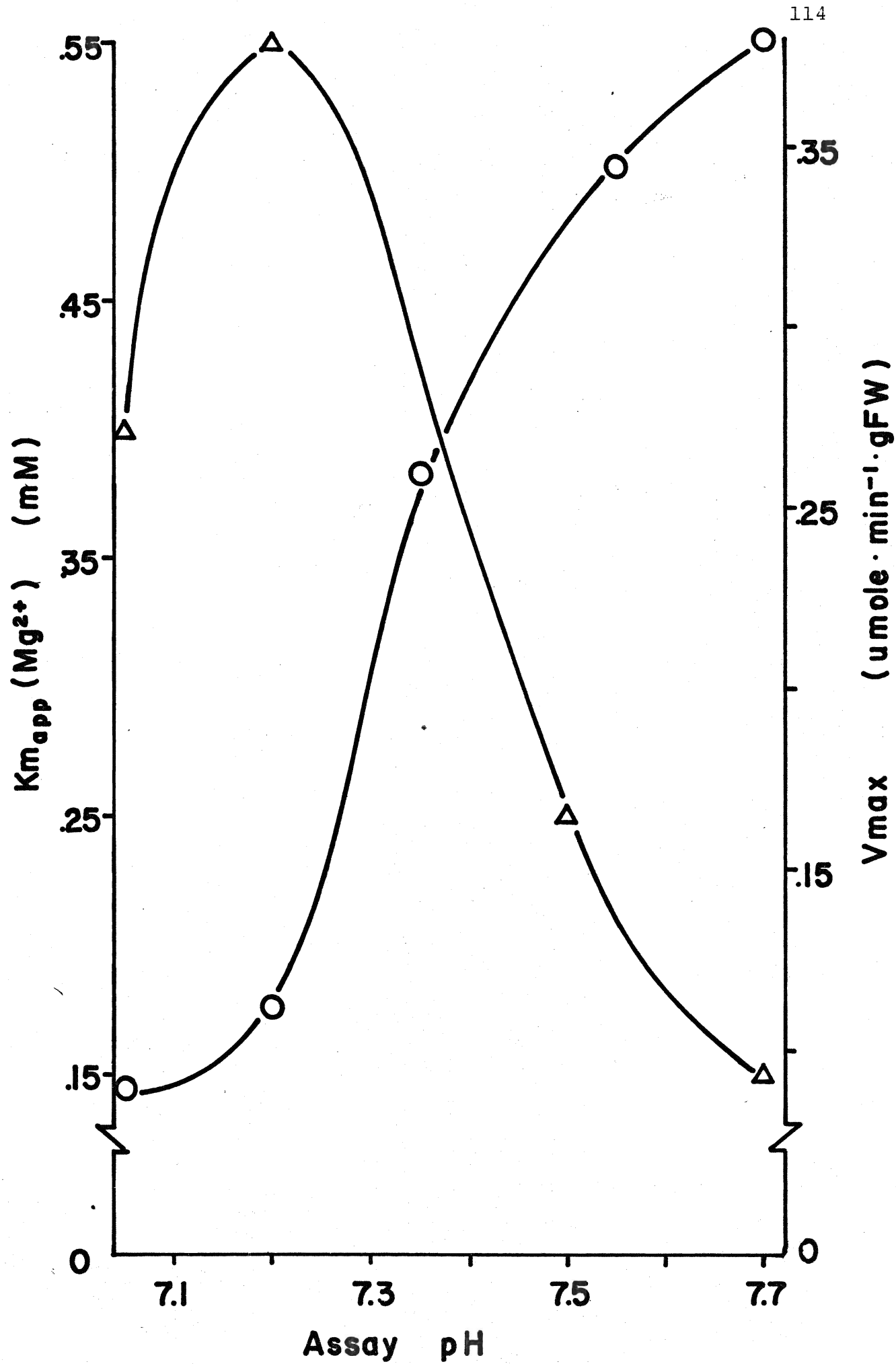


Figure 15: Effect of pH on the  $K_{m_{app}}(\text{MgCl}_2)$  and  $V_{max}$  of PEP carboxylase.

Enzyme activity was assayed spectrophotometrically at 340 nm in the presence of 10.7 mM K-Pi buffer pH 6.9 to 7.4, 16.7 mM  $\text{NaHCO}_3$ , 0.05 mM NADH, 0.5 mM PEP, 0.17 to 3.33 mM  $\text{MgCl}_2$  and 0.2 ml enzyme extract.  $K_{m_{app}}$  for  $\text{Mg}^{2+}$  ( $\Delta$ ) and  $V_{max}$  ( $\square$ ) were estimated from linear transformations of the  $V \times [\text{Mg}^{2+}]$  data.



assayed in a variety of buffer systems. The initial objective was to determine whether a single buffer system could be used for the extraction and assay of both PEPC and the malic enzyme over the pH range of 6.0 to 8.0.

(1) General survey of the effects of buffer species and pH on PEP carboxylase and malic enzyme activities

(a) PEP carboxylase

Protein was extracted and assayed in potassium phosphate, BES-KOH, BES-NaOH or Tris-BES buffers. Extraction buffers were adjusted to pH 7.4 and the assay buffers were prepared over a pH range of 6.9 to 7.9. Enzyme activity was measured with 0.5 mM PEP. Figure 16 indicates that maximum activity was observed when extracted and assayed with 20 mM potassium phosphate buffer. Activity in BES-KOH (25 or 50 mM), BES-NaOH (25 mM), or Tris-BES (25 mM) was 20 to 30% of the activity in phosphate buffer at all pH values tested. Enzyme activity in phosphate buffers using a Tris-BES (250 mM) extracted protein preparation was 20% (pH 7.1) to 50% (pH 7.5) of the activity obtained with phosphate extraction and assay buffers. However, in all assay systems activity increased with pH. This is good evidence that PEPC activity increases with pH independently of the buffer system. The ionic strength of each assay system used was approximately  $75 \text{ mM} \pm 15$ , and increases in pH from 7.0 to 7.5 increased the ionic concentration by at most 15%. Furthermore, the addition of 10 mM KCl, NaCl, or K-Pi (adjusted

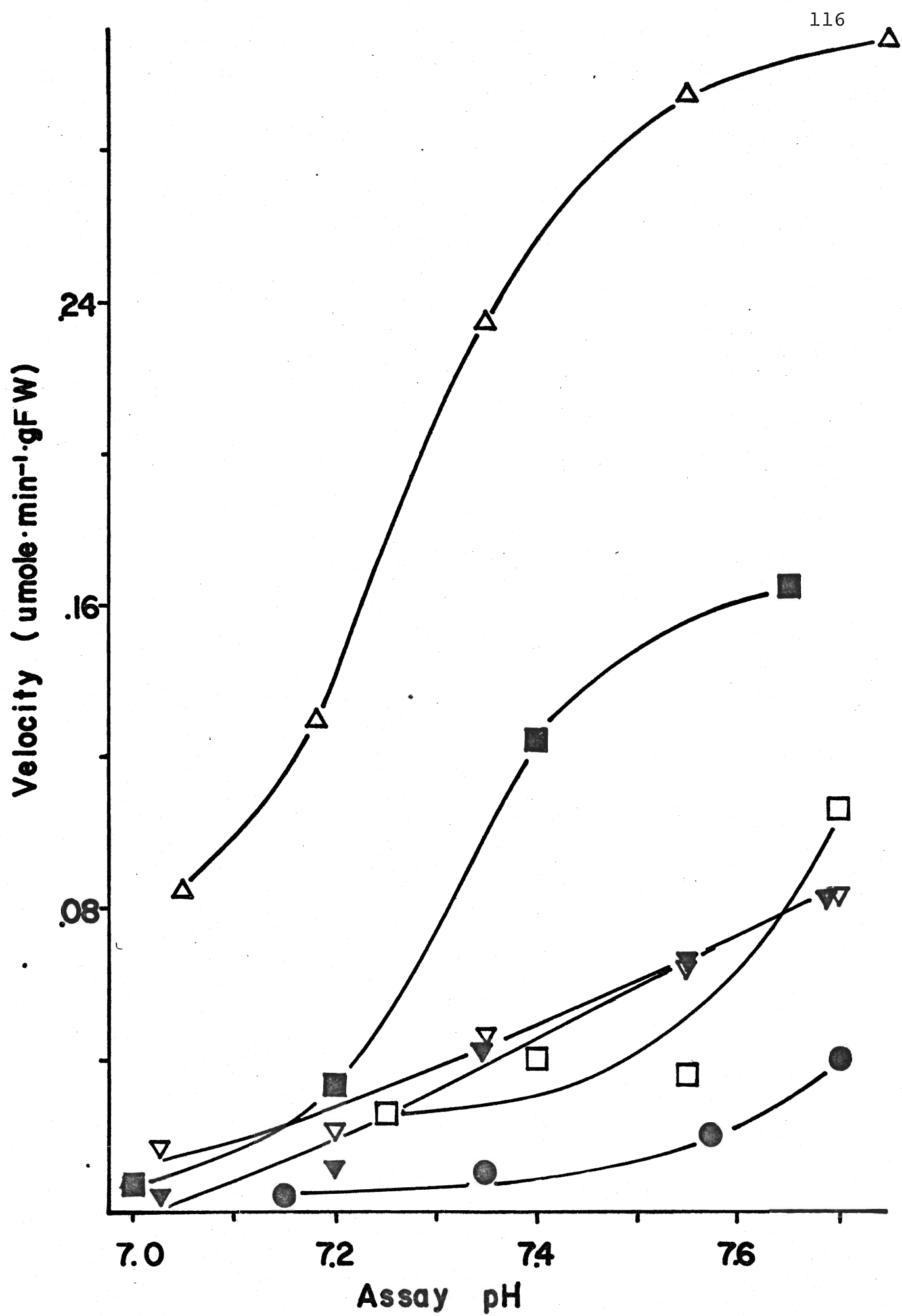
Figure 16: Effect of pH and various extraction and assay buffer species on PEP carboxylase activity.

Enzyme activity was assayed spectrophotometrically at 340 nm in the presence of 16.7 mM  $\text{NaHCO}_3$ , 3.3  $\text{MgCl}_2$ , 0.05 mM NADH, 0.5 mM PEP and 0.2 ml protein preparation extracted and assayed in the following buffers (pH 6.9 to 7.5):

	Extraction Buffer <sup>1</sup>	Assay Buffer <sup>2</sup>
△	20 mM K-Pi	10.7 mM K-Pi
●	250 mM Tris-BES	12.5 mM Tris-BES
▽	50 mM BES-KOH	12.5 mM BES-KOH
▼	50 mM BES-KOH	25 mM BES-KOH
□	25 mM BES-NaOH	12.5 mM BES-NaOH
■	250 mM Tris-BES	10.7 mM K-Pi

<sup>1</sup> Extraction buffer, initial concentration, pH 7.4

<sup>2</sup> Assay buffer, assay concentration



to the pH of the assay) to activity measured in 25 or 50 mM BES-NaOH or 25 mM Tris-BES did not significantly affect the rates of absorbance change. The results indicate that optimal PEPC activity required the presence of  $K^+$  and/or  $P_i$  in the extraction and assay medium.

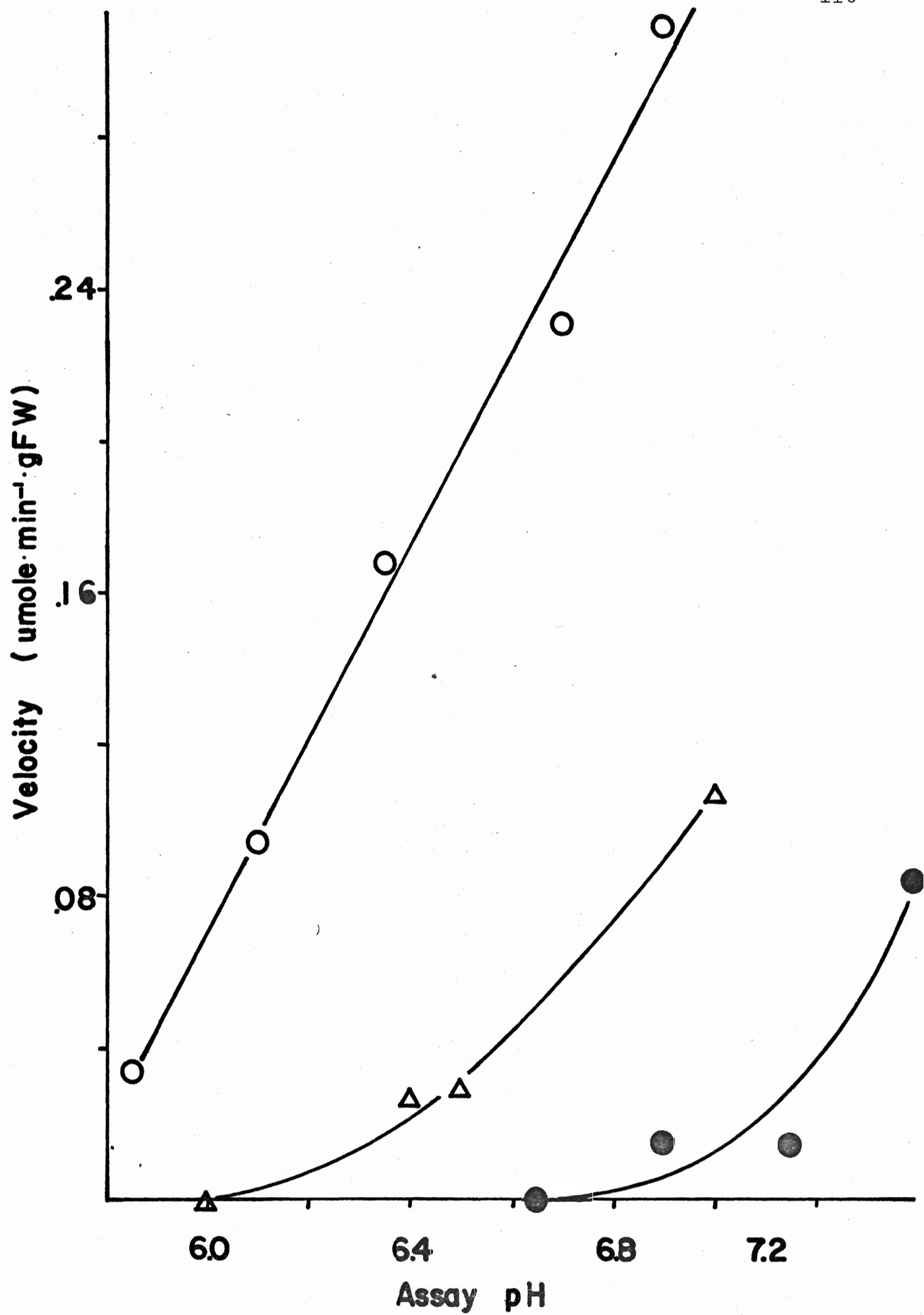
(b) The malic enzyme

Malic enzyme activity was extracted with 20 mM potassium phosphate buffers and assayed with 0.5 mM malate in 20 mM potassium phosphate, 50 mM Tris-HCl, or 50 mM histidine-KOH buffers pH 5.8 to 7.4 (Figure 17). Activity in Tris-HCl was not detectable at pH values lower than 6.8. At pH 7.0, activity in phosphate buffers was nine-fold higher than activity in Tris-HCl. However, at assay pH values greater than 7.0, an erratic increase in absorbance was observed in the presence or absence of malate, making these conditions unsuitable for activity measurements. The difference between these assays and those used for PEPC was the presence of  $NADP^+$  and  $MnCl_2$  rather than NADH and  $MgCl_2$ . However, the total absorbance increase was too large to account for an enzymic reduction of  $NADP^+$ . It is possible that  $MnCl_2$  and potassium phosphate may induce a general change in protein structure and aggregations at alkaline conditions, resulting in the large absorbance increases and decreases observed. Histidine buffers increased activity three- to five-fold over the phosphate system and extended pH range of detectable enzyme activity in the acidic region to less than pH 6.0.

Figure 17: Effect of assay buffer species and pH on malic enzyme activity from potassium phosphate extracted protein.

Enzyme activity was assayed spectrophotometrically at 340 nm in the presence of 1.0 mM  $\text{MnCl}_2$ , 0.5 mM  $\text{NADP}^+$ , 0.5 mM malate, 0.2 ml protein preparation extracted in 20 mM K-Pi buffer pH 7.4 and 25 mM histidine-KOH buffer pH 5.8 to 6.8 (○), 25 mM Tris-HCl buffer pH 6.6 to 7.4 (●) or 10.0 mM K-Pi buffer pH 6.0 to 7.0 (△). Extraction buffer levels indicate initial concentrations and assay buffer levels indicate assay concentrations.





Enzyme activity was also determined from proteins extracted with histidine-KOH (5 and 50 mM), BES-KOH (5 and 50 mM), or Tris-BES (5 and 250 mM) buffers at pH 7.4 using the procedure outlined in Methods (I,B). Assays were conducted with 50 mM histidine-KOH, 25 or 50 mM BES-KOH, or 25 mM Tris-BES respectively (pH 6.0 to 7.8) and 0.5 mM malate. Figure 18 demonstrates that maximal activity was observed when extraction and assay involved histidine-KOH or Tris-BES buffers. Additionally, protein extracted with either potassium phosphate or histidine-KOH resulted in similar activities when assayed in histidine-KOH (compare Figures 17 and 18). In contrast, extraction and assay with BES-KOH reduced the observed activity 70 to 90% compared with histidine or tris-BES buffers.

The ionic concentration of all assays employed was  $40 \text{ mM} \pm 10$ , with the exception of the Tris-BES assay having an ionic strength of approximately 12.5 mM. Additionally, the ionic strength of these systems changes at most by 15% as the pH is increased from 6.0 to 7.0. The results indicate that malic enzyme activity was not dependent on ionic strength. It is possible, however, that optimal activity requires a net neutral or positively charged buffer species in the assay medium. Protein aggregation due to a negatively charged species (i.e.,  $\text{BES}^-$  or  $\text{HPO}_4^{2-}/\text{H}_2\text{PO}_4^-$ ) and  $\text{Mn}^{+2}$  complexing may provide an explanation for the low activities observed in BES-KOH and phosphate buffer systems.

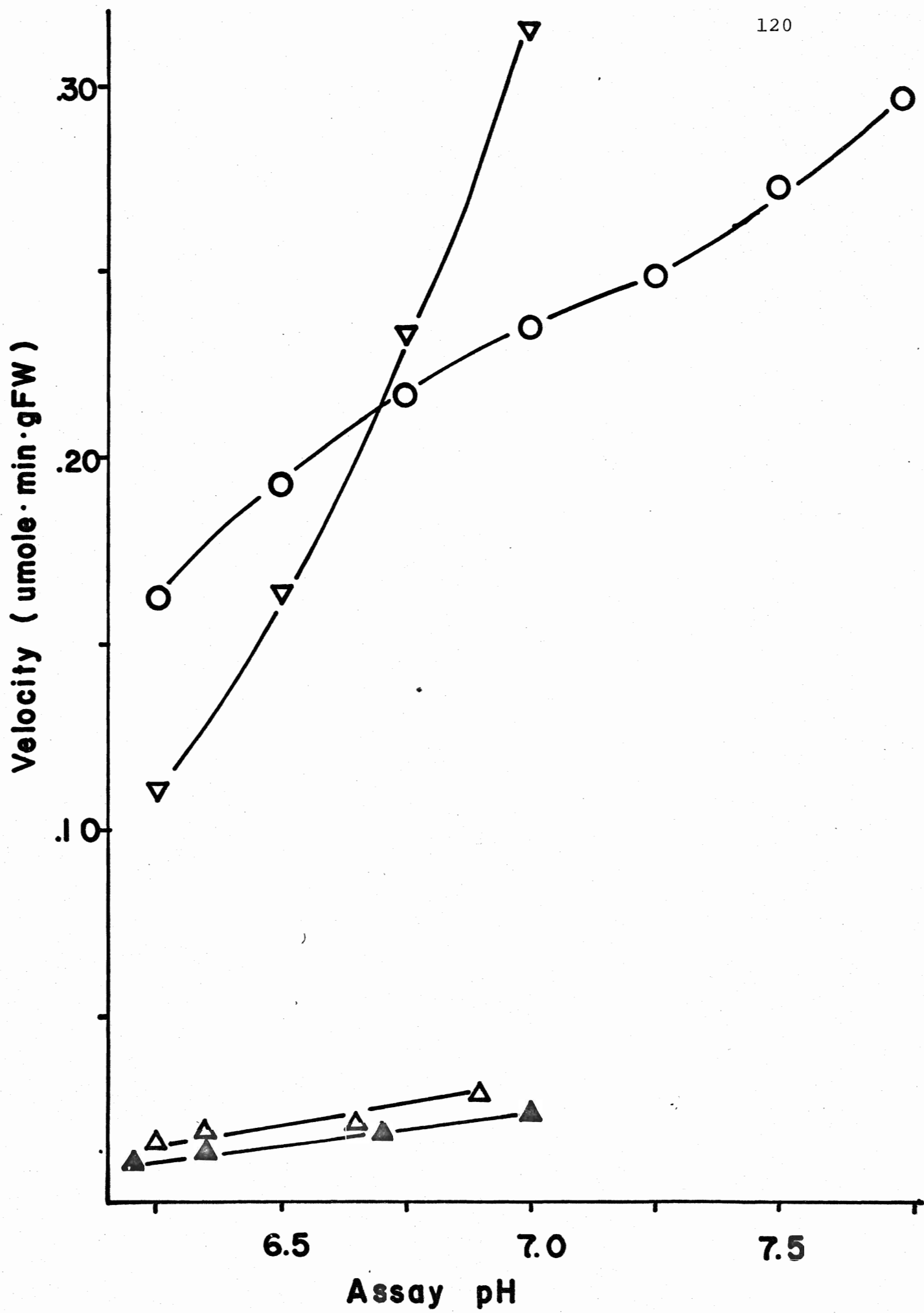
Figure 18: Effect of pH and various extraction and assay buffer species on malic enzyme activity

Enzyme activity was assayed spectrophotometrically at 340 nm in the presence of 1.0 mM  $\text{MnCl}_2$ , 0.5 mM  $\text{NADP}^+$ , 0.5 mM malate and 0.2 ml protein preparation extracted and assayed in the following buffers.

Extraction Buffer	Assay Buffer
○ 250 mM Tris-BES pH 7.4	12.5 mM Tris-BES pH 6.25-7.75
▽ 50 mM histidine-KOH pH 6.8	25 mM histidine-KOH pH 6.25-7.00
△ 50 mM BES-KOH pH 7.4	12.5 mM BES-KOH pH 6.25-7.00
▲ 50 mM BES-KOH pH 7.4	25 mM BES-KOH pH 6.25-7.00

<sup>1</sup> Extraction buffer, initial concentration

<sup>2</sup> Assay buffer, assay concentration



In conclusion, histidine buffers resulted in optimal malic enzyme activity between pH 6.0 and 7.0. However, it was necessary to assay malic enzyme activity at pH values above 7.0. Since the pK of histidine·HCl is 6.0, the buffering capacity would be greatly reduced above neutrality, limiting the pH range for malic enzyme assay. Tris-BES buffers, on the other hand, resulted in similar rates of absorbance change and permitted the assay of activity above neutrality due to the wide range of buffering.

(2) Tris-BES buffers: Effect of various concentrations on PEP carboxylase and malic enzyme activities.

The Tris-BES buffer system contains high buffering power between pH 7.0 and 9.0, and thus would be ideal for assaying PEPC and the malic enzyme over a physiological pH range. Previous results (I,B,1.a) demonstrated that PEPC activity was extremely low when extracted and assayed in Tris-BES buffers compared with potassium phosphate buffers. An attempt was made to attain higher PEPC activity by investigating the effects of a range of Tris-BES extraction and assay concentrations on enzyme activity. The conditions resulting in maximal malic enzyme activity are also reported.

(a) PEP carboxylase

Protein was extracted in 5 mM, and 25 or 250 mM Tris-BES buffers pH 7.4. Enzyme activity was measured with 0.5 mM PEP and Tris-BES buffers pH 7.15 or 7.70 (25, 100, 250 or 500 mM).

Table 12 indicates that maximum activity was obtained in 25 mM assay buffers extracted with the 250 mM buffer. The maximum activity observed was 70% lower than activity obtained in the standard potassium phosphate extraction and assay buffers.

Plots of activity versus assay ionic strength for each Tris-BES concentration used indicate a decrease in activity of  $0.01 \mu\text{mole} \cdot \text{min}^{-1} \cdot \text{g FW}$  for each 20 mM increase in assay ionic strength at pH 7.15 and 7.70 (Figure 19). The ionic strength of the potassium phosphate assay system was approximately 75 mM. However, in an ionic concentration of 75 mM, the activity observed in Tris-BES buffers was approximately 15% that observed in phosphate buffers (see Table 12). This suggests that the differences in observed activities in the two buffer systems was not due to a non-specific ionic concentration requirement. In all further experiments PEPC activity was extracted and assayed in potassium phosphate buffers.

(b) The malic enzyme

Malic enzyme activity was measured with 0.5 mM malate and the same permutations of Tris-BES employed in the previous section for PEPC activity. Assay pH values of 6.5 and 7.2 were used. Results indicate that the protein extracted in 250 mM Tris-BES and assayed in 25 mM gave maximum or near maximum activity at pH 6.5 and 7.2 (Table 13).

Plots of activity versus assay ionic strength for each Tris-BES concentration used indicate that activity at pH 7.2

Table 12: Effect of Tris-BES extraction buffer concentrations, and Tris-BES assay buffer concentrations and pH on PEP carboxylase activity

Assay Buffer		mM Extraction Buffer (pH 7.4)	
pH	mM	25	250
7.0	25	21.0 (14.5)	100.0 (29.0)
	100	5.0 (3.5)	66.0 (19.5)
	250	2.5 (1.0)	50.0 (14.5)
	500	5.0 (3.5)	8.0 (2.5)
7.5	25	10.0 (5.0)	100.0 (22.0)
	100	11.0 (5.5)	84.0 (19.0)
	250	5.0 (0.5)	40.5 (9.0)
	500	8.0 (4.5)	47.0 (10.5)

Enzyme was extracted in 25 or 250 mM Tris-BES buffer pH 7.4, or 20 mM K-Pi buffer pH 7.4. Assays were performed in the presence of 12.5, 50, 125 or 250 mM Tris-BES buffer pH 7.0 or 7.5 (Tris-BES extracted protein) or 10.7 mM K-Pi buffer pH 6.9 or 7.4 (K-Pi extracted protein). Assays contained 3.3 mM  $\text{MgCl}_2$ , 16.7 mM  $\text{NaHCO}_3$ , 0.05 mM NADH, 0.5 mM PEP and 0.2 ml enzyme extract. Activities in Tris-BES buffers are expressed as a percentage of the maximal activity observed at each assay buffer pH. Bracketed values indicate the activity observed in Tris-BES buffers as a percentage of activity observed in K-Pi buffers.

Figure 19: Effect of pH and assay ionic strength on PEP carboxylase activity assayed in various Tris-BES buffers.

Enzyme activity was assayed spectrophotometrically at 340 nm in the presence of 12.5 to 250 mM Tris-BES buffer pH 7.9 (●) or 7.5 (○), 16.7 mM  $\text{NaHCO}_3$ , 3.3 mM  $\text{MgCl}_2$ , 0.05 mM NADH, 0.5 mM PEP and 0.2 ml protein preparation extracted with 250 mM Tris-BES buffer pH 7.4. Assay u indicates total ionic concentration of the assay.



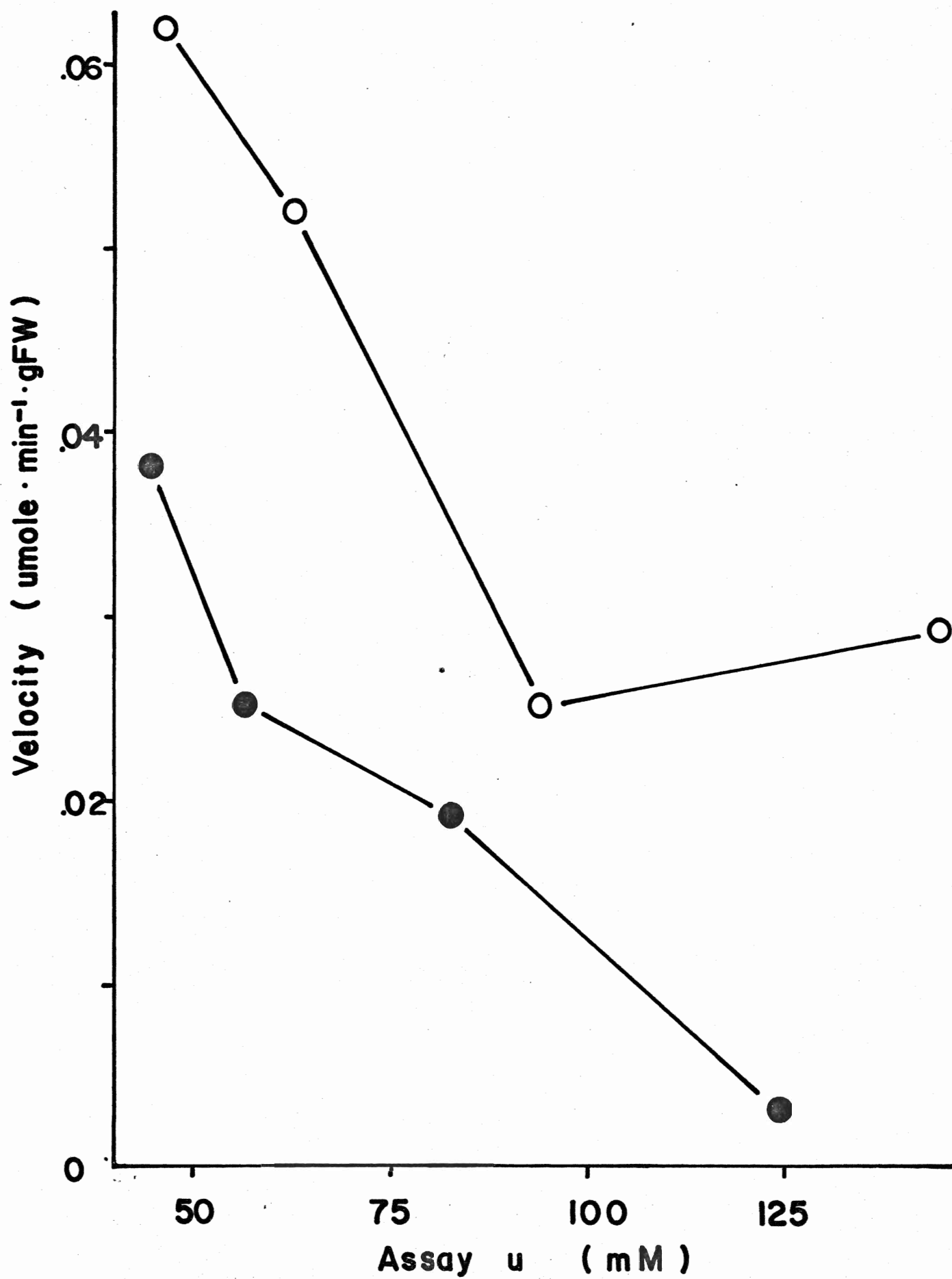


Table 13: Effect of Tris-BES extraction buffer concentrations, and Tris-BES assay buffer concentrations and pH on malic enzyme activity.

Assay Buffer		mM Extraction Buffer (pH 7.4)		
pH	mM	25	100	250
6.5	25	10.0	34.5	100.0
	100	14.5		71.8
	250	10.9		57.3
	500	34.5		83.6
7.2	25	35.1	100.0	100.0
	100	49.9		105.8
	250	44.8		123.4

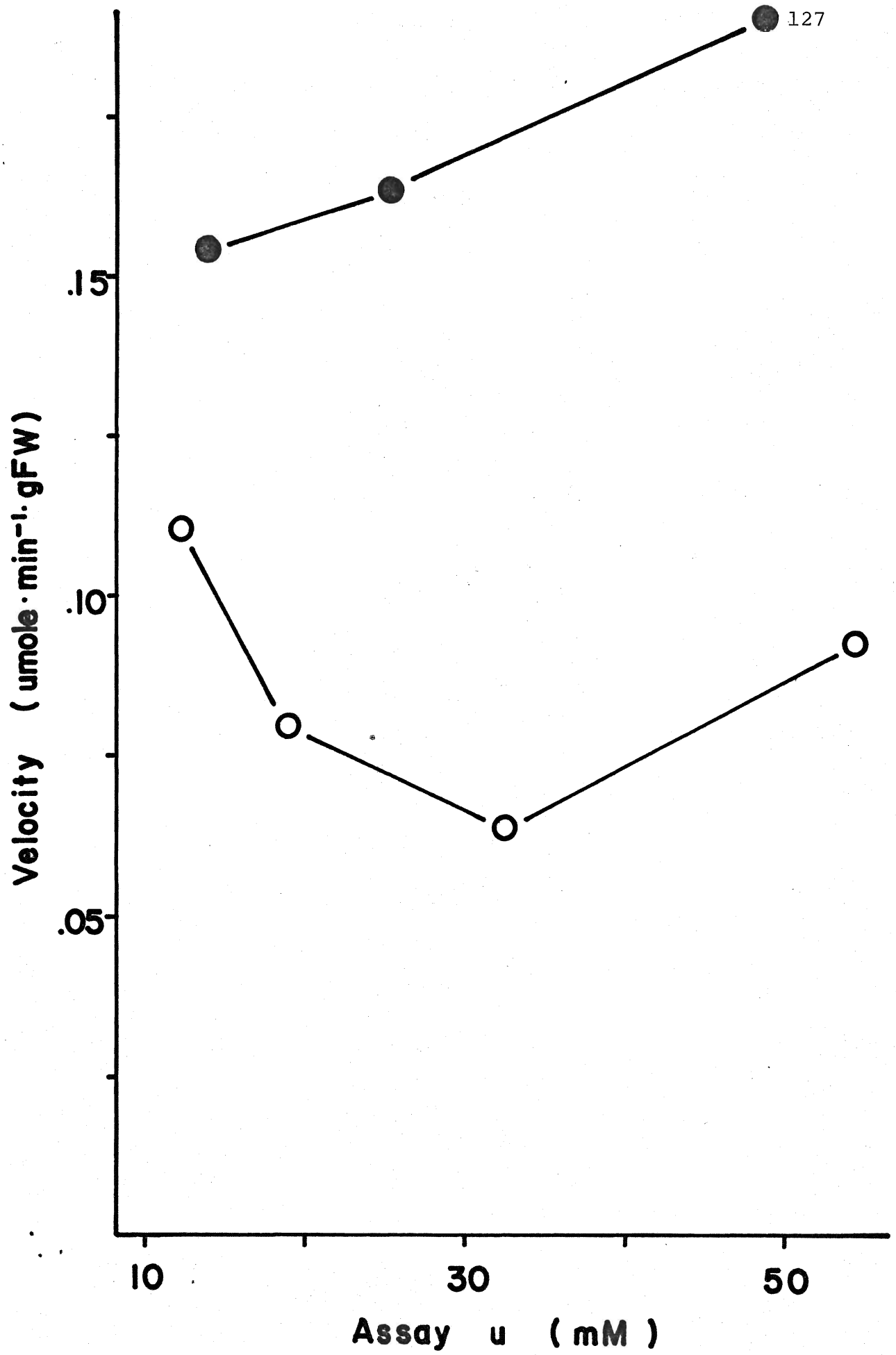
Enzyme was extracted in 25, 100 or 250 mM Tris-BES buffer pH 7.4. Assays were performed in the presence of 12.5, 50, 125 or 250 mM Tris-BES buffer pH 6.5 or 7.2. Assays contained 1.0 mM  $\text{MnCl}_2$ , 0.5 mM  $\text{NADP}^+$ , 0.5 mM malate and 0.2 ml enzyme extract. Activities are expressed as a percentage of activity extracted in 250 mM Tris-BES and assayed in 25 mM Tris-BES pH 6.5 or 7.2.

increased  $0.01 \mu\text{mole} \cdot \text{min}^{-1} \cdot \text{g}$  FW for each 10 mM increase in ionic strength (Figure 20). Activity at pH 6.5 did not show any proportionality with increases in ionic concentration.

The results presented in this section demonstrate that maximum PEPC activity was obtained when extracted and assayed in phosphate buffers, whereas maximal malic enzyme activity was observed in protein extracted and assayed with Tris-BES buffers. Therefore, in all further experiments, these separate systems were employed for assaying PEPC and malic enzyme activities.

Figure 20: Effect of pH and assay ionic strength on malic enzyme activity assayed in various Tris-BES buffers.

Enzyme activity was assayed spectrophotometrically at 340 nm in the presence of 1.0 mM  $\text{MnCl}_2$ , 0.5 mM  $\text{NADP}^+$ , 0.5 mM malate, 12.5 to 250 mM Tris-BES buffer pH 6.5 (○) or 12.5 to 125 mM Tris-BES buffer pH 7.2 (●), and 0.2 ml protein preparation extracted with 250 mM Tris-BES buffer pH 7.4. Assay u indicates total ionic concentration of the assay.



## II. Characterization of malic enzyme activity

This section is divided into three sub-sections. The first deals with spectrophotometric assays demonstrating the dependence of the rate of absorbance change on all substrates. The second section presents results obtained from radiochemical assays in determining the reaction product(s), and their substrate dependence. The last section reports the effects of pH on the kinetics of the malic enzyme.

### A. Substrate, coenzyme and cofactor dependence of the spectrophotometric reaction rate

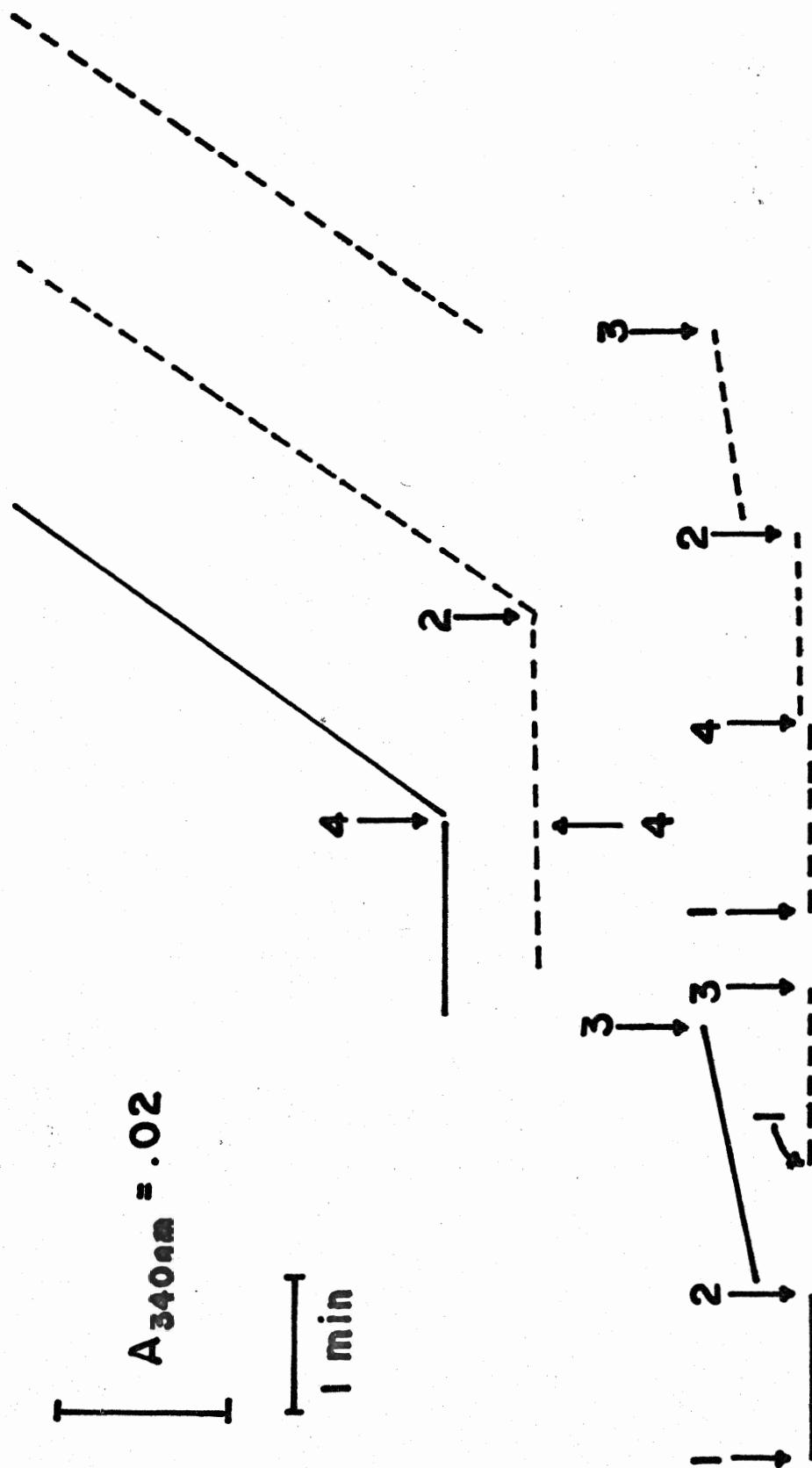
#### (1) $\text{NADP}^+$ reduction

Enzyme activity was measured at pH 7.25 using the standard assay system (Table 6).  $\text{MnCl}_2$ ,  $\text{NADP}^+$  and malate were added to the cuvette consecutively and rates of absorbance change were determined after each addition. The order of addition was varied so that the assay system was completed with malate,  $\text{MnCl}_2$ , or  $\text{NADP}^+$ . The results indicate that rates of absorbance increase rose dramatically when all components of the assay system were present and confirm the presence of malic enzyme activity (Figure 21). In the absence of  $\text{NADP}^+$ , or  $\text{NADP}^+$  and malate, absorbance increases of 6 to 12% of the maximal rate were observed. Preliminary results indicated that this was a malic enzyme independent phenomenon involving  $\text{Mn}^{2+}$ , Tris-BES buffer, and protein (Methods (II,B,1(i))).

Figure 21: Effect of malate,  $\text{MnCl}_2$  and  $\text{NADP}^+$  on the rates of absorbance change at 340 nm.

Enzyme was incubated at 30°C in the presence of 12.5 mM Tris-BES buffer pH 7.4. Three separate recorder traces are shown, each with the following additions.

- (1) 0.2 ml enzyme extract + 12.5 mM Tris-BES pH 7.4
- (2) 1.0 mM  $\text{MnCl}_2$
- (3) 0.5 mM  $\text{NADP}^+$
- (4) 0.5 mM malate





When 0.5 mM  $\text{NAD}^+$  was substituted for  $\text{NADP}^+$  in the standard assay, there was no detectable increase in absorbance during a five minute assay. 1.0 mM  $\text{MgCl}_2$  substitution for 1.0 mM  $\text{MnCl}_2$  in the standard assay resulted in an 80 to 90% decrease in the rate of absorbance increase. These results indicate that the malic enzyme catalyzed reaction has specific coenzyme ( $\text{NADP}^+$ ) and cofactor ( $\text{Mn}^{2+}$ ) requirements.

## (2) NADPH oxidation

Conditions resulting in maximal activity at pH 7.25 were determined by varying the assay concentrations of pyruvate and  $\text{NaHCO}_3$ , and assaying with 1.0 mM  $\text{MnCl}_2$  and 0.04 mM NADPH. Table 14 indicates that maximal activity was obtained with 1.0 mM  $\text{MnCl}_2$ , 33.3 mM  $\text{NaHCO}_3$ , and 13.3 mM pyruvate. NADPH concentrations between 400 and 40  $\mu\text{M}$  did not change the maximal rate of absorbance decrease observed.  $\text{MnCl}_2$ , NADPH, pyruvate, and  $\text{NaHCO}_3$  were added consecutively to the cuvette and the rates of absorbance change were determined after each addition. Figure 22 demonstrates that the maximal rate of absorbance decrease was obtained on addition of pyruvate to the otherwise complete assay system. Similar results were obtained when NADPH,  $\text{MnCl}_2$ , or  $\text{NaHCO}_3$  were added last.

Maximal rates of  $\text{NADP}^+$  reduction (Figure 21) and NADPH oxidation (Figure 22) at pH 7.25 indicate an activity ratio of 4:1.

Table 14: Effect of various concentrations of pyruvate and  $\text{NaHCO}_3$  on the rates of pyruvate carboxylation.

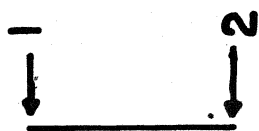
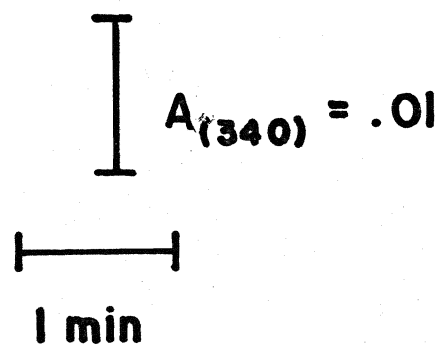
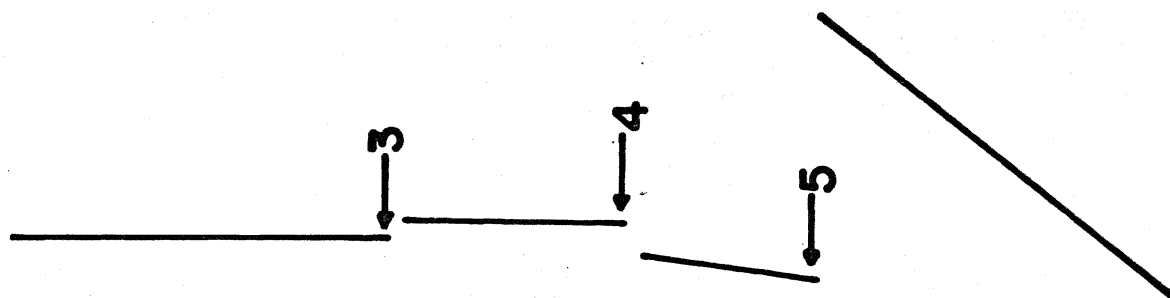
mM Pyruvate	mM $\text{NaHCO}_3$		
	1.67	6.67	33.33
0.67	28.0	18.5	20.5
6.67	48.7	51.2	62.5
13.33	56.5	50.0	100.0
26.67	54.2	57.0	96.5

Spectrophotometric assays were performed in the presence of 1.0 mM  $\text{MnCl}_2$ , 0.05 mM NADPH, 12.5 mM Tris-BES buffer pH 7.25, 0.2 ml enzyme extract and various concentrations of pyruvate and  $\text{NaHCO}_3$  as tabulated. Activities are expressed as a percentage of activity observed with 13.33 mM pyruvate and 33.33 mM  $\text{NaHCO}_3$ .

Figure 22: Effect of pyruvate,  $\text{NaHCO}_3$ ,  $\text{MnCl}_2$  and NADPH  
on the rates of absorbance change at 340 nm.

Enzyme was incubated at 30°C in the presence of 12.5 mM Tris-BES buffer pH 7.25. Additions to the reaction mixture were made as follows.

- (1) 0.2 ml enzyme extract + 12.5 mM Tris-BES pH 7.25
- (2) 0.05 mM NADPH
- (3) 1.0 mM  $\text{MnCl}_2$
- (4) 33.3 mM  $\text{NaHCO}_3$
- (5) 13.3 mM pyruvate



## B. Radiochemical assays

(1) Dependence of labelled product accumulation on all substrates, cofactor, and coenzyme.

Malate decarboxylation was assayed at pH 7.25 in the presence of 0.5 mM U-[ $^{14}\text{C}$ ]-malate using the standard assay system (Table 6), or omitting  $\text{MnCl}_2$  or  $\text{NADP}^+$ . The ethylacetate fraction was analyzed in one experiment for labelled pyruvate-DNP, and the ethanolamine fraction was analyzed for labelled  $\text{CO}_2$  in another (Methods (II,B,2 (iii))). Pyruvate carboxylation was assayed in the presence of 33.3 mM [ $^{14}\text{C}$ ]- $\text{NaHCO}_3$  at pH 7.25 under standard assay conditions (Table 10), or in the absence of  $\text{MnCl}_2$ , pyruvate, or NADPH. The aqueous fraction was analyzed for labelled malate (Methods II,B,2 (iii))). Results indicated that maximal recovery of radioactivity in the ethyl acetate, ethanolamine, and aqueous fractions required the presence of all substrates, cofactor and coenzymes (Table 15). This data indicates the presence of malic enzyme activity in the protein extract.

(2) Evidence for pyruvate being the major product of a malate dependent reaction.

Enzyme activity was assayed at pH 7.25 in the presence of U[ $^{14}\text{C}$ ]-malate and  $\text{MnCl}_2$  and/or  $\text{NADP}^+$  (Table 9). 2,4-Dinitro-phenylhydrazine (-DNP) derivatives in the reaction mixture were analyzed for label using the procedure outlined in Methods (II,B, 2 (iv))). Figure 23 illustrates the thin layer chromatogram of authentic OAA- and pyruvate-DNP, 2,4-DNP and a sample of the

Table 15: Radioactivity recovered in the ethyl acetate (pyruvate-DNP), ethanolamine (CO<sub>2</sub>) and aqueous (malate) fractions of a malic enzyme catalyzed reaction: Dependence on substrates, coenzyme and cofactor.

Assay	Malate Decarboxylation		Pyruvate Carboxylation
Components	Ethyl Acetate Fraction	Ethanolamine Fraction	Aqueous Fraction
Full Assay	100.0	100.0	100.0
-MnCl <sub>2</sub>	6.5	7.5	0.0
-NADP <sup>+</sup>	2.0	0.0	N.A.
-NADPH	N.A. <sup>1</sup>	N.A.	0.0
-Pyruvate	N.A.	N.A.	0.0

<sup>1</sup>N.A., not applicable as these reagents are not components of the assay system.

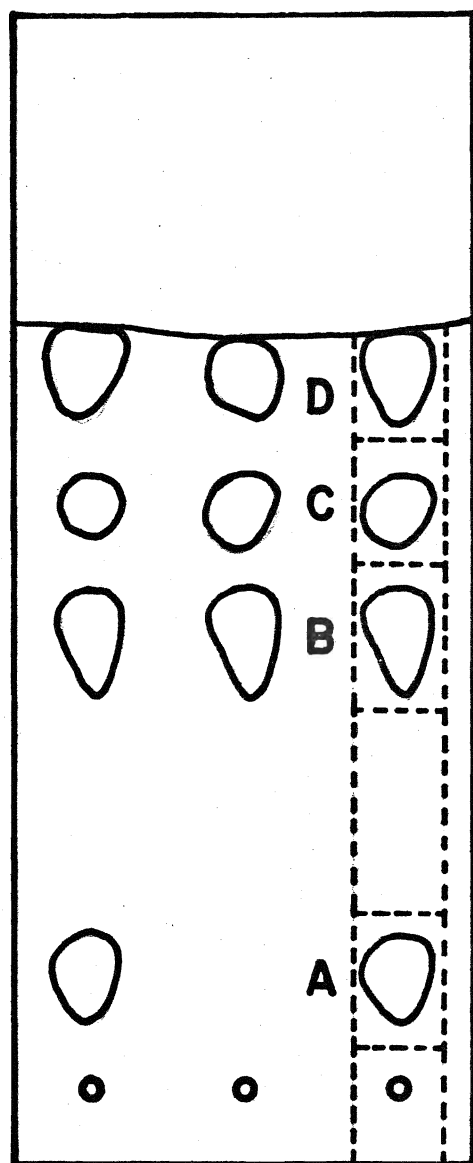
Accumulation of label in the ethyl acetate or ethanolamine fraction was measured in the presence of 12.5 mM Tris-BES buffer pH 7.25, 0.5 mM malate (2  $\mu\text{Ci}\cdot\mu\text{mole}^{-1}$ ) and 0.1 ml enzyme extract  $\pm$  1.0 mM MnCl<sub>2</sub>, 0.5 mM NADP<sup>+</sup>. Accumulation of label in the aqueous fraction was measured in the presence of 12.5 mM Tris-BES buffer pH 7.25, 33.3 mM NaHCO<sub>3</sub> (0.1  $\mu\text{Ci}\cdot\mu\text{mole}^{-1}$ ) and 0.1 ml enzyme extract  $\pm$  1.0 mM MnCl<sub>2</sub>, 0.05 mM NADPH or 13.3 mM pyruvate. Accumulated label is expressed as a percentage of label accumulated in the presence of all assay components (full assay).

Figure 23: Chromatogram of the 2,4-dinitrophenylhydrazine derivatives of OAA, pyruvate, and a malate,  $\text{MnCl}_2$ ,  $\text{NADP}^+$  utilizing reaction, including the scheme for gel sectioning.

Enzyme was assayed radiochemically in the presence of 12.5 mM Tris-BES buffer pH 7.25, 1.0 mM  $\text{MnCl}_2$ , 0.5 mM  $\text{NADP}^+$  0.5 mM U- $[^{14}\text{C}]$ -malate and 0.1 ml enzyme extract. 2,4-DNP derivatives were collected in the ethyl acetate fraction (1) and chromatographed on Silica gel G alongside authentic OAA- (2) and pyruvate-DNP (3). A solvent system of butanol: $\text{H}_2\text{O}$ :ethanol in a 70:20:10 (v:v:v) ratio was employed. The migration path of the sample was sectioned as indicated.

Figure 24: Autoradiogram of the 2,4-dinitrophenylhydrazine derivatives of a malate,  $\text{MnCl}_2$  and  $\text{NADP}^+$  utilizing reaction.

The chromatogram produced in Figure 23 was exposed to X-ray film for three weeks and then developed. The regions of radioactivity corresponding to the migration of OAA- and pyruvate-DNP are noted.

**Chromatogram**

solvent  
front

Pyruvate-  
DNP

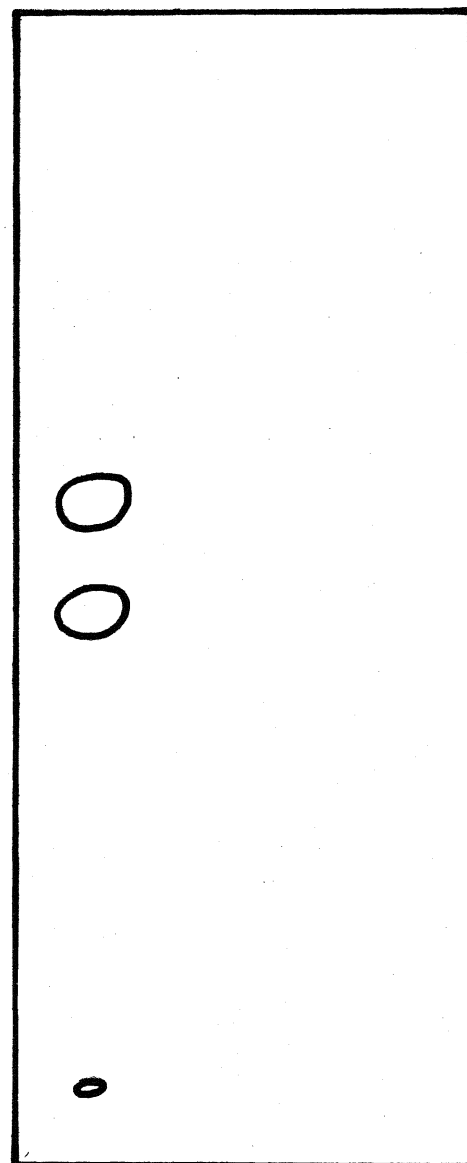
OAA-DNP

origin

2

3

1

**Autoradiogram**

1

2

3



ethyl acetate fraction from a standard reaction mixture. This figure demonstrates that authentic OAA-DNP migrated to three distinct yellow coloured regions, the two faster moving components migrating the same distance as the yellow coloured authentic pyruvate-DNP. OAA is highly unstable and decarboxylates non-enzymatically to pyruvate. Pyruvate was presumably present in two isomeric forms, one migrating slightly in front of the other. Unreacted 2,4-DNP was deep yellow in colour and migrated with the solvent front. When the ethyl acetate fraction was chromatographed alone, only the yellow unreacted 2,4-DNP region was detectable in day light. Under ultraviolet radiation, one weakly fluorescing region was observed which coincided with the migration pattern of authentic pyruvate-DNP.

Sections of gel were removed from the plate according to the pattern illustrated in Figure 23. Results indicated that the majority of the radioactivity from a complete assay system was recovered in the section coinciding with the slower moving pyruvate-DNP component (Table 16). A relative percentage (38%) of radioactivity was also recovered in the faster moving pyruvate-DNP component, and in further experiments both of these areas were combined and counted. No radioactivity was detected in the slowest moving OAA-DNP component. In the absence of  $\text{MnCl}_2$  or  $\text{NADP}^+$ , no detectable radioactivity was recovered in any region of the gel sections analyzed.

Autoradiography of the chromatogram demonstrates radioactivity at the origin of all ethyl acetate samples (Figure 24).

Table 16: Radioactivity recovered in gel sections of the ethyl acetate fraction of a malic enzyme catalyzed reaction: Dependence on  $\text{MnCl}_2$  and  $\text{NADP}^+$ .

Spot	Full Assay	- $\text{MnCl}_2$	- $\text{NADP}^+$
A (OAA-DNP)	0	0	0
B (Pyruvate-DNP)	100	2.8	1.3
C (Pyruvate-DNP)	38	2.5	0
D (2,4-DNP)	0	0	0

Spot, refers to the position of authentic OAA- and pyruvate-DNP and unreacted 2,4-DNP after silica gel thin layer chromatography in a 70:20:10 (v:v:v) butanol: $\text{H}_2\text{O}$ :ethanol solvent (see Figure 23)

The ethyl acetate fraction of a reaction performed in the presence of 12.5 mM Tris-BES buffer pH 7.25, 0.5 mM malate ( $2.0 \mu\text{Ci} \cdot \mu\text{mole}^{-1}$ ) and 0.1 ml enzyme extract  $\pm 1.0$  mM  $\text{MnCl}_2$  or 0.5 mM  $\text{NADP}^+$  was subjected to thin layer chromatography with a mixture of authentic OAA- and pyruvate-DNP. Accumulated label is expressed as a percentage of the label in Spot B.

However, radioactivity at any other region was observed only for the assays which contained  $\text{MnCl}_2$  and  $\text{NADP}^+$ . This region of high radioactivity coincided with the migration pattern of authentic pyruvate-DNP. Malate did not migrate significantly in the solvent system employed in these experiments. This indicates that the region of high radioactivity at the origin was probably due to unreacted labelled malate which had been carried over into the ethyl acetate fraction.

(3) Evidence for malate being the major product of a pyruvate dependent reaction.

Enzyme activity was assayed following the protocol outlined in Table 10. Samples of the aqueous fraction were co-chromatographed with L-malate (Methods (II,B,2 (iii))). Figure 25 illustrates the migration pattern of L-malate to three distinct areas. Additional yellow regions appeared when the aqueous fraction was chromatographed due to other organic acids (e.g., pyruvate) present in the reaction mixture. Radioactivity was recovered in the section coinciding with the intermediate malate component. When either  $\text{MnCl}_2$ , NADPH, or pyruvate were missing from the assay, no detectable radioactivity was recovered in any of the gel sections (Table 17).

#### C. Kinetics of the malic enzyme as a function of pH

Malic enzyme activity was assayed spectrophotometrically with 0.01 to 0.97 mM malate in 25 mM Tris-BES buffers pH 6.0 to

Figure 25: Chromatogram of malate and the aqueous fraction of a pyruvate,  $\text{NaHCO}_3$ ,  $\text{MnCl}_2$  and NADPH utilizing reaction including the scheme for gel sectioning.

Enzyme activity was assayed radiochemically in the presence of 12.5 mM Tris-BES buffer pH , 1.0 mM  $\text{MnCl}_2$ , 0.05 mM NADPH, 13.3 mM pyruvate, 33.33  $[\text{}^{14}\text{C}]$ - $\text{NaHCO}_3$  and 1.0 ml enzyme extract. The aqueous fraction (1) was chromatographed on cellulose alongside authentic malate (2) in a phenol:  $\text{H}_2\text{O}$ :formic acid solvent solution (75:25:1; v:v:v). The migration path of the samples was sectioned as indicated.

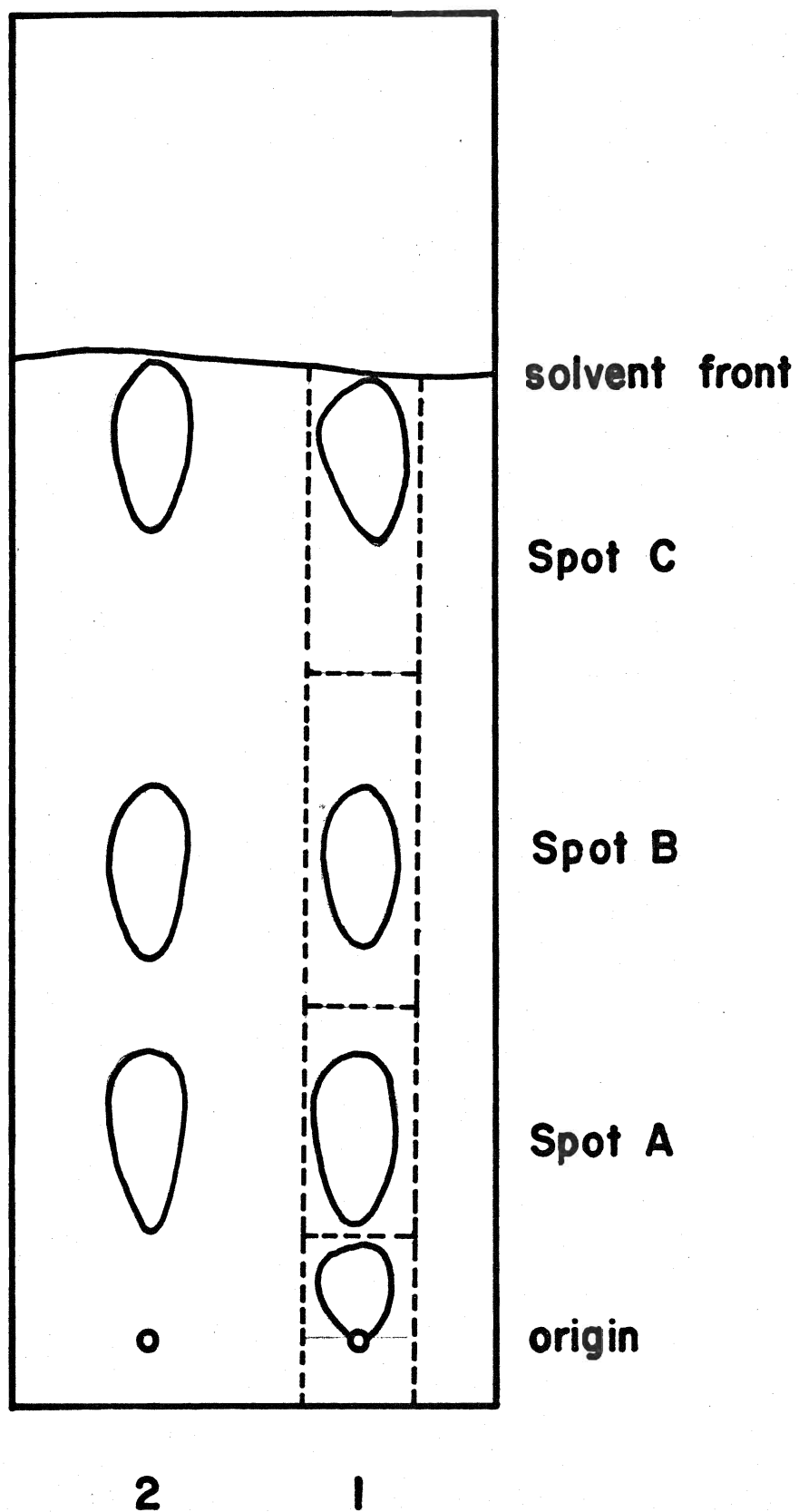


Table 17: Radioactivity recovered in gel sections of the aqueous fraction of a malic enzyme catalyzed reaction: Dependence on pyruvate,  $\text{MnCl}_2$  and NADPH

Spot <sup>1</sup>	Full Assay	-pyruvate	- $\text{MnCl}_2$	-NADPH
A	0	0	0	0
B	100.0	0	0	0
C	0	0	0	0

<sup>1</sup> Spot, refers to the positions of authentic malate after cellulose thin layer chromatography in a 75:25:1 (v:v:v) phenol:H<sub>2</sub>O:formic acid solvent (refer to Figure 25).

The aqueous fraction of a reaction performed in the presence of 12.5 mM Tris-BES buffer pH 7.25, 33.3 mM [<sup>14</sup>C]-NaHCO<sub>3</sub> (0.1  $\mu\text{Ci} \cdot \mu\text{mole}^{-1}$ ) and 0.1 ml enzyme extract  $\pm$  1.0 mM  $\text{MnCl}_2$ , 13.3 mM pyruvate or 0.05 mM NADPH was subjected to thin layer chromatography with authentic malate. Accumulated label is expressed as a percentage of label accumulated in Spot B.

7.75 (Table 6). The following results were obtained from one representative experiment.

pH profiles indicate that activity measured in the presence of malate concentrations greater than 0.1 mM increased as pH was increased (Figure 26). In contrast, activity assayed with low malate levels was not significantly affected by pH changes. Maximum activity was observed with malate concentrations between 0.3 mM (pH 6.5) and 0.5 mM (pH 7.5). Higher malate concentrations inhibited activity at all pH values tested. Activity decreased 50% at pH 6.0 and 20% at pH 7.5 when malate levels were increased from 0.50 to 0.97 mM.

Velocity versus malate concentration plots were constructed for activity measured from pH 6.5 to 7.25 (Figure 27). The plots indicate substrate inhibition at all pH values. At malate concentrations less than 0.1 mM activity was not affected by pH changes.

The apparent  $K_m(\text{malate})$  and  $V_{\max}$  were determined for each assay pH using linear transformations of the Michaelis-Menton hyperbola for the previous data (Figure 28a, b and c). The plots indicate that the  $K_{m_{\text{app}}}(\text{malate})$  of 0.1 mM and  $V_{\max}$  of  $0.3 \mu\text{mole} \cdot \text{min}^{-1} \cdot \text{g FW}$  were not affected by pH. Each of the linear plots demonstrated the substrate inhibition phenomenon in a characteristic manner. At high malate levels, the Lineweaver-Burk (Figure 28a) and Hanes (Figure 28c) plots are concave upwards, and the Eadie-Hofstee plot (Figure 28b) is concave downwards. These deviations from linearity indicate

Figure 26: pH profiles of malic enzyme activity at near-saturated and malate-limited substrate levels.

Enzyme activity was assayed spectrophotometrically at 340 nm in the presence of 12.5 mM Tris-BES buffer pH 6.0 to 7.75, 1.0 mM  $\text{MnCl}_2$ , 0.5 mM  $\text{NADP}^+$ , 0.2 ml enzyme extract and 0.97 ( $\Delta$ ), 0.5 ( $\nabla$ ), 0.1 ( $\bigcirc$ ) and 0.03 ( $\square$ ) mM malate.



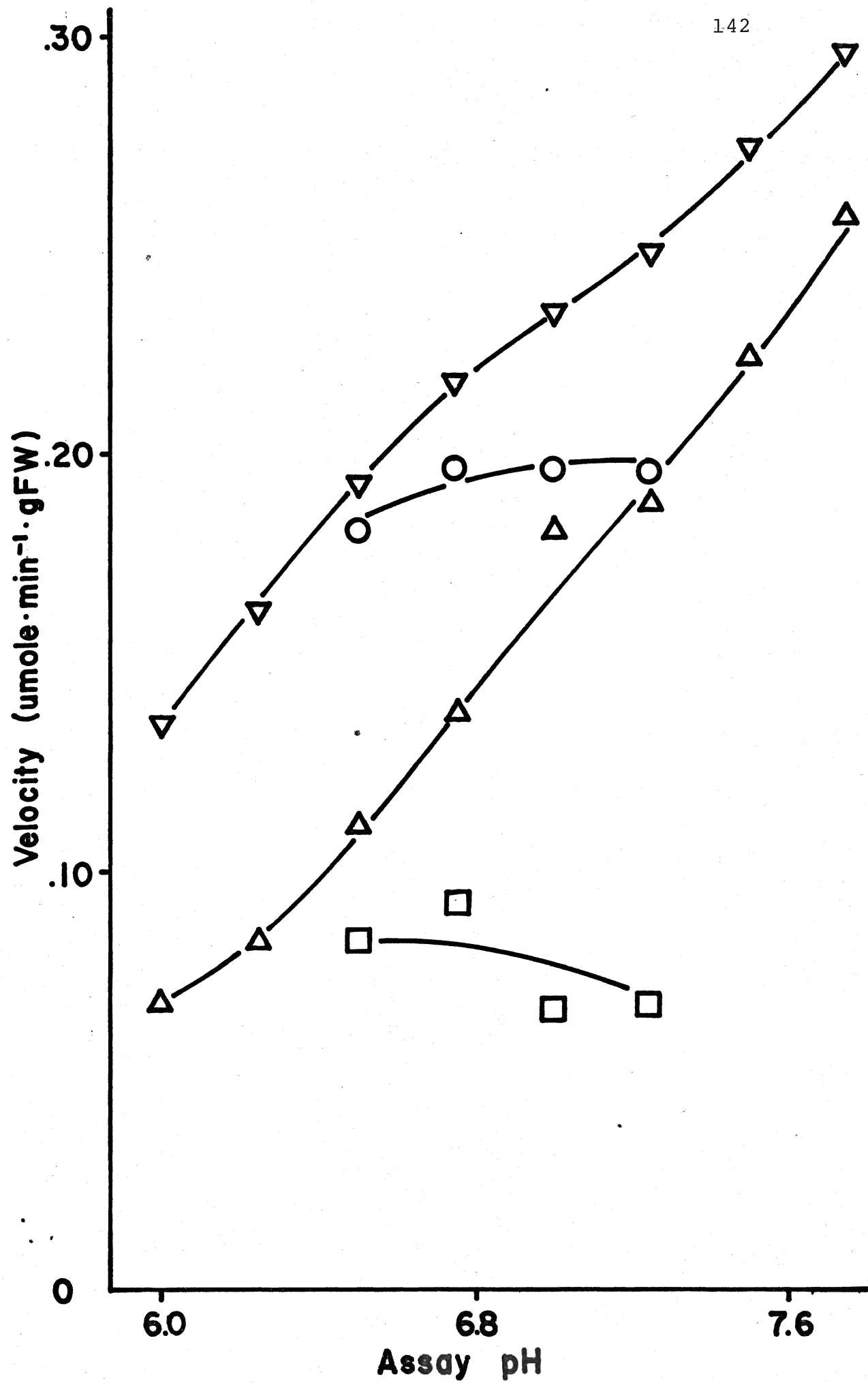


Figure 27: Effect of pH on malic enzyme activity as a function of the malate concentration.

Enzyme activity was assayed spectrophotometrically at 340 nm in the presence of 1.0 mM  $\text{MnCl}_2$ , 0.5 mM  $\text{NADP}^+$ , 0.005 to 0.97 mM malate, 0.2 ml enzyme extract and 12.5 mM Tris-BES buffer pH 6.5 (●), 6.75 (○), 7.00 (▲) and 7.25 (△).

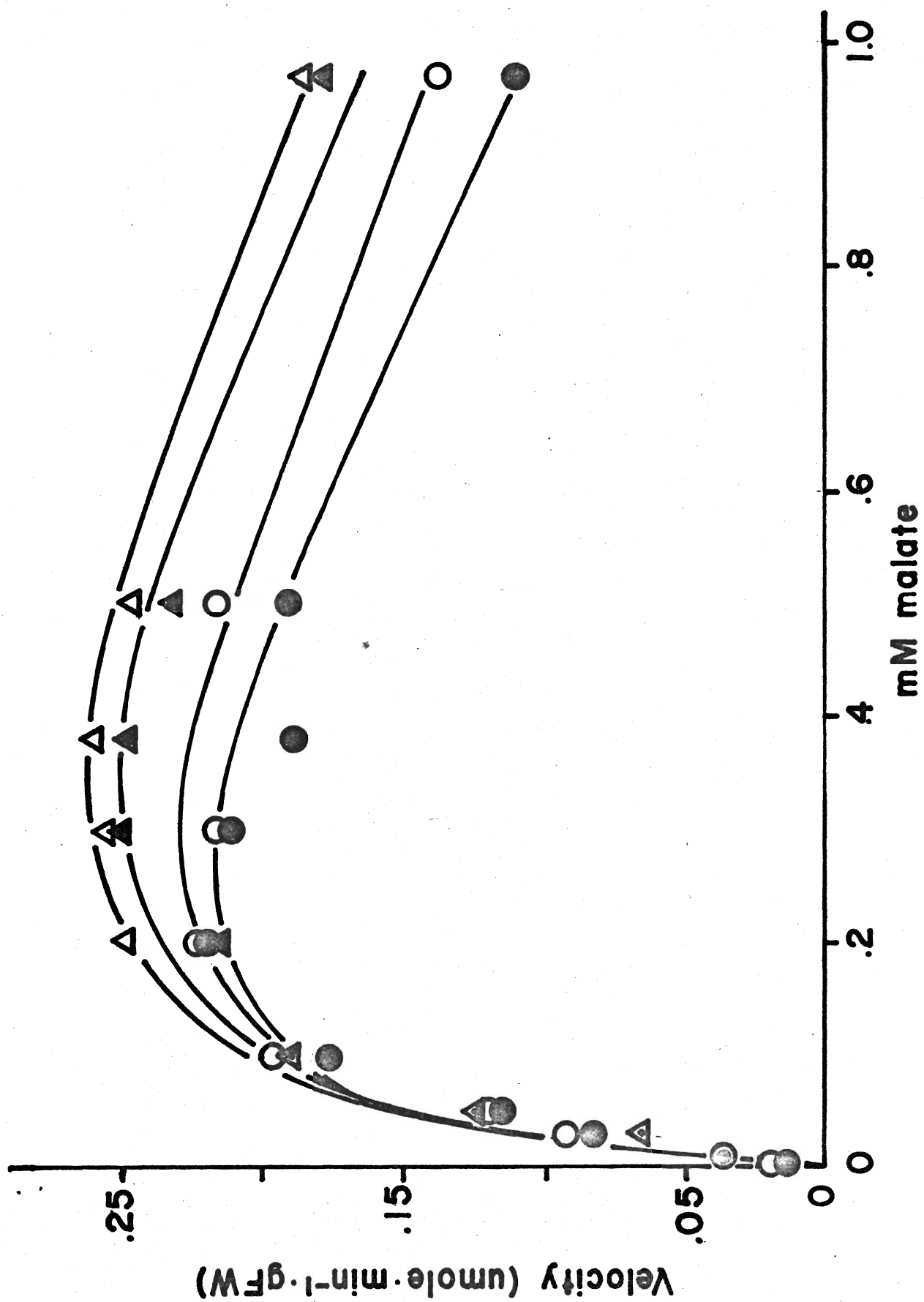


Figure 28: Effect of pH on linearly transformed plots of malic enzyme activity as a function of the malate concentration.

Enzyme activity was assayed spectrophotometrically at 340 nm in the presence of 1.0 mM  $\text{MnCl}_2$ , 0.5 mM  $\text{NADP}^+$ , 0.005 to 0.97 mM malate, 0.2 ml enzyme extract and 12.5 mM Tris-BES buffer pH 6.5 ( $\square$ ), 6.75 ( $\circ$ ), 7.00 ( $\blacktriangledown$ ) and 7.25 ( $\triangle$ ).

Figure 28(a): Lineweaver-Burk plot

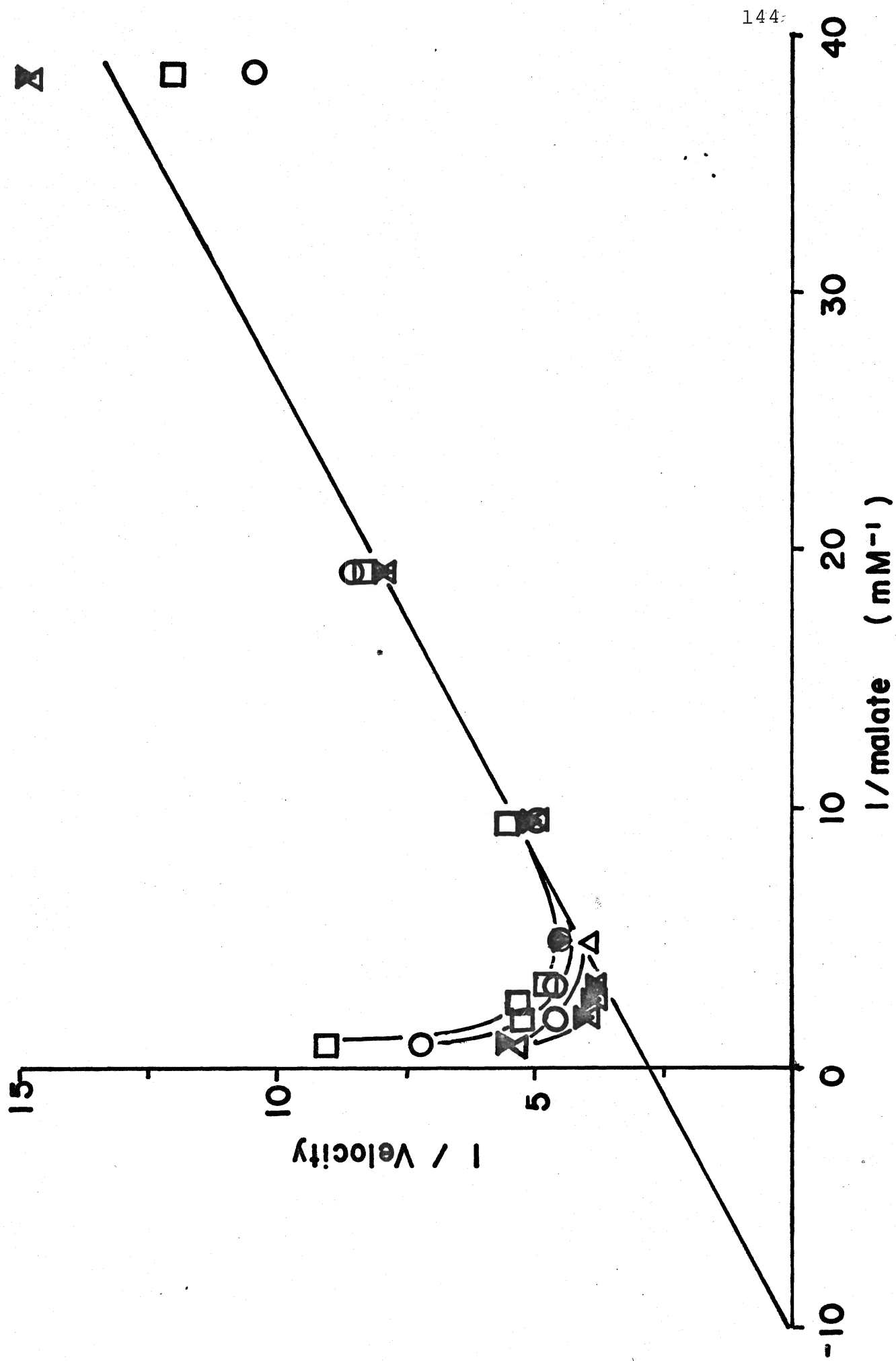


Figure 28(b): Eadie-Hofstee plot

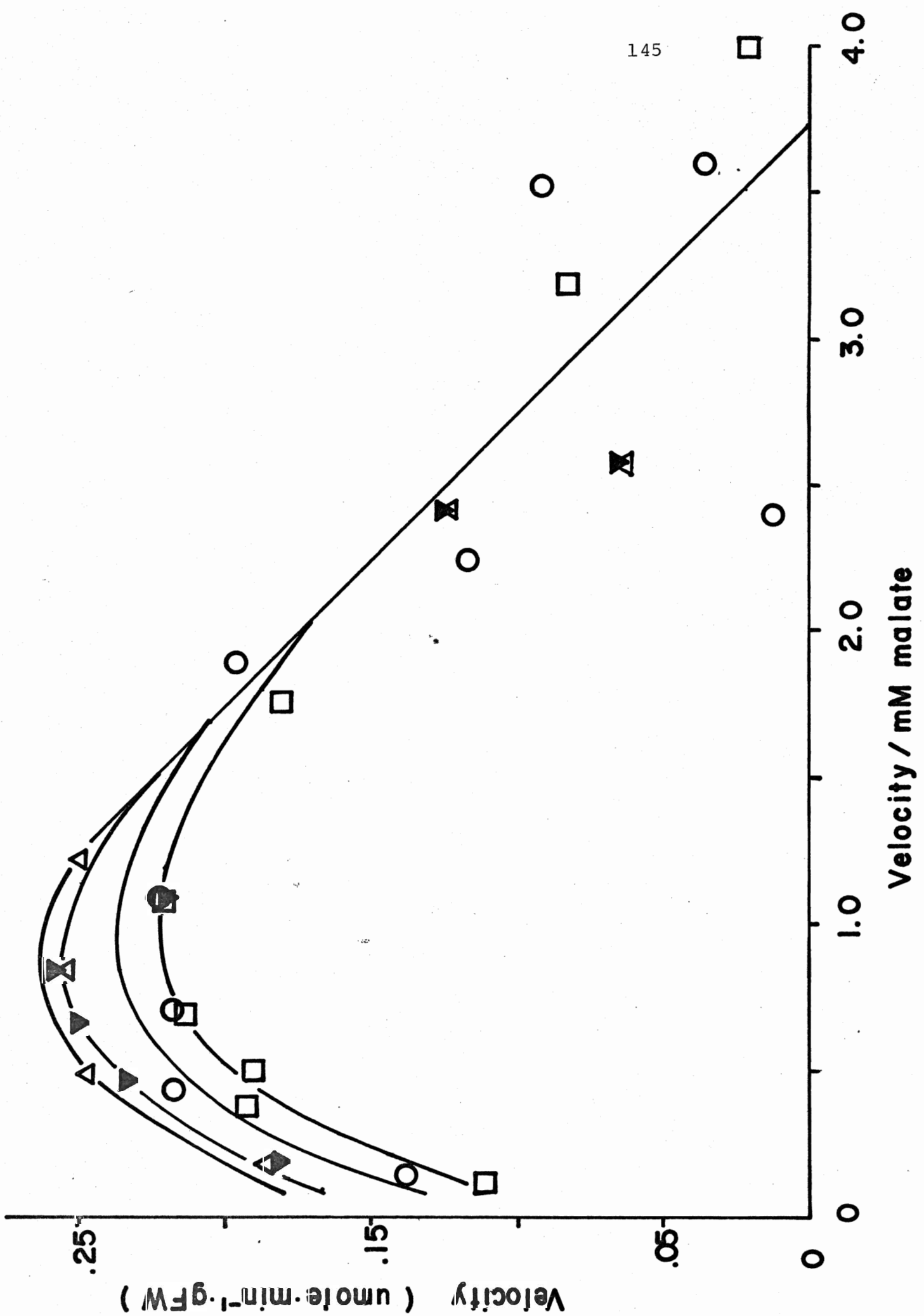
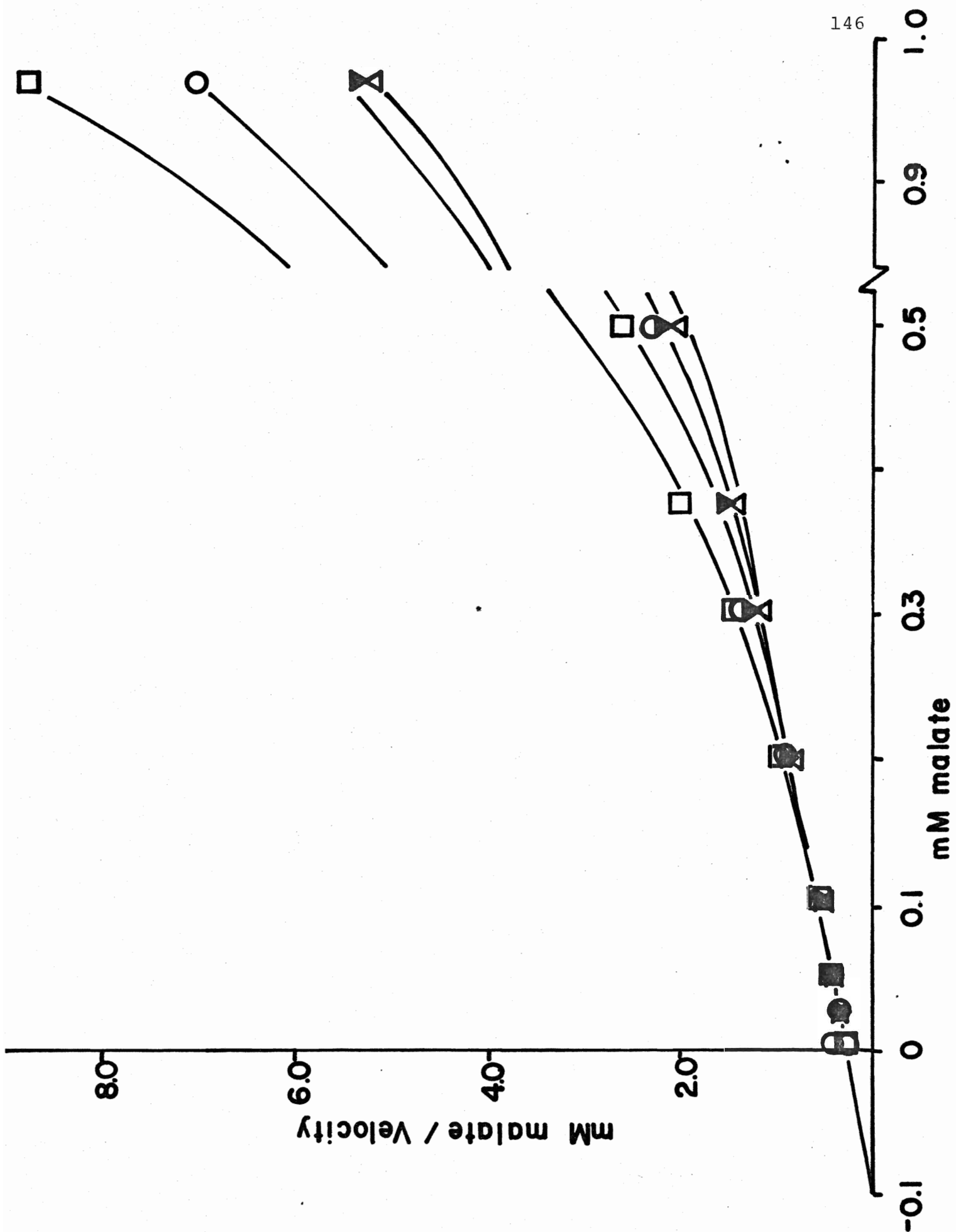


Figure 28(c): Hanes plot





the malate concentrations at which inhibition was exhibited, and this appeared to be pH dependent. At pH 6.5 malate levels greater than 0.1 mM became inhibitory, whereas at pH 7.25 inhibition was observed at malate levels greater than 0.5 mM.

Hill coefficients determined from Hill plots of the data were equal to 1.0 and were not affected by changes in pH (Figure 29).

The  $K_{m_{app}}(\text{MnCl}_2)$  was determined by assaying the enzyme with 0.5 mM malate and a range of  $\text{MnCl}_2$  concentrations (0.05 to 3.0 mM) at pH values 6.5 to 7.25. The data was analyzed using linear transformations of the Michaelis-Menton equation. Figure 30 demonstrates that the  $K_{m_{app}}(\text{MnCl}_2)$  decreased from 0.33 mM at pH 6.5 to 0.11 mM at pH 7.25. The results indicate that the binding affinity of the malic enzyme for  $\text{MnCl}_2$  increases as pH is increased.

In summary, the results indicate that the kinetic parameters of the malic enzyme which are pH sensitive are substrate inhibition at high malate levels, and  $\text{Mn}^{2+}$  binding affinity. Binding affinity for malate and catalytic efficiency appeared to be pH insensitive.

Figure 29: Effect of pH on the Hill plot of malic enzyme activity.

Enzyme activity was assayed spectrophotometrically at 340 nm in the presence of 1.0 mM  $\text{MnCl}_2$ , 0.5 mM  $\text{NADP}^+$ , 0.005 to 0.97 mM malate, 0.2 ml enzyme extract and 12.5 mM Tris-BES buffer pH 6.5 ( $\square$ ), 6.75 ( $\circ$ ), 7.00 ( $\blacktriangledown$ ) and 7.25 ( $\triangle$ ).

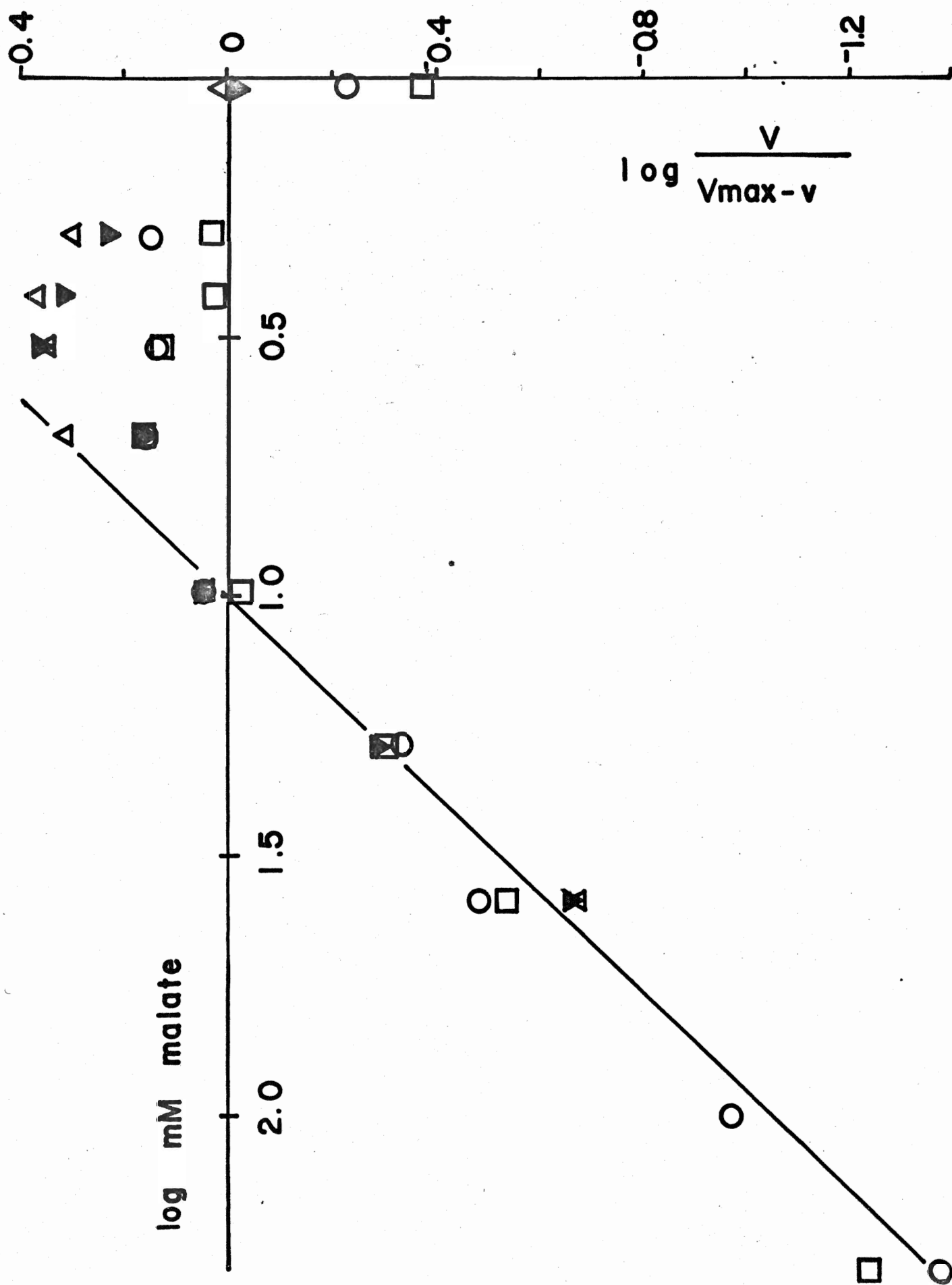
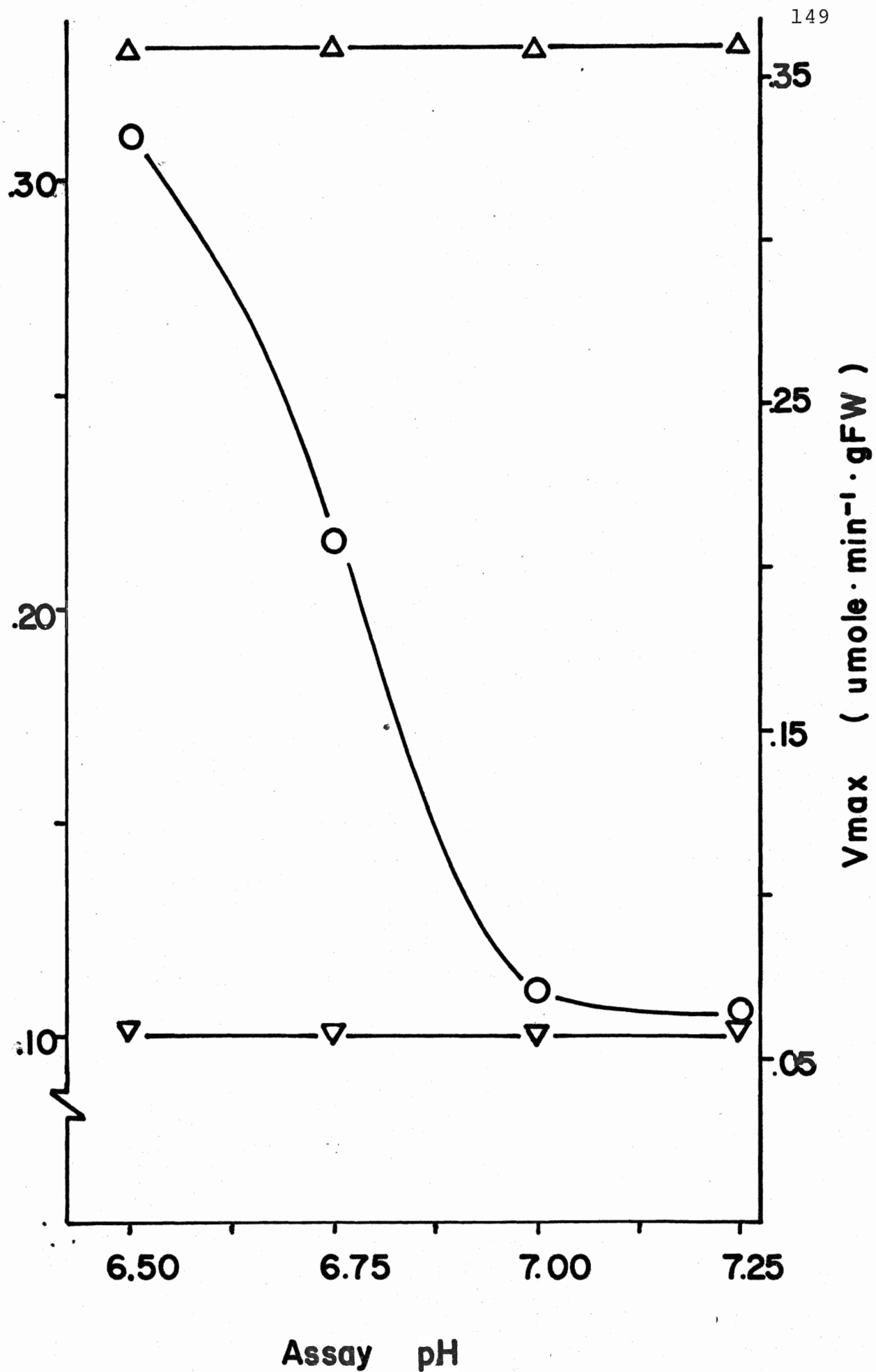


Figure 30: Effect of pH on the  $K_{m_{app}}(\text{MnCl}_2)$ , the  $K_{m_{app}}(\text{malate})$  and  $V_{max}$  of the malic enzyme.

Enzyme activity was assayed spectrophotometrically at 340 nm in the presence of 12.5 mM Tris-BES buffer pH 6.50 to 7.25, 0.5 mM  $\text{NADP}^+$  and 0.2 ml enzyme extract. Further additions to the reaction mixture were 0.01 to 0.05 malate and constant 1.0 mM  $\text{MnCl}_2$ , or 0.05 to 3.0 mM  $\text{MnCl}_2$  and constant 0.5 mM malate. The  $K_{m_{app}}$  for malate ( $\nabla$ ),  $K_{m_{app}}$  for  $\text{Mn}^{2+}$  ( $\bigcirc$ ) and  $V_{max}$  ( $\Delta$ ) were estimated from linear transformations of the  $V \times S$  data.

$K_{m_{app}}$  ( malate;  $Mn^{+2}$  ) ( mM )



6.50

6.75

7.00

7.25

Assay pH

### III. Determination of the kinetic constants of PEP carboxylase and the malic enzyme from radiochemical assays

This section deals with a comparison of the kinetics obtained from spectrophotometric and radiochemical assays of PEPC and malic enzyme activities. In all experiments, spectrophotometric assays were performed concurrently in the presence of labelled or unlabelled substrates to determine whether an isotope effect was influencing activity. Spectrophotometric and radiochemical assays were conducted using a range of substrate levels. Activities at each substrate concentration are plotted as a percentage of  $V_{\max}$ . Apparent  $K_m$  and  $V_{\max}$  are reported for each assay procedure.

#### A. PEP carboxylase

Radiochemical assays were conducted at pH 7.55 in the presence of  $[^{14}\text{C}]\text{-NaHCO}_3$  or  $1\text{-}[^{14}\text{C}]\text{-PEP}$  as outlined in the methods (Table 4). Spectrophotometric assays (0.5 mM PEP, pH 7.55) were not significantly altered when labelled or unlabelled  $\text{HCO}_3^-$  was used. However, when labelled PEP was employed, the activity of the spectrophotometric assay was decreased 60 to 80% from assays performed with unlabelled PEP. Cyclohexylammonium salts of labelled and unlabelled PEP were used. The results suggest that the large difference in rates of NADH oxidation could be due to  $^{14}\text{C}$  inhibition of activity.

Plots of velocity as a percentage of  $V_{\max}$  versus PEP concentrations indicate that  $V_{\max}$  and  $K_{m_{\text{app}}}(\text{PEP})$  were increased

in the radiochemical assays compared with the spectrophotometric assay (Figure 31). The  $K_{m_{app}}(PEP)$  was increased eleven-fold from 0.03 mM (spectrophotometric) to 0.32-0.35 mM (radiochemical), and  $V_{max}$  was increased approximately 1.5-fold from 0.32  $\mu\text{mole}\cdot\text{min}^{-1}\cdot\text{g FW}$  (spectrophotometric) to 0.48-0.52  $\mu\text{mole}\cdot\text{min}^{-1}\cdot\text{g FW}$  (radiochemical). These results are summarized in Table 18. In all experiments, Lineweaver-Burk plots were linear, although radiochemical data showed much greater deviation about sample means when compared with spectrophotometric data (see Tables 3 and 5). The results indicate that an isotope effect involving labelled PEP was probably not changing the kinetics of the radiochemical assay compared with the spectrophotometric assay, as labelled  $\text{HCO}_3^-$  changed the kinetics in a similar manner.

The kinetic differences observed between the  $^{14}\text{C}$  and  $^{12}\text{C}$  assays may have been due to the presence of NADH in the coupled spectrophotometric technique. This could have been tested by comparing the rate of OAA production in the absence and presence of NADH by adding NADH midway during the assay period. This would presumably result in a biphasic pattern of absorbance decrease at 340 nm. The rate of OAA production in the absence of OAA could be calculated from the change in absorbance observed over the initial fast phase. This would be compared with the rate of absorbance decrease over the slower final phase. The results could indicate whether PEPC activity measured spectrophotometrically is modified in the presence



Figure 31: Effect of spectrophotometric or radiochemical measurement of activity on the kinetics of PEP carboxylase.

Spectrophotometric assays ( $\Delta$ ) were performed at 340 nm in the presence of 10.7 mM K-Pi buffer pH 7.4, 16.7 mM  $\text{NaHCO}_3$ , 3.3 mM  $\text{MgCl}_2$ , 0.01 to 0.5 mM PEP and 0.2 ml enzyme extract. Radiochemical assays were performed in the presence of the same reagents with the exception of NADH which was omitted and 0.1 ml enzyme extract was used. When  $[^{14}\text{C}]\text{-NaHCO}_3$  was employed ( $\bigcirc$ ) unlabelled PEP was added and vice versa ( $\square$ ). Activities are expressed as a percentage of  $V_{\text{max}}$  estimated from linear transformations of the data.

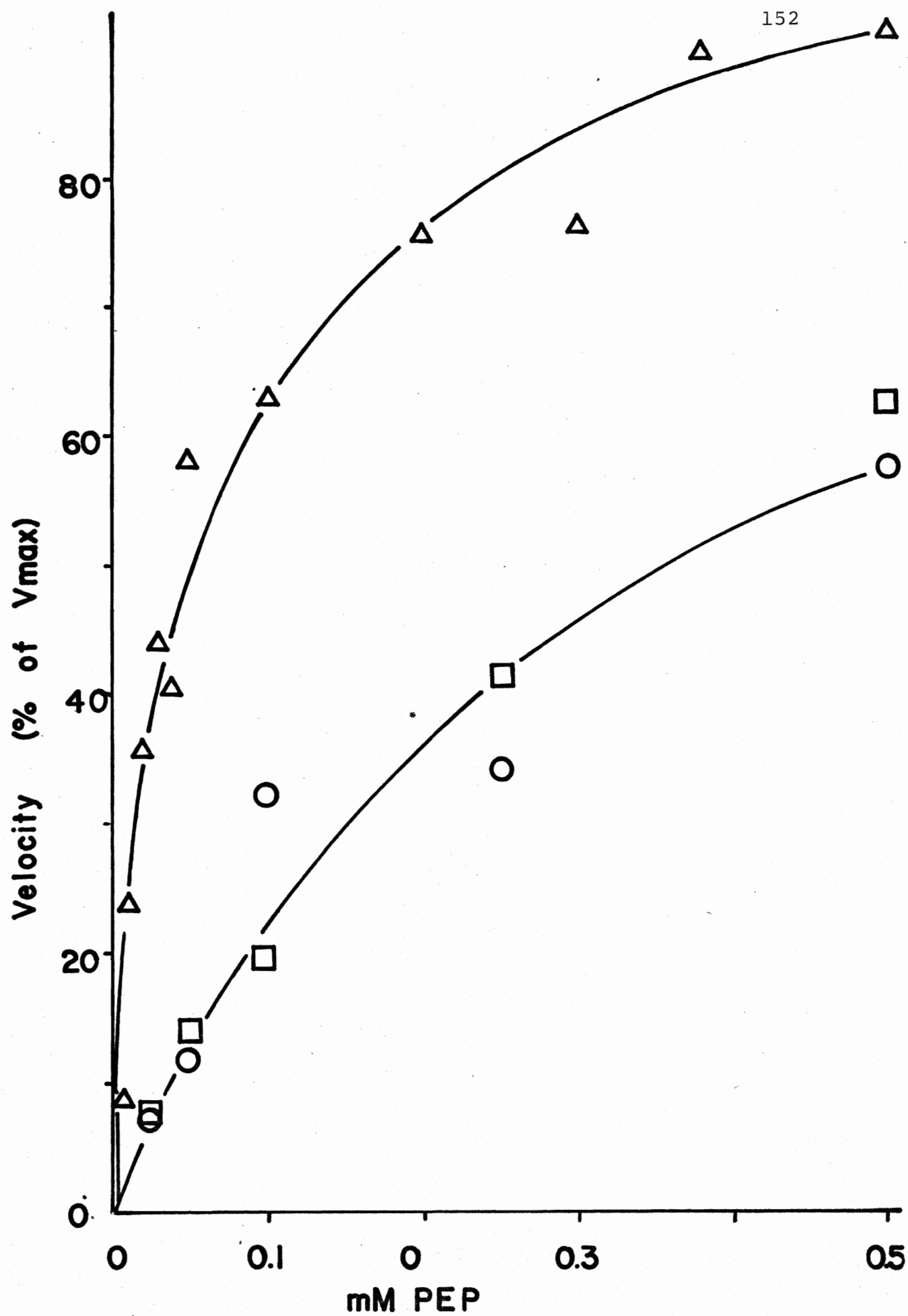


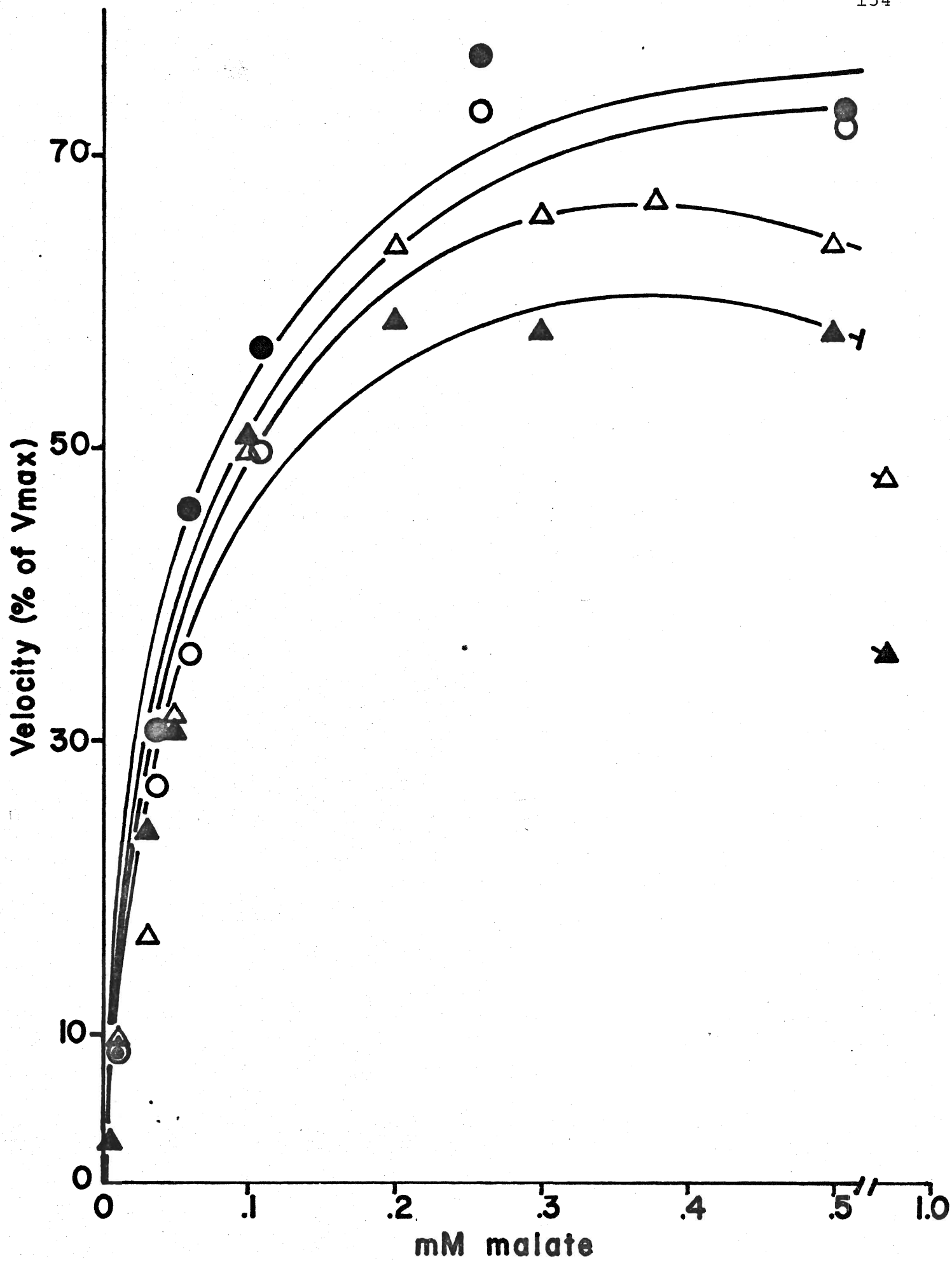
Table 18: Effect of spectrophotometric or radiochemical assays on the apparent  $K_m$ (PEP) and  $V_{max}$  for PEP carboxylase.

Assay Technique	$K_{m_{app}}$ (PEP) mM	$V_{max}$ $\mu\text{mole}\cdot\text{min}^{-1}\cdot\text{g FW}$
Spectrophotometric	0.03	0.32
Radiochemical		
(1) $[^{14}\text{C}]\text{-NaHCO}_3$	0.35	0.52
(2) $1\text{-}[^{14}\text{C}]\text{-PEP}$	0.32	0.48

Spectrophotometric assays were performed in the presence of 10.7 mM K-Pi buffer pH 7.4, 16.7 mM  $\text{NaHCO}_3$ , 3.3 mM  $\text{MgCl}_2$ , 0.05 mM NADH, 0.01 to 0.5 mM PEP and 0.2 ml enzyme extract. Radiochemical assays were performed in the presence of the same reagents with the exception of NADH which was omitted and 0.1 ml enzyme extract was used. When  $[^{14}\text{C}]\text{-NaHCO}_3$  was employed unlabelled PEP was added and vice versa. Kinetic constants were determined from linear transformations of the data.

Figure 32: Effect of spectrophotometric or radiochemical measurement of activity on the kinetics of the malic enzyme.

Spectrophotometric assays (○/●) were performed in the presence of 12.5 mM Tris-BES buffer pH 6.75 (closed symbols) or pH 7.25 (open symbols), 1.0 mM  $\text{MnCl}_2$ , 0.5 mM  $\text{NADP}^+$ , 0.01 to 0.5 mM malate and 0.2 ml enzyme extract. Radiochemical assays were performed under the same conditions with the exception that U- $^{14}\text{C}$ -malate and 0.1 ml enzyme were employed. Activities are expressed as a percentage of  $V_{\text{max}}$  estimated from linear transformations of the data.



of MDH activity.

#### B. The malic enzyme

Radiochemical and spectrophotometric assays were conducted between pH 6.75 and 7.4 with labelled, and labelled or unlabelled malate respectively. Spectrophotometric assays (0.5 mM malate, pH 7.25) were not significantly different in the presence of labelled or unlabelled substrate. When both assays were performed with a range of malate concentrations (0.01 to 0.97 mM) plots of activity as a percentage of  $V_{\max}$  versus the substrate concentration indicate similar hyperbolic curves (Figure 32). The apparent  $K_m$ (malate) was 0.1 mM under all assay conditions. However, the  $V_{\max}$  decreased from  $0.38 \mu\text{mole} \cdot \text{min}^{-1} \cdot \text{g FW}$  in the spectrophotometric assays to  $0.20 \mu\text{mole} \cdot \text{min}^{-1} \cdot \text{g FW}$  in the radiochemical assays under all conditions of pH (Table 19). This may reflect a constant loss of radioactivity in pyruvate-DNP which may be due to the recovery procedure. Thus, the apparent activity would decrease if some proportion of the product were not recovered, whereas the apparent binding affinity would not be affected.

Radiochemical assays were performed as checks on the effects of potential modulators of PEPC and malic enzyme activities as measured spectrophotometrically (Results IV). However, if the kinetics of the two assay systems are not similar (as for PEPC), the value of one system as a check on another may be limited.

Table 19: Effect of spectrophotometric or radiochemical assays on the apparent  $K_m$ (malate) and  $V_{max}$  for the malic enzyme.

Assay Technique	$K_{mapp}$ (malate) mM	$V_{max}$ $\mu\text{mole}\cdot\text{min}^{-1}\cdot\text{g FW}$
Spectrophotometric	0.1	0.3
Radiochemical	0.1	0.20

Spectrophotometric assays were performed in the presence of 12.5 mM Tris-BES buffer pH 6.75 and 7.25, 1.0 mM  $\text{MnCl}_2$ , 0.5 mM  $\text{NADP}^+$ , 0.01 to 0.5 mM malate and 0.2 ml enzyme extract. Radiochemical assays were performed under the same conditions with the exception that U- $^{14}\text{C}$ -malate and 0.1 ml enzyme extract were employed. Kinetic constants were determined from linear transformations of the data.

#### IV. Effects of pH and various metabolites on PEP Carboxylase and malic enzyme activities

The results are divided into three sections. The first section involves a general survey of enzyme activities in the presence and absence of various carboxylic and amino acids, and sugar phosphates. In the second section, evidence is presented indicating whether the influence of apparent effectors result from direct or indirect action on enzyme activity. The final section deals with the influence of apparent strong effectors and pH on the kinetic constants of PEPC and malic enzyme activities. PEPC was assayed in potassium phosphate buffers, and malic enzyme in Tris-BES buffers.

##### A. General survey of potential effectors of PEPC and malic enzyme activities.

###### (1) Effects on rates of absorbance change.

Assays were conducted for PEPC (0.5 mM PEP, assay pH 7.15 and 7.55) and the malic enzyme (0.5 mM malate, assay pH 6.5 and 7.1) in the presence and absence of various metabolites (3.0 mM) (Methods (II,A,1(ii); II,B,1(ii))). The results indicate that representatives from each of the three classes of metabolites tested were apparent effectors of enzyme activity (Table 20). Furthermore, all effectors which inhibited PEPC activity also inhibited malic enzyme activity, and no activators were found. The strongest influence of effectors on enzyme activity were under conditions of low assay pH and low substrate levels.



Table 20: Effects of various metabolites on the spectrophotometric activities of PEPC and the malic enzyme.

Metabolite	PEPC [PEP] (mM)				Malic enzyme [malate] (mM)			
	0.1		0.5		0.1		0.5	
	Assay pH		Assay pH		Assay pH		Assay pH	
	7.15	7.55	7.15	7.55	6.10	7.10	6.50	7.10
<b>Carboxylic acids</b>								
succinate	--	--	--	--	--	--	--	--
citrate	--	--	--	--	--	--	--	--
phenylsuccinate	--	--	--	--	--	--	--	--
4-aminobutyrate	--	0	0	0	0	0	0	0
acetate	--	0	0	0	0	0	0	0
malate	--	--	--	--	N.A.	N.A.	N.A.	N.A.
pyruvate	--	0	0	0	0	0	0	0
PEP	N.A.	N.A.	N.A.	N.A.	--	0	0	0
<b>Amino acids</b>								
glutamate	--	0	0	0	--	0	0	0
aspartate	--	0	0	0	--	0	0	0
histidine	--	0	0	0	0	0	0	0
glycine	0	0	0	0	0	0	0	0
leucine	0	0	0	0	0	0	0	0
<b>Phosphorylated sugars</b>								
G-6-P	--	0	0	0	0	0	0	0
G-1-P	0	0	0	0	0	0	0	0
F-6-P	0	0			0	0	0	0
F-1-P	0	0	0	0	0	0	0	0
F-1,6-diP	--	--	--	--	--	--	--	--
3-PGA	--	--	--	--	--	--	--	--

PEPC activity was assayed in the presence of 10.7 mM K-Pi buffer pH 7.0 or 7.4, 3.3 mM MgCl<sub>2</sub>, 16.7 NaHCO<sub>3</sub>, 0.05 mM NADH, 0.1 or 0.5 mM PEP and 0.2 ml enzyme extract ± 2.0 mM metabolites. Malic enzyme activity was assayed in the presence of 12.5 mM Tris-BES pH 6.5 or 7.1, 1.0 mM MnCl<sub>2</sub>, 0.5 mM NADP<sup>+</sup>, 0.1 or 0.5 mM malate and 0.2 ml enzyme extract ± 3.0 mM metabolites. 0 indicates no effect of metabolites on activity; -- indicates inhibition of activity by metabolites; N.A. indicates metabolite effects are not applicable as these reagents are normal substrates.

(2) Effects on accumulation of [ $^{14}\text{C}$ ]-labelled reaction products

Radiochemical assays of PEPC and malic enzyme activities were conducted using the standard assay systems (Tables 4 and 9) modified to contain 0.01 or 0.5 mM substrates in the presence and absence of potential effectors (3.0 mM). Radioactivity recovered in OAA-DNP (PEPC) or pyruvate-DNP (malic enzyme) was corrected for artifacts resulting from potential effectors by performing various control assays (Methods II, A&B(ii)). In addition, spectrophotometric assays were conducted concurrently with 0.5 mM substrates in the presence and absence of the same potential effectors (3.0 mM).

(a) PEP carboxylase

Table 21 indicates that the effect of malate was similar in the spectrophotometric and radiochemical assays. In contrast, succinate, citrate, fructose-1,6-diphosphate and 3-phosphoglycerate increased the accumulation of radioactivity in OAA-DNP at low PEP concentrations but inhibited the analogous spectrophotometric assays. With saturating levels of PEP these metabolites inhibited both assay techniques similarly. The value of the results obtained from radiochemical assays conducted with low levels of PEP may be limited in that low levels of radioactivity were recovered with high standard deviations (20-30% of mean, Table 5) and the kinetics are radically different from those obtained in the spectrophotometric assay (Results III, A). Glutamate, and to a lesser extent aspartate, were unique in that they mildly inhibited the rate of absorbance change (5 to 25%)

Table 21: Effects of various metabolites on the spectrophotometric or radiochemical assay of PEPC activity.

Metabolite	Percent Remaining Activity			
	Spectrophotometric Assay		Radiochemical Assay	
	mM PEP		mM PEP	
	0.01	0.5	0.01	0.5
Glutamate	95-100	100	0	0
Aspartate	75-85	90-95	0	5-15
Succinate	0-5	10-15	105	10
Citrate	40-50	50-60	500	25
Malate	0-5	10-15	0	10
F-1,6-diP	25	45-50	500	20
3-PGA	25-30	50	300	25-30

PEPC activity was assayed spectrophotometrically in the presence of 10.7 mM K-Pi buffer pH 7.25, 3.3 mM MgCl<sub>2</sub>, 16.7 mM NaHCO<sub>3</sub>, 0.05 mM NADH, 0.01 or 0.5 mM PEP and 0.2 ml enzyme extract ± metabolites. Radiochemical assays were assayed at similar conditions with the exceptions that NADH was omitted, 0.1 ml enzyme extract and 1-[<sup>14</sup>C]-PEP were used. Activities are expressed as a percentage of the metabolite containing assay over the standard assay.

but completely inhibited accumulation of label in OAA-DNP. Autoradiography of the chromatograms indicated that glutamate, aspartate and malate reduced the amount of radioactivity detectable in OAA-DNP (Figure 33). Furthermore, no other radioactive region was detected indicating the absence of other ethyl acetate extractable DNP derivatives of reaction products. Succinate, citrate, fructose-1,6-diphosphate and 3-phosphoglycerate did not significantly affect the density of the OAA-DNP region, and did not result in new areas of radioactivity as detectable by autoradiography.

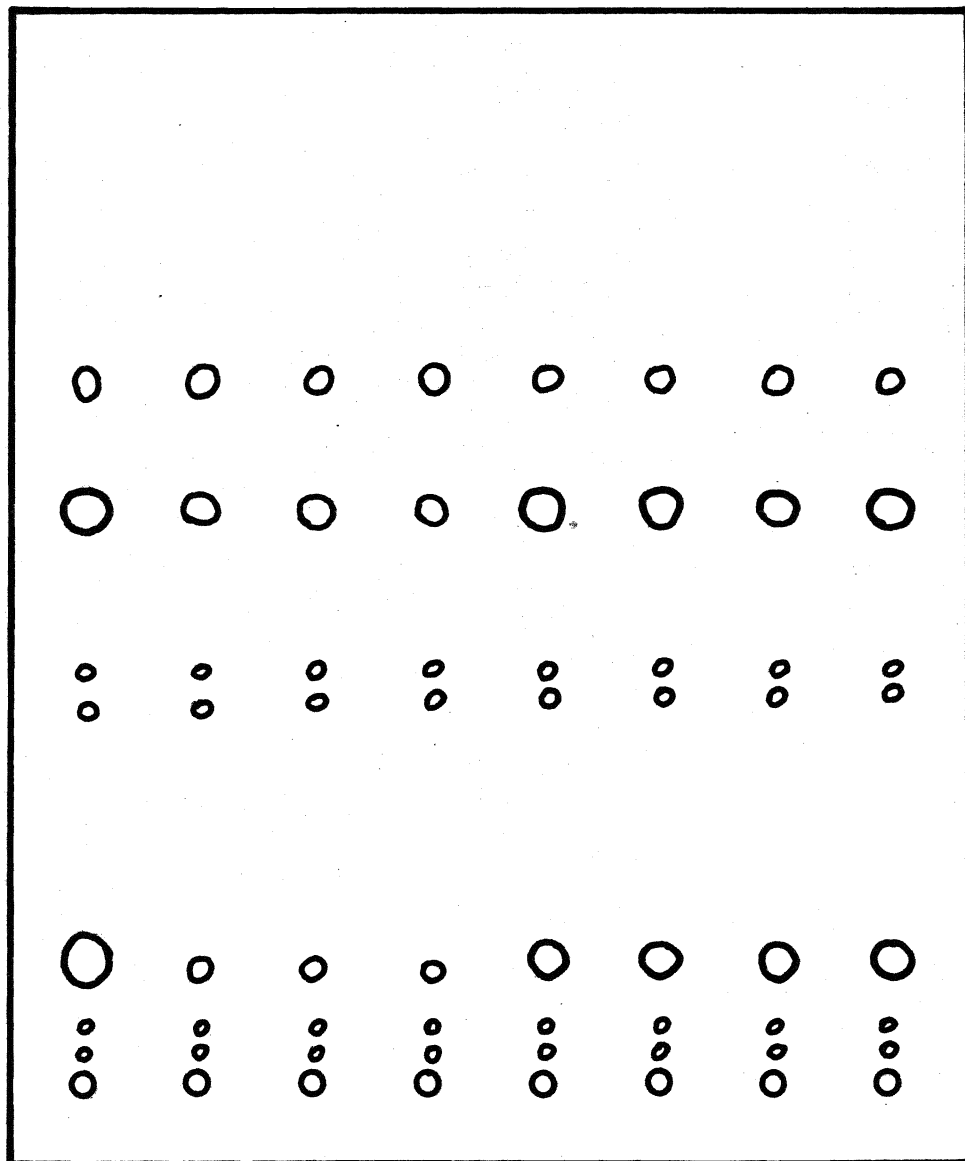
The results indicate that glutamate and aspartate do not interfere with the rate of NADH oxidation, but do affect OAA accumulation. This suggests that in the radiochemical assay, labelled OAA is removed (e.g., by transamination to aspartate) thus inhibiting its accumulation but not affecting its rate of production. Further evidence for this interpretation is presented in Results (IV,B,1).

(b) The malic enzyme

The same metabolites used in the previous section were used in spectrophotometric and radiochemical assays of the malic enzyme. Table 22 indicates that aspartate, citrate, F-1,6-diP, and 3-PGA exhibit similar effects on activity assayed with 0.5 mM malate in either assay system. With the exception of 3-PGA, the same trend was observed in the malate limited systems. Whereas 3-PGA increased the percent radioactivity recovered in

Figure 33: Autoradiogram of the chromatography of 2,4-dinitrophenylhydrazine derivatives of the PEP carboxylase reaction in the presence of various metabolites.

Enzyme activity was assayed radiochemically in the presence of 10.7 mM K-Pi buffer pH 7.0, 3.3 mM  $\text{MgCl}_2$ , 16.7 mM  $\text{NaHCO}_3$ , 0.05 mM NADH, 0.5 mM 1- $^{14}\text{C}$ -PEP and 0.1 ml enzyme extract - (1) or + 3.0 mM malate (2), glu(3), asp (4), succinate (5), citrate (6), F-1,6-diP (7) or 3-PGA (8). The ethyl acetate fractions were chromatographed and exposed to X-ray film for three weeks. The region of radioactivity corresponding to the migration of OAA-DNP is noted.



OAA-DNP  
origin

1 2 3 4 5 6 7 8

Table 22: Effects of various metabolites on the spectrophotometric or radiochemical assay of malic enzyme activity.

Metabolite	Percent Remaining Activity			
	Spectrophotometric Assay		Radiochemical Assay	
	mM malate		mM malate	
	0.01	0.5	0.01	0.5
Glutamate	100	100	65-70	60-65
Aspartate	90-95	95-100	100	95-100
Succinate	70-75	85-90	115-120	125-130
Citrate	100-105	90-95	90	100
F-1,6-diP	55-60	60-65	75-80	50
3-PGA	75-80	75-80	130	80-85

Malic enzyme activity was assayed spectrophotometrically in the presence of 12.5 mM Tris-BES buffer pH 7.25, 1.0 mM  $\text{MnCl}_2$ , 0.5 mM  $\text{NADP}^+$ , 0.01 or 0.5 mM malate and 0.2 ml enzyme extract  $\pm$  3.0 mM metabolites. Radiochemical assays were performed under the same conditions with the exception that U- $^{14}\text{C}$ -malate and 0.1 ml enzyme extract were employed. Activities are expressed as a percentage of the metabolite containing assay over the standard assay.

pyruvate-DNP (130% of the standard assay), it inhibited the rates of absorbance change (75-80%). However, the calculated standard deviation of the radiochemical assay at low malate levels are high (20-30% of mean, Table 11) indicating that the 3-PGA effect may or may not result from a real stimulation of malic enzyme activity. The same thesis could explain the discrepancies observed in each assay system with respect to the apparent activation of pyruvate-DNP formation by succinate. Aspartate was observed to mildly inhibit the spectrophotometric and radiochemical assays. Glutamate did not influence the rate of absorbance change. In contrast, glutamate inhibited pyruvate-DNP formation 30-40%. This may have resulted from the removal of labelled pyruvate by a transamination reaction.

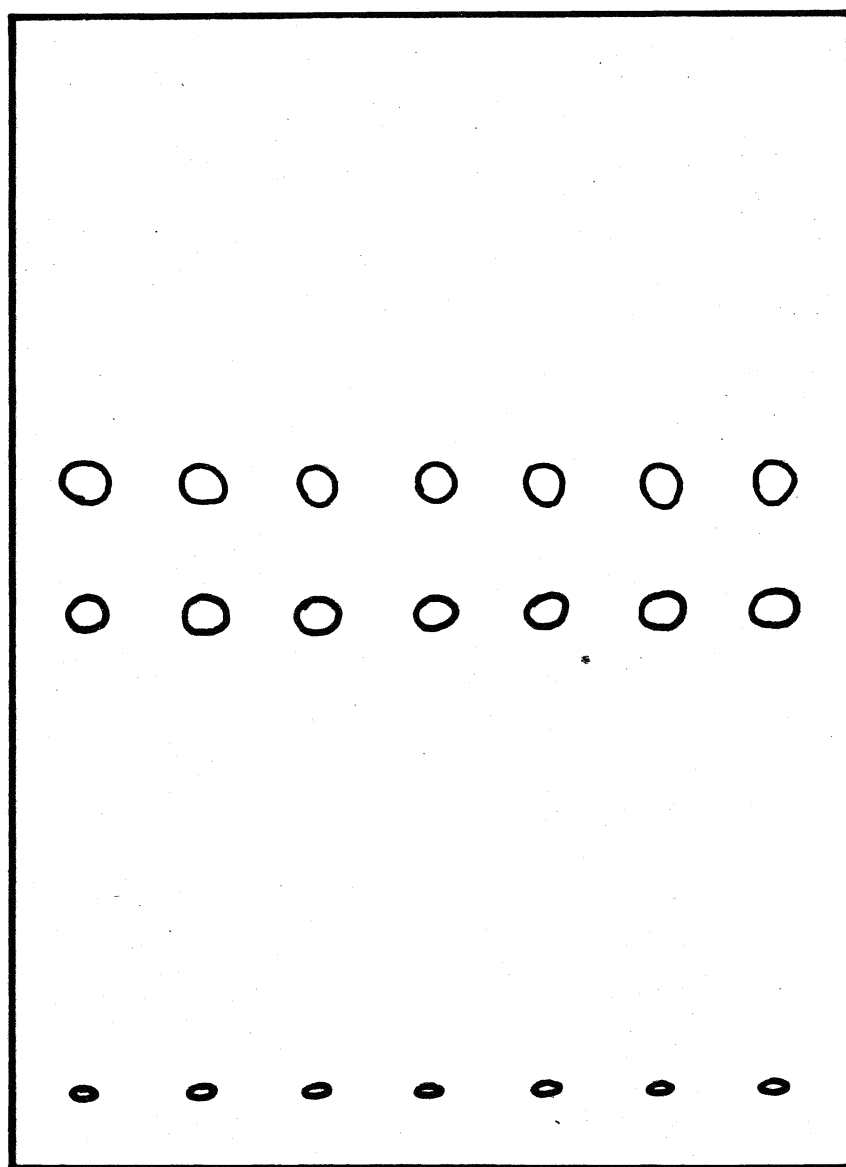
Autoradiograms of the thin layer chromatographs in the presence <sup>or</sup> of absence of these metabolites indicate no detectable change in the density of pyruvate-DNP (Figure 34). Furthermore, no additional regions of radioactivity were observed.

In general, the influence of all metabolites on malic enzyme activity measured spectrophotometrically or radiochemically were mild. This may indicate a common mechanism of inhibition. Chelation of essential  $Mn^{2+}$  could be one mechanism as the  $K_{m_{app}}$  ( $MnCl_2$ ) is highly pH-dependent (Results II,C). Experiments designed to provide evidence for or against modulation of activity through metabolite chelation of  $Mn^{2+}$  is presented in the following section.



Figure 34: Autoradiogram of the chromatography of 2,4-dinitrophenylhydrazine derivatives of the malic enzyme catalyzed reaction in the presence of various metabolites.

Enzyme activity was assayed radiochemically in the presence of 12.5 mM Tris-BES pH 7.25, 1.0 mM  $\text{MnCl}_2$ , 0.5 mM  $\text{NADP}^+$ , 0.5 mM U- $^{14}\text{C}$ -malate and 1.0 ml enzyme extract-(1) or + 3.0 mM glu (2), asp (3), succinate (4), citrate (5), F-1,6-diP (6) or 3-PGA (7). The ethyl acetate fractions were chromatographed and exposed to X-ray film for three weeks. The regions of radioactivity corresponding to the migration of OAA- and pyruvate-DNP are noted.



1 2 3 4 5 6 7

## B. Evidence for a direct or indirect effect of potential effectors on enzyme activities

In this section apparent effects of various metabolites on enzyme activity were investigated to determine whether these were artifacts of the assay system. Results are presented which deal with the effects of glutamate and aspartate on the accumulation of radioactive OAA-DNP (PEPC) and pyruvate-DNP (malic enzyme). The results of experiments investigating the possibility of metabolite chelation of essential metal ions are also presented.

### (1) Effects of glutamate and aspartate on the accumulation of [ $^{14}\text{C}$ ]-labelled reaction products of PEP carboxylase and the malic enzyme

Standard radiochemical assays (Tables 4 and 9) were run with 0.5 mM substrate for 5 minutes, at which time 3 mM glutamate or aspartate was added and the reaction was stopped after an additional 5 minutes (Methods II,A,2). Additional radiochemical assay systems were incubated for five minutes in the presence or absence of glutamate or aspartate. The ethyl acetate fractions were chromatographed and analyzed for OAA-DNP (PEPC) or pyruvate-DNP (malic enzyme) as previously described (Methods II,A,s).

#### (a) PEP carboxylase

Table 23 indicates that addition of glutamate or aspartate at the beginning of the reaction reduces OAA-DNP formation 90 to 100%. If inhibition was the result of a direct effect on the enzyme, we could expect to see approximately the same dpm in a

Table 23: Effect of glutamate or aspartate on the radioactive accumulation of OAA-DNP for a PEP carboxylase catalyzed reaction

Standard assay conditions	dpm <sup>1</sup>	% remaining dpm	
1. 5 min assay	29023.5±2320	-- <sup>2</sup>	-- <sup>3</sup>
2. +glutamate (5 min)	860.3± 64.5	3.0	--
3. +aspartate (5 min)	2721.5± 231.3	9.4	--
4. 10 min assay	62572.7±5631.5	--	--
5. 5 min + glutamate (5 min)	11699.7±1085.0	18.7	39.2
6. 5 min + aspartate (5 min)	11046.9± 935.3	17.7	34.8

dpm, total radioactivity accumulated in OAA-DNP expressed as dpm per 1.0 ml assay.

% dpm remaining in the presence of glu or asp as a function of dpm in the standard assay, 5 or 10 min.

% dpm remaining in assay (5) or (6) as a function of the combined dpm in assay (1) + assay (2) (glu) or + assay (3) (asp).

0.1 ml enzyme extract was incubated in the presence of 10.7 mM K-Pi buffer pH 6.9, 3.3 mM MgCl<sub>2</sub>, 16.7 mM [<sup>14</sup>C]-NaHCO<sub>3</sub> (1.0 µCi·µmole<sup>-1</sup>), 0.05 mM NADH and 0.5 mM PEP for 5 (1) or 10 minutes (4). 3.0 mM glutamate or aspartate was added at the beginning of a 5 minute assay (2), (3) or for the final 5 minutes of a 10 minute assay (5), (6).

ten minute assay (incubated with inhibitor during the last five minutes) as the combined dpm obtained from a standard five minute assay and a five minute assay incubated with the inhibitor. On the other hand, if inhibition of label accumulation was the result of labelled OAA removal, the dpm in the ten minute assay relative to the sum of dpm in the two five minute assays should be reduced. The results demonstrate that ten minute assays containing glutamate or aspartate during the last 5 minutes contained 35 to 40% of the label observed in the standard five minute assay plus label in the five minute assay in the presence of glutamate or aspartate. This indicates that the majority of labelled OAA initially formed had been converted to another compound and that inhibition of the radiochemical assay by aspartate or glutamate results from product removal, not inhibition of PEP carboxylase.

The spectrophotometric assays in the presence of glutamate or aspartate converted PEP to OAA and NADH to  $\text{NAD}^+$  in a 1:1 stoichiometry indicating that practically all OAA is converted to malate, and transamination of OAA is not occurring. Conversely, in the radiochemical assay where NADH is not present, it appears that OAA may be removed in transamination reactions, resulting in amino acid inhibition of this system.

(b) The malic enzyme

Table 24 indicates that glutamate or aspartate inhibited the five minute assay of enzyme activity 30 or 10% respectively.

Table 24: Effect of glutamate or aspartate on the radioactive accumulation of pyruvate-DNP for a malic enzyme catalyzed reaction.

Standard assay conditions	dpm <sup>1</sup>	% remaining dpm	
1. 5 min assay	23545.7±3296.4	-- <sup>2</sup>	-- <sup>3</sup>
2. +glutamate (5 min)	16385.1±2048.1	69.6	--
3. +aspartate (5 min)	20627.4±1095.8	87.6	--
4. 10 min assay	45191.5±5874.9	--	--
5. 5 min + glutamate (5 min)	35930.2±4250.7	79.5	90.0
6. 5 min + aspartate (5 min)	38947.5±3305.3	86.2	88.2

<sup>1</sup> dpm, total radioactivity accumulated in pyruvate-DNP expressed as dpm per 1.0 ml assay

<sup>2</sup> % dpm remaining in the presence of glu or asp as a function of dpm in the standard assay, 5 or 10 min.

<sup>3</sup> % dpm remaining in assay (5) or (6) as a function of the combined dpm in assay (1) + assay (2) (glu) or + assay (3) (asp).

0.1 ml enzyme extract was incubated in the presence of 12.5 mM Tris-BES buffer pH 7.0, 1.0 mM MnCl<sub>2</sub>, 0.5 mM NADP<sup>+</sup>, and 0.5 mM malate for 5 (1) or 10 minutes (5). 3.0 mM glutamate or aspartate was added at the beginning of a 5 minute assay (2), (3) or for the final 5 minutes of a 10 minute assay (5), (6).

Additionally, the label accumulated in the ten minute assays (Final five minutes in the presence of glutamate or aspartate) contained approximately 90% (+/- a standard deviation of 20%) of the label accumulated in the combined five minute assays in the absence or presence of glutamate or aspartate. The results indicate that glutamate or aspartate do not remove pyruvate from the assay by converting it to another compound.

(2) Chelation of essential metal ions.

Standard spectrophotometric assays (Tables 1 and 6) of PEPC and malic enzyme activities were performed in the presence and absence of potential effectors (1.7 mM). After rates were obtained in the presence of effectors, additional  $MgCl_2$  or  $MnCl_2$  was added to the PEPC or malic enzyme assays respectively and rates were obtained in the subsequent two to three minute period.

(a) PEP carboxylase

Table 25 summarizes the effects of additional  $MgCl_2$  on rates of absorbance decrease inhibited by various metabolites. The results demonstrate that additional  $MgCl_2$  inhibits the rates of absorbance decrease further. For example, succinate (1.7 mM) inhibited the standard assay containing 3.3 mM  $MgCl_2$  33.3%. When the  $MgCl_2$  concentration was increased to 6.6 mM, and further to 9.9 mM the standard assay was inhibited 37% and 44.4% respectively (See Figure 35 and Table 25). The results indicate

Table 25: Effect of  $\text{MgCl}_2$  on PEP carboxylase activity in the presence and absence of various metabolites

Standard Assay Conditions	Activity		
	3.3 mM $\text{MgCl}_2$	6.6 mM $\text{MgCl}_2$	9.9 mM $\text{MgCl}_2$
- PEP	0.000	0.000	0.000
Standard Assay	0.027	0.024	0.021
+ malate	0.003	0.002	0.002
+ glutamate	0.026	0.022	0.020
+ aspartate	0.021	0.019	0.018
+ succinate	0.018	0.017	0.015
+ citrate	0.020	0.019	0.018
+ F-1,6-diP	0.015	0.013	0.012
+ 3-PGA	0.015	0.013	0.012

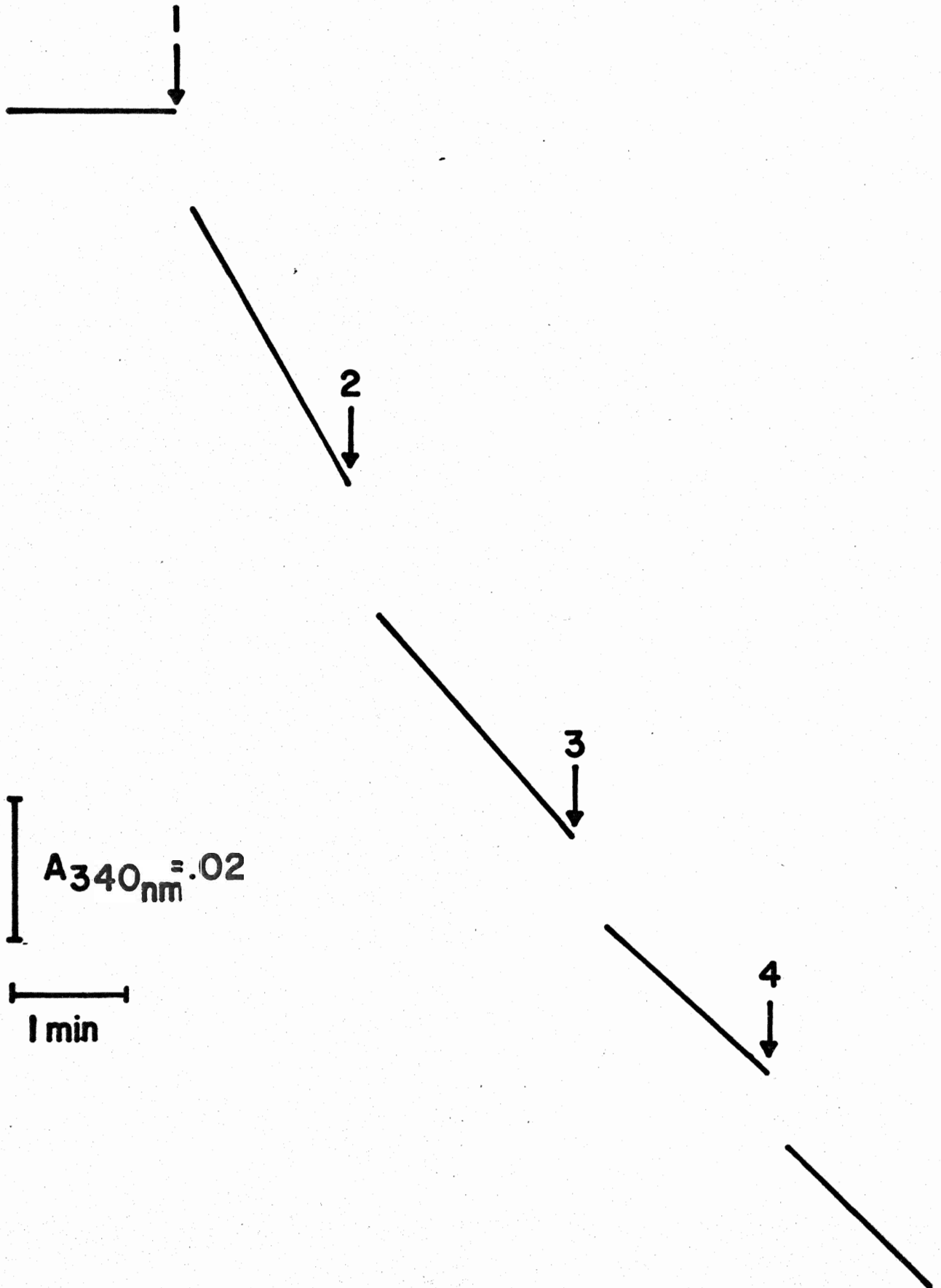
Enzyme activity was assayed spectrophotometrically at 340 nm in the presence of 10.7 mM K-Pi buffer pH 7.2, 3.3 mM  $\text{MgCl}_2$ , 16.7 mM  $\text{NaHCO}_3$ , 0.05 mM NADH, 0.5 mM PEP, 0.2 ml enzyme extract  $\pm$  1.7 mM of each metabolite. Two additional volumes containing 3.3 mM  $\text{MgCl}_2$  were added consecutively. Rates (expressed as  $\Delta\text{A}\cdot\text{min}^{-1}$ ) were determined after the addition of PEP, metabolite, 6.6 mM and 9.9 mM  $\text{MgCl}_2$ .



Figure 35: Effect of succinate and  $\text{MgCl}_2$  on the PEP carboxylase catalyzed rate of absorbance decrease at 340 nm.

0.2 ml enzyme extract was incubated at 30°C in the presence of 3.3 mM  $\text{MgCl}_2$ , 0.05 mM NADH, 16.7 mM  $\text{NaHCO}_3$  and 10.7 mM K-Pi buffer pH 7.4. Additions to the reaction mixture are as indicated:

- (1) 0.5 mM PEP
- (2) 1.7 mM succinate
- (3) 3.3 mM  $\text{MgCl}_2$
- (4) 3.3 mM  $\text{MgCl}_2$



that apparent metabolite inhibition of PEPC activity is probably not due to chelation of essential  $\text{MgCl}_2$  by the metabolite.

(b) The malic enzyme

The successive additions of 1.0 mM  $\text{MnCl}_2$  to all metabolite<sup>5</sup> inhibited assays increased the rates of absorbance change back to the uninhibited rate, and further  $\text{MnCl}_2$  addition to the same assays increased the rate of absorbance change beyond the standard assay rate (Table 26). For example, 1.7 mM succinate decreased the rate of absorbance increase observed for the standard assay 42%. When the  $\text{MnCl}_2$  concentration was increased to 3.3 and 5.0 mM, the standard assay was 'activated' 10.5 and 42.1% (see Figure 36 and Table 26). Furthermore, these observed increases in rates of absorbance change after  $\text{MnCl}_2$  addition were transitory and decreased to a rate smaller than the standard assay within 15 to 30 minutes. This phenomenon was demonstrated to be malic enzyme independent (Methods II,B,1; Figure 3). In order to eliminate this phenomenon, and still investigate the possible chelation of  $\text{MnCl}_2$  by potential effectors, the enzyme preparation was pre-incubated for 30 minutes with 50 mM  $\text{MnCl}_2$ . The resulting preparation was highly turbid and a white precipitate was plainly visible. However, malic enzyme activity was not significantly different from that obtained with the standard protein preparation (Table 26). In contrast, the inhibitory effects of 3-PGA were decreased from 35 to 15% when assayed with the  $\text{MnCl}_2$  pre-incubated enzyme. A phenomenon unique to fructose-1,6-

Table 26: Effect of  $\text{MnCl}_2$  on malic enzyme activity in the presence and absence of various metabolites

Standard Assay Conditions	Activity				
	Enzyme- $\text{MnCl}_2$ <sup>1</sup>			Enzyme+50 mM $\text{MnCl}_2$ <sup>2</sup>	
	1.7 mM $\text{MnCl}_2$	3.3 mM $\text{MnCl}_2$	5.0 mM $\text{MnCl}_2$	1.7 mM $\text{MnCl}_2$	3.3 mM $\text{MnCl}_2$
- malate	0.001	0.006	0.003	0.006	0.004
Standard Assay	0.019	0.028	0.032	0.022	0.022
+ succinate	0.011	0.021	0.027	0.018	0.020
+ citrate	0.018	0.023	0.034	0.021	0.021
+F-1,6-diP	0.007	0.010	0.022	0.022	0.021
+ 3-PGA	0.012	0.016	0.023	0.023	0.022

<sup>1</sup>Enzyme -  $\text{MnCl}_2$ , enzyme stored in buffer

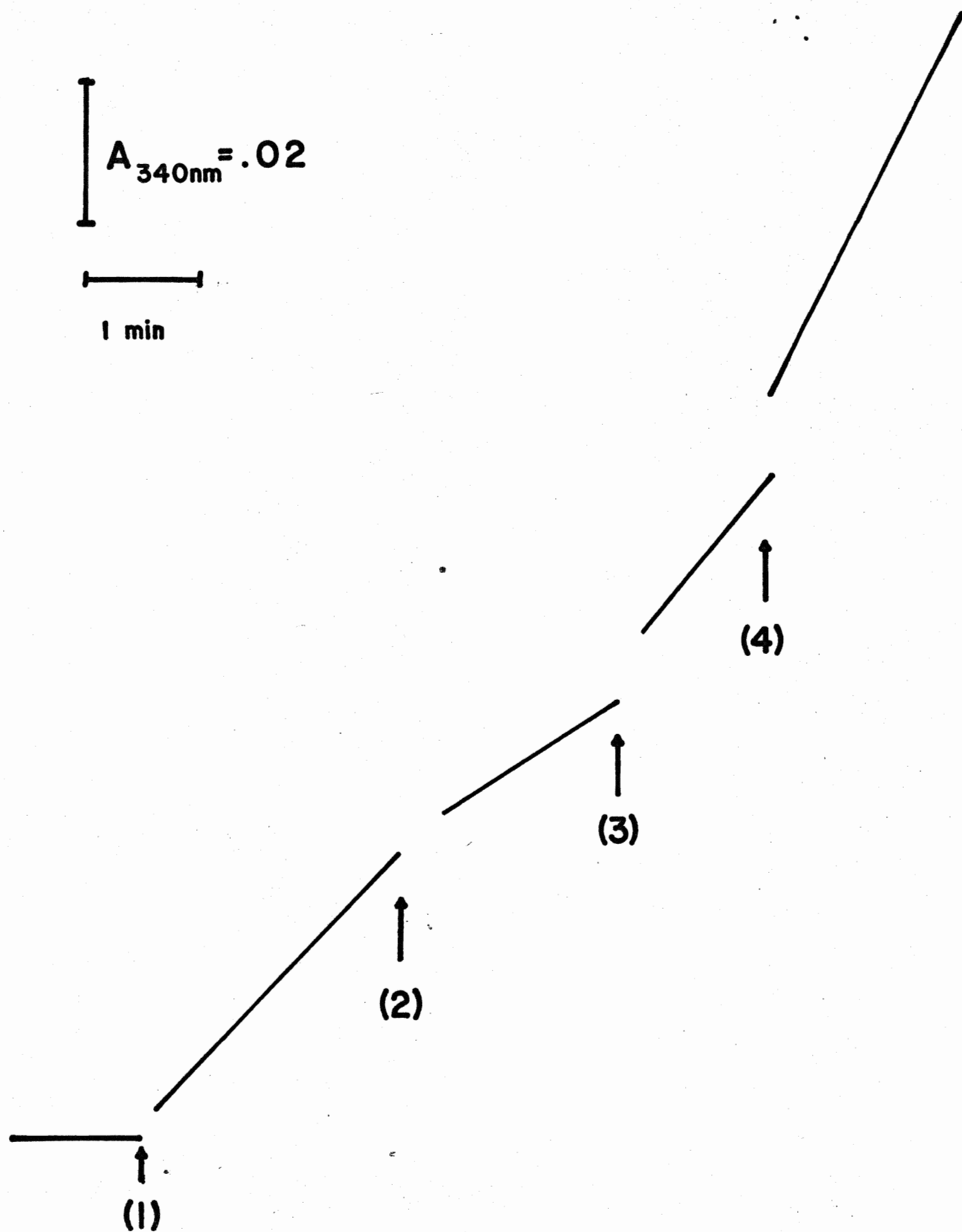
<sup>2</sup>Enzyme + 50 mM  $\text{MnCl}_2$ , enzyme pre-incubated for 30 min with 50 mM  $\text{MnCl}_2$

Enzyme activity was assayed spectrophotometrically at 340 nm in the presence of 12.5 mM Tris-BES buffer pH 6.9, 1.0 mM  $\text{MnCl}_2$ , 0.5 mM  $\text{NADP}^+$ , 0.5 mM malate and 0.2 ml enzyme in the presence or absence of 50 mM  $\text{MnCl}_2 \pm 1.7$  mM of each metabolite. Additional  $\text{MnCl}_2$  was added consecutively to a final volume as indicated. Rates (expressed as  $\Delta A \cdot \text{min}^{-1}$ ) were determined after the addition of malate, metabolite and  $\text{MnCl}_2$  additions.

Figure 36: Effect of succinate and  $\text{MnCl}_2$  on the malic enzyme catalyzed rate of absorbance increase at 340 nm.

0.2 ml enzyme extract was incubated at 30°C in the presence of 1.0 mM  $\text{MnCl}_2$ , 0.5 mM  $\text{NADP}^+$  and 12.5 mM Tris-BES buffer pH 7.25. Additions to the reaction mixture are as indicated:

- (1) 0.5 mM malate
- (2) 1.7 mM succinate
- (3) 1.0 mM  $\text{MnCl}_2$
- (4) 3.0 mM  $\text{MnCl}_2$



diphosphate inhibition of malic enzyme activity is that assays with non-pre-incubated enzyme produced biphasic 'initial' rates in which the initial rate was faster than the final rate. In contrast, assays with the pre-incubated protein resulted in monophasic initial rates of the same magnitude as the slower segment of the biphasic assays (Figure 37).

In general, the results indicate that  $\text{MnCl}_2$  chelation by the metabolites may possibly be the mechanism of inhibition. This is reinforced by the low  $K_{m_{app}}$  ( $\text{MnCl}_2$ ) of 0.1 mM at pH 7.25 (see Results II,C).

#### C. Effects of pH and effectors on the apparent kinetic constants of PEP carboxylase and the malic enzyme

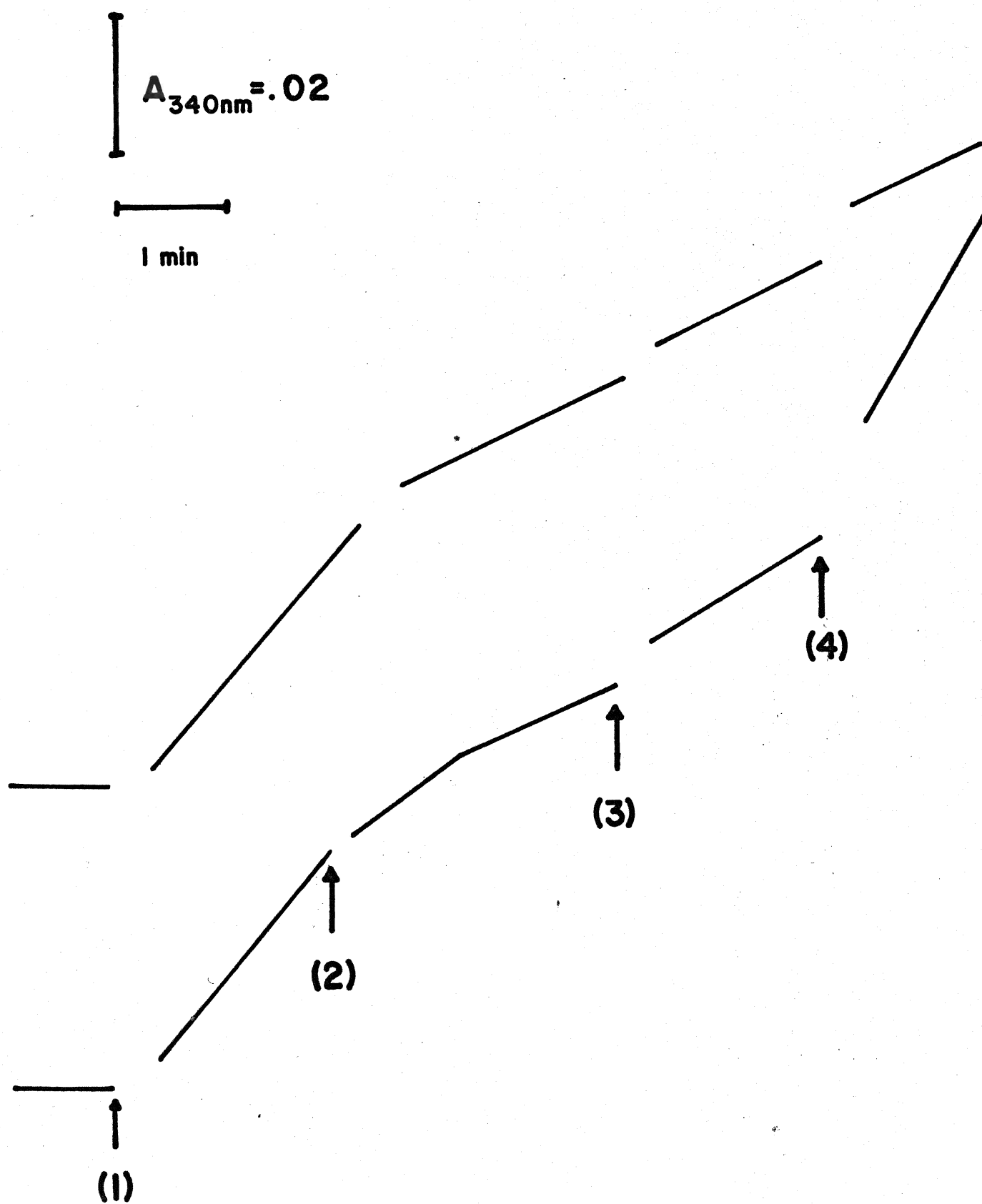
In this section, standard spectrophotometric assays were conducted in the presence and absence of apparent effectors of PEPC and the malic enzyme as determined in Results (IV,A and B). All rates reported here are corrected for endogenous activities by running appropriate control assays (Methods II,A,1(ii); II,B,1(ii)). The addition to the cuvette of effector before substrate or vice versa, did not influence the final rate obtained in the presence of substrate and effector. Apparent affinity constants for substrates and  $V_{max}$  were determined in the presence and absence of the effectors using the linear transformations of the Michaelis-Menton equation (Methods V). In most cases, only one potential effector concentration was employed, thus not permitting the calculation of inhibitor

Figure 37: Effect of fructose-1,6-diphosphate and  $\text{MnCl}_2$  on the malic enzyme catalyzed rate of absorbance increase at 340 nm using the standard protein preparation, or protein pre-incubated with  $\text{MnCl}_2$ .

0.2 ml standard enzyme extract (lower trace) or 0.2 ml protein pre-incubated for 30 minutes in the presence of 50 mM  $\text{MnCl}_2$  (upper trace) was incubated at 30°C in the presence of 1.0 mM  $\text{MnCl}_2$ , 0.5 mM  $\text{NADP}^+$  and 12.5 mM Tris-BES buffer pH 7.25. Additions to the reaction mixtures are as indicated:

- (1) 0.5 mM malate
- (2) 1.7 mM fructose-1,6-diphosphate
- (3) 1.0 mM  $\text{MnCl}_2$
- (4) 3.0 mM  $\text{MnCl}_2$





binding affinity constants. Results with potential effectors of PEPC activity are reported first, followed by results with effectors of malic enzyme activity.

(1) PEP carboxylase

Malate, succinate, citrate, fructose-1,6-diphosphate and 3-phosphoglycerate were tested to determine their effects on the kinetics, apparent  $K_m(\text{PEP})$  and  $V_{\max}$  of PEPC between pH 7.0 and 7.7. Figure 38 demonstrates that the % inhibition of saturating activity by each metabolite decreased as pH was increased.

(a) Malate inhibition of PEPC activity

pH profiles of activity in the presence of 0.1 mM malate indicate that activity increased as pH was increased at all concentrations of PEP (Figure 39). The most pronounced increases in activity were between pH 7.2 and 7.5

Plots of percent inhibition as functions of pH indicate that inhibition decreased linearly as the pH was increased for all PEP concentrations (Figure 40). Malate inhibited PEPC activity 70 to 90% at pH, 7.1 and 25 to 55% at pH 7.5

Linear transformations of the data indicate biphasic plots (Figures 41a,b, and c). Under conditions of high binding affinity for PEP (low PEP levels) or low binding affinity (high PEP levels), malate did not change the  $K_{m_{\text{app}}}(\text{PEP})$ . In contrast, both the high and low  $V_{\max}$  estimations were decreased. These results are summarized in Table 27 at the end of this section.

Figure 38: Effect of pH on the percent inhibition of near-saturated PEP carboxylase activity by malate, succinate, citrate, fructose-1,6-diphosphate and 3-phosphoglycerate.

Enzyme activity was assayed spectrophotometrically at 340 nm in the presence of 10.7 mM K-Pi buffer pH 6.9 to 7.5, 3.3 mM  $\text{MgCl}_2$ , 16.7 mM  $\text{NaHCO}_3$ , 0.05 mM NADH, 0.5 mM PEP, 0.2 ml enzyme extract and  $\pm 1.7$  mM succinate ( $\Delta$ ), 0.1 mM malate ( $\bigcirc$ ), 1.7 mM citrate ( $\square$ ), 1.7 mM fructose-1,6-diphosphate ( $\nabla$ ), or 1.0 mM 3-phosphoglycerate ( $\blacktriangledown$ ). Percent inhibition was calculated for metabolite inhibited activity as a percentage of activity in the absence of the metabolite.

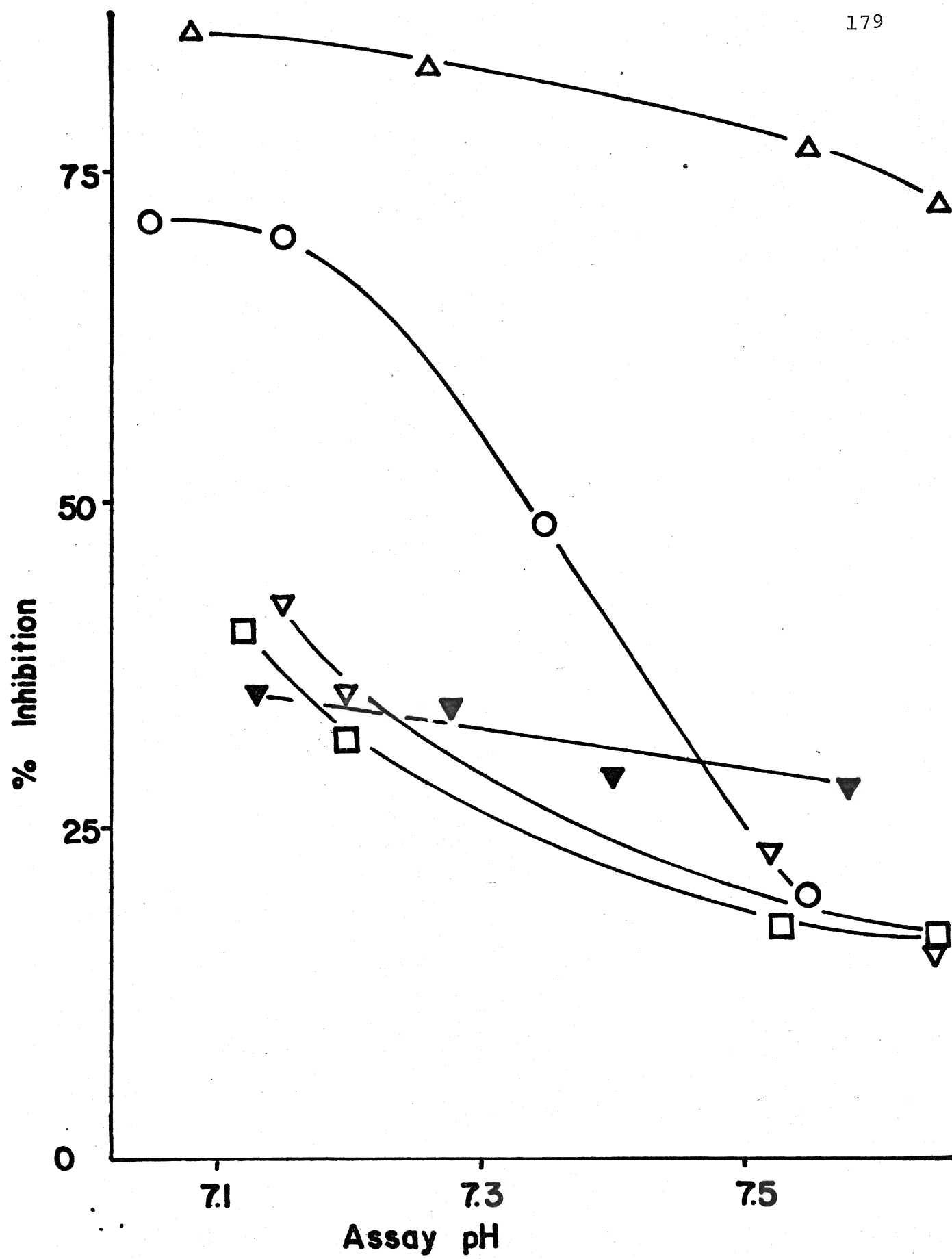


Figure 39: Effect of 0.1 mM malate on the pH profiles of PEP carboxylase activity at near-saturated and PEP limited substrate levels.

Enzyme activity was assayed spectrophotometrically at 340 nm in the presence of 10.7 mM K-Pi buffer pH 6.9 to 7.4, 3.3 mM  $\text{MgCl}_2$ , 16.7 mM  $\text{NaHCO}_3$ , 0.05 mM NADH, 0.2 ml enzyme extract and 0.5 ( $\Delta$ ), 0.3 ( $\bigcirc$ ), 0.1 ( $\nabla$ ) or 0.05 ( $\square$ ) mM PEP in the presence (closed symbols) or absence (open symbols) of 0.1 mM malate .

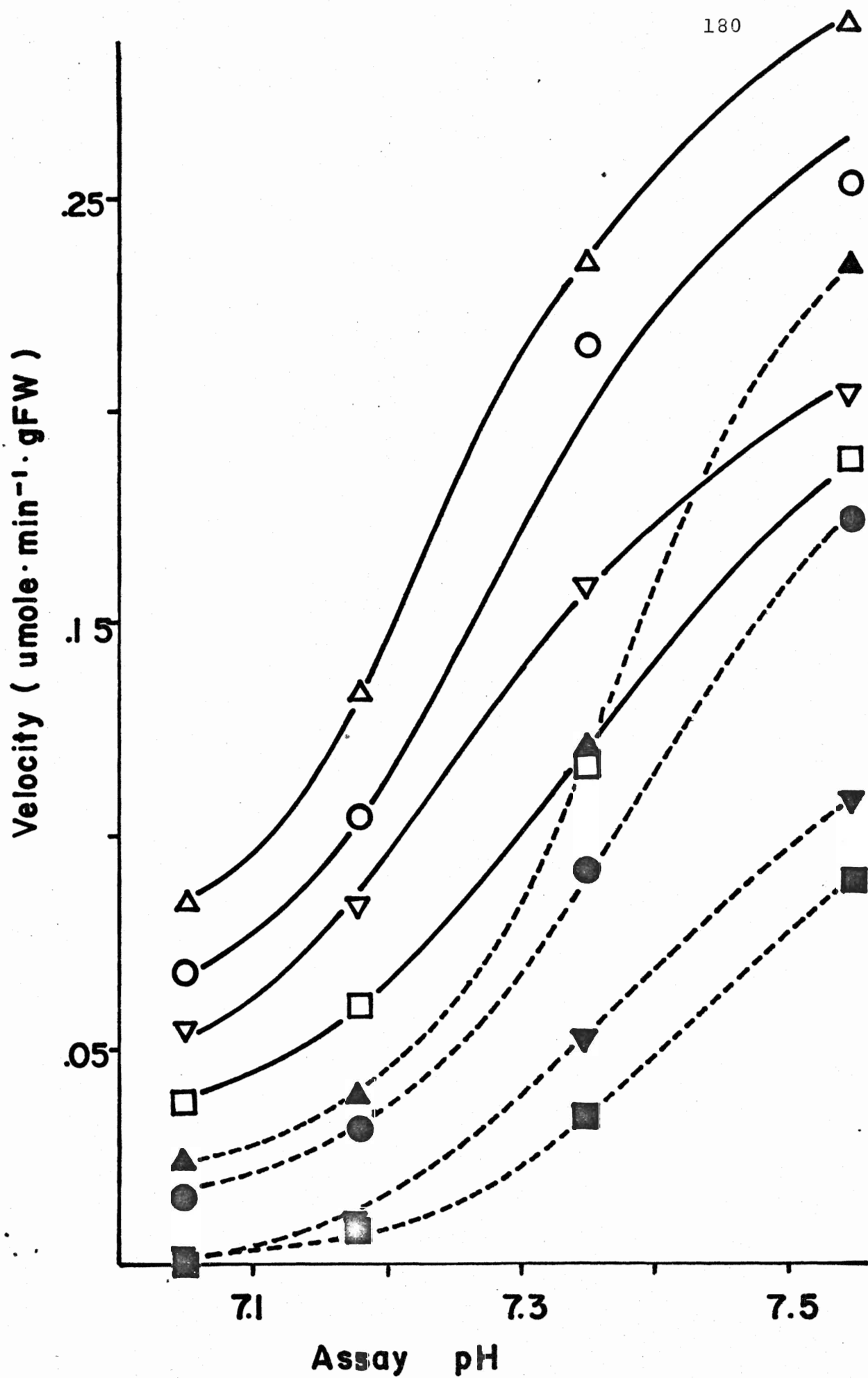


Figure 40: Effect of pH on the percent inhibition of PEP carboxylase activity by 0.1 mM malate.

Enzyme activity was assayed spectrophotometrically at 340 nm in the presence of 10.7 mM K-Pi buffer pH 6.9 to 7.4, 3.3 mM  $\text{MgCl}_2$ , 16.7 mM  $\text{NaHCO}_3$ , 0.05 mM NADH, 0.2 ml enzyme extract and 0.5 ( $\blacktriangle$ ), 0.3 ( $\blacktriangledown$ ), 0.1 ( $\bullet$ ) or 0.05 ( $\blacksquare$ ) mM PEP in the presence and absence of 0.1 mM malate. Percent inhibition was calculated for malate inhibited activity as a percentage of activity in the absence of malate.

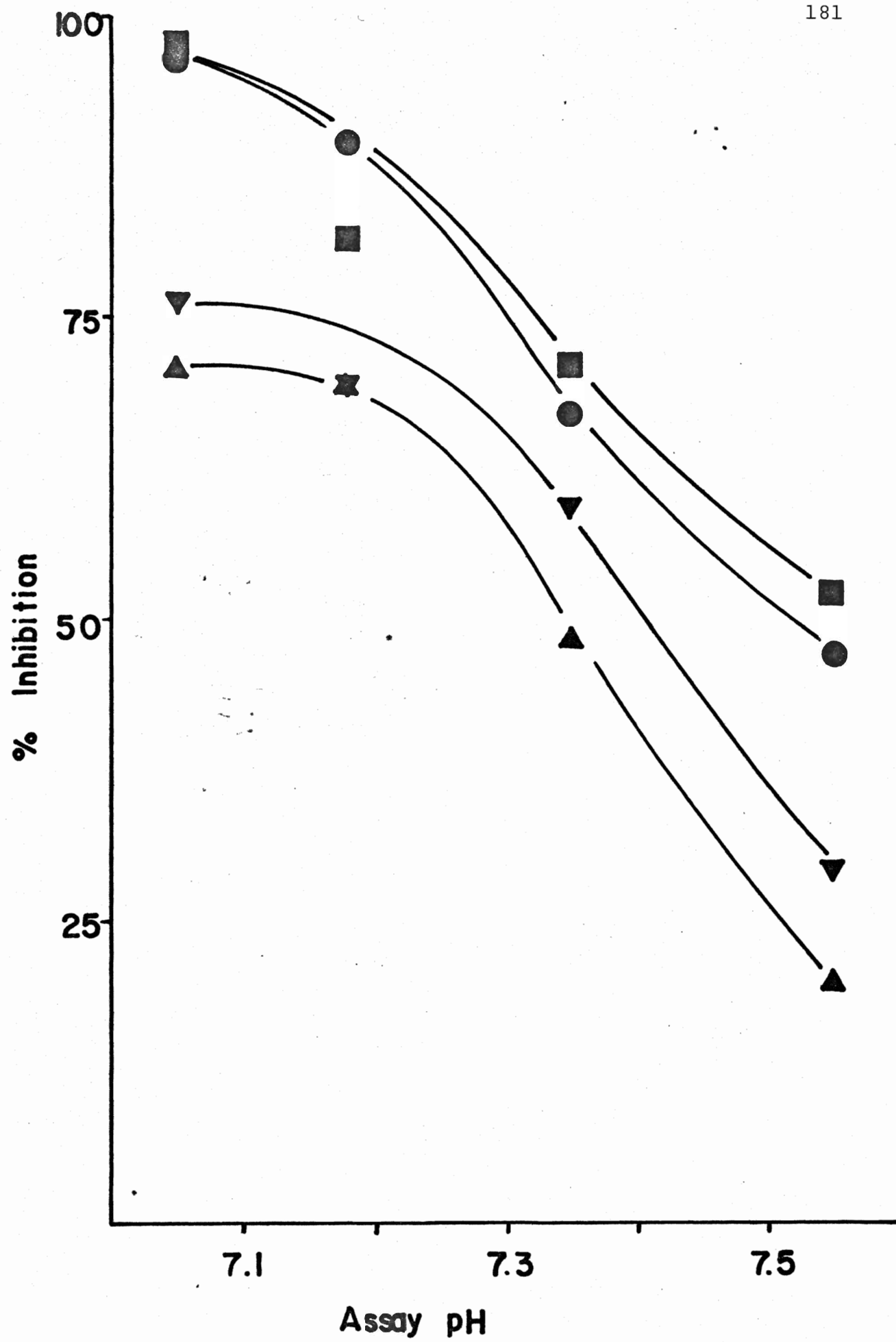




Figure 41: Effect of pH and 0.1 mM malate on the linear transformations of PEP carboxylase activity as a function of PEP concentrations.

Enzyme activity was assayed spectrophotometrically at 340 nm in the presence of 10.7 mM K-Pi buffer pH 6.9 ( $\square$ ), 7.1 ( $\nabla$ ), 7.25 ( $\bigcirc$ ) and 7.4 ( $\triangle$ ), 3.3 mM  $\text{MgCl}_2$ , 16.7 mM  $\text{NaHCO}_3$ , 0.05 mM NADH, 0.2 ml enzyme extract and 0.01 to 0.5 mM PEP in the absence (open symbols) and presence (closed symbols) of 0.1 mM malate.

Figure 41(a): Lineweaver-Burk plot

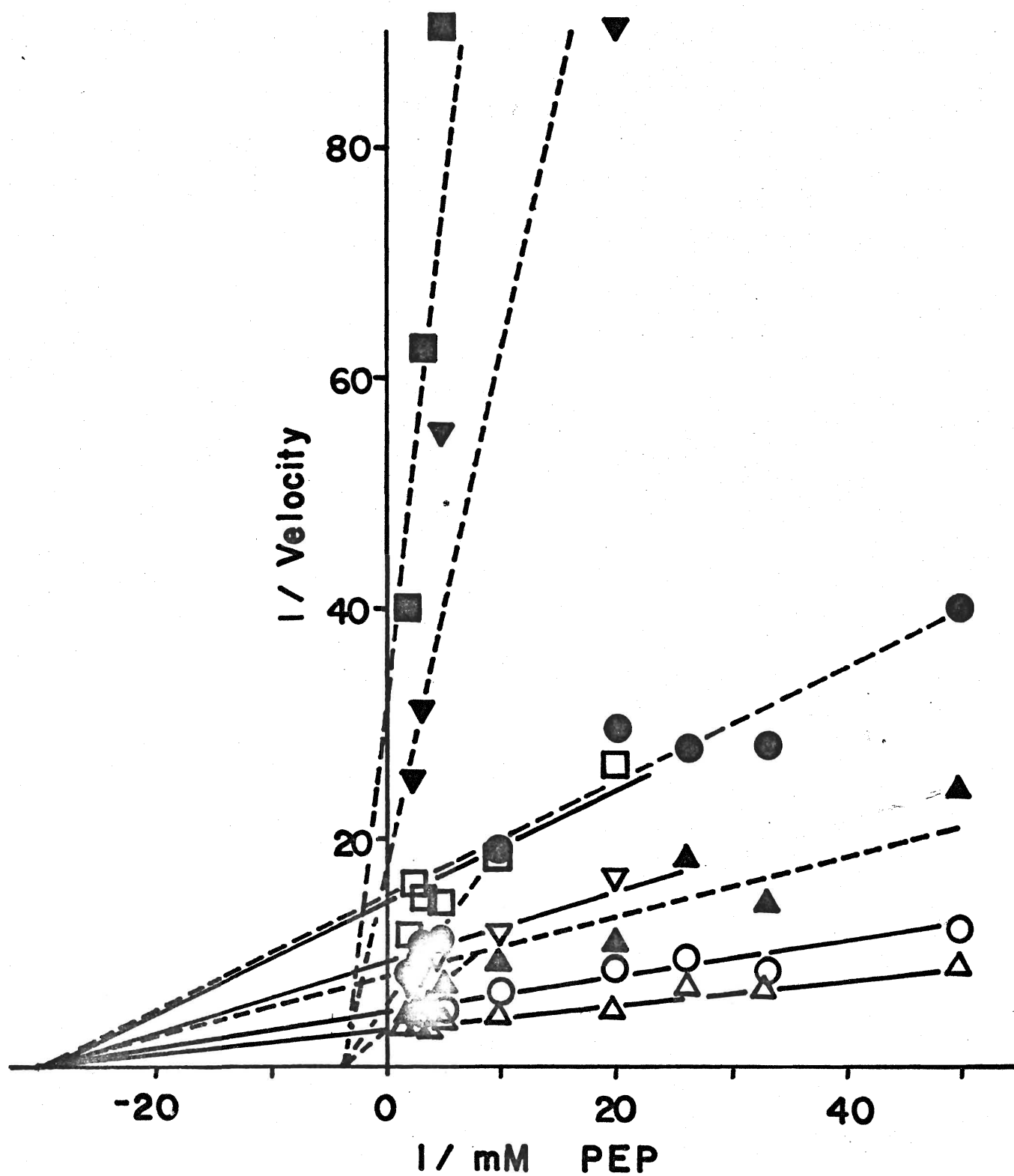


Figure 41(b): Eadie-Hofstee plot

Buffer pH 7.25 (●) and 7.4 (▲); + 0.1 mM malate  
(closed symbols), - malate (open symbols). For further  
details refer to legend of Figure 41.

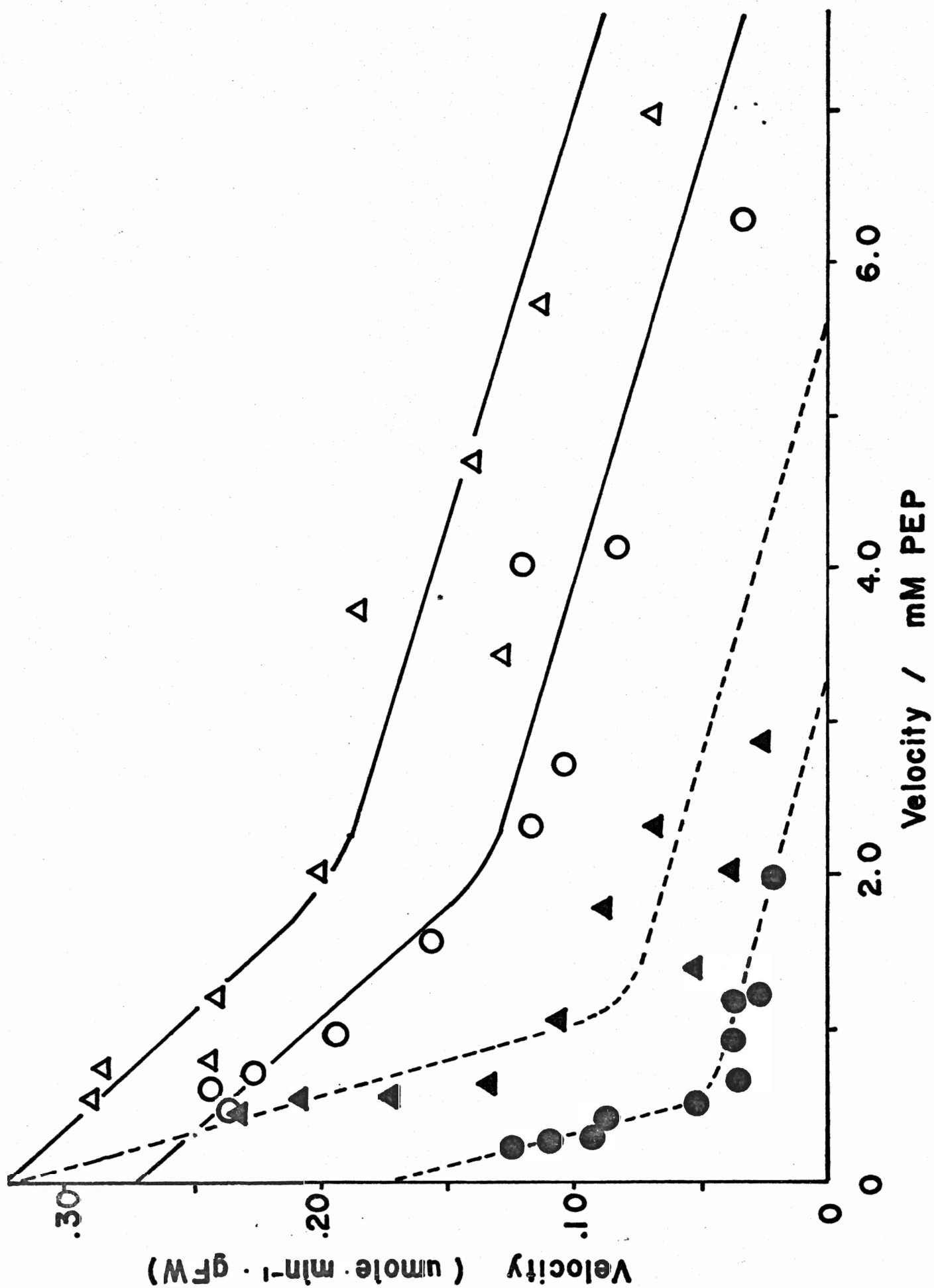
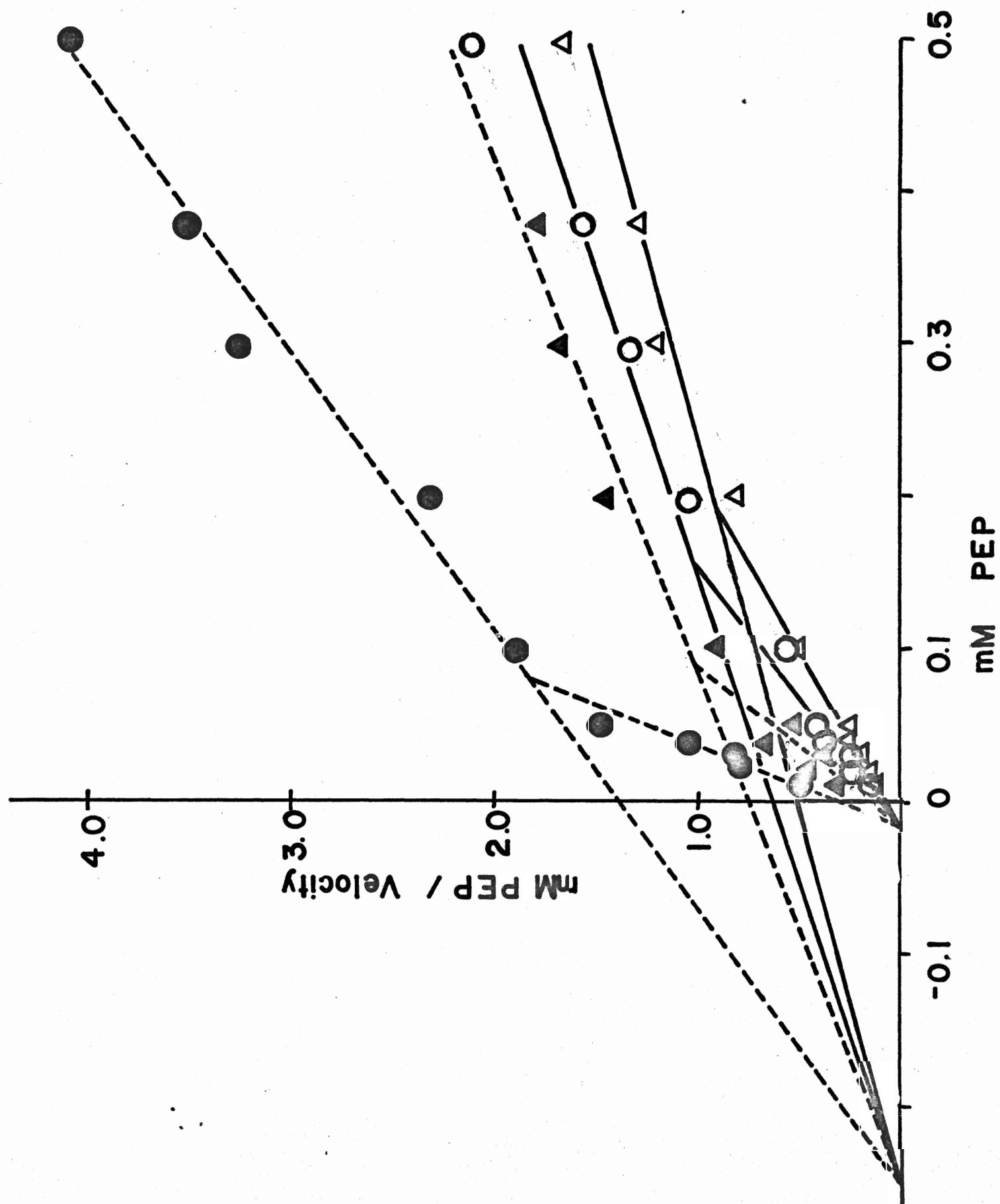


Figure 41(c) Hanes plot

Buffer pH 7.25 (●) and 7.4 (Δ); + 0.1 mM malate  
(closed symbols), - malate (open symbols). For further  
details refer to legend of Figure 41.



Estimations of the effect of pH on the  $K_{i_{app}}^{(malate)}$  were determined from Dixon plots. Activity was assayed between pH 7.0 and 7.6 with 0.05 or 0.5 mM PEP in the presence and absence of 0.02 to 0.29 mM malate. Figure 42 demonstrates that under all assay conditions, the curves intersect at one point on the abscissa. This indicates that the  $K_{i_{app}}^{(malate)}$  of 0.04 to 0.06 mM was pH independent, and that inhibition was non-competitive in nature, confirming the results obtained earlier for 0.1 mM malate inhibition of PEPC activity.

(b) Succinate, citrate, fructose-1,6-diphosphate, 3-phosphoglycerate inhibition of PEPC activity.

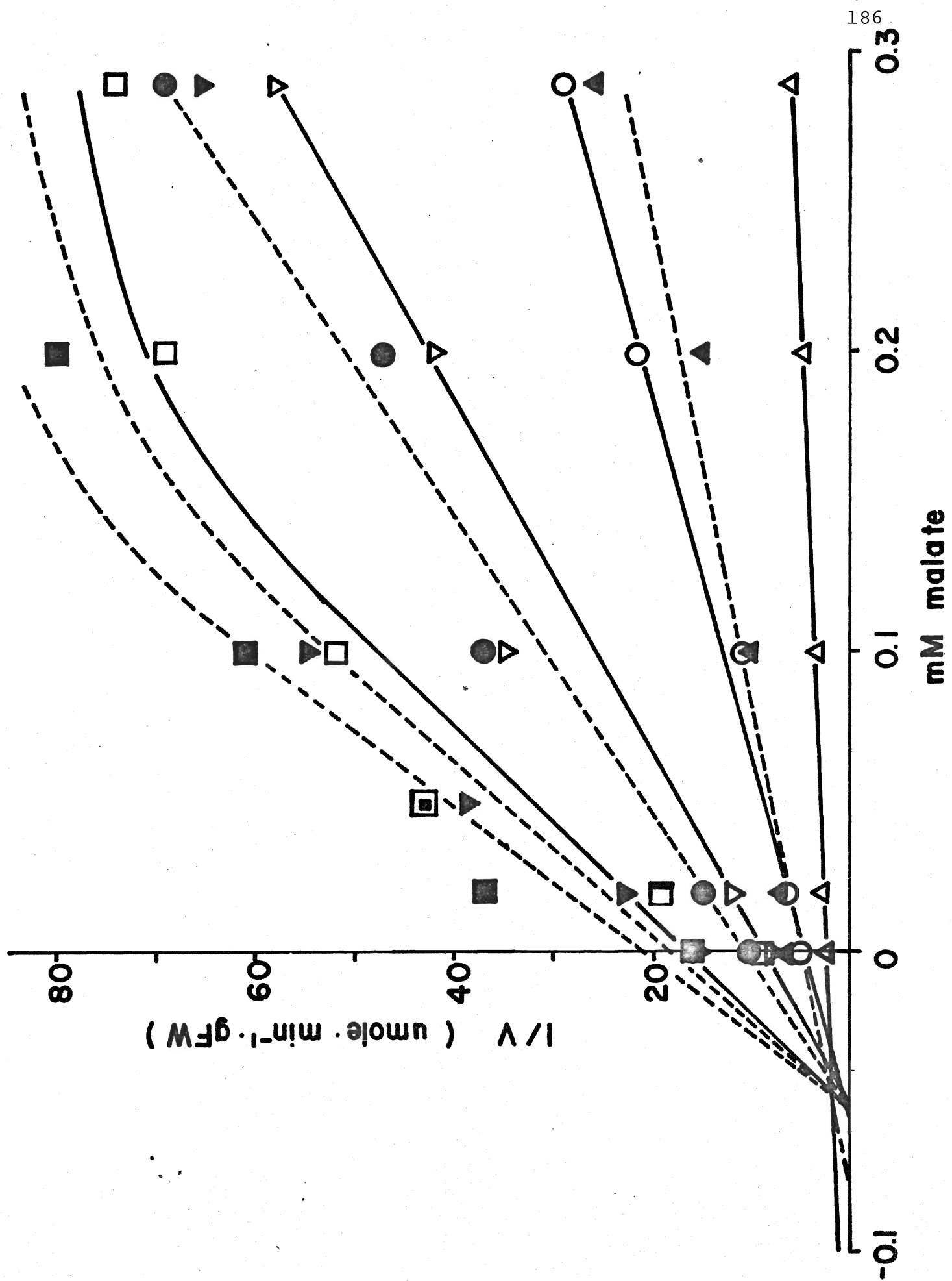
1.7 mM succinate, citrate, fructose-1,6-diphosphate or 1.0 mM 3-phosphoglycerate were assayed with separate protein extracts. In all cases, the percent inhibition of saturated activity decreased as pH was increased (Figure 38). Succinate was a much stronger inhibitor than the other metabolites, with the exception of malate. At pH 7.3, activity assayed with 0.5 mM PEP was inhibited 55% by 0.10 mM malate, 85% by 1.7 mM succinate, and 25 to 35% by 1.7 mM fructose-1,6-diphosphate, citrate and 1.0 mM 3-phosphoglycerate. The addition of 0.1 mM malate to metabolite inhibited assays (0.5 mM PEP, pH 7.05 and 7.55), or vice versa, increased the inhibition of enzyme activity further.

Linear transformations of activity in the presence and absence of the metabolites demonstrated distinct effects of each metabolite on the kinetic constants of PEPC. Lineweaver-Burk

Figure 42: Effect of pH on the Dixon plot of PEP carboxylase activity in the presence of malate.

Enzyme activity was assayed spectrophotometrically at 340 nm in the presence of 10.7 mM K-Pi buffer pH 6.9 ( $\square$ ), 7.1 ( $\nabla$ ), 7.25 ( $\bigcirc$ ) and 7.4 ( $\triangle$ ), 3.3 mM  $\text{MgCl}_2$ , 16.7 mM  $\text{NaHCO}_3$ , 0.05 mM NADH, 0.2 ml enzyme extract and 0.5 (open symbols) or 0.05 (closed symbols) mM PEP.





plots are illustrated, however, Eadie-Hofstee and Hanes plots of the data indicated similar results. Figure 43 indicates that Lineweaver-Burk plots of succinate inhibition of activity are non-linear at pH 7.55 and 7.26. At PEP concentrations greater than 0.1 mM, succinate increased the  $K_{m_{app}}(PEP)$  from 0.03 to 0.13 mM and this increase was pH independent. Maximal succinate inhibited activity was pH dependent, decreasing from 0.09 to 0.05  $\mu\text{mole}\cdot\text{min}^{-1}\cdot\text{g FW}$  as pH was decreased from 7.55 to 7.26. In contrast, succinate inhibited activity in the presence of PEP concentrations less than 0.1 mM was of an uncompetitive type as indicated by parallel curves of activity in the presence or absence of succinate (Figure 43).

Lineweaver-Burk plots of activity in the presence of 1.7 mM citrate demonstrate that  $V_{max}$  was not affected by citrate (Figure 44). However, the apparent  $K_m(PEP)$  was increased by citrate from 0.03 mM to 0.09 mM in a pH independent manner. The results indicate that citrate inhibited PEPC activity competitively with respect to PEP.

Figure 45 indicates that 1.7 mM F-1,6-diP inhibition of PEPC activity was non-competitive at high pH, since  $V_{max}$  was decreased from 0.45 to 0.41  $\mu\text{mole}\cdot\text{min}^{-1}\cdot\text{g FW}$  at pH 7.72 and from 0.38 to 0.29  $\mu\text{mole}\cdot\text{min}^{-1}\cdot\text{g FW}$  at pH 7.53, and the  $K_{m_{app}}$  for PEP (0.04 mM) was not changed. Conversely, inhibition at low pH was dependent on the PEP concentration. Levels of PEP greater than 0.2 mM caused an increase in the  $K_{m_{app}}(PEP)$  from 0.04 mM to 0.33 mM, and  $V_{max}$  was not influenced. These results indicate

Figure 43: Effect of pH and 1.7 mM succinate on the Lineweaver-Burk plot of PEP carboxylase activity.

Enzyme activity was assayed spectrophotometrically at 340 nm in the presence of 10.7 mM K-Pi buffer pH 7.1 (○) and 7.4 (Δ), 3.3 mM MgCl<sub>2</sub>, 16.7 mM NaHCO<sub>3</sub>, 0.05 mM NADH, 0.026 to 0.5 mM PEP, 0.2 ml enzyme extract and plus (closed symbols) or minus (open symbols) 1.7 mM succinate.

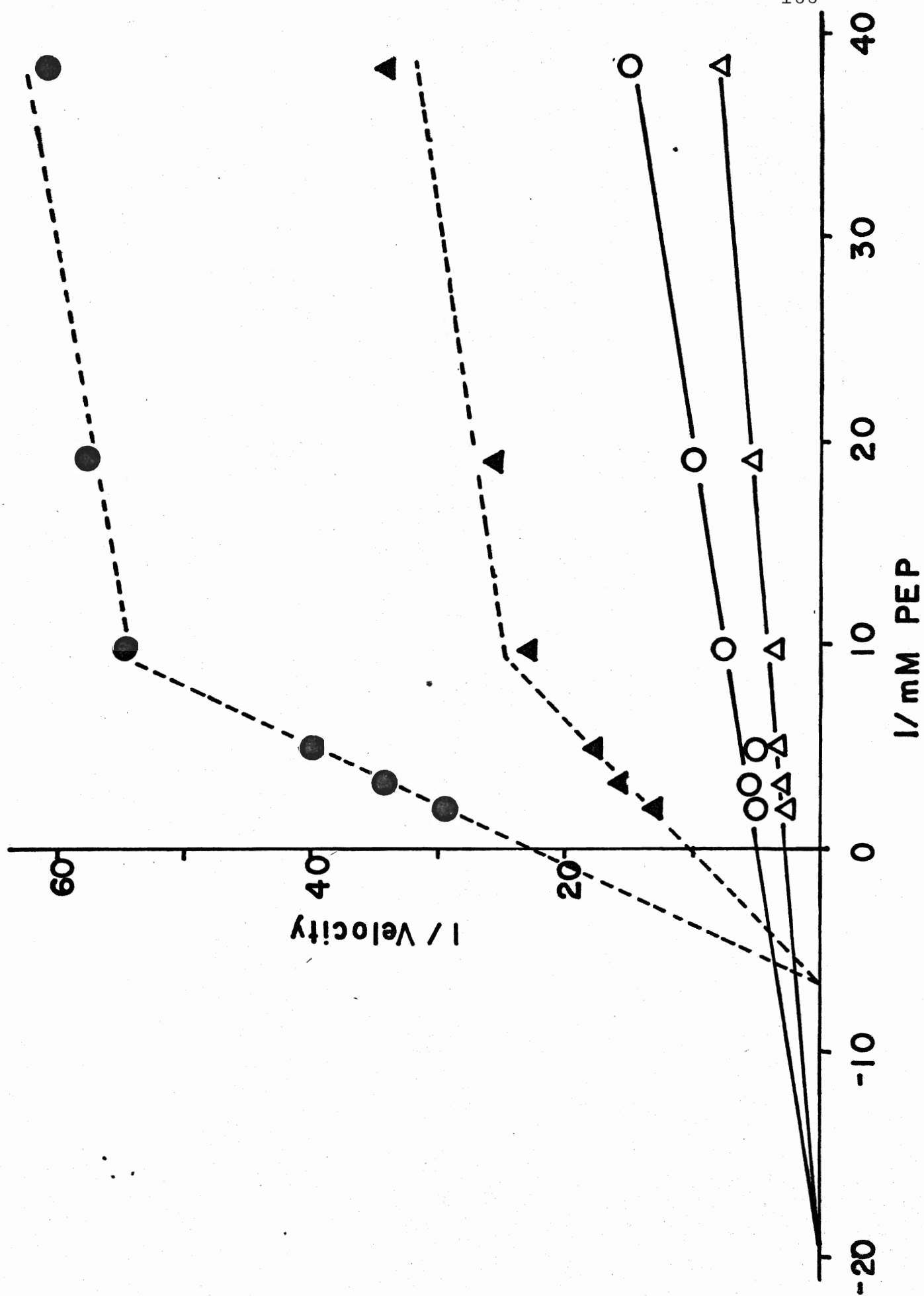


Figure 44: Effect of pH and 1.7 mM citrate on the Lineweaver-Burk plot of PEP carboxylase activity.

Enzyme activity was assayed spectrophotometrically at 340 nm in the presence of 10.7 mM K-Pi buffer pH 6.9 ( $\square$ ), 7.1 ( $\bigcirc$ ), 7.25 ( $\nabla$ ) and 7.4 ( $\triangle$ ), 3.3 mM  $\text{MgCl}_2$ , 16.7 mM  $\text{NaHCO}_3$ , 0.05 mM NADH, 0.03 to 0.5 mM PEP, 0.2 ml enzyme extract and plus (closed symbols) or minus (open symbols) 1.7 mM citrate.

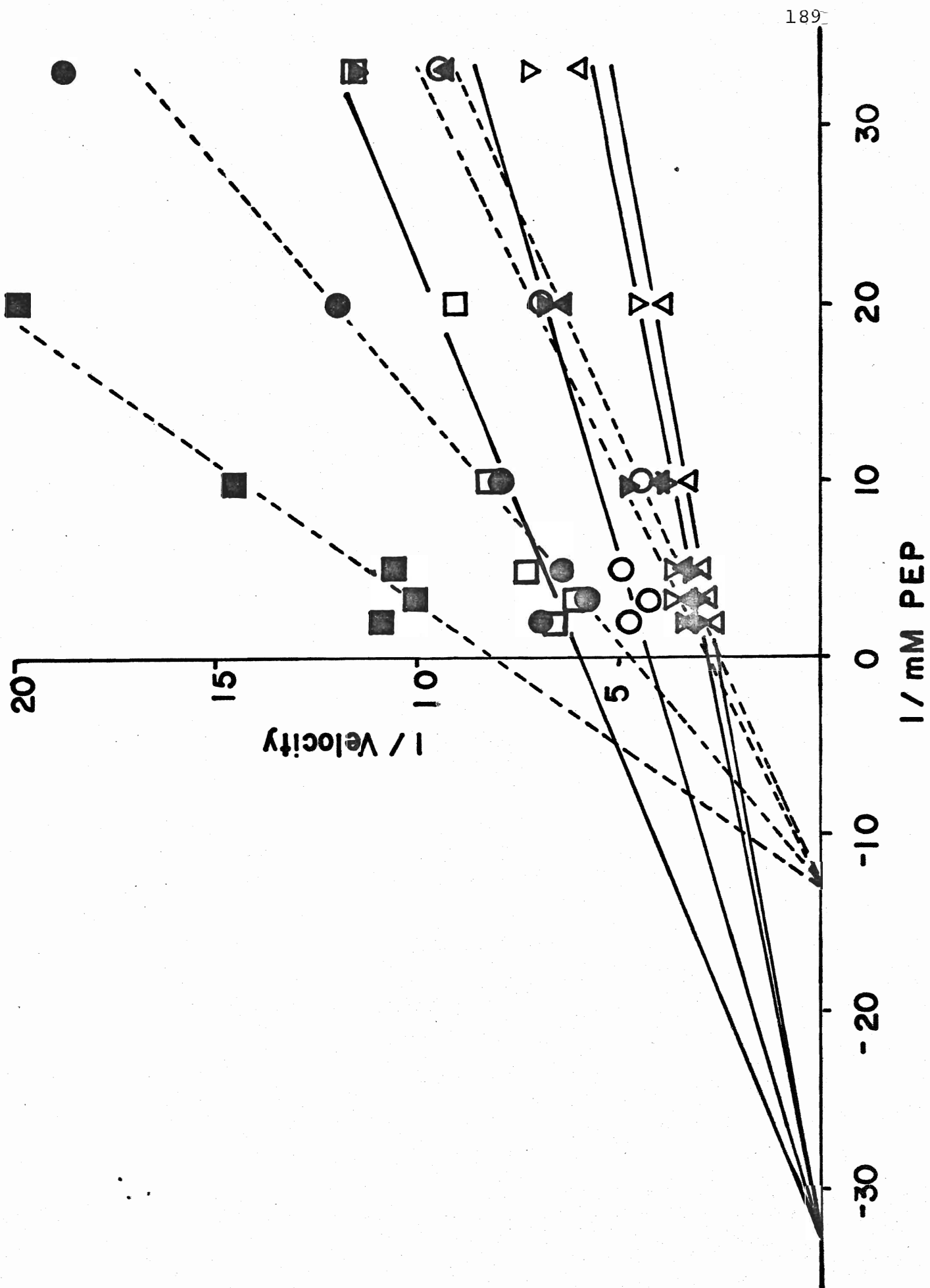
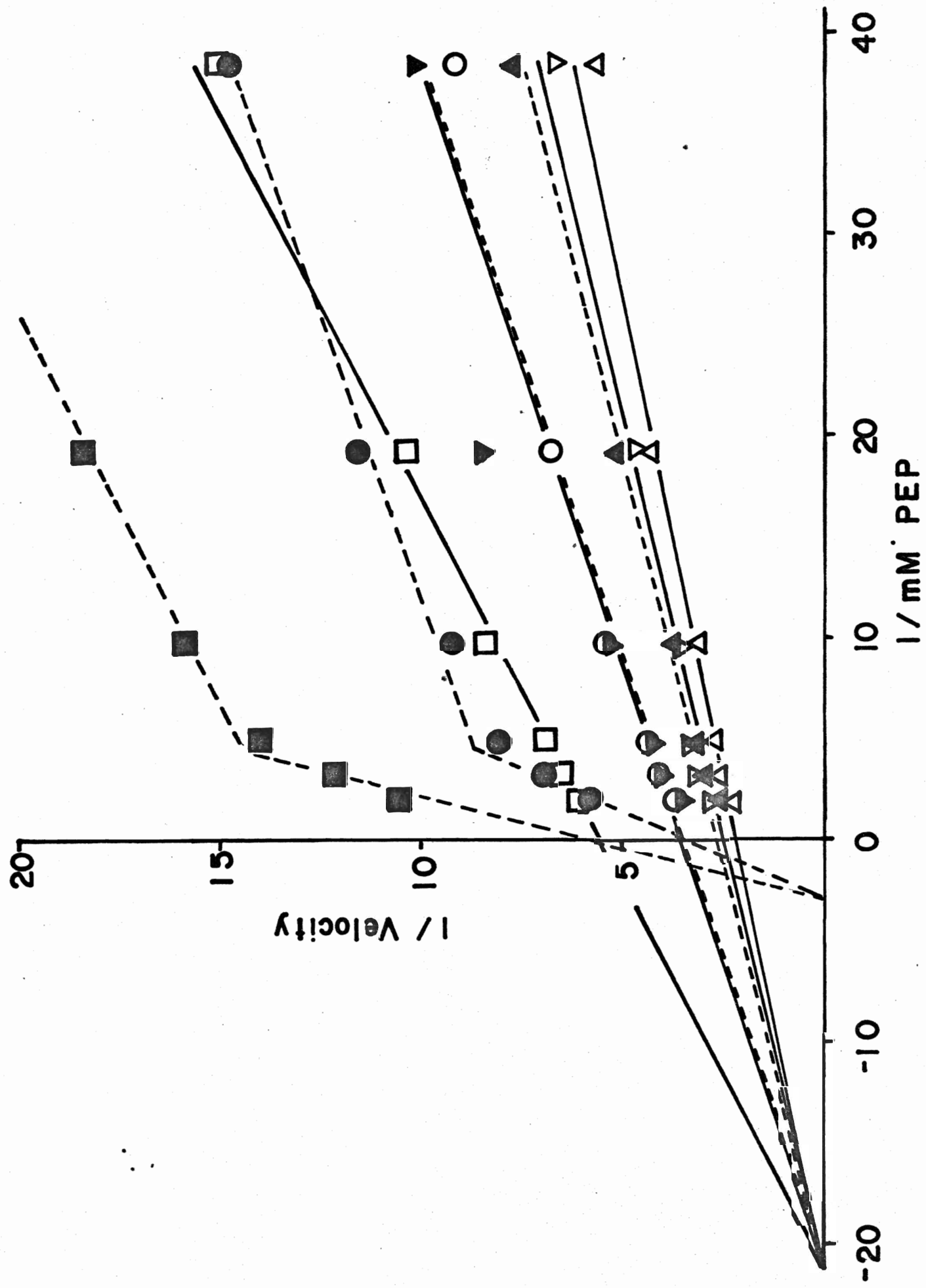


Figure 45: Effect of pH and 1.7 mM fructose-1,6-diphosphate on the Lineweaver-Burk plot of PEP carboxylase activity.

Enzyme activity was assayed spectrophotometrically at 340 nm in the presence of 10.7 mM K-Pi buffer pH 6.9 ( $\square$ ), 7.1 ( $\bigcirc$ ), 7.25 ( $\nabla$ ) and 7.4 ( $\triangle$ ), 3.3 mM  $\text{MgCl}_2$ , 16.7 mM  $\text{NaHCO}_3$ , 0.05 mM NADH, 0.03 to 0.5 mM PEP, 0.2 ml enzyme extract and plus (closed symbols) or minus (open symbols) 1.7 mM fructose-1,6-diphosphate.





competitive inhibition. When assayed at low pH with PEP concentrations less than 0.2 mM, Figure 45 demonstrates parallel curves in the presence or absence of F-1,6-diP, indicative of uncompetitive inhibition.

3-PGA influenced PEPC activity in a non-competitive manner by decreasing the  $V_{\max}$  from 0.38 to 0.24  $\mu\text{mole}\cdot\text{min}^{-1}\cdot\text{g FW}$  at pH 7.58, and from 0.12 to 0.08  $\mu\text{mole}\cdot\text{min}^{-1}\cdot\text{g FW}$  at pH 7.13 (Figure 46). The  $K_{m\text{app}}$ (PEP) of 0.06 mM was not affected by pH and/or 3-PGA.

Table 27 summarizes the effects of pH and malate, succinate, citrate, F-1,6-diP or 3-PGA on the apparent  $K_m$ (PEP) and  $V_{\max}$  of PEPC.

## (2) The malic enzyme

Inhibition of malic enzyme activity by 1.7 mM succinate, F-1,6-diP and 3-PGA was investigated at pH 6.4, 6.9 and 7.4 over a range of malate concentrations (0.025 to 0.5 mM). Figure 47 demonstrates that near-saturating activity was inhibited most strongly by F-1,6-diP, followed by 3-PGA, succinate and citrate (1.7 mM). Furthermore, inhibition by all metabolites decreased with an increase in pH. The decrease in inhibition as pH was increased from 6.4 to 7.4 was approximately 50% for all metabolites, possibly indicating a similar mechanism of inhibition.

All metabolites tested inhibited enzyme activity non-competitively as indicated by a decrease in  $V_{\max}$  and no effect on the apparent  $K_m$ (malate). No effect of pH on  $K_m$  or  $V_{\max}$  was

Figure 46: Effect of pH and 1.0 mM 3-phosphoglycerate on the Lineweaver-Burk plot of PEP carboxylase activity.

Enzyme activity was assayed spectrophotometrically at 340 nm in the presence of 10.7 mM K-Pi, buffer pH 7.1 (○) and 7.4 (△), 3.3 mM MgCl<sub>2</sub>, 16.7 mM NaHCO<sub>3</sub>, 0.05 mM NADH, 0.026 to 0.5 mM PEP, 0.2 ml enzyme extract and plus (closed symbols) or minus (open symbols) 1.0 mM 3-phosphoglycerate.

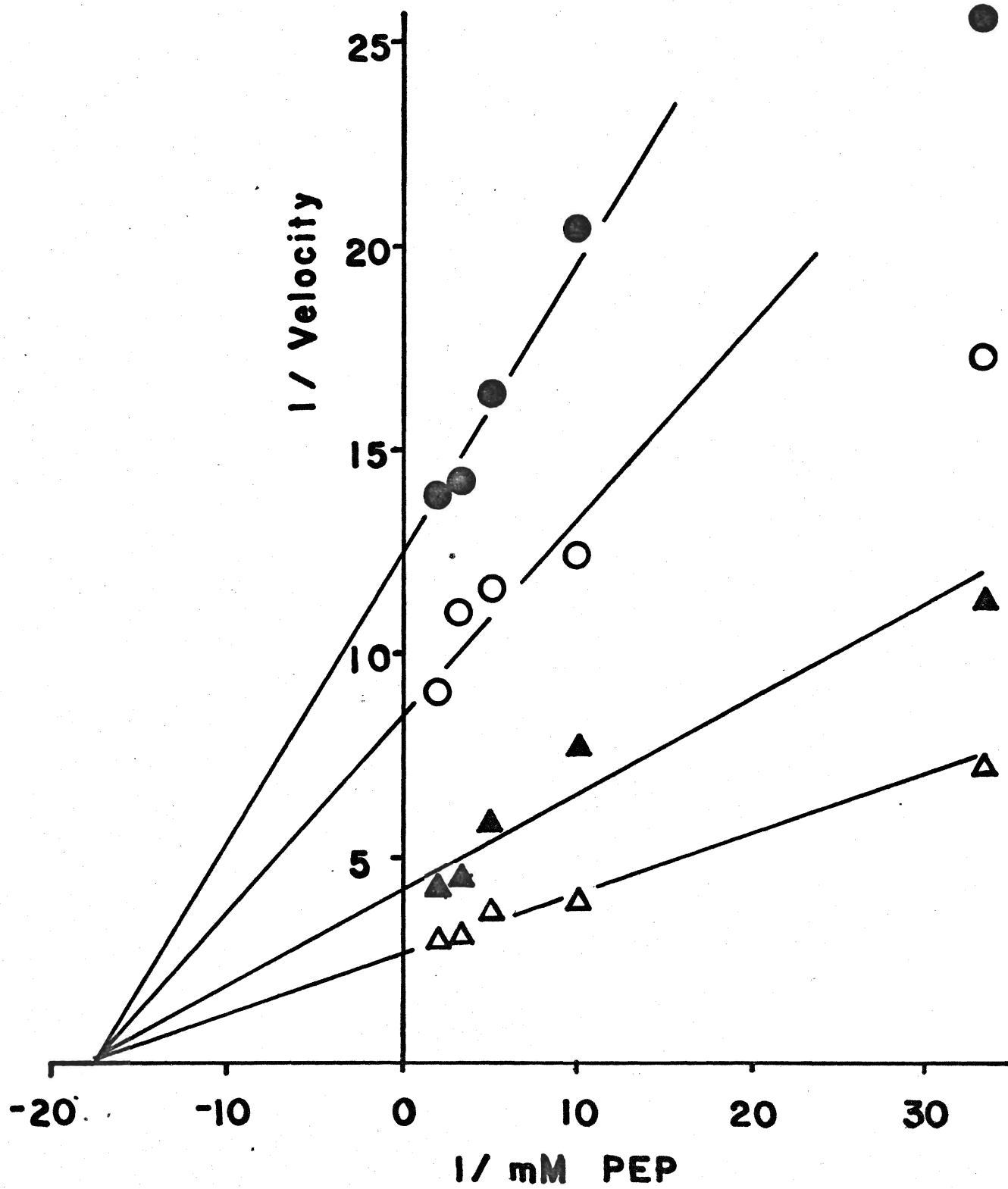


Table 27: Effects of pH and various metabolites on the apparent  $K_m$ (PEP) and  $V_{max}$  of PEPC.

Metabolite	$V_{max}^0$	$K_{m_{app}}^0$	Inh. <sup>1</sup> Type	$V_{max}^2$	$K_{m_{app}}^2$	Inh. Type	$V_{max}^3$	$K_{m_{app}}^3$	Inh. Type
—	—	—	—	.09→.40 (7.05→7.55)	0.6-1.0	—	.09→.23 (7.05→7.55)	0.03	—
Malate (0.1 mM)	—	—	—	.16;.35 (7.35;7.55)	0.6-1.0	N.C.	.05;.10 (7.35;7.55)	0.03	N.C.
Succinate (1.7 mM)	—	—	—	.04;.09 (7.26;7.55)	0.13	Mix.	.02;.05 (7.26;7.55)	0.03	U.C.
Citrate (1.7 mM)	.17→.39 (7.12→7.72)	0.09	C.	—	—	—	—	—	—
F·1,6·diP (1.7 mM)	.28;.40 (7.53;7.72)	0.05	N.C.	.28;.04 (7.12;7.20)	0.33	C.	.08;.14 (7.12;7.20)	0.03	U.C.
3·PGA (1.0 mM)	.08;.24 (7.13;7.58)	0.06	N.C.	—	—	—	—	—	—

<sup>0</sup>Kinetic constants for systems exhibiting linear curves of Michaelis-Menton transformations

<sup>1</sup>Inhibition type (C.-competitive; N.C.-non-competitive; U.C.-un-competitive)

<sup>2</sup>Kinetic constants at high [PEP] for systems exhibiting non-linear curves of Michaelis-Menton transformations

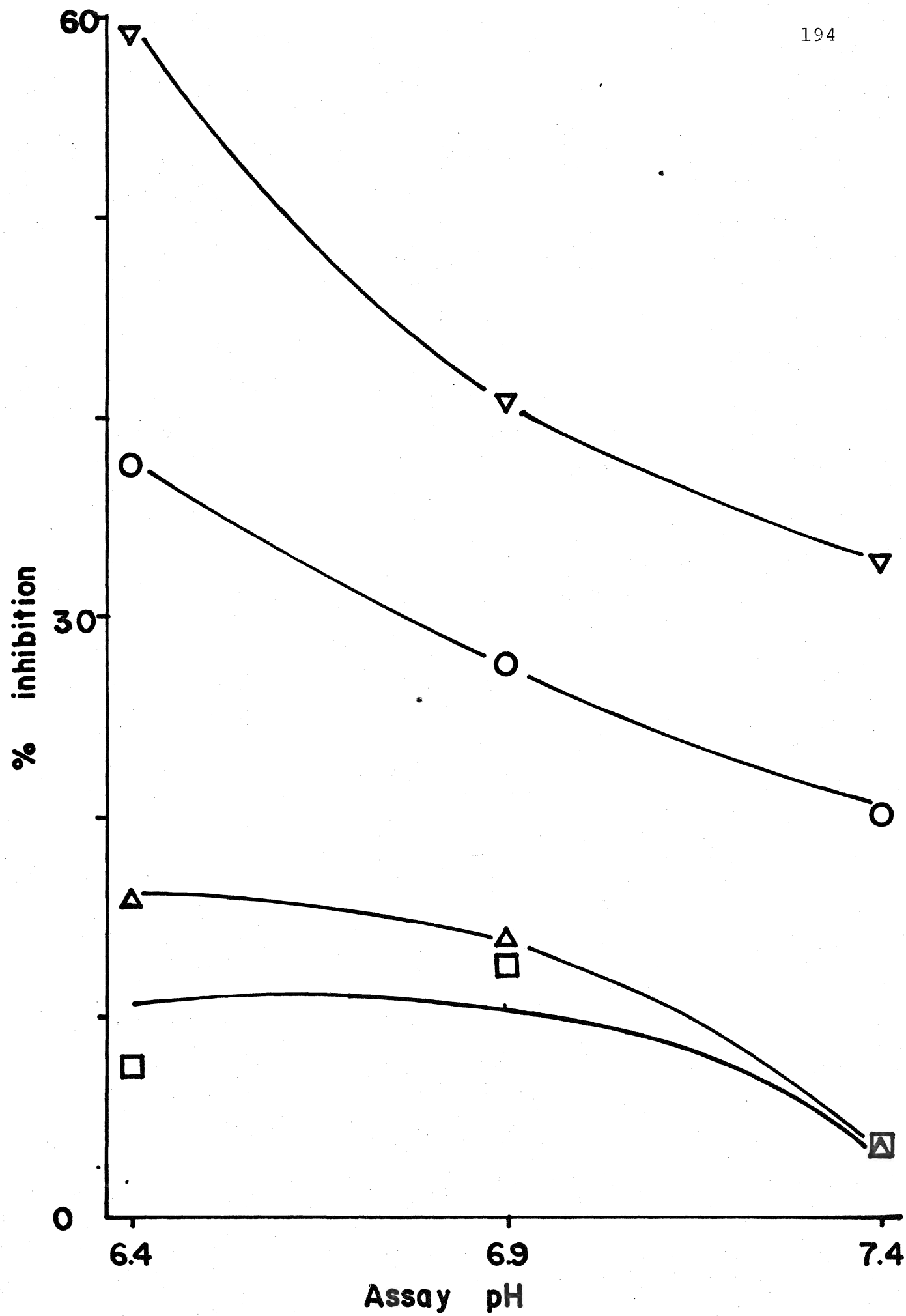
<sup>3</sup>Kinetic constants at low [PEP] for systems exhibiting non-linear curves of Michaelis-Menton transformations

$V_{max}$  ( $\mu\text{mole} \cdot \text{min}^{-1} \cdot \text{gFW}$ );  $K_m$  (mM); ( ) indicate assay pH

Assay components: 10.7 mM K-Pi buffer pH 6.9-7.4; 3.3 mM  $\text{MgCl}_2$ ; 16.7 mM  $\text{NaHCO}_3$ ; 0.05 mM NADH; 0.01-0.5 mM PEP; 0.2 ml enzyme extract  $\pm$  metabolite.

Figure 47: Effect of pH on the percent inhibition of near-saturated malic enzyme activity by fructose-1,6-diphosphate, 3-phosphoglycerate, succinate and citrate.

Enzyme activity was assayed spectrophotometrically at 340 nm in the presence of 12.5 mM Tris-BES buffer pH 6.4 to 7.4, 1.0 mM  $\text{MnCl}_2$ , 0.5 mM  $\text{NADP}^+$ , 0.5 mM malate, 0.2 ml enzyme extract  $\pm$  1.7 mM levels of fructose-1,6-diphosphate ( $\nabla$ ), 3-phosphoglycerate ( $\bigcirc$ ), succinate ( $\Delta$ ) or citrate ( $\square$ ). Percent inhibition was calculated for metabolite inhibited activity as a percentage of activity in the absence of the metabolite.



observed in any experiments. The influence of succinate on the Lineweaver-Burk plot of malic enzyme activity was typical of malic enzyme inhibition by metabolites (Figure 48). Table 28 indicates that the  $V_{\max}$  was decreased 30% by succinate, 70% by fructose-1,6-diphosphate, 20% by 3-phosphoglycerate and 25% by citrate.

It is apparent from the results presented that the phosphorylated sugars are stronger inhibitors of malic enzyme activity than the carboxylic acids, and that amino acids did not significantly influence activity. The results have also reported the loss of activity when the malic enzyme was extracted and/or assayed in potassium phosphate buffers. The combined data suggest that malic enzyme activity may be negatively effected by inorganic phosphate and/or the phosphate groups of organic compounds.

Figure 48: Effect of pH and 1.7 mM succinate on the  
Lineweaver-Burk plot of malic enzyme activity.

Enzyme activity was assayed spectrophotometrically at 340 nm in the presence of 12.5 mM Tris-BES buffer pH 6.4 (○), 6.9 (▽) and 7.4 (△), 1.0 mM  $\text{MnCl}_2$ , 0.5 mM  $\text{NADP}^+$ , 0.026 to 0.5 mM malate, 0.2 ml enzyme extract and plus (closed symbols) or minus (open symbols) 1.7 mM succinate.



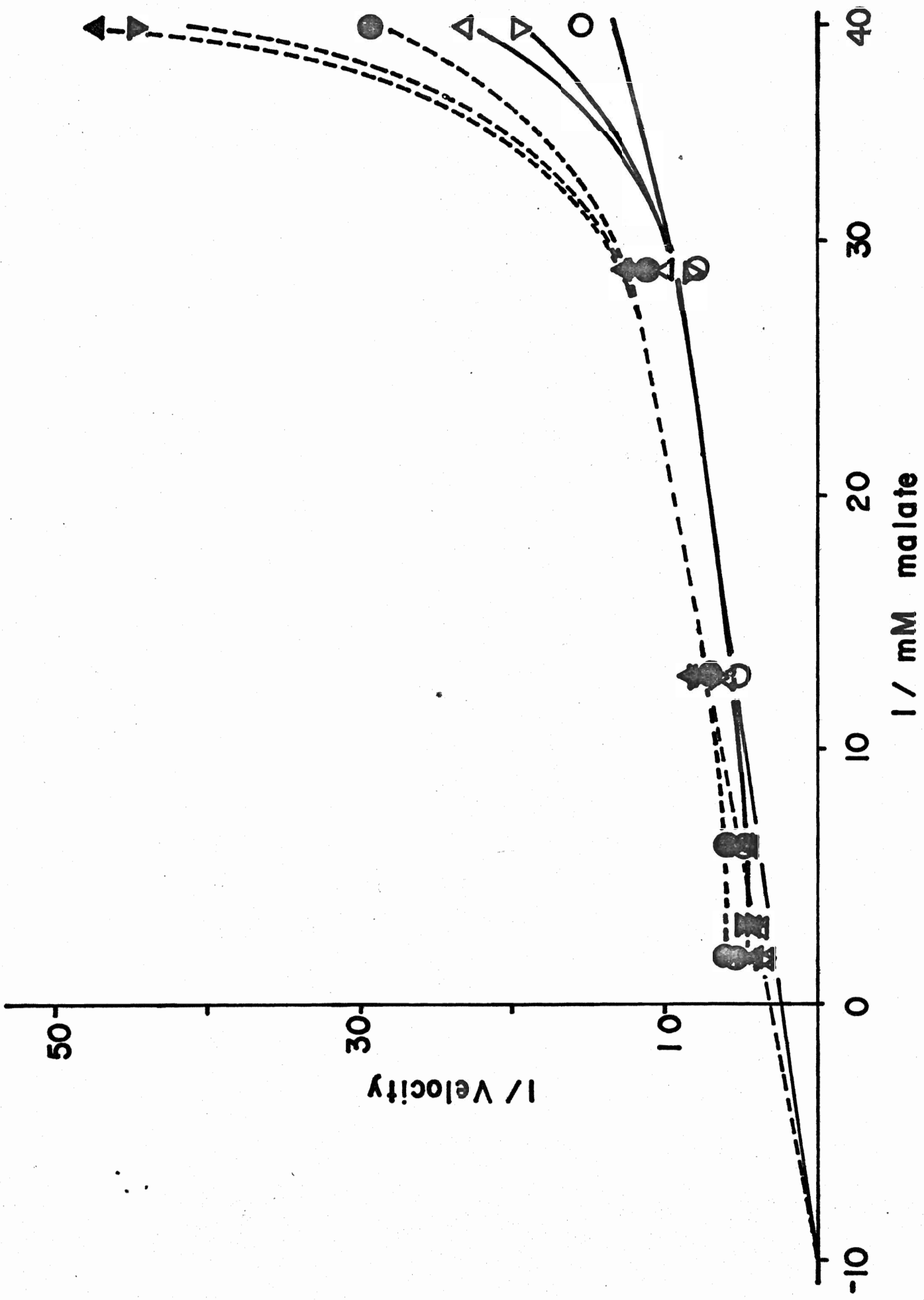


Table 28: Effects of pH and various metabolites on the apparent  $K_m$ (malate) and  $V_{max}$  of the malic enzyme

Metabolite	no pH effect		Inhibition Type
	$V_{max}$ ( $\mu\text{mole}\cdot\text{min}^{-1}\cdot\text{g FW}$ )	$K_{m\text{app}}$ (malate) (mM)	
--	$0.42 \pm 0.03$	0.1	00
succinate	0.27	0.1	non-comp.
citrate	0.32	0.1	non-comp.
F-1,6-diP	0.13	0.1	non-comp.
3-PGA	0.29	0.1	non-comp.

Enzyme activity was assayed spectrophotometrically at 340 nm in the presence of 12.5 mM Tris-BES buffers pH 6.4, 6.9 or 7.4, 1.0 mM  $\text{MnCl}_2$ , 0.5 mM  $\text{NADP}^+$  + 0.01 to 0.5 mM malate  $\pm$  1.7 mM of each metabolite. Apparent  $K_m$ (malate) and  $V_{max}$  in the presence and absence of metabolites were estimated from linear transformations of the data.

## Discussion

Davies (1973) suggested that the carboxylation of PEP by PEPC and the decarboxylation of malate by the malic enzyme could serve to regulate cytosolic pH of plant cells. Implicit in this hypothesis is the antagonistic modulation of the activities of these two enzymes by  $H^+$  and metabolites. Increases in cytosol pH could be countered by increased PEPC activity, and decreases in cytosol pH could be countered by increased malic enzyme activity. Metabolites which positively effect PEPC activity would negatively affect malic enzyme activity and vice versa. Furthermore, Davies (1973) suggested that these modulatory effects would be most pronounced at the cytosolic pH, thus reinforcing the control of enzyme activity by  $H^+$  (Literature Review III, C). The cytosolic pH of plant cells has been estimated as between pH 7.0 and 7.5 (Spanswick and Miller, 1977; Kurkdjian and Guern, 1978). The results of the present investigation indicate that malic enzyme activity is present in Avena coleoptile tissue, but that kinetic changes in response to pH are incompatible with its proposed role in pH regulation. In contrast, the kinetics of Avena PEPC are consistent with its postulated role in a pH-stat.

The present study confirmed the preliminary observations of Howe (1969) and Bown and Lampman (1971) that malic enzyme activity is present in soluble protein extracts of Avena coleotpile tissue. Figures 21 and 22 demonstrate the dependence

of rates of absorbance change of the forward reaction (malate decarboxylation) and the reverse reaction (pyruvate carboxylation) on all substrates, cofactor and coenzyme. Further evidence was obtained from analysis of the reaction products of the forward and reverse reactions and demonstration of dependence on all reactants for their formation (Figures 23 and 25, Tables 16 and 17). Additionally, the ratio of 4.0:1 observed for maximal activity in the forward and reverse reactions agrees well with the 3.3:1 and 3.5:1 ratios obtained for enzyme isolated from pigeon liver (Schimerlik and Cleland, 1977a) and Solanum tubers (Davies and Patil, 1974).

Malic enzyme activity from a variety of species and tissues exhibits a strict requirement for  $\text{NADP}^+$ , and substitution with  $\text{NAD}^+$  renders the enzyme inactive (Rutter and Lardy, 1958; Davies and Patil, 1974). Results presented here also demonstrated strict specificity for  $\text{NADP}^+$ . Additionally, the  $K_m(\text{NADP}^+)$  for the Avena enzyme was very low (less than 0.4 nM) and therefore not rate limiting in the reaction system employed in these studies (Results II, A).

Divalent metal ions are required for maximal malic enzyme activity from all tissues. In some studies, the enzyme was assayed with  $\text{Mg}^{2+}$  (Schimerlik and Cleland, 1977 a and b; Davies and Patil, 1974) but in most reports,  $\text{Mn}^{2+}$  was employed. In this study, the substitution of  $\text{Mg}^{2+}$  for equimolar saturating  $\text{Mn}^{2+}$  at high (near saturating) levels of malate reduced enzyme activity by 80 to 90% (Results II,A). Enzyme isolated from

Solanum tuberosum (Davies and Patil, 1974) and pigeon liver (Schimerlik, Grimshaw and Cleland, 1977) exhibited non-linear kinetics with respect to malate levels when assayed with  $Mn^{2+}$  and Michaelis-Menten type kinetics when assayed with  $Mg^{2+}$ . In contrast, all other studies demonstrated hyperbolic kinetics when substrate levels were varied and the  $Mn^{2+}$  level was constant. The Avena enzyme conformed with the latter kinetic pattern in that Michaelis-Menton type kinetics were observed when assayed with a constant level of  $Mn^{2+}$  and varied malate levels (Figure 27). Further evidence for non-allosteric behaviour was obtained from Hill plots which demonstrated Hill coefficients of 1.0 (Figure 29).

Evidence for the involvement of the malic enzyme in the proposed pH-stat would include an acidic pH optimum, and decreasing activity as pH is increased towards neutrality and proposed cytosol pH values. However,  $V_{max}$  pH optima for enzyme activity isolated from all reported species and tissues was between pH 7.0 and 8.5 (Literature Review I,B,2). pH profiles of Solanum enzyme activity demonstrated that decreases in malate levels resulted in shifts of optimal activity to lower pH values (Davies, 1973). The author suggested that at these more physiological conditions of malate, the in vitro activity profiles are consistent with a role in the pH-stat. In the present study, activity at near-saturating malate levels increased with pH increases from 6.5 to 7.25, and decreases in malate concentration to below 0.3 mM resulted in elimination

of the influence of pH on activity (Figure 25).

In apparent contradiction to the near-saturating pH profiles,  $V_{\max}$  was demonstrated to be pH independent (Figure 30). However, velocity versus malate concentration plots indicated that high malate levels inhibited activity as demonstrated by a modification of the hyperbolic curve (Figure 27). Furthermore, the degree of substrate inhibition diminished as pH was raised from 6.5 to 7.25, in agreement with previous studies (Rutter and Lardy, 1958; Pupillo and Bossi, 1979). It is possible that a Michaelian  $V_{\max}$  is never reached in practice as a result of inhibition by high malate levels, and that pH decreases further prevent the attainment of  $V_{\max}$ .

Inhibition of activity by high substrate levels is generally interpreted as resulting from binding of excess substrate to the enzyme and rendering the complex inactive. In the results presented here an increased  $H^+$  concentration intensified this phenomenon. However, since increased  $H^+$  levels did not affect  $V_{\max}$  or the apparent  $K_m(\text{malate})$ , it is unlikely that changes in ionization states at the active site were influencing substrate inhibition. The only other parameter investigated in this study which was influenced by pH was the  $K_{m_{\text{app}}}(\text{Mn}^{2+})$ . Figure 30 demonstrated that the  $K_{m_{\text{app}}}(\text{Mn}^{2+})$  decreased 65% as the pH was increased from 6.5 to 7.25. The results of this study indicate that pH increases may be correlated with a decreased affinity of a second site for malate, which may or may not be independent of an increased

affinity for  $Mn^{2+}$ . The results do not permit a mechanistic interpretation of these phenomena, and further explanation would necessarily be highly speculative.

Davies and Patil (1974) observed that, in general, the Solanum malic enzyme was activated by carboxylic acids and inhibited by phosphorylated sugars. In contrast, most other studies demonstrated that carboxylic acids were inhibitors (Rutter and Lardy, 1958; Sanwal and Smando, 1969; Schimerlik and Cleland, 1977a). Table 20 and Figure 47 indicate that succinate, citrate, fructose-1,6-diphosphate and 3-phosphoglycerate inhibited the Avena enzyme at near-saturating and limiting malate levels and these effects decreased as pH was increased. Additionally, inhibition was non-competitive in all cases, and changes in pH did not influence the  $K_{m_{app}}$  (malate) in the presence of these metabolites (Table 28). Rutter and Lardy (1958) suggested that inhibition by negatively charged molecules may result from chelation of essential divalent metal cations. The results presented in Table 26 indicate that inhibition of activity by carboxylic acids and phosphorylated sugars may be due to chelation of  $Mn^{2+}$  since, when a three-fold excess of  $Mn^{2+}$  over metabolite was present in the assay inhibition was almost completely abolished. In contrast, kinetic studies of the effects of these compounds on enzyme activity were conducted with equimolar levels of  $Mn^{2+}$  and apparent effector. The weak non-competitive inhibition observed under these conditions was likely due to metabolite chelation of  $Mn^{2+}$  resulting in

decreased levels of  $Mn^{2+}$  available to the enzyme. pH increases resulting in decreased inhibition could be explained in terms of an increased affinity of the enzyme for  $Mn^{2+}$  and decreased affinity of apparent effectors for  $Mn^{2+}$ .

Near-saturating and maximal activity was more strongly inhibited by the phosphorylated sugars than the carboxylic acids (Table 22 and Figure 47). This observation provides further evidence that inhibition resulted from  $Mn^{2+}$  chelation, and that phosphate binds  $Mn^{2+}$  tighter than carboxylate groups. In addition, fructose-1,6-diphosphate presumably has the potential to complex with twice as much  $Mn^{2+}$  as the dicarboxylic acids because of the presence of four negative charges (two phosphate groups) compared with two negative charges (two carboxylate groups).

The effects of various buffer species may also be tentatively interpreted in terms of metal ion chelation. Optimal activity was obtained in histidine-KOH and Tris-BES buffers, whereas activity in phosphate, Tris-HCl, or BES-KOH buffers was greatly reduced (Figures 17 and 18). Between pH 6.0 and 7.0, the majority of histidine molecules would be in the zwitterionic form and thus be unable to complex with  $Mn^{2+}$ . Conversely, potassium phosphate buffers have the potential to complex  $Mn^{2+}$  through ionic interactions with phosphate (Ingraham and Green, 1958). If BES and Tris chelate  $Mn^{2+}$ , then it is difficult to see why buffers made with both species resulted in significantly greater activity than buffers made with Tris or BES.



In summary, the results obtained for the malic enzyme indicate that activity at concentrations of malate less than 0.3 mM,  $V_{\max}$  and  $K_{m_{app}}$  (malate) were not influenced by pH increases from 6.5 to 7.25. Additionally, pH increases were correlated with an increased affinity of the enzyme for  $Mn^{2+}$ , and a decrease in the degree of substrate inhibition decreased with pH increases. All of these observations of the kinetic characteristics of the Avena enzyme are inconsistent with its postulated role in pH regulation.

Saturated and PEP-limited Avena coleoptile PEPC has a pH optimum of 7.7 to 8.0 (Hill and Bown, 1978; Smith, Doo and Bown, 1979). These authors extracted PEPC activity using the same procedure employed in the present study, with the exception that ammonium sulphate was removed from the protein preparation by dialysis instead of gel filtration. Figure 10 demonstrated that dialysis reduced the maximal activity, but did not significantly affect the  $K_{m_{app}}$  (PEP) when compared with gel filtrated enzyme. This may have resulted from the removal of a small endogenous tightly bound non-competitive inhibitor molecule which would have been retained on the Sephadex G-25 column. Inactivation or denaturation of a large fraction of the population of enzyme molecules in the dialyzed preparation compared with the filtrated protein could alternatively account for the decrease in maximal activity.

PEPC activity from a variety of plant species and tissues exhibits non-hyperbolic kinetics under some assay conditions. Non-linear transformations of velocity versus substrate concentration data can indicate the presence of an allosteric site, a random-order two substrate mechanism, two conformational states of the enzyme, or the presence of multiple enzymes catalyzing the same reaction (i.e., isozymes). Non-linear PEPC kinetics are most often interpreted in terms of allosteric regulation of its activity. Hill (1976) observed that activity of the Avena enzyme assayed at pH 7.6 and low levels of PEP had a Hill coefficient of 2.0, indicative of positive co-operativity. In contrast, Smith (1977) reported a Hill number of 0.87 at pH 7.1, 1.08 at pH 7.36, and 1.18 at pH 7.58. The author suggested that the allosteric nature of PEPC varied with pH, and at values greater than the cytosol pH, the enzyme exhibited positive co-operativity, whereas at values less than the cytosol pH, the enzyme exhibited negative co-operativity. However, the numbers reported are probably not significantly different from 1.0 as the assay system, apparatus and graphical procedure employed would not permit differentiation between the cited Hill numbers. In the present study, PEPC appeared to exhibit normal Michaelis-Menten kinetics although PEP levels less than five percent of  $V_{\max}$  were not employed (Figure 12). The lack of co-operativity over this range of PEP concentrations was also indicated by Hill coefficients approximating 1.0 between pH 7.05 and 7.55 (Figure 14). However, linear transformations

of the data indicated deviations from Michaelis-Menten kinetics in that all plots were non-linear (Figure 13 a, b and c). For an allosteric interpretation, the results indicated negative co-operativity at all pH values employed, in that Lineweaver-Burk plots were concave downwards and Eadie-Hofstee plots were concave upwards. However, inspection of the velocity versus PEP concentrations plots indicate  $S_{0.9}/S_{0.1}$  numbers of less than 81, suggestive of positive co-operativity. In addition, inhibition of PEPC activity by malate, a well-documented non-competitive inhibitor, increased the deviation from linearity of the transformed data (Figure 41 a, b and c). A non-competitive inhibitor of an enzyme exhibiting co-operative kinetics normally abolishes the co-operativity rather than enhancing it (Segel, 1975).

The results obtained in this study may also be interpreted in terms of the presence of two isozymes of PEPC present in the protein extract. Evidence is available indicating that greening of etiolated plant tissue is correlated with the development of a PEPC isozyme exhibiting different properties than activity extracted from dark grown tissue (Mukerji and Ting, 1971; Goatly, Coombs and Smith, 1975; Mukerji, 1977a, b and c). In the present study, the linear transformations may describe the combined kinetics of two PEPC isozymes, one with a lower affinity for PEP and higher catalytic efficiency than the other. Since the mechanism of PEPC is not understood, further explanation of the results obtained would be highly speculative.

Smith et al. (1979) reported that the  $K_m(\text{PEP})$ ,  $K_i(\text{malate})$  and  $V_{\max}$  for Avena PEPC were pH dependent and suggested that increases in cytosol pH would increase the binding affinity for PEP, decrease the binding affinity for malate, and increase catalytic efficiency. In the present investigation, greater than twice as many PEP concentrations were assayed over the same range employed in the study of Smith et al. (1979). The non-linear transformations previously discussed indicate the presence of two affinities for PEP and malate and two  $V_{\max}$  estimations. Furthermore,  $V_{\max}$  only was influenced by pH, increasing with pH increases between 7.0 and 7.6 (Figure 15).

Figure 15 indicated that the affinity of PEPC for  $\text{Mg}^{2+}$  increased with pH increases. Experiments conducted by Mukerji (1977b) led him to suggest that corn leaf PEPC requires a PEP- $\text{Mg}^{2+}$  complex as substrate and that  $\text{Mg}^{2+}$  binds in a negatively co-operative manner. If the same mechanism of catalysis is employed by the Avena enzyme, then increases in activity with pH increases would not necessitate an increased binding affinity for PEP, but would explain the pH dependency of  $K_{m\text{app}}(\text{Mg}^{2+})$ . In other words, an active site residue having a pK around 7.5 and binding  $\text{Mg}^{2+}$  when deprotonated would become increasingly available to the PEP- $\text{Mg}^{2+}$  complex as pH is increased from 7.0. Mukerji (1977b) suggests that high levels of  $\text{Mg}^{2+}$  would act as an activator of enzyme activity through binding at a regulatory site. Thus, the observed pH independent non-competitive inhibition by malate may result from inhibition

of  $\text{Mg}^{2+}$  binding at this regulatory site, inducing a decreased efficiency of catalysis. Figure 40 demonstrates that the percent inhibition of PEPC activity by 0.1 mM malate decreased from 70% at pH 7.05 to 30% at pH 7.55. Additionally, the degree of non-linearity of linear transformations of the data decreased as pH was increased over the same range (Figure 41a, b and c). Thus the affinity of  $\text{Mg}^{2+}$  binding at a regulatory site increases with pH increases and this characteristic may decrease the probability of malate binding at the same site.

Bonugli and Davies (1977) observed that phosphorylated sugar compounds activated Solanum PEPC activity whereas carboxylic acids inhibited activity, and these effects were most pronounced at the cytosol pH (around pH 7.3). The present study demonstrated that malate, succinate, citrate, fructose-1,6-diphosphate and 3-phosphoglycerate inhibited Avena PEPC activity, and in all cases the percent inhibition of maximal and PEP-limited activity decreased as pH was increased from 7.0 to 7.6 (Figure 38 and Table 21). In contrast to the results obtained for the malic enzyme, each of the metabolites affected PEPC differently (Figure 41, 43-46). Table 25 indicated that inhibition of activity by each metabolite was not due to  $\text{Mg}^{2+}$  chelation. Furthermore, the addition of 0.1 mM malate to metabolite inhibited assays always resulted in a further decrease in activity, possibly indicating binding at separate regulatory sites on the enzyme (Results IV,C,1(b)).

The carboxylic acids inhibited PEPC activity more than the phosphorylated sugars, and malate and succinate were the strongest inhibitors (Figure 38 and Table 28). Wong and Davies (1973) have suggested that Zea mays PEPC activity is regulated by the cytosolic level of TCA cycle and glycolytic intermediates. However, the physiological role of succinate and citrate inhibition is speculative as these compounds are probably not present in the cytosol at levels which regulate in vitro PEPC activity.

Extraction and/or assay buffers containing phosphate resulted in higher activity than systems not containing phosphate (Figure 16). This observation is in agreement with other studies which indicate that phosphate activates PEPC activity (Wong and Davies, 1973). Ionic strength of the assay system may affect PEPC activity although results in the present study were obtained by varying Tris-BES buffer concentrations only (Figure 19). The decrease in activity observed as Tris-BES concentrations were increased was more likely a result of inhibition by Tris and/or BES, as similar assay ionic concentrations using potassium phosphate buffers resulted in much higher activity (Figure 16). The experiments conducted here cannot distinguish between a general ionic strength effect and a specific species effect on activity.

PEPC activity generates  $H^+$  by fixing  $HCO_3^-$  into organic acids, thus resulting in a shift of the  $CO_2 \longleftrightarrow HCO_3^-$  equilibrium. In summary, pH increases from 7.0 to 7.6 were

correlated with increases in maximal and PEP-limited activity, increases in affinity of the enzyme for  $\text{Mg}^{2+}$ , and decreased sensitivity to inhibitor molecules. All of these results are consistent with a role for PEPC in countering increases in cytosolic pH.

In vitro evidence for a pH-stat involving PEPC and the malic enzyme should ideally involve similar assay conditions which reflect in vivo cytosol conditions. The results of this study, and those of Davies and co-workers (1974; 1977) were obtained with quite different assay conditions for the two enzymes. Thus, although the same metabolites inhibited both PEPC and the malic enzyme isolated from Avena coleoptiles, and inversely affected the Solanum enzymes, the comparative effects of these compounds on PEPC and malic enzyme activity should be interpreted with caution. In general, the results of this study indicated that malic enzyme activity decreases (at high malate levels) or remained constant (at low malate levels) as pH is decreased, indicating that it could not account for increased production of  $\text{OH}^-$  (or consumption of  $\text{H}^+$ ) and therefore could not counter pH decreases. Conversely, the pH-dependent kinetics of PEPC were consistent with its postulated role in countering increased cytosol alkalinity.

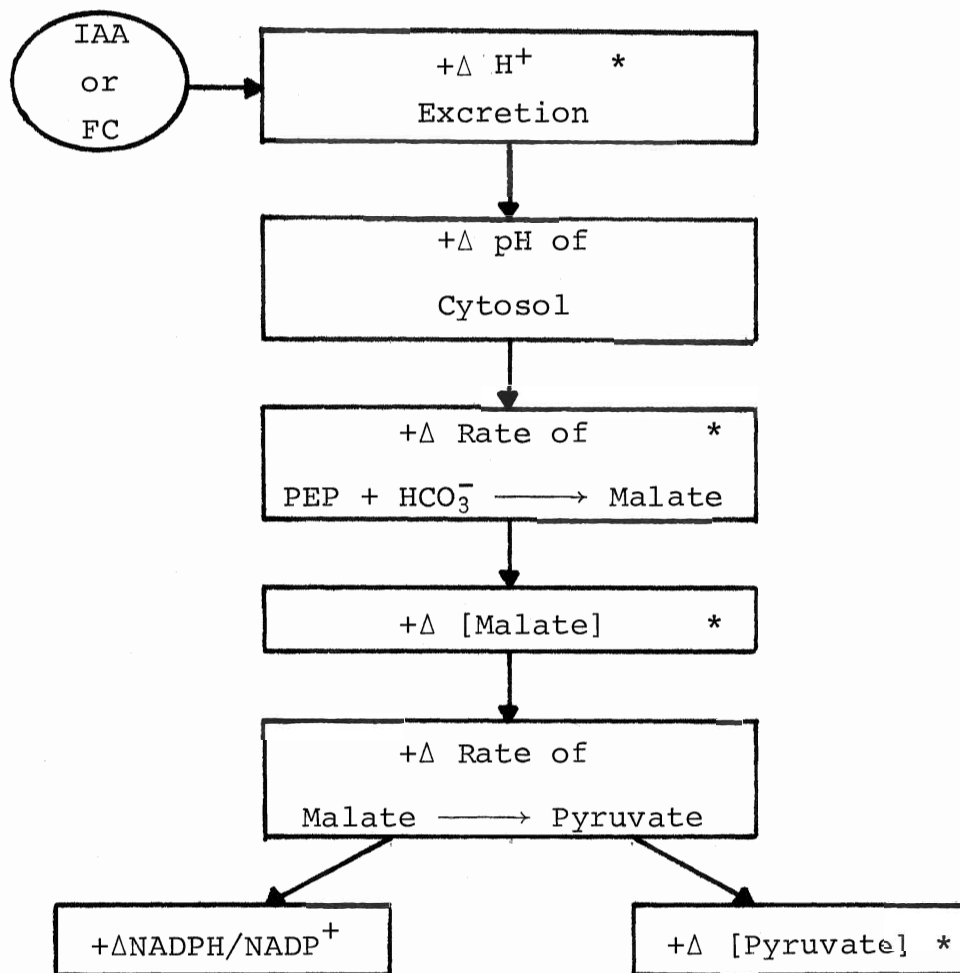
In vivo evidence for a pH-stat has been obtained from studies of tissues which excrete  $\text{H}^+$ , and increase their rates of non-autotrophic  $\text{CO}_2$  fixation during hormone stimulated

growth (Literature Review IV). However, recent work by Calgogno et al. (1978) demonstrated that tissue levels of malate and pyruvate increase when treated with IAA or FC. This makes it difficult to envisage PEPC and malic enzyme activity varying inversely as required by Davies' pH-stat. Marrè (1979) interpreted these observations as consequences of increased malic enzyme activity such that cytosol levels of malate, pyruvate,  $\text{CO}_2$ , NADPH and  $\text{NADP}^+$  are maintained close to equilibrium (Figure 49). The pH profiles of PEPC and malic enzyme activities obtained in this study provide new and further evidence in support of this proposal. Thus the hypothesized increases in cytosol pH resulting from auxin stimulated  $\text{H}^+$  excretion would serve to stimulate both PEPC and the malic enzyme such that the flux of carbon through malate and pyruvate is increased.

Smith and Raven (1979) have postulated that carboxylate synthesis and degradation are indirectly coupled with membrane  $\text{H}^+$  transport such that cytosol pH regulation is an inherent consequence of cellular homeostasis. However, in vivo evidence for the mechanism of regulation of carboxylate metabolism in higher plants is lacking. The observations that metabolically separate malate pools exist in plant cells (Lips and Beevers, 1966) implicate the need for a fine control of malate flux through the malic enzyme and across the tonoplast or mitochondrial membrane into the vacuole or mitochondrion, respectively. In vivo fluxes of malate and in vitro



Figure 49: A model for the mechanism of action of growth hormones



+Δ, increase

\* experimentally detected changes induced by IAA or FC,  
IAA, indoleacetic acid/ FC, fusicoccin

modified from Marrè, 1979

characteristics of tonoplast and mitochondrial transport systems, in combination with the kinetic characteristics of PEPC and the malic enzyme observed in this study would undoubtedly increase our understanding of the role of these enzymes in malate metabolism and growth.

## Literature cited

- Beffagna, N., S. Coccuci and E. Marrè. 1977. Stimulating effect of fusaric acid on  $K^+$ -activated ATPase in plasmalemma preparations from higher plant tissues. *Pl. Sci. Lett.* 8:91-98.
- Bergmeyer, H. U. (Editor). *Methods of Enzyme Analysis*. 1963. Vol. III. Academic Press, New York.
- Bonugli, K. J. and D. D. Davies. 1977. The regulation of potato phosphoenolpyruvate carboxylase in relation to a metabolic pH-stat. *Planta* 133:281-287.
- Bown, A. W. and I. Aung. 1974. The influence of 0.03% carbon dioxide on protein metabolism of etiolated *Avena sativa* coleoptiles. *Plant Physiol.* 54:19-22.
- Bown, A. W., I. J. Dymock and I. Aung. 1974. A synergistic stimulation of *Avena sativa* coleoptile elongation by IAA and  $CO_2$ . *Plant Physiol.* 54:15-18.
- Bown, A. W., I. J. Dymock and B. C. Hill. 1976. An investigation into the influence of IAA and malate on *in vivo* and *in vitro* rates of dark carbon dioxide fixation in coleoptile tissue. *Can. J. Bot.* 55:1641-1645.
- Bown, A. W. and W. W. Lampman. 1971. The presence and role of phosphopyruvate carboxylase in etiolated coleoptiles of *Avena sativa*. *Can. J. Bot.* 49:321-326.
- Burton, K. and M. A. Krebs. 1953. The free energy changes associated with the individual steps of the TCA cycle, glycolysis and alcohol fermentation and with the hydrolysis of the pyrophosphate groups of adenosine triphosphate. *Biochem. J.* 54:94-107.
- Caldagno, R., P. Lado, R. Colombo, R. Cerana and M. Pugliarello. 1978. Changes in cellular metabolism associated with the activation of  $H^+/K^+$  exchange by auxin or fusaric acid in pea internode segments. Presented at Fed. Eur. Soc. Plant Physiol. meet. Edinburgh.
- Cleland, R. 1976. Fusaric acid-induced growth and hydrogen ion excretion of *Avena* coleoptiles: Relation to auxin response. *Planta* 128:201-206.

- Cleland, R. 1973. Auxin-induced hydrogen ion excretion from Avena coleoptiles. P.N.A.S. (U.S.A.) 70:3092.
- Cleland, R. 1976. Fusaric acid-induced growth and hydrogen ion excretion of Avena coleoptiles: Relation to auxin response. Planta 128:201-206.
- Coombs, J., C. W. Baldry and D. Bucke. 1973. The C<sub>4</sub> pathway in Pennisetum purpureum. I. The allosteric nature of PEP carboxylase. Planta. 110: 95-107.
- Coombs, J., S. L. Maw and C. W. Baldry. 1975. Metabolic regulation in C<sub>4</sub> photosynthesis: PEP carboxylase and energy charge. Planta 117:279-292.
- Cooper, T. G. and H. G. Wood. 1971. The carboxylation of phosphoenolpyruvate and pyruvate. II. The active species of "CO<sub>2</sub>" utilized by PEP carboxylase and pyruvate carboxylase. J. Biol. Chem. 246:5488-5490.
- Corwin, L. M. and G. R. Fanning. 1968. Studies of parameters affecting the allosteric nature of PEP carboxylase of Escherichia coli. J. Biol. Chem. 243:3517-3525.
- Cram, W. J. - 1974. Effects of Cl<sup>-</sup> on HCO<sub>3</sub><sup>-</sup> and malate fluxes and CO<sub>2</sub> fixation in carrot and barley root cells. J. Exp. Bot. 25:253-268.
- Cram, W. J. 1976. Negative feedback regulation of transport in cells. The maintenance of turgor, volume and nutrient supply. In Encyclopaedia of Plant Physiology, New Ser., ed. U. Lüttge and M. G. Pitman. Vol. 2A:284-316. Springer, Berlin.
- Danner, M. and I. P. Ting. 1967. CO<sub>2</sub> metabolism in corn roots. II. Intracellular distribution of enzymes. Plant Physiol. 42:719-724.
- Davies, D. D. 1973. Control of and by pH. Symp. Soc. Exp. Biol. 27:513-529.
- Davies, D. D. 1979. The central role of phosphoenolpyruvate in plant metabolism. Ann. Rev. Plant Physiol. 30:131-158.
- Davies, D. D., J. Giovanelli and T. ApRees. 1964. Plant Biochemistry. Blackwell Scientific Publications, Oxford.
- Davies, D. D., Nascimento, K. H. and K. D. Patil. 1974. The distribution and properties of NADP malic enzyme in flowering plants. Phytochem. 13:2417-2425.

- Davies, D. D. and K. D. Patil. 1974. Regulation of malic enzyme of Solanum tuberosum by metabolites. Biochem. J. 137:45-53.
- Dhindsa, R. S., C. A. Beasley and I. P. Ting. 1975. Osmoregulation in cotton fibre: Accumulation of  $K^+$  and malate during growth. Plant Physiol. 56:394-398.
- Goatly, M. B., J. Coombs and H. Smith. 1975. Development of C4 photosynthesis in sugar cane: Changes in properties of PEP carboxylase during greening. Planta 125:15-24.
- Haschke, H. P. and U. Lüttge. 1975. Stoichiometric correlation of malate accumulation with auxin-dependent  $K^+$ - $H^+$  exchange and growth in Avena coleoptile segments. Plant Physiol. 56:696-698.
- Haschke, H. P. and U. Lüttge. 1977. Action of auxin on  $CO_2$  dark fixation in Avena coleoptile segments as related to elongation growth. Plant Sci. Lett. 8:53-58.
- Hiatt, A. J. 1967. Relationship of cell sap pH to organic acid change during ion uptake. Plant Physiol. 42:294-298.
- Hill, B. C. 1976. A kinetic study of the regulatory properties of Avena sativa coleoptile PEP carboxylase. B.Sc. (Hons.) Thesis, Brock University.
- Hill, B. C. and A. W. Bown. 1978. Phosphoenolpyruvate carboxylase activity from Avena coleoptile tissue. Regulation by  $H^+$  and malate. Can. J. Bot. 56:404-407.
- Hishikido, T. and H. Takanashi. 1973. Glycine activation of PEP carboxylase from monocotyledonous C4 plants. Biochem. Biophys. Res. Commun. 53(1):126-133.
- Hong, S. L. 1973. Identification of the product of PEP carboxylase activity in crude enzyme preparations from Avena sativa coleoptiles. B.Sc. (Hons.) Thesis, Brock University.
- Howe, R. C. 1969. Carbon fixation in the oat coleoptile. B.Sc. (Hons.) Thesis, Brock University.
- Jacoby, G. and G. G. Laties. 1971. Bicarbonate fixation and malate compartmentation in relation to salt-induced stoichiometric synthesis of organic acids. Plant Physiol. 47:525-553.

- Kluge, M. and C. B. Osmond. 1972. Studies on phosphoenolpyruvate carboxylase and other enzymes of Crassulacean acid metabolism of Bryophyllum tubiflorum and Sedum praelatum. Z. Pflanzenphysiol. 66:97-105.
- Koshland, D. E. 1970. The molecular basis for enzyme regulation. In The Enzymes V. I and II (Editor) P. D. Boyer. Academic Press. New York.
- Kraemer, L. M., E. E. Conn and B. Vennesland. 1951. The  $\beta$ -carboxylases of plants. III. Oxalacetic carboxylase of wheat germ. J. Biol. Chem. 188:583-591.
- Krebs, H. A. and F. J. Roughton. 1948. Carbonic anhydrase as a tool in studying the mechanism of reactions involving  $\text{H}_2\text{CO}_3$ ,  $\text{CO}_2$  or  $\text{HCO}_3^-$ . Biochem. J. 43:550-555.
- Kurkdjian, A. and J. Guern. 1978. Intracellular pH in higher plant cells. I. Improvements in the use of the 55-dimethyl-oxazolidine-2- $[^{14}\text{C}]$ ,4-dione distribution technique. Plant Sci. Lett. 11:337-344.
- Lee, S.-H. and E. J. Davis. 1979. Carboxylation and decarboxylation reactions. Anaplerotic flux and removal of citrate cycle intermediates in skeletal muscle. J. Biol. Chem. 254:420-430.
- Lin, R. C. and E. J. Davis. 1974. Malic enzymes of rabbit heart mitochondria. J. Biol. Chem. 249:3867-3875.
- Lips, S. H. and H. Beevers. 1966a. Compartmentation of organic acids in corn roots. I. Differential labelling of two malate pools. Plant Physiol. 41:709-712.
- Lowry, D. H., N. J. Rosenbrough, A. L. Farr and R. J. Randall. 1951. Protein measurement with the Folin phenol reagent. J. Biol. Chem. 193:265-275.
- Maren, T. H. 1967. Carbonic anhydrase: Chemistry, physiology and inhibition. Physiol. Rev. 595-781.
- Marrè, E. 1979. Fusicoccin: A tool in plant physiology. Ann. Rev. Plant Physiol. 30:273-288.
- Maruyama, H., R. L. Easterday, H. C. Chang and M. D. Lane. 1966. The enzymatic carboxylation of PEP. J. Biol. Chem. 241:2405-2412.
- Metzler, D. E. 1977. Biochemistry. The Chemical Reactions of Living Cells. Academic Press. New York.

- Meyers, W. F. and K. Y. Huang. 1972. Thin Layer Chromatography. In *Methods in Enzymology*. Vol. XIII, p. 431. Colowick, S. P. and N. O. Kaplan (editors). Academic Press. New York.
- Mukerji, S. K. 1977a. Corn leaf phosphoenolpyruvate carboxylases. I. Purification and properties of two isoenzymes. *Arch. Biochem. Biophys.* 182:343-351.
- Mukerji, S. K. 1977b. Ibid. II. The effect of divalent cations on activity. *Arch. Biochem. Biophys.* 182:352-359.
- Mukerji, S. K. 1977c. Ibid. III. Inhibition of  $^{14}\text{CO}_2$  fixation by  $\text{SO}_3^{2-}$  and activation by glucose-6-phosphate. *Arch. Biochem. Biophys.* 182:360-365.
- Mukerji, S. K. and I. P. Ting. 1971. Phosphoenolpyruvate carboxylase isoenzymes: Separation and properties of three forms from cotton leaf tissue. *Arch. Biochem. Biophys.* 143:297-317.
- Nesius, K. K. and J. S. Fletcher. 1975. Contribution of non-autotrophic  $\text{CO}_2$  fixation to protein synthesis in suspension cultures of Paul's Scarlet Rose. *Plant Physiol.* 55: 643-645.
- Newsholme, E. A. and C. Start. 1973. *Regulation in Metabolism*. John Wiley and Sons. New York.
- Nishikido, T. and T. Wada. 1974. Comparative studies of NADP-malic enzyme from C4- and C3-plants. *Biochem. Biophys. Res. Comm.* 61:243-249.
- Ochoa, S., A. H. Mehler and A. Kornberg. 1947. Reversible oxidative decarboxylation of malic acid. *J. Biol. Chem.* 167:871.
- Osmond, C. B. 1976. Ion absorption and carbon metabolism in cells of higher plants. In *Encyclopaedia of Plant Physiology*, New Ser., ed. U. Lüttge and M. G. Pitman. Vol. 2A:347-372. Springer. Berlin.
- Pupillo, P. and P. Bossi. 1979. Two forms of NADP-dependent malic enzyme in expanding maize leaves. *Planta* 144:283-289.
- Raven, J. A. and F. A. Smith. 1976. Cytoplasmic pH regulation and electrogenic  $\text{H}^+$  extrusion. *Curr. Adv. Pl. Sci.* 8: 649-660.
- Rayle, D. L. 1973. Auxin-induced hydrogen ion secretion in *Avena* coleoptiles and its implications. *Planta* 114:63-73.

- Reeves, R. B. 1977. The interaction of body temperature and acid-base balance in ectothermic vertebrates. *Ann. Rev. Physiol.* 34
- Reibach, P. H. and C. R. Benedict. 1977. Fractionation of stable carbon isotopes by phosphoenolpyruvate carboxylase from C<sub>4</sub> plants. *Plant. Physiol.* 59:564-568.
- Rubinstein, B. and E. N. Light. 1973. Indole acetic acid-enhanced chloride uptake into coleoptile cells. *Planta* 110:43-56.
- Rutter, W. J. and H. A. Lardy. 1958. Purification and properties of pigeon liver malic enzyme. *J. Biol. Chem.* 233:374-382.
- Sanwal, B. D. and R. Smando. 1969. Malic enzyme of *Escherichia coli*; possible mechanism for allosteric effects. *J. Biol. Chem.* 244:1824-1830.
- Schimerlik, M. I. and W. W. Cleland. 1977a. Inhibition and alternate-substrate studies on the mechanism of malic enzyme. *Biochem.* 16:565-570.
- Schimerlik, M. I. and W. W. Cleland. 1977b. pH variation of the kinetic parameters and the catalytic mechanism of malic enzyme. *Biochem.* 16:576-583.
- Schimerlik, M. I., C. E. Grimshaw and W. W. Cleland. 1977. Determination of the rate-limiting steps for malic enzyme by the use of isotope effects and other kinetic studies. *Biochem.* 16:571-576.
- Segel, I. H. 1975. *Enzyme Kinetics*. John Wiley and Sons, Toronto.
- Smith, C. E. 1977. The regulation of *Avena sativa* phosphoenolpyruvate carboxylase in relation to cytoplasmic pH control. B.Sc. (Hons.) Thesis, Brock University.
- Smith, C. E., A. C. Doo and A. W. Bown. 1979. The influence of pH on kinetic parameters of coleoptile phosphoenolpyruvate carboxylase. Relationship to auxin-stimulated dark fixation. *Can. J. Bot.* 57: 543-547.
- Smith, T. E. 1968. Partial purification and characteristics of potato phosphoenolpyruvate carboxylase. *Arch. Biochem. Biophys.* 125:178-188.
- Smith, F. A. and J. A. Raven. 1979. Intracellular pH and its regulation. *Ann. Rev. Plant Physiol.* 30:289-312.
- Smith, I. 1960. *Chromatographic and electrophoretic techniques*. p. 263. Intersciences Publishers Inc., New York.



- Spanswick, R. M. and A. G. Miller. 1977. Measurement of the cytoplasmic pH in Nitella translucens. Comparison of values obtained by microelectrode and weak acid methods. Plant Physiol. 59:664-666.
- Splittstoesser, W. E. 1966. Dark CO<sub>2</sub> fixation and its role in the growth of plant tissue. Plant Physiol. 41:755-759.
- Stout, R. and R. Cleland. 1978. Effects of fusaric acid on the activity of a key pH-stat enzyme, PEP-carboxylase. Planta 139:43-45.
- Stout, R. G., K. D. Johnson and D. L. Rayle. 1978. Rapid auxin- and fusaric acid-enhanced Rb<sup>+</sup> uptake and malate synthesis in Avena coleoptile sections. Planta 139:35-41.
- Tchen, T. T. and B. Vennesland. 1955. Enzymatic carbon fixation into oxaloacetate in wheat germ. J. Biol. Chem. 213:533-546.
- Thimann, K. V. and C. L. Schneider. 1938. The role of salts, hydrogen ion concentration and agar in the response of the Avena coleoptile to auxins. Am. J. Bot. 25:270-280.
- Ting, I. P. 1968. CO<sub>2</sub> metabolism in corn roots. III. Inhibition of PEP carboxylase by L-malate. Plant Physiol. 43:1919-1924.
- Ting, I. P. and D. Dugger. 1966. CO<sub>2</sub> metabolism in corn roots. I. Kinetics of carboxylation and decarboxylation. Plant Physiol. 42:712-718.
- Ting, I. P. and C. B. Osmond. 1973. Photosynthetic phosphoenolpyruvate carboxylases: Characteristics of alloenzymes from leaves of C<sub>3</sub> and C<sub>4</sub> plants. Plant Physiol. 51:439-447.
- Umbreit, W. W., R. H. Burris and J. F. Stauffer. 1964. Manometric Techniques. Fourth Edition. Burgess Publishing Co., Minneapolis.
- Waygood, E. R., R. Mache, and C. K. Tan. 1969. Carbon dioxide: The substrate for PEP carboxylase from leaves of maize. Can. J. Bot. 47:1455-1458.
- Went, S. 1928. In: Philips, I. D. 1971. Introduction to the Biochemistry and Physiology of Plant Growth Hormones. McGraw-Hill, New York.
- Wong, J. T. 1975. Kinetics of Enzyme Mechanisms. Academic Press. New York.
- Wong, K. F. and D. D. Davies. 1973. Regulation of PEP carboxylase of Zea mays by metabolites. Biochem. J. 131:451-458.

Zimmerman, U. 1978. Physics of turgor and osmoregulation.  
Ann. Rev. Plant Physiol. 29:121-148.

Zimmerman, U. and F. Beckers. 1978. Generation of action  
potentials in Chara corallina by turgor pressure. Planta  
138:173-179.